THE SIMULATION OF MULTICOMPONENT ION EXCHANGE IN FIXED-BED COLUMNS

A THESIS PRESENTED FOR THE DEGREE OF
DOCTOR OF PHILOSOPHY IN CHEMICAL ENGINEERING
UNIVERSITY OF CANTERBURY
CHRISTCHURCH, NEW ZEALAND.

by

A. DECHAPUNYA

1981 AD
2524 BD

THIS WORK IS DEDICATED TO ALL RESEARCH ENGINEERS AND ROMADEE

ACKNOWLEDGEMENTS

I would like to thank Dr R.M. Allen, my supervisor, for his help and guidance throughout this work. Through his kindness, tolerance and encouragement, the author has brought the work to a meaningful conclusion.

Many thanks to all the technicians of the Chemical Engineering Department for their help.

Thanks to Mrs C. McEntee for trying to type everything.

Thanks to Thomas Steele for drawing all the graphs and proof reading this thesis.

Thanks to Mrs P. Thomas for transforming one copy into many.

The author is grateful to Professor A.M. Kennedy for arranging a teaching fellowship toward the end of this work.

Thanks to Dr G. Wilson for writing software for the data acquisition system.

CONTENTS

SUMMARY

A mathematical model based on the Nernst-Planck equations has been developed to describe multicomponent ion exchange process.

Digital computer programs have been written in FORTRAN IV to solve the equations of the model with the following features:

- mass transfer coefficients are determined from fundamental properties of exchanging ions and ion exchange resins
- allowing three exchanging ions for combined mass transfer resistance or any number for a single phase resistance
- constant or variable self-diffusion coefficients
- constant or variable separation factors
- allowing partial column presaturation or arbitrary column initial concentration profiles.

To verify the equations of the model a comparison between experimental and predicted breakthrough curves has been made. This involved obtaining independent equilibrium data and measuring column effluent concentration histories.

Equilibrium studies of K-H, Na-H and K-Na-H systems with Dowex 50W X8 at solution concentration of 0.1 N showed that variable separation factors must be used in the breakthrough curve predictions.

Effluent concentrations and temperature from a 5 cm ID and 200 cm long fixed-bed ion exchange column, measured by ion selective electrodes and a LX5700 temperature sensor

respectively, were recorded by a data logging system consisting of a Motorola MEK 6800D2 evaluation kit, an Orion 701A ionalyzer, a teletype and a 10-bit analog to digital converter.

A comparison of computed results with experimental data has shown that the model developed can be used to accurately predict the breakthrough curve behaviour from a multicomponent fixed-bed ion exchange column.

CHAPTER 1

INTRODUCTION

There are numerous publications on the science of binary ion exchange operations. The literature was reviewed by Kelly (1966) up to 1966 with the emphasis on experimental work, and by Allen (1973) concentrating on computer simulation work.

Frequently, however, ion exchange operations involve more than two counter ions. An examination of the literature reveals that references to multicomponent ion exchange in fixed-bed columns are rare. Few experimental breakthrough curves have been published involving more than two counter ions. One of the reasons for the lack of experimental multicomponent breakthrough curves has been difficulties in analytical measurements. Titrations of samples collected from the columns are tedious and time-consuming. New analytical tools and the low cost of microcomputers allow automatic data logging of continuous column effluent analysis.

The aim of the work is to generate a useful mathematical model of the multicomponent fixed-bed ion exchange process. Experimental results are recorded to verify this model and its numerical solution. This will broadly involve:-

(1) obtaining multicomponent equilibrium data;
(2) obtaining experimental multicomponent breakthrough curves;
(3) developing a model or models for multicomponent ion exchange in fixed-bed columns;
(4) developing a computer program to solve these equations.

Previous Work on Multicomponent Ion Exchange in Fixed-Bed Columns

Dranoff and co-workers (1958, 1961) extended the second order kinetic rate model developed for binary ion exchange to ternary ion exchange. They assumed that equilibrium ratio for any two ions was the same in binary and ternary systems. Breakthrough curve predictions were performed by solving rate, material balance and equilibrium equations using the method of characteristics. Shallow bed experiments (column diameter 1.5 cm, bed height .25 cm and solution flow rates of 30-116 ml/sq.cm min) were employed to determine rate constants. For each deep bed ternary run (bed height 0.4 - 5.52 cm) three binary shallow bed runs were prerun to obtain the necessary rate constants for the breakthrough curve prediction of the ternary run. Experimental results showed good agreement between experimental and predicted breakthrough curves. This was to be expected since the exchange was mass transfer controlled and the mass transfer constants were experimentally determined. The exchange was said to be mass transfer controlled due to the high flow rates used. (Samuelson, 1963, recommended flow rates of 3-10 ml/sq.cm min for normal ion exchange operations). Also due to high flow rates, intermediate plateau zones were not developed in one run and were not reached in the others.

A multicomponent ion exchange equilibrium theory (Klein, Tondeur and Vermeulen, 1967) was based on the assumption that at a very low flow-rate mass transfer coefficients were high and the ion exchange operation was under equilibrium control, i.e. local equilibrium existed at all points in the bed. This allowed plateau zones to fully develop. Therefore the prediction

of breakthrough curves involved only mass balances and equilibrium relationships. They showed that the number of plateau zones equalled, in general, the number of exchanging ions. These plateau zones were separated by transition zones. The multicomponent equilibrium theory is capable of predicting only the locations of the plateau zones and the transition zones. In the design of any ion exchange operation, actual dynamics must be known. Work on the dynamic behaviour, the predicting of the whole breakthrough curves, was carried out by Clazie et al. (1968) and Omatete (1971).

Clazie applied multicomponent diffusion equations based on irreversible thermodynamics to ion exchange operations. It was shown that the multicomponent diffusion equation, the Nernst-Planck equation and the Fick's law equation can be put into the same form:-

$$J_i = C_o \sum_{\substack{j=1 \\ j \neq i}}^{n} D_{ij} \nabla X_j \qquad (1.1)$$

J_i diffusion flux of species i with respect to weight equivalent velocity

C_o total solution concentration

D_{ij} multicomponent diffusion coefficient

∇X_j driving force for species j.

The difference between the three models is the way in which D_{ij} was related to basic parameters. The multicomponent rate equations were obtained by considering the mean concentrations at a column cross section and applying the linear driving force approximation to the flux equations. The resulting rate equations were then combined with the column mass balance

equations and were solved with appropriate equilibrium data. Predictions of ternary component breakthrough curves involved obtaining mass transfer data from binary column experiments. Ternary equilibrium properties were assumed to be constant and obtained from mass balances on the binary and ternary breakthrough curves assuming constant pattern conditions applied. The Ag-Na-H system with Duolite C-25 porous resin was employed and a total solution concentration of 1.5 N was used to ensure particle phase mass transfer control.

Omatete employed the Ag-Na-H system with Dowex 50W X8 non-porous resin. The experiments were carried out at solution concentrations of 0.05 N for solution phase diffusion control and 1.5 N for particle phase diffusion control.

Both Clazie and Omatete experimentally obtained equilibrium and rate parameters from binary and ternary breakthrough curves. Even so their agreement between predicted and experimental breakthrough curves was not good. This may have been because the ion exchange was predominantly under equilibrium control and the equilibrium model used in the breakthrough curve predictions was not correct. One of their conclusions that the predicted breakthrough curves were insensitive to the rate terms supported that the exchanging processes were under equilibrium control.

Gopola Rao and co-workers (1969, 1974) studied the rate of ternary ion exchange with particle phase diffusion controlling. A single particle method was used in obtaining experimental rate data. A feed solution was passed through a column containing a single ion exchange particle charged with a radioactive tracer ion. The rate of concentration change inside the resin was

monitored directly by a radioactive tracer technique. Since the bed contained only one particle, the amount of exchange occurring was small and it was assumed that the composition of the feed solution remained constant. A model (Viswanathan et al., 1969) was developed to compute the rate of change of ionic concentration in a resin particle for ternary ion exchange. The model was a combination of flux equations based on irreversible thermodynamics and continuity equations. The resulting rate equations consisted of the time derivatives of counter ionic concentrations as functions of particle diameter and particle phase diffusion coefficients. A finite difference approximation with forward difference formulae was used in solving the rate equations. The experimental characteristics were: Ba-Sr-Na-Dowex 50W X8, bed diameter 1 cm, total solution concentration 0.1 N and solution feed flow rate of more than 1500 ml/sq.cm min. High flow rates were employed to ensure particle phase diffusion control. Satisfactory agreement between experimental and predicted rate data were obtained in the favourable equilibrium cases, i.e. when counter ions of higher selectivity coefficients replacing other counter ions.

Extensive experimental data under unfavourable equilibrium conditions for ternary ion exchange in a single particle was carried out by Bajpai et al. (1974). The Nernst Planck equations were applied instead of those of irreversible thermodynamics. They pointed out that both principles gave the same equations if cross phenomenological coefficients were dropped. The systems under investigation were Mn-Cs-Na, Ba-Mn-Na and Sr-Mn-Cs with Dowex 50W X8. Agreement between experiment and prediction was poor for unfavourable equilibrium and this may have been because particle phase diffusion was not the sole controlling

mechanism. Reasonable improvement was obtained after combined diffusion was introduced into their model. However the equations used were not presented in the paper.

There appears to be no general analytical solution for multicomponent ion exchange. The existing analytical solutions are for special cases, namely constant pattern and those derived from equilibrium theory (Cooney and Strusi, 1972; Bradley and Sweed, 1975).

The science of multicomponent ion exchange in fixed bed columns is far from complete. Current technique needed to be improved and refined as follows:-

(1) The rate terms, Ri, are obtained from binary data; to be able to predict a breakthrough curve of ternary component 1, 2 and 3, binary breakthrough curves of 1-2, 1-3 and 2-3 are needed. Chapter Three considers the possibility of determining the rate terms from fundamental properties of counter ions and ion exchange resins.

(2) Constant separation factors are employed in breakthrough curve predictions. Binary and ternary equilibrium data will be independently obtained (Chapter 5).

(3) Combined rate resistances have not been included. Chapter Four considers the possibility.

(4) Few ternary breakthrough curves have been presented (Clazie 2 curves and Omatete 3 curves). This was due to the method of obtaining experimental breakthrough curves. In this work, continuous monitoring of effluent concentrations will be investigated.

CHAPTER 2

MULTICOMPONENT FIXED-BED ION EXCHANGE EQUATIONS

2.1 The Flux Equations

The application of irreversible thermodynamics to multicomponent diffusion led to a generalized diffusion equation (Clazie et al., 1968; Viswanathan et al., 1969). For n dependent fluxes and n dependent forces the equations are:

$$J_i = -\sum_{j=1}^{n} L_{ij} \nabla\Gamma_j \qquad i = 1,2,...n \qquad (2.1)$$

J_i weight equivalent flux of species i with respect to weight equivalent average reference frame velocity;

L_{ij} weight equivalent phenomonological coefficient for diffusion;

Γ_j electrochemical potential of species j;

$\nabla\Gamma_j$ gradient of Γ_j with respect to distance;

n total number of species in the system, i.e. number of counter ions plus number of co-ions plus solvent.

The following assumptions are made regarding the evaluation of the number of species, n:-

(1) The effect of the solvent is negligible during ion exchange operations.

(2) The fluxes are considered at the solution-particle interfaces and due to Donnan exclusion principle (Helfferich, p.134, 1962) there will be negligible co ions fluxes at the interfaces.

With these assumptions, n is taken as the number of counter ions.

The electrochemical potential is the sum of chemical and

electrical energies; it can be considered as the driving force of the ion exchange operation (Helfferich, 1962):

$$\Gamma_j = \mu_j + Z_j f\phi \qquad (2.2)$$

in which μ_j, Z_j, f and ϕ are chemical potential, valence, Faraday constant and electrostatic potential respectively.

The chemical potential of species j can be shown to be (Appendix 2B):

$$\mu_j = \mu_j^{\Delta}(T,P) + RT \ln X_j \qquad (2.3)$$

where $\mu_j^{\Delta}(T,P)$, R, T, and X_j are μ_j at standard state, universal gas constant, absolute temperature and normalized concentration of species j respectively. Combining Eqn. 2.2 with Eqn. 2.3 gives:

$$\Gamma_j = \mu_j^{\Delta}(T,P) + RT \ln X_j + Z_j f\phi$$

Upon taking the derivative:

$$\nabla\Gamma_j = \frac{RT\nabla X_j}{X_j} + Z_j f\nabla\phi$$

Substituting $\nabla\Gamma_j$ in Eqn. 2.1 gives:

$$J_i = -\sum_{j=1}^{n} \frac{L_{ij}RT}{X_j}\left[\nabla X_j + \frac{Z_j X_j f}{RT}\nabla\phi\right] \qquad (2.4)$$

The above flux equations are limited in application due to the difficulties in obtaining L_{ij} values and therefore an approximation will be considered.

The Nernst Planck Approximation

The Nernst Planck equation was derived by Nernst and Planck in 1889-1890. There are two basic assumptions in the model (Helfferich 1962):-

(1) the contribution of electrical potential is significant;

(2) each ionic species interacts with the solvent independently of the other ions.

The first is a basic principle in electrochemistry. The second applies in a dilute solution where the cross coefficients (L_{ij}; $i \neq j$) can be considered negligible in comparison with the main coefficients (Miller; 1966, 1967). Thus Eqn. 2.4 becomes:

$$J_i = - \frac{L_{ii} RT}{X_i} [\nabla X_i + \frac{Z_i X_i f \nabla \phi}{RT}]$$

defining the self-diffusion coefficient as:

$$D_i = \frac{L_{ii} RT}{C_i}$$

where C_i is the concentration of species i, thus

$$J_i = -D_i C_o [\nabla X_i + \frac{Z_i X_i f \nabla \phi}{RT}] \qquad (2.5)$$

where C_o is the weight equivalent total solution phase concentration.

Eqn. 2.5 is applicable to both solution and particle phases. The availability of self-diffusion coefficient data (Chapter 3) makes the Nernst-Planck equation practical to implement in ion exchange process calculations.

The electrical potential term in the Nernst-Planck equation can be eliminated with the following conditions:-

(a) Ion exchange is an equi-equivalent counter diffusion. Thus, at the solution-particle interface the number of equivalents in the solution and particle phases are constant:

$$\sum_{i=1}^{n} X_i \Big|_i = 1.0 \qquad (2.6A)$$

$$\sum_{i=1}^{n} Y_i \Big|_i = 1.0 \qquad (2.6B)$$

where $X_i|_i$ and $Y_i|_i$ are the normalized concentrations at the interface in the solution and particle phases respectively. In the film region, the co-ion concentrations would not be expected to be constant because of the possibility of the movement of the ions of different mobilities (Helfferich, 1962). However, recent investigation by Bajpai et al. (1974) showed that the total concentration of co-ions in the film region can be assumed to be constant. But in the bulk solution far from the interface, the CO-ion concentrations are constant.

(b) The absence of electrical current flow gives the condition that the fluxes of counter ions and co-ions sum to zero. Due to Donnan exclusion of co-ions, the fluxes of co-ions at the interface are negligible; thus

$$\sum_{i=1}^{n} J_i|_i = 0.0 \qquad (2.7A)$$

$$\sum_{i=1}^{n} \bar{J}_i|_i = 0.0 \qquad (2.7B)$$

where $J_i|_i$ and $\bar{J}_i|_i$ are the fluxes at the interface in the solution and particle phases respectively.

The Nernst-Planck equation for the solution phase with Eqn. 2.6A and Eqn. 2.7A gives (Appendix 2C):

$$J_i|_i = C_o \sum_{\substack{j=1 \\ j\neq i}}^{n} D_{ij} \nabla X_j|_i \qquad (2.8)$$

where the multicomponent solution phase diffusion coefficient D_{ij} is given by:

$$D_{ij} = D_i\left[1 + \frac{Z_i X_i (D_j - D_i)}{\sum_{k=1}^{n} Z_k X_k D_k}\right] \qquad (2.9)$$

The Nernst-Planck equation for the particle phase with Equations 2.6B and 2.7B gives:

$$\bar{J}_i\Big|_i = Q \sum_{\substack{j=1 \\ j\neq i}}^{n} \bar{D}_{ij} \nabla Y_j\Big|_i \qquad (2.10)$$

where Q is the ion exchange capacity and $\bar{D}_{ij}$ is the multicomponent particle phase diffusion coefficient given by:

$$\bar{D}_{ij} = \bar{D}_i\left[1 + \frac{Z_i Y_i (\bar{D}_j - \bar{D}_i)}{\sum_{k=1}^{n} Z_k Y_k \bar{D}_k}\right] \qquad (2.11)$$

Eqn. 2.8 and Eqn. 2.10 indicate that the flux of species i is influenced by the concentration gradient of other species. In other words, if there is no concentration gradient of species i there may still be a flux of species i, provided that other concentration gradients exist. This fact has been illustrated experimentally by Cussler and Breuer (1972) and Arnold and Toor (1967).

The qualitative picture of the Nernst-Planck model is as follows. When ions of different mobilities diffuse, an elastic potential gradient is set up; this gradient will slow down the fast ions and speed up the slower ones, i.e. electroneutrality is maintained.

The Nernst-Planck equations were first applied to the analysis of particle diffusion in binary ion exchange by Helfferich and Plesset (1958). Since then, others have applied the Nernst-Planck equations to various binary ion exchange systems (Dranoff and Smith, 1964; Hering and Bliss, 1963; Morig and Rao, 1965; Turner and co-workers, 1966, 1968, 1970; Kataoka and co-workers, 1968, 1973).

Difficulties in analytical measurements have hindered the application of the Nernst-Planck equations to multicomponent ion exchange in fixed-bed columns (Clazie et al., 1968; Omatete, 1971).

2.2 The Diffusional Mass Transfer Rate Equations

In a fixed bed process, ion exchange takes place because the feed is not in equilibrium with the bed. The driving force for the operation is the electrochemical gradient between the solution phase and the particle phase. For a species i in the solution phase, its overall concentration gradient is given by the difference of X_i and Y_i.

For strong acid/strong base synthetic ion exchange materials the transfer mechanism from the solution phase into the particle phase occurs in three steps:-

(1) Solution phase diffusion

Species i diffuse from the bulk solution to the interface.

(2) Adsorption

Species i are adsorbed into the inside of the interface.

(3) Particle phase diffusion

Species i diffuse from the inside of the interface into the particle.

The adsorption step is usually very fast compared to the other two, thus its rate does not affect the transfer of species i into the particle. Consequently, solution phase diffusion and particle phase diffusion are employed here as a mechanism for the ion exchange rate.

Solution Phase Diffusion

For one particle at a particular cross-section of a fixed-bed column, the rate of diffusion of species i into the particle is obtained by considering a mass balance between the solution layer around the particle and the particle itself. The rate equation for solution phase diffusion is given by:

$$Q\left[\frac{\partial Y_i}{\partial t}\right]_V = -\nabla N_i\Big|_i \qquad (2.12)$$

N_i weight equivalent flux relative to a fixed co-ordinate

$N_i|_i$ N_i at the solution-particle interface

V bed volume

t time

The weight equivalent flux relative to a fixed co-ordinate, N_i, is related to the weight equivalent flux relative to the weight equivalent average frame reference velocity, J_i, by (Appendix 2A):

$$N_i = J_i + C_i V_F$$

where V_F is the weight equivalent average frame reference velocity. It can be shown that, Appendix 2A, for an ion exchange operation V_F equals zero, thus Eqn. 2.12 becomes:

$$Q\left[\frac{\partial Y_i}{\partial t}\right]_V = -\nabla J_i\Big|_i \qquad (2.13)$$

Particle Phase Diffusion

The rate equation for particle phase diffusion is given by:

$$Q\left[\frac{\partial Y_i}{\partial t}\right]_V = -\nabla \bar{J}_i\Big|_i \qquad (2.14)$$

Rate Equations at a Column Cross-Section

The rate equations, Eqn. 2.13 and Eqn. 2.14, were considered at a point at a particular cross-section of a fixed bed ion

exchange column, and therefore the concentrations here are point concentrations. To convert these point concentrations to mean concentrations at a particular cross-section so that they can be coupled with the column material balance equations, the rate equations are integrated over a closed volume θ bounded by a surface area S. For solution phase diffusion the integration gives:

$$\iiint_{\theta} Q\left[\frac{\partial Y_i}{\partial t}\right] d\theta_V = -\iiint_{\theta} \nabla J_i \Big|_i \, d\theta \qquad (2.15)$$

The Gauss theorem gives that

$$\iiint_{\theta} \nabla . J_i \Big|_i \, d\theta = \oiint_S \underset{\sim}{U} . J_i \Big|_i \, dS \qquad (2.16)$$

where $\underset{\sim}{U}$ is the unit vector normal to the particle surface.

Applying Eqn. 2.16 to Eqn. 2.15 gives:

$$\iiint_{\theta} Q\left[\frac{\partial Y_i}{\partial t}\right] d\theta_V = -\oiint_S \underset{\sim}{U} . J_i \Big|_i \, dS$$

Carrying out the integration gives:

$$Q\left[\frac{\partial \bar{Y}_i}{\partial t}\right] \theta'_V = - \underset{\sim}{U} . J_i \Big|_i S \qquad (2.17)$$

where θ', S and $\bar{Y}_i$ are bed volume per unit depth, surface area of the particles in the volume per unit depth and mean normalized concentration at a cross-section of a fixed-bed column respectively.

A mass transfer area, A_p, for ion exchange operation in a fixed-bed column is (Vermeulen, 1958):

$$A_p = \frac{6(1 - \varepsilon)}{d_p}$$

where ε and d_p are void volume per unit bed volume and a particle diameter respectively. The relationship between A_p, θ' and S is, therefore, given by:

$$A_p = \frac{S}{\theta},$$

Combining the above equation with Eqn. 2.17 results in

$$\left[\frac{\partial \bar{Y}_i}{\partial t}\right]_V = - \frac{A_p}{Q} \underset{\sim}{U}.J_i\Big|_i \qquad (2.18)$$

For particle phase diffusion Eqn. 2.17 becomes:

$$Q\left[\frac{\partial \bar{Y}_i}{\partial t}\right]_V^{\theta''} = - \underset{\sim}{U}.\bar{J}_i\Big|_i S \qquad (2.19)$$

where θ'' is the particle volume per unit depth, related to A_p and S by

$$A_p = \frac{(1 - \varepsilon).S}{\theta''}$$

and Eqn. 2.19 becomes

$$\left[\frac{\partial \bar{Y}_i}{\partial t}\right]_V = - \frac{A_p}{Q(1-\varepsilon)} \underset{\sim}{U}.\bar{J}_i\Big|_i \qquad (2.20)$$

Eqn. 2.18 and Eqn. 2.20 are simplified by substituting J_i and $\bar{J}_i$ from Eqn. 2.8 and Eqn. 2.10 respectively:

$$\left[\frac{\partial \bar{Y}_i}{\partial t}\right]_V = - \frac{A_p C_o}{Q} \sum_{\substack{j=1 \\ j\neq i}}^{n} D_{ij} \underset{\sim}{U}.\nabla X_j\Big|_i \qquad (2.21)$$

$$\left[\frac{\partial \bar{Y}_i}{\partial t}\right]_V = - \frac{A_p}{(1-\varepsilon)} \sum_{\substack{j=1 \\ j\neq i}}^{n} \bar{D}_{ij} \underset{\sim}{U}.\nabla Y_j\Big|_i \qquad (2.22)$$

Eqn. 2.21 and Eqn. 2.22 can be further simplified using the concept of the film diffusion theory.

Film Diffusion Approximation

The film diffusion theory is based on the following assumptions:-

(1) The diffusion is a quasi-stationary process; the diffusion across the film is fast compared with the concentration changes

at the film boundaries so that the flux can be computed from boundary concentrations.

(2) The film is treated as a planar layer, i.e. the diffusion is one dimensional.

The theory states that all the mass transfer resistances occur with linear gradients across the film thicknesses (Treybal, 1968). The applications of the film theory to particle phase diffusion and solution phase diffusion are shown in Figures 2.1a and 2.1b respectively. From Fig. 2.1a the varying concentration gradient is written as:

$$\underset{\sim}{U}.\nabla Y_i\Big|_i = -\frac{\bar{Y}_i - \bar{Y}_i^*}{\bar{\delta}} \tag{2.23}$$

The negative sign indicates that the unit vector $\underset{\sim}{U}$ is normal outward from the particle surface. Similarly for solution phase diffusion, Fig. 2.1b,

$$\underset{\sim}{U}.\nabla X_i\Big|_i = \frac{\bar{X}_i - \bar{X}_i^*}{\delta} \tag{2.24}$$

By combining Eqn. 2.23 with Eqn. 2.22 the particle phase rate equation is obtained

$$\left[\frac{\partial \bar{Y}_i}{\partial t}\right]_V = \frac{A_p}{(1-\epsilon)\bar{\delta}} \sum_{\substack{j=1 \\ j\neq i}}^{n} \bar{D}_{ij}(\bar{Y}_j - \bar{Y}_j^*) \tag{2.25}$$

Also by combining Eqn. 2.24 with Eqn. 2.21 the solution phase rate equation is obtained

$$\left[\frac{\partial \bar{Y}_i}{\partial t}\right]_V = -\frac{A_p C_o}{\delta Q} \sum_{\substack{j=1 \\ j\neq i}}^{n} D_{ij}\,(\bar{X}_j - \bar{X}_j^*) \tag{2.26}$$

Defining a multicomponent particle phase mass transfer coefficient, $\bar{k}_{ij}$, and a multicomponent solution phase mass transfer coefficient, k_{ij}, as

$$\bar{k}_{ij} = \frac{Q\, A_p}{C_o(1 - \varepsilon)\,\bar{\delta}}\, \bar{D}_{ij} \qquad (2.27)$$

$$k_{ij} = \frac{A_p\, D_{ij}}{\delta} \qquad (2.28)$$

Thus Eqn. 2.25 and Eqn. 2.26 become:

$$\left[\frac{\partial \bar{Y}_i}{\partial t}\right]_V = \frac{C_o}{Q} \sum_{\substack{j=1 \\ j\neq i}}^{n} \bar{k}_{ij}\, (\bar{Y}_j - \bar{Y}_j^*) \qquad (2.29)$$

$$\left[\frac{\partial \bar{Y}_i}{\partial t}\right]_V = -\frac{C_o}{Q} \sum_{\substack{j=1 \\ j\neq i}}^{n} k_{ij}\, (\bar{X}_j - \bar{X}_j^*) \qquad (2.30)$$

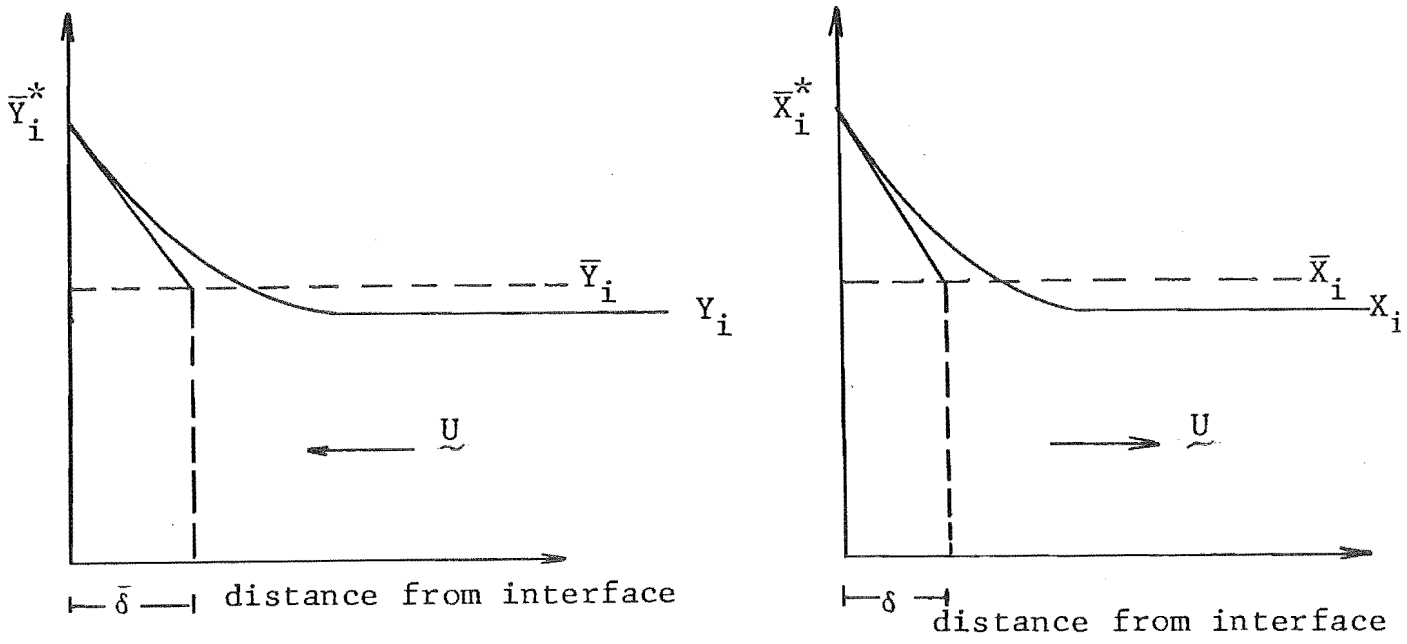

(a) (b)

$\underset{\sim}{U}$. unit vector normal to particle surface

X_i normalised solution phase concentration

Y_i normalised particle phase concentration

$\bar{X}_i$ mean value of X_i at a cross-section of a column

$\bar{X}_i^*$ value of $\bar{X}_i$ at a particle-solution interface

$\bar{Y}_i$ mean value of Y_i at a cross-section of a column

$\bar{Y}_i^*$ value of $\bar{Y}_i$ at a particle-solution interface

δ, $\bar{\delta}$ film thickness, assumed to be constant time average values for the entire duration of mass transfer. It is also depended on the nature of the flows. The film model works well when δ/d_p and $\bar{\delta}/d_p$ are less than unity.

d_p particle diameter

Figure 2.1

Normalized Rate Equations

The normalized column material balance equation, Eqn. 2.37, shows that $\bar{Y}_i$ is a function of V and ZV, i.e.

$$\bar{Y}_i = f(V, ZV)$$

where Z is a throughput ratio and is defined as (Vermeulen, 1958):

$$Z = \frac{C_o}{QV}(Ft - V\varepsilon)$$

Using the chain rule of partial differentiation on $\bar{Y}_i$

$$d\bar{Y}_i = \left[\frac{\partial \bar{Y}_i}{\partial V}\right]_{ZV} dV + \left[\frac{\partial \bar{Y}_i}{\partial ZV}\right]_V dZV$$

$$\frac{dY_i}{dt} = \left[\frac{\partial \bar{Y}_i}{\partial V}\right]_{ZV} \frac{dV}{dt} + \left[\frac{\partial \bar{Y}_i}{\partial ZV}\right]_V \frac{dZV}{dt}$$

$$\therefore \quad \left[\frac{\partial \bar{Y}_i}{\partial t}\right]_V = \left[\frac{\partial \bar{Y}_i}{\partial ZV}\right]_V \left[\frac{dZV}{dt}\right]_V \tag{2.31}$$

By definition $ZV = \frac{C_o}{Q}[Ft - V\varepsilon]$

$$\therefore \quad \left[\frac{\partial ZV}{\partial t}\right]_V = \frac{C_o F}{Q} \tag{2.32}$$

Combining Eqn. 2.31 with Eqn. 2.32 gives

$$\left[\frac{\partial \bar{Y}_i}{\partial t}\right]_V = \frac{C_o F}{Q}\left[\frac{\partial \bar{Y}_i}{\partial ZV}\right]_V \tag{2.33}$$

Applying Eqn. 2.33 to Eqn. 2.29 and Eqn. 2.30 respectively results in:

$$\left[\frac{\partial \bar{Y}_i}{\partial ZV}\right]_V = \frac{1}{F} \sum_{\substack{j=1 \\ j \neq i}}^{n} \bar{k}_{ij} (\bar{Y}_j - \bar{Y}_j^*) \tag{2.34}$$

$$\left[\frac{\partial \bar{Y}_i}{\partial ZV}\right]_V = -\frac{1}{F} \sum_{\substack{j=1 \\ j\neq i}}^{n} k_{ij} \left(\bar{X}_j - \bar{X}_j^*\right) \tag{2.35}$$

2.3 The Column Material Balance Equation

The wellknown equation describing a material balance of a species i taken over a cross-section perpendicular to the direction of the flow in a fixed-bed ion exchange column, assuming that molecular diffusions and axial effects are negligible, is given by (Hiester et al., 1952):

$$\left[\frac{\partial \bar{X}_i}{\partial V}\right]_{V_s} + \frac{Q}{C_o}\left[\frac{\partial \bar{Y}_i}{\partial V_s}\right]_V + \varepsilon\left[\frac{\partial \bar{X}_i}{\partial V_s}\right]_V = 0 \tag{2.36}$$

where V_s is the solution volume.

By employing the throughput ratio, Z, Eqn. 2.36 can be shown to be (Allen, 1973):

$$\left[\frac{\partial \bar{X}_i}{\partial V}\right]_{ZV} + \left[\frac{\partial \bar{Y}_i}{\partial ZV}\right]_V = 0 \tag{2.37}$$

2.4 Equilibrium Relations

A separation factor α_j^i, which measures a resin selectively of species i relative to species j at equilibrium, is defined

$$\alpha_j^i = \frac{\bar{Y}_i^* / \bar{X}_i^*}{\bar{Y}_j^* / \bar{X}_j^*} \tag{2.38}$$

Eqn. 2.38 can be written as (Appendix 2D)

$$\bar{Y}_i^* = \frac{\alpha_n^i \bar{X}_i^*}{\sum_{j=1}^{n} \alpha_n^j \bar{X}_j^*} \tag{2.39}$$

$$\bar{X}_i^* = \frac{\alpha_i^n \bar{Y}_i^*}{\sum_{j=1}^{n} \alpha_j^n \bar{Y}_j^*} \tag{2.40}$$

Equations 2.39 and 2.40 are useful when the diffusion in a single phase is the controlling mechanism. For example, when the particle diffusion is the controlling one, $\bar{X}_i^*$ equals $\bar{X}_i$ and one can use Eqn. 2.39 as

$$\bar{Y}_i^* = \frac{\alpha_n^i \bar{X}_i}{\sum_{j=1}^{n} \alpha_n^j \bar{X}_j}$$

APPENDIX 2A

RELATIONSHIP BETWEEN THE WEIGHT EQUIVALENT FLUX RELATIVE TO A FIXED CO-ORDINATE AND THE WEIGHT EQUIVALENT FLUX RELATIVE TO WEIGHT EQUIVALENT AVERAGE REFERENCE FRAME VELOCITY

Let V_i^o be velocity of species i relative to fixed co-ordinates. Then V_F the weight equivalent average reference frame velocity is given by:

$$V_F = \sum_{i=1}^{n} \frac{C_i V_i^o}{C_o} \tag{2A.1}$$

C_i weight equivalent concentration

C_o total concentration

Now let N_i be weight equivalent flux relative to fixed co-ordinates and J_i be weight equivalent flux relative to weight equivalent average reference frame velocity, therefore

$$N_i = C_i V_i^o \tag{2A.2}$$

$$J_i = C_i (V_i^o - V_F) \tag{2A.3}$$

The relationship between N_i and J_i is then

$$N_i = J_i + C_i V_F \tag{2A.4}$$

An ion exchange operation is an equi-equivalent counter diffusion process i.e. at any time the net fluxes relative to fixed co-ordinates at the interface are zero so that

$$\sum_{i=1}^{n} N_i = 0$$

Substituting N_i from Eqn. 2A.2 in the above equation results in

$$\sum_{i=1}^{n} C_i V_i^o = 0 \qquad (2A.5)$$

Combining Eqn. 2A.5 with Eqn. 2A.1 gives

$$V_F = 0$$

and Eqn. 2A.4 becomes

$$N_i = J_i \qquad (2A.6)$$

APPENDIX 2B

DERIVATION OF EQUATION 2.3

The chemical potential of a species i, μ_i, is given by (Robinson and Stokes, 1959)

$$\mu_i = \mu_1^o(T,P) + RT \ln \gamma_i M_i \qquad (2B.1)$$

$\mu_i^o(T,P)$ chemical potential at a standard state

R universal gas constant

T absolute temperature

P pressure

M_i molar concentration

γ_i molar activity coefficient

The weight equivalent concentration of species i, C_i, is related to the molar concentration of species i, M_i, by

$$C_i = Z_i M_i \qquad (2B.2)$$

where Z_i is the valence of species i.

Substituting C_i from Eqn. 2B.2 in Eqn. 2B.1 gives

$$\mu_i = \mu_i^o(T,P) + RT \ln \left(\frac{\gamma_i C_i}{Z_i}\right)$$

$$\mu_i = \mu_i^o(T,P) - RT \ln Z_i + RT \ln \gamma_i C_i \qquad (2B.3)$$

Since Z_i is constant then Eqn. 2B.3 can be written as

$$\mu_i = \mu_i^\phi(T,P) + RT \ln \gamma_i C_i \qquad (2B.4)$$

The standard state is chosen such that the activity coefficient approaches unity when the concentration approaches zero at any temperature and pressure. In Eqn. 2B.4, by definition μ_i equals $\mu_i^\phi(T,P)$ at the standard state since at the standard

state RT ln γ_i C_i equals zero at any temperature and pressure.

The concentration in Eqn. 2B.4 can be written in terms of normalized concentration by

$$\mu_i = \mu_i^{\phi}(T,P) + RT \ln \gamma_i C_i \frac{C_o}{C_o}$$

$$\mu_i = \mu_i^{\phi}(T,P) + RT \ln \gamma_i C_o + RT \ln X_i$$

$$\mu_i = \mu_i^{\phi}(T,P,\gamma_i,C_o) + RT \ln X_i \qquad (2B.5)$$

In an ion exchange operation the total number of equivalents in any one phase is constant provided that electrolyte sorption is negligible and if swelling is also negligible then C_o is constant, Eqn. 2B.5 becomes

$$\mu_i = \mu_i^{\phi}(T,P,\gamma_i) + RT \ln X_i \qquad (2B.6)$$

For dilute solutions containing homovalent ions, molar activity coefficients, γ_i, are functions of total solution ionic strength alone (Appendix 6B). Since C_o is constant, then the total ionic strength is also constant, and consequently γ_i are also constant, Eqn. 2B.6 becomes

$$\mu_i = \mu_i^{\Delta}(T,P) + RT \ln X_i \qquad (2B.7)$$

APPENDIX 2C

DERIVATION OF MULTICOMPONENT FLUX EQUATIONS FROM THE NERNST-PLANCK EQUATIONS

The Nernst-Planck equation of a counter ion i at the solution-particle interface is given by (dropping "$|_i$" from $\nabla X_i|_i$ & $J_i|_i$ for clarity).

$$J_i = -C_o D_i (\nabla X_i + \frac{Z_i X_i f \nabla \phi}{RT}) \qquad (2C.1)$$

The absence of electrical current gives the following conditions, Eqn. 2.7A,

$$\sum_{j=1}^{n} J_j = 0 \qquad (2C.2)$$

Eqn. 2C.2 can be written as

$$J_i + \sum_{\substack{j=1 \\ j\neq i}}^{n} J_j = 0 \qquad (2C.3)$$

Substituting J_j from Eqn. 2C.1 in Eqn. 2C.3 gives

$$J_i - \sum_{\substack{j=1 \\ j\neq i}}^{n} C_o D_j (\nabla X_j + \frac{Z_j X_j f \nabla \phi}{RT}) = 0$$

Solving for $\frac{f \nabla \phi}{RT}$ gives

$$\frac{f \nabla \phi}{RT} = \frac{J_i - \sum_{j=1, j\neq i}^{n} C_o D_j \nabla X_j}{\sum_{\substack{j=1 \\ j\neq i}}^{n} Z_j X_j D_j C_o} \qquad (2C.4)$$

Substituting $f \nabla \phi / RT$ in Eqn. 2C.1 gives

$$J_i = -C_o D_i (\nabla X_i + Z_i X_i [\frac{J_i - \Sigma C_o D_j \nabla X_j}{\Sigma Z_j X_j D_j C_o}])$$

Solving for J_i

$$J_i = \frac{-C_o D_i \nabla X_i \sum_{j\neq 1} Z_j X_j D_j C_o + C_o D_i X_i \sum_{j\neq i} C_o D_j \nabla X_j}{\sum_{\substack{j=1 \\ j\neq i}}^{n} C_o Z_j X_j D_j + Z_i X_i D_i C_o}$$

$$J_i = \frac{-\sum_{j\neq 1} C_o Z_j X_j D_j D_i \nabla X_i + \sum_{j\neq i} C_o D_j \nabla X_j \, Z_i X_i D_i}{\sum_{j=1}^{n} Z_j X_j D_j} \qquad (2C.5)$$

Now $\sum_{j=1}^{n} X_j = 1.0$; Eqn. 2.6A

or $\sum_{j=1}^{n} \nabla X_j = 0$

or $\nabla X_i = -\sum_{\substack{j=1 \\ j\neq i}}^{n} \nabla X_j \qquad (2C.6)$

Substitute ∇X_i from Eqn. (2C.6) in Eqn. (2C.5)

$$J_i = \frac{\sum_{\substack{j=1 \\ j\neq i}}^{n} C_o Z_j X_j D_j D_i \sum_{\substack{j=1 \\ j\neq i}}^{n} \nabla X_j + \sum_{\substack{j=1 \\ j\neq i}}^{n} C_o D_j \nabla X_j Z_i X_i D_i}{\sum_{j=1}^{n} Z_j X_j D_j}$$

$$J_i = \frac{\sum_{\substack{j=1 \\ j\neq i}}^{n} \left(\sum_{\substack{j=1 \\ j\neq i}}^{n} C_o Z_j X_j D_j D_i \right) \nabla X_j + \sum_{\substack{j=1 \\ j\neq i}}^{n} C_o D_j Z_i X_i D_i \nabla X_j}{\sum_{j=1}^{n} Z_j X_j D_j}$$

$$J_i = \frac{\sum_{\substack{j=1 \\ j\neq i}}^{n} C_o \left(\sum_{\substack{j=1 \\ j\neq i}}^{n} Z_j X_j D_i D_j + Z_i X_i D_i D_j \right) \nabla X_j}{\sum_{j=1}^{n} Z_j X_j D_j}$$

$$J_i = \sum_{\substack{j=1 \\ j\neq i}}^{n} C_o D_i \left[1.0 + \frac{Z_i X_i (D_j - D_i)}{\sum_{j=1} Z_j X_j D_j} \right] \nabla X_j$$

Comparing this equation with Eqn. 1.1

$$J_i = C_o \sum_{\substack{j=1 \\ j \neq i}}^{n} D_{ij} \nabla X_j$$

the multicomponent diffusion coefficients D_{ij} can be expressed in terms of the self-diffusion coefficients D_i

$$D_{ij} = D_i \left[1 + \frac{Z_i X_i (D_j - D_i)}{\sum_{j=1}^{n} Z_j X_j D_j}\right]$$

APPENDIX 2D

DERIVATION OF EQUATIONS 2.39 AND 2.40

A separation factor α_n^i is given by Eqn. 2.38,

$$\alpha_n^i = \frac{\bar{Y}_i^* \bar{X}_n^*}{\bar{X}_i^* \bar{Y}_n^*} \tag{2D.1}$$

The total solution concentration and the total exchange capacity can be assumed to be constant, i.e.

$$\sum_{i=1}^{n} \bar{Y}_i^* = 1 \tag{2D.2}$$

$$\sum_{i=1}^{n} \bar{X}_i^* = 1.0 \tag{2D.3}$$

Eqn. 2D.1 can be written as

$$\bar{Y}_i^* = \alpha_n^i \bar{X}_i^* \frac{\bar{Y}_n^*}{\bar{X}_n^*} \tag{2D.4}$$

Summing Eqn. 2D.4 from 1 to n gives

$$\sum_{i=1}^{n} \bar{Y}_i^* = \frac{\bar{Y}_n^*}{\bar{X}_n^*} \sum_{i=1}^{n} \alpha_n^i \bar{X}_i^* \tag{2D.5}$$

Combining Eqn. 2D.5 with Eqn. 2D.2 and Eqn. 2D.4 gives

$$\bar{Y}_i^* = \frac{\alpha_n^i \bar{X}_i^*}{\sum_{j=1}^{n} \alpha_n^j \bar{X}_j^*} \tag{2D.6}$$

Similarly for $\bar{X}_i^*$ it can be shown that

$$\bar{X}_i^* = \frac{\alpha_i^n \bar{Y}_i^*}{\sum_{j=1}^{n} \alpha_j^n \bar{Y}_j^*} \tag{2D.7}$$

CHAPTER 3

EVALUATION OF MASS TRANSFER COEFFICIENTS

The rate equations which were derived in section 2.2 are

$$\left[\frac{\partial \bar{Y}_i}{\partial t}\right]_V = -\frac{C_o}{Q} \sum_{\substack{j=1 \\ j\neq i}}^{n} k_{ij}(\bar{X}_j - \bar{X}_j^*) \quad \text{for solution phase diffusion}$$

$$\left[\frac{\partial \bar{Y}_i}{\partial t}\right]_V = \frac{C_o}{Q} \sum_{\substack{j=1 \\ j\neq i}}^{n} \bar{k}_{ij} (\bar{Y}_j - \bar{Y}_j^*) \quad \text{for particle phase diffusion}$$

k_{ij} and $\bar{k}_{ij}$ are given by Equations 2.27 and 2.28.

$$\bar{k}_{ij} = \frac{Q A_p \bar{D}_{ij}}{C_o(1-\epsilon)\bar{\delta}}$$

$$k_{ij} = \frac{A_p D_{ij}}{\delta}$$

The multicomponent mass transfer coefficients, k_{ij} and $\bar{k}_{ij}$, are not usually determined from the above relations due to difficulties in obtaining the film thicknesses. A more practical way is to correlate mass transfer coefficients with fundamental properties using experimental breakthrough curves. The advantage of using an empirical correlation is that it includes hydrodynamic effects and fundamental properties for which values are available.

While mass transfer coefficients are available for isotopic and binary ion exchange there are none presently available for multicomponent ion exchange.

This chapter examines some of the existing correlations and their use for computing multicomponent mass transfer coefficients.

3.1 Particle Phase Mass Transfer Coefficients

To find a particle phase self mass transfer coefficient, $\bar{k}_i$, an isotopic ion exchange is considered. The flux of isotope i at any point inside an ion exchange resin is given by the Nernst-Planck equation

$$\bar{J}_i = -\bar{D}_i Q(\nabla Y_i + \frac{Y_i Z_i f}{RT} \nabla\phi)$$

However, since different isotopes are the same counter ion, $\nabla\phi$ is zero.

$$\bar{J}_i = -\bar{D}_i Q \frac{\partial Y_i}{\partial r} \tag{3.1}$$

The rate of change of concentration in the spherical ion exchange particle is given by the continuity equation

$$Q\frac{\partial Y_i}{\partial t} = -\nabla\bar{J}_i = -\frac{1}{r^2}\frac{\partial}{\partial r}(r^2 \bar{J}_i) \tag{3.2}$$

Equations 3.1 and 3.2 are combined to give

$$\frac{\partial Y_i}{\partial t} = \frac{1}{r^2}\frac{\partial}{\partial r}[r^2 \bar{D}_i \frac{\partial Y_i}{\partial r}] \tag{3.3}$$

For isotopic exchange $\bar{D}_i$ is constant and Eqn. 3.3 becomes

$$\frac{\partial Y_i}{\partial t} = \bar{D}_i[\frac{\partial^2 Y_i}{\partial r^2} + \frac{2}{r}\frac{\partial Y_i}{\partial r}] \tag{3.4}$$

Eqn. 3.4 has been solved by many workers (for example Boyd et al, 1947) under the condition that at t equals zero the surface concentration changes from $\bar{Y}_i^o \rightarrow \bar{Y}_i^*$ and remains constant at $\bar{Y}_i^*$.

$$\frac{\bar{Y}_i(t) - \bar{Y}_i^o}{\bar{Y}_i^* - \bar{Y}_i^o} = 1 - \frac{6}{\pi}\sum_{n=1}^{\infty}\frac{1}{n^2}\exp(\frac{-4\, n^2\, \pi^2\, \bar{D}_i\, t}{d_p^2}) \tag{3.5}$$

where $\bar{Y}_i(t)$ is the mean concentration in the particle at time t. Solving for $\bar{Y}_i(t)$ gives

$$\bar{Y}_i(t) = \bar{Y}_i^o + (\bar{Y}_i^* - \bar{Y}_i^o)[1 - \frac{6}{\pi}\sum_{n=1}^{\infty}\frac{1}{n^2}\exp(\frac{-4n^2\, \pi^2\, \bar{D}_i t}{d_p^2})] \tag{3.6}$$

Eqn. 3.6 was derived under the condition that the surface concentration is constant. In ion exchange operations the surface concentrations are not constant, and the equation has to be modified before it can be applied to ion exchange operations.

Work of Glueckauf (1955)

Gleuckauf applied Eqn. 3.6 to a condition in which the surface concentrations were not constant. It was shown by successive integration by parts, that when $\frac{4\bar{D}_i t}{d_p^2} > 0.1$ the rate of diffusion in a particle is given by

$$\frac{d\bar{Y}_i}{dt} = \frac{4\pi^2 \bar{D}_i}{d_p^2}(\bar{Y}_i^* - \bar{Y}_i) + (1 - \frac{\pi^2}{15}) \frac{d\bar{Y}_i^*}{dt} - (\frac{1}{15} - \frac{2\pi^2}{315}) \frac{d^2\bar{Y}_i^*}{dt^2} + \ldots \quad (3.7)$$

By ignoring the third and higher terms and assuming that

$$\frac{d\bar{Y}_i}{dt} = \frac{d\bar{Y}_i^*}{dt} \quad (3.8)$$

Eqn. 3.7 becomes

$$\frac{d\bar{Y}_i}{dt} = \frac{60\bar{D}_i}{d_p^2} (\bar{Y}_i^* - \bar{Y}_i) \quad (3.9)$$

Eqn. 3.9 can be applied at any level in a fixed-bed ion exchange column.

$$[\frac{\partial \bar{Y}_i}{\partial t}]_V = \frac{60\bar{D}_i}{d_p^2} (\bar{Y}_i^* - \bar{Y}_i) \quad (3.10)$$

While $\bar{Y}_i$ in Eqn. 3.9 is a mean concentration inside a particle, $\bar{Y}_i$ in Eqn. 3.10 is the mean concentration at a cross section of a fixed-bed column (Section 2.2).

Work of Hiester and Co-workers (1954, 1956)

Their rate equations were

$$[\frac{\partial \bar{Y}_i}{\partial t}]_V = \frac{A_p D \varepsilon C_o}{\delta Q}(\bar{X}_i - \bar{X}_i^*) \text{ for solution phase diffusion} \quad (3.11)$$

$$\left[\frac{\partial \bar{Y}_i}{\partial t}\right]_V = \frac{A_p \bar{D}}{\bar{\delta}}(\bar{Y}_i^* - \bar{Y}_i) \text{ for particle phase diffusion} \quad (3.12)$$

$$\left[\frac{\partial \bar{Y}_i}{\partial t}\right]_V = \frac{k_r \varepsilon C_o}{Q}\left[\bar{X}_i(1 - \bar{Y}_i) - \frac{\bar{Y}_i}{\alpha_n^i}(1 - \bar{X}_i)\right] \text{ for reaction kinetic model} \quad (3.13)$$

D effective solution phase diffusion coefficient

$\bar{D}$ effective particle phase diffusion coefficient

k_r reaction kinetic mass transfer coefficient

A mid-point slope technique was used to determine values of k_r from experimental breakthrough curves. The procedure can be summarized as follows: (1) from an experimental breakthrough curve, a plot of $\bar{X}$ vs Z, the slope at mid-point $\frac{d\bar{X}(0.5)}{dZ}$ is evaluated; (ii) the value $\frac{d\bar{X}(0.5)}{dZ}$ is compared to an analytical plot of $\frac{d\bar{X}(0.5)}{dZ}$ vs Nr where Nr is the number of transfer units related to reaction kinetic mass transfer coefficient by

$$k_r = \frac{F\ Nr}{Ah}$$

F solution flow rate

A column cross section area

h bed height

Film thicknesses, δ and $\bar{\delta}$, from Equations 3.11 and 3.12 are related to fundamental properties by:

$$\frac{\delta}{d_p} = a\ Re^{-m}\ Sc^{-w} \quad (3.14)$$

$$\frac{\bar{\delta}}{d_p} = b \quad (3.15)$$

where a, m, w and b are constants, Re and Sc are Reynolds and Schmidt numbers given by

$$Re = \frac{d_p F \rho}{6(1-\varepsilon)A\mu} \quad (3.16)$$

$$Sc = \frac{\mu}{\rho D} \tag{3.17}$$

where ρ and μ are solution phase density and solution phase viscosity respectively.

Substituting δ and $\bar{\delta}$ from Equations 3.14 and 3.15 in Equations 3.11 and 3.12 give

$$\left[\frac{\partial \bar{Y}_i}{\partial t}\right]_V = \frac{A_p D \varepsilon C_o}{a d_p Re^{-m} Sc^{-w} Q} (\bar{X}_i - \bar{X}_i^*) \tag{3.18}$$

$$\left[\frac{\partial \bar{Y}_i}{\partial t}\right]_V = \frac{A_p \bar{D}}{b d_p} (\bar{Y}_i^* - \bar{Y}_i) \tag{3.19}$$

The relationship between k_r, a, b, m and w were shown to be

$$\frac{BQ \bar{D} 6(1-\varepsilon)\bar{D}}{\varepsilon C_o D d_p^2 k_r} = \frac{a Q \bar{D} Re^{-m} Sc^{-w}}{\varepsilon C_o D} + b \tag{3.20}$$

where B is a correction term for mixed diffusion control.

Using a number of experimental breakthrough curves from various workers the constants a, b, m and w were evaluated to be 0.29, 0.06, 0.5 and 0.5 respectively. Therefore Equations 3.18 and 3.19 become

$$\left[\frac{\partial \bar{Y}_i}{\partial t}\right]_V = \frac{A_p D \varepsilon C_o}{0.29 d_p Q} (ReSc)^{0.5} (\bar{X}_i - \bar{X}_i^*) \tag{3.21}$$

$$\left[\frac{\partial \bar{Y}_i}{\partial t}\right]_V = \frac{A_p \bar{D}}{0.06 d_p} (\bar{Y}_i^* - \bar{Y}_i) \tag{3.22}$$

Equation 3.22 can be simplified by substituting $6(1-\varepsilon)/d_p$ for A_p

$$\left[\frac{\partial \bar{Y}_i}{\partial t}\right]_V = \frac{100(1 - \varepsilon)\bar{D}}{d_p^2} (\bar{Y}_i^* - \bar{Y}_i) \tag{3.22a}$$

The average value of voidage used in Eqn. 3.20 was 0.4, thus the above equation becomes

$$\left[\frac{\partial \bar{Y}_i}{\partial t}\right]_V = \frac{60\ \bar{D}}{d_p^2}(\bar{Y}_i^* - \bar{Y}_i) \qquad (3.22b)$$

Work of Jury (1967)

The Glueckuaf equation, Eqn. 3.9, was verified by an alternative mathematical approach. In this work Eqn. 3.6 was solved for variable boundary conditions using a frequency domain analysis. It was shown that only one assumption, namely $\frac{4\bar{D}_i t}{d_p^2} > \frac{1}{\pi^2}$ was required in the proof.

Multicomponent Particle Phase Mass Transfer Coefficients

For a single component system Eqn. 2.29 becomes

$$\left[\frac{\partial \bar{Y}_i}{\partial t}\right]_V = \frac{C_o}{Q}\bar{k}_i(\bar{Y}_i^* - \bar{Y}_i)$$

Comparing the above equation to Eqn. 3.10 or Eqn. 3.22b gives

$$\bar{k}_i = \frac{60\ \bar{D}_i}{d_p^2}\frac{Q}{C_o} \qquad (3.23)$$

The following relation, Eqn. 3.24, will be used to compute multicomponent particle phase mass transfer coefficients.

$$\bar{k}_{ij} = \frac{60\bar{D}_{ij}}{d_p^2}\ \frac{Q}{C_o} \qquad (3.24)$$

where the multicomponent particle phase diffusion coefficient $\bar{D}_{ij}$ is given by Eqn. 2.11

$$\bar{D}_{ij} = \bar{D}_i\left[1 + \frac{Z_i\bar{Y}_i(\bar{D}_j - \bar{D}_i)}{\sum_{j=1}^{n} Z_j\bar{Y}_j\bar{D}_j}\right]$$

3.2 Solution Phase Mass Transfer Coefficients

The flux of isotope i at any point in the film layer between the particle and the bulk solution is given by

$$J_i = -D_i C_o \nabla X_i \qquad (3.25)$$

The application of the film theory (section 2.2) to Eqn. 3.25 leads to

$$J_i|_i = -D_i C_o \frac{(\bar{X}_i - \bar{X}_i^*)}{\delta} \tag{3.26}$$

The rate of change of mean concentration of isotope i in the resin phase is given by the continuity equation

$$Q\frac{d\bar{Y}_i}{dt} = -A_p \underset{\sim}{U} \cdot J_i|_i \tag{3.27}$$

Combining Eqn. 3.27 with Eqn. 3.26 results in

$$\frac{d\bar{Y}_i}{dt} = \frac{A_p C_o D_i}{\delta Q}(\bar{X}_i - \bar{X}_i^*) \tag{3.28}$$

Defining k_i as the solution phase self mass transfer coefficient

$$k_i = \frac{A_p D_i}{\delta}$$

Thus, Eqn. 3.28 becomes

$$\frac{d\bar{Y}_i}{dt} = \frac{k_i C_o}{Q}(\bar{X}_i - \bar{X}_i^*) \tag{3.29}$$

Eqn. 3.29 can be solved under a constant boundary condition and linear equilibrium (Boyd et al., 1947) to give

$$\frac{\bar{X}_i - \bar{X}_i^o}{\bar{X}_i^* - \bar{X}_i^o} = 1 - \exp[-\frac{k_i C_o t}{Q}] \tag{3.30}$$

$\bar{X}_i$ mean normalized concentration at time t

$\bar{X}_i^*$ $\bar{X}_i$ at the interface at time t

$\bar{X}_i^o$ $\bar{X}_i$ at the interface at time 0

Eqn. 3.30 can be used to correlate k_i with fundamental properties for isotopic exchange in a single particle ion exchange column in which the conditions of constant boundary and linear equilibrium are met.

Work of Hiester et al. (1956)

A relationship between the reaction kinetic mass transfer coefficient and solution phase and particle phase mass transfer coefficients was derived for a nonlinear equilibrium. The mid-point slope technique was used to compute reaction kinetic mass transfer coefficients from a number of published breakthrough curves. It was shown that for the solution phase diffusion, the rate equation is given by:

$$\left[\frac{\partial \bar{Y}_i}{\partial t}\right]_V = \frac{6(1-\varepsilon)D\varepsilon C_o}{0.29\ d_p^2\ Q}(ReSc)^{0.5}(\bar{X}_i - \bar{X}_i^*)$$

The term $6(1-\varepsilon)\varepsilon D(ReSc)^{0.5}/0.29\ d_p^2$ is rearranged to give $3.4482\ F\varepsilon(ReSc)^{-0.5}/A\ d_p$. Thus

$$\left[\frac{\partial \bar{Y}_i}{\partial t}\right]_V = \frac{3.4482\ F\varepsilon\ C_o}{A\ d_p\ Q}(ReSc)^{-0.5}(\bar{X}_i - \bar{X}_i^*) \qquad (3.31)$$

Work of Kataoka et al. (1973)

The hydraulic radius model was applied to laminar flow in packed beds by assuming that the voids in the packed beds should be regarded as a bundle of tubes. The mass transfer between the particles and the flowing solution becomes the mass transfer between the inner tube surfaces and the flowing solution. It was shown that the entrance length, Le, required for a velocity profile to become fully developed is given by

$$\frac{Le}{d_p'} = \frac{\beta\varepsilon Re'}{(1-\varepsilon)} \qquad (3.32)$$

where β has a value from 0.022 to 0.029, Re' is Reynolds number given by $\frac{d_p F\rho}{(1-\varepsilon)A\mu}$ and d_p' is a distance corresponding to a spherical diameter based on the hydraulic radius model.

Equation 3.32 indicates that at low Reynolds numbers the entrance lengths are less than d_p' i.e. the flow will be fully

developed at the inlets of imaginary pipes. By solving a differential mass balance equation for a solute diffusing from the surface of a tube wall to the flowing solution, a theoretical liquid phase mass transfer coefficient at high Schmidt number was shown to be

$$j = \left[\frac{1-\varepsilon}{\varepsilon}\right]^{1/3} k^* Sc^{2/3} = \frac{1.85\ F\ Re'^{-2/3}}{A\varepsilon} \qquad (3.33)$$

Equation 3.33 was tested for ion exchange operations by comparison with experimental mass transfer coefficients. Experimental data were obtained using isotopic exchange in a single particle radioactive tracer technique. The relation used for correlating the experimental results was

$$-\ln\left(1 - \frac{\bar{X}_i - \bar{X}_i^o}{\bar{X}_i^* - \bar{X}_i^o}\right) = A_p\, k^*\, \frac{C_o}{Q}\, t \qquad (3.34)$$

Plots of $\ln\left(1 - \frac{\bar{X}_i - \bar{X}_i^o}{\bar{X}_i^* - \bar{X}_i^o}\right)$ against t for R-C_s-C_s/0.01N and R-Zn-Zn/0.01N showed linear relationships. A plot of j against Re' (see Eqn. 3.33) on a log-log scale was obtained using experimental data and experimental values of k^* from the earlier plots. The plot showed that for Sc > 360 and Re' < 10 the experimental data fitted the line drawn by Eqn. 3.33 well.

Multicomponent Solution Phase Mass Transfer Coefficients

For a single component system Eqn. 2.30 becomes

$$\left[\frac{\partial \bar{Y}_i}{\partial t}\right]_V = \frac{k_i\, C_o}{Q} (\bar{X}_i - \bar{X}_i^*)$$

Comparing the above equation with Eqn. 3.31 gives

$$k_i = \frac{3.4482\ F\varepsilon (ReSc)^{-0.5}}{A\ d_p} \quad \text{for Hiester relation} \qquad (3.35)$$

also by comparing Eqn. 3.34 with Eqn. 3.30

$$k_i = 1.85\left(\frac{\varepsilon}{1-\varepsilon}\right)^{1/3} \frac{FA_p}{A\varepsilon}(Re'Sc)^{-2/3} \quad \text{for Kataoka relation} \tag{3.36}$$

where Sc in the above relations is given by

$$Sc = \frac{\mu}{\rho D_i}$$

The following relations will be used to compute multicomponent solution phase mass transfer coefficients.

$$k_{ij} = \frac{3.4482\ F\varepsilon}{A\ d_p}\left(Re\ \frac{\mu}{\rho D_{ij}}\right)^{-0.5} \quad \text{for Hiester relation} \tag{3.37}$$

$$k_{ij} = 1.85\left(\frac{\varepsilon}{1-\varepsilon}\right)^{1/3} \frac{FA_p}{A\varepsilon}\left(Re'\ \frac{\mu}{\rho D_{ij}}\right)^{-2/3} \quad \text{for Kataoka relation} \tag{3.38}$$

where the multicomponent solution phase diffusion coefficient D_{ij} is given by Eqn. 2.9,

$$D_{ij} = D_i\left[1 + \frac{Z_i \bar{X}_i (D_j - D_i)}{\sum_{j=1}^{n} Z_j \bar{X}_j D_j}\right]$$

3.3 Self Diffusion Coefficients

Self diffusion coefficient data, in both solution and particle phases, are required for mass transfer coefficient calculations.

Table 3.1 and Table 3.2 show D_i and $\bar{D}_i$ respectively for a number of ions at various concentrations at 25°C.

It is clear from these two tables that self diffusion coefficients are a function of concentration.

In ion exchange operations, concentration of each ionic species varies throughout the whole operation and consequently the self diffusion coefficient will also vary. Therefore an

Electrotyle	Ion	Concentration (N)	D_i ($m^2 s^{-1}$)x10^9	References	D_i^o
NaCl	Na^+	.000225	1.335	Mills & Godbole	1.333
		.00102	1.327	(1960)	
		.00500	1.319		
		.0101	1.312		
		.0495	1.294		
		.0970	1.280		
LiCl	Li^+	0.2	.962	Anderson &	1.027
		0.5	.946	Patterson (1975)	
		1.0	.919		
		2.0	.868		
NaCl	Na^+	0.2	1.295	"	1.333
		0.5	1.279		
		1.0	1.234		
		2.0	1.133		
KCl	K^+	0.2	1.92	"	1.956
		0.5	1.87		
		1.0	1.85		
		2.0	1.84		
CsCl	Cs^+	0.2	1.952	"	2.054
		0.5	1.947		
		1.0	1.935		
		2.0	1.906		

Self diffusion coefficient at infinite dilution is given by the Nernst equation

$$D_i^o = \frac{RT\ \lambda_i^o}{|Z_i| f^2} \qquad \text{(section 6.3)}$$

Table 3.1: Self diffusion coefficients in solution phase at 25°C.

Counter Ion	Concentration (N)	Self diffusion coefficient ($m^2 s^{-1}$) x 10^{10}	References
Na^+	1.0	1.6	Rao and David (1964)
Na^+	0.1	2.035	Viswanathan et al (1969)
Sr^+	0.1	0.190	
Ba^{+2}	0.1	0.116	
Na^+	0.1	2.05	Bajpai et al (1974)
Mn^{+2}	0.1	0.222	
Sr^{+2}	0.1	0.195	
Ba^{+2}	0.1	0.116	
Cs^+	0.1	3.0	
Na^+	1.0	1.61	Kataoka, Yoshida and
Zn^{+2}	1.0	0.180	Savada (1974)
Ba^{+2}	1.0	0.0698	
Co^{+2}	1.0	0.160	
Na^+	0.2	1.57	Graham (1970)
Cs^+	0.2	2.41	

Table 3.2: Self diffusion coefficients in Dowex 50W X8 at 25°C

algorithm, which estimates self diffusion coefficients in both the solution and the particle phases at any concentration is required for breakthrough curve prediction.

Particle Phase Self Diffusion Coefficients

Kataoka and co-workers (1974, 1976) measured self-diffusion coefficients of H, Li, Na, Cs, Sr, Cu, Ce, Zn, Ba and Co in many types of ion exchange resin. The isotopic single ion exchange particle method was used for the experiments. The effects of resin diameter, solution concentration, valence, degree of crosslinking and atomic weight were studied. The following equations were proposed to estimate self diffusion coefficients in sulfonated styrene type resin in the range of degree of crosslinking 3-16%.

$$\frac{\bar{D}_i}{D_i^o} = 0.55 \exp\left(-0.174 \frac{V_H^w}{V} X Z_i\right) \quad (3.39)$$

$$\frac{\bar{D}_{Ba}}{D_{Ba}^o} = 0.36 \exp\left(-0.348 \frac{V_H^w}{V} X\right) \quad (3.40)$$

D_i^o solution phase self diffusion coefficient at infinite dilution

V_H^w bed volume of H-type resin in water

V bed volume in a solution

X degree of crosslinking

Z_i valence of species i

When data of V_H^w/V are not available, they can be estimated using the following relations. If E is the equivalent weight of the ion, then for E > 15

$$\frac{V_H^w}{V} = [1 + 0.52(C_o - 1)\exp(-.205X)][\exp(.023EP \exp(-.192X))] \quad (3.41)$$

$$P = 1.51 - .51\ C_o \text{ for } 0 < C_o < 1.0 \qquad (3.42)$$

$$P = 1.03 + 0.01C_o - 0.04C_o^2 \text{ for } 1 < C_o < 4 \qquad (3.43)$$

or for E < 15.

$$\frac{V_H^w}{V} = \frac{V_H^w}{V_H} \qquad (3.44)$$

where the values of V_H^w/V_H are estimated from Figure 3.1.

Solution Phase Self-diffusion Coefficients

The following relations will be used to determine solution phase self diffusion coefficients.

Step (1) B_i is evaluated at infinite dilution

$$B_i = \frac{\bar{D}_i^o}{D_i^o} \qquad (3.45)$$

where $\bar{D}_i^o$ is the particle phase self diffusion coefficient at infinite dilution.

Step (2) assuming that B_i is constant for species i, then

$$B_i = \frac{\bar{D}_i^o}{D_i^o} = \frac{\bar{D}_i}{\bar{D}_i} \qquad (3.46)$$

$$\text{i.e. } D_i = \frac{\bar{D}_i}{B_i} \qquad (3.47)$$

Comparisons between D_i computed from Equations 3.45-3.47 and D_i from literature are shown in Table 3.3. Agreement between experimental and predicted values are good at low concentrations. Since ion exchange usually involves operation at low concentrations this method of computing solution phase self diffusion coefficients is acceptable.

In multicomponent ion exchange operations, all counter ions diffuse from the same resin. Thus, from Eqn. 3.39

$$B_i = \frac{\bar{D}_i^o}{D_i^o} = f(V_H^w/V) = \frac{\bar{D}_j^o}{D_j^o} = \ldots . \quad (3.48)$$

for homo valent ions

i.e. $B_i = B_j = B_n$

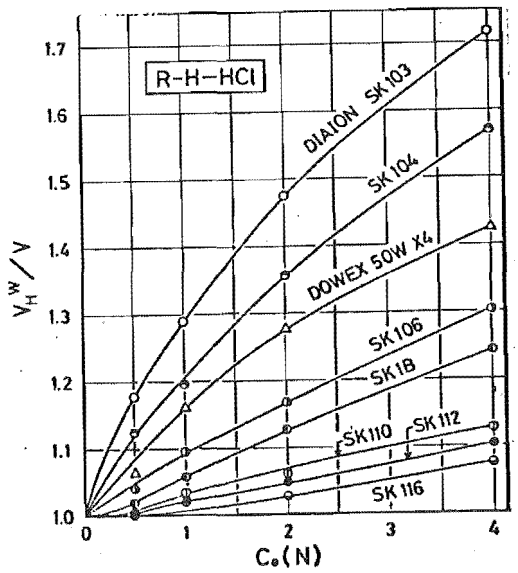

Figure 3.1: Effect of C_o on V_H^w/V for R-H-HCl system.

Ion	Concentration (N)	D_i From Table 3.1	D_i From Eqns 3.45-3.47
Na^+	0.000225	1.335	1.333
	0.2	1.295	1.312
	0.5	1.279	1.283
	1.0	1.234	1.239
	2.0	1.033	1.081
K^+	0.2	1.92	1.948
	0.5	1.87	1.939
	1.0	1.85	1.931
	2.0	1.84	1.693

Table 3.3: Comparison between the estimated and published values of solution phase self diffusion coefficients

CHAPTER 4

NUMERICAL SOLUTION OF MULTICOMPONENT ION EXCHANGE EQUATIONS

Up to now, no general analytical methods have been developed to predict breakthrough curves from multicomponent fixed-bed ion exchange columns. It is possible but unlikely that there will be an analytical method to solve general purpose multicomponent ion exchange equations.

Kelly, Allen and Kennedy (1970) stated "there is little to be gained in trying to obtain more precise analytical descriptions of fixed-bed ion exchange behaviour. Computer studies allow the considerations of such factors as variable interdiffusion coefficients, variable separation factor, axial dispersion, resin volume changes and electrolyte sorption".

This chapter describes the numerical solution of the multicomponent ion exchange equations developed in chapter 2 and chapter 3. The solution is verified against analytical methods and established solutions for binary components. Comparison is then made with experimental results.

4.1 Equations and Method of Solving

The equations to be solved are presented in Table 4.1 and can be put in the form:-

$$\left(\frac{\partial \bar{Y}_i}{\partial Z\bar{V}}\right)_V = R_i \qquad i = 1,....n-1 \tag{4.1}$$

$$\left(\frac{\partial \bar{X}_i}{\partial \bar{V}}\right)_{ZV} = -R_i \qquad i = 1,....n-1 \tag{4.2}$$

Table 4.1: Multicomponent fixed-bed ion exchange equations

Equation	Physical Form	Normalised Form
Column material balance	$\left(\frac{\partial \bar{X}_i}{\partial V}\right)_{Vs} + \frac{Q}{C_o}\left(\frac{\partial \bar{Y}_i}{\partial V_s}\right)_V + \varepsilon\left(\frac{\partial \bar{X}_i}{\partial V_s}\right)_V = 0$	$\left(\frac{\partial \bar{X}_i}{\partial V}\right)_{ZV} + \left(\frac{\partial \bar{Y}_i}{\partial ZV}\right)_V = 0$
Solution phase diffusion	$\left(\frac{\partial \bar{Y}_i}{\partial t}\right)_V = \frac{C_o}{Q} \sum_{\substack{j=1 \\ j\neq i}}^{n} k_{ij}(\bar{X}_j^* - \bar{X}_j)$	$\left(\frac{\partial \bar{Y}_i}{\partial ZV}\right)_V = \frac{1}{F} \sum_{\substack{j=1 \\ j\neq i}}^{n} k_{ij}(\bar{X}_j^* - \bar{X}_j)$
Particle phase diffusion	$\left(\frac{\partial \bar{Y}_i}{\partial t}\right)_V = \frac{C_o}{Q} \sum_{\substack{j=1 \\ j\neq i}}^{n} \bar{k}_{ij}(\bar{Y}_j - \bar{Y}_j^*)$	$\left(\frac{\partial \bar{Y}_i}{\partial ZV}\right)_V = \frac{1}{F} \sum_{\substack{j=1 \\ j\neq i}}^{n} \bar{k}_{ij}(\bar{Y}_j - \bar{Y}_j^*)$
Equilibrium	$\bar{Y}_i^* = \frac{\alpha_n^i \bar{X}_i^*}{\sum_{j=1}^{n} \alpha_n^j \bar{X}_j^*}$	$\bar{Y}_i^* = \frac{\alpha_n^i \bar{X}_i^*}{\sum_{j=1}^{n} \alpha_n^j \bar{X}_j^*}$
	$\bar{X}_i^* = \frac{\alpha_i^n \bar{Y}_i^*}{\sum_{j=1}^{n} \alpha_j^n \bar{Y}_j^*}$	$\bar{X}_i^* = \frac{\alpha_i^n \bar{Y}_i^*}{\sum_{j=1}^{n} \alpha_j^n \bar{Y}_j^*}$

C_o Total solution concentration, equivalents/litre

F Solution flow rate (L^3/T)

k_{ij} Multicomponent mass transfer coefficient in solution phase (1/T)

$\bar{k}_{ij}$ Multicomponent mass transfer coefficient in particle phase (1/T)

n Total number of counter ions

Q Resin capacity, equivalents/litre of packed bed

t Time; from a first drop of solution to column (T)

V Bed volume (L^3)

$\bar{X}_i$ Normalised mean solution concentration at a bed cross section

$\bar{Y}_i$ Normalised mean concentration in resin at a bed cross section

Z Throughput ratio, $Z = (C_o/QV)(Ft-V\varepsilon)$

V_s Solution volume (L^3)

ε Voidage

α_n^i Separation factor

$*$ Denotes properties at a solution-particle interface

In which

$$R_i = \frac{1}{\bar{F}} \sum_{\substack{j=1 \\ j\neq i}}^{n} k_{ij}(\bar{X}_j^* - \bar{X}_j) \quad \text{for solution phase diffusion} \tag{4.3}$$

$$= \frac{1}{\bar{F}} \sum_{\substack{j=1 \\ j\neq i}}^{n} \bar{k}_{ij}(\bar{Y}_j - \bar{Y}_j^*) \quad \text{for particle phase diffusion} \tag{4.4}$$

The numerical method used is known as the method of characteristics, and applied to ion exchange calculations by Acrivos (1956), and later by Dranoff et al., 1958 and 1961; Clazie et al., 1968; Allen, 1973. In this method the partial differential equations are replaced by ordinary differential equations valid along characteristic lines as shown in Fig. 4.1. Therefore Equations 4.1 and 4.2 become (Allen, 1973)

For V constant

$$\frac{d\bar{Y}_i}{dZV} = R_i \qquad i = 1,.....n-1 \tag{4.5}$$

For ZV constant

$$\frac{d\bar{X}_i}{dV} = -R_i \qquad i = 1,.....n-1 \tag{4.6}$$

4.2 Initial and Boundary Conditions

Equations 4.5 and 4.6 are solved subjected to initial and boundary conditions. For a constant feed concentration and a uniform partially or completely presaturated column concentration the initial and boundary conditions are:

$$\bar{Y}_i = \bar{Y}_i^o \quad \text{for } V \geq 0 \text{ and } ZV = 0 \tag{4.7}$$

$$\bar{X}_i = \bar{X}_i^o \quad \text{for } V = 0 \text{ and } ZV \geq 0 \tag{4.8}$$

Eqn. 4.7 applies along the line ZV = 0

Eqn. 4.8 applies along the line V = 0.

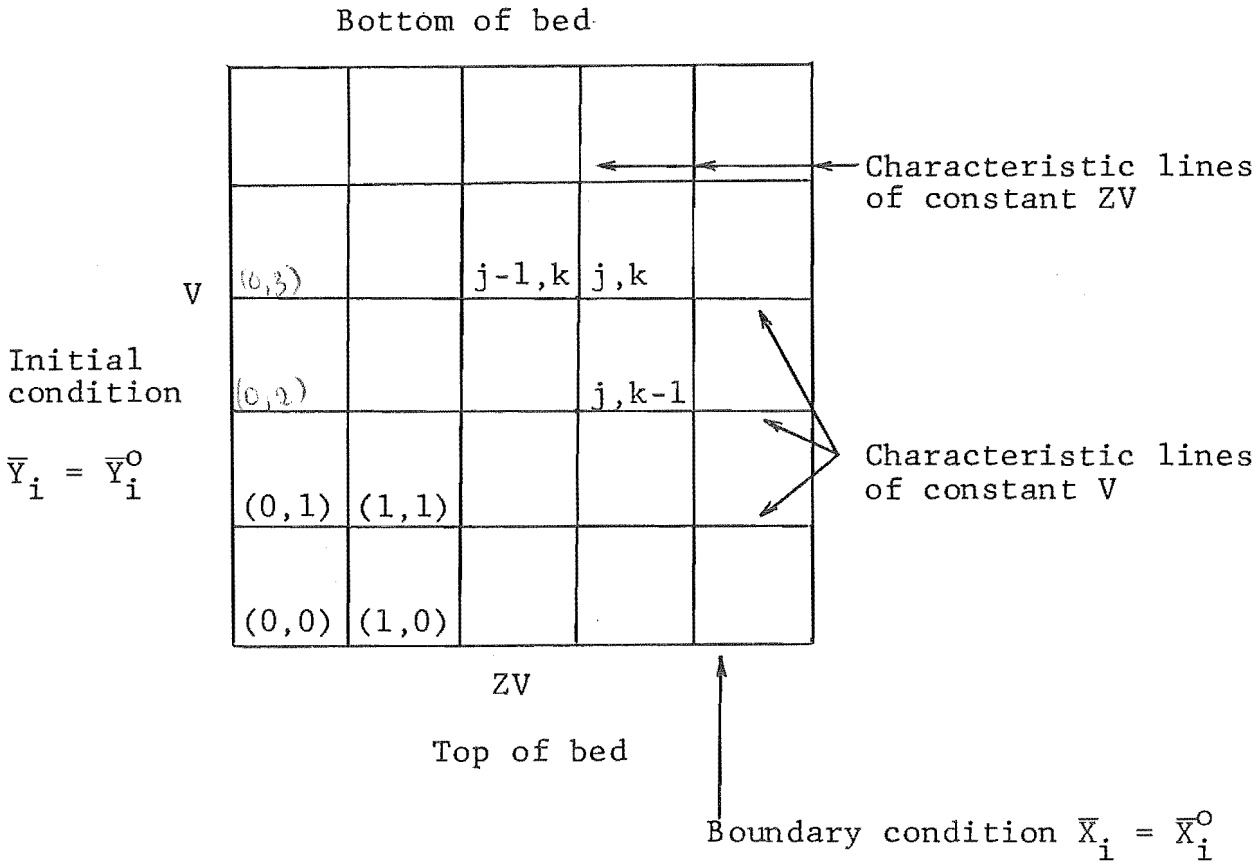

$\overline{Y}_i^o$ presaturated column normalized concentration

$\overline{X}_i^o$ feed normalized concentration

$$\sum_{i=1}^{n} \overline{Y}_i^o = 1$$

$$\sum_{i=1}^{n} \overline{X}_i^o = 1$$

Figure 4.1: Characteristic lines of the fixed-bed equations.

4.3 Calculation Procedure

Considering the characteristic lines, Figure 4.1, the lines in the V direction correspond to distance down an ion exchange column, whereas the lines in the ZV direction correspond to operation time.

The starting point of the calculation is at the point (0,1) (the values of $\bar{X}_i$ and $\bar{Y}_i$ at point (0,0) are known from initial and boundary conditions), and proceeds to points (0,2), (0,3), ... i.e. the calculation proceeds in the V direction from top of the column to the bottom of the column.

To calculate $\bar{X}_i$ and $\bar{Y}_i$ at a point (j,k) the procedure is:

- $\bar{X}_i$ is calculated from point (j, k-1), Eqn. 4.6,
- $\bar{Y}_i$ is calculated from point (j-1, k), Eqn. 4.5

4.4 Numerical Integration Technique

Having used the method of characteristics to transform the partial differential equations (PDE) to ordinary differential equations (ODE), a suitable integration technique is required to solve the ordinary differential equations.

Clazie et al. (1968) compared the following integration techniques; modified Euler, Runge-Kutta-Gill and explicit central difference. All three methods converged toward the same solution as the increments were decreased. The modified Euler method converged significantly faster than the other two and the Runge-Kutta-Gill method was the slowest.

Allen (1973) discussed various integration techniques for use in binary ion exchange calculation and suggested that the modified Euler technique was suitable.

The modified Euler integration technique is as follows: if the ODE to be solved is $\frac{dY}{dt} = f(Y,t)$, and a value of Y_j at point j is known then a value of Y_{j+1} at point j+1, which is h away from point j, is given by

$$Y_{j+1} = \frac{Y'_{j+1} + Y''_{j+1}}{2} \qquad (4.9)$$

where $Y'_{j+1} = Y_j + hf(Y_j,t)$

$$Y''_{j+1} = Y_j + hf(Y'_{j+1}, t_{j+1})$$

Figure 4.2 illustrates how the modified Euler integration technique is employed to solve values of X and Y from previously computed values.

4.5 Combined Rate Mechanism

In binary ion exchange, solution phase diffusion control (SPDC) can be distinguished from particle phase diffusion control (PPDC) by the mechanism parameter, ξ, i.e.

$\xi \to 0$ for PPDC

$\xi \to \infty$ for SPDC

In multicomponent ($n \geq 3$) systems the concept of a mechanism parameter is no longer valid since there are more than one species to be exchanged and therefore there may be more than one value of the mechanism parameter. In a multicomponent system SPDC can be distinguished from PPDC by considering the term Q/C_o.

Knowing X, Y at point (j, k-1) and (j-1, k), then to calculate X, Y at point (j, k) the procedure is:

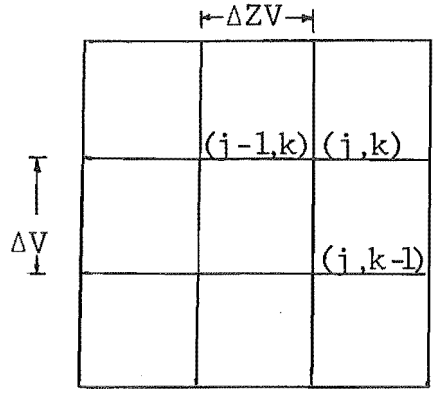

Step 1

$$X' = X(j, k-1) - R(j, k-1)\Delta V$$

$$Y' = Y(j-1, k) + R(j-1, k)\Delta ZV$$

$$R' = RATE(X', Y')$$

Step 2

$$X'' = X(j, k-1) - R'\Delta V$$

$$Y'' = Y(j-1, k) + R'\Delta ZV$$

Step 3

$$X(j, k) = (X' + X'')/2$$

$$Y(j, k) = (Y' + Y'')/2$$

$$R(j, k) = RATE\ \{X(j, k), Y(j, k)\}$$

Figure 4.2

$$\frac{Q}{C_o} \rightarrow 0 \quad \text{for PPDC}$$

$$\frac{Q}{C_o} \rightarrow \infty \quad \text{for SPDC}$$

because

$$\frac{\bar{k}_{ij}}{k_{ij}} \alpha \frac{Q}{C_o} \quad \text{(Equations 2.27 and 2.28)}$$

The concepts of SPDC and PPDC were developed to allow solutions to be derived to the ion exchange equations. In reality neither pure solution phase diffusion or pure particle phase diffusion can exist alone but only as a combined diffusion.

It is the aim of this section to develop an algorithm to compute equilibrium concentrations for the combined diffusion case.

Interfacial concentrations for combined diffusion in multicomponent ion exchange systems can be calculated by equating the SPDC rate equation to the PPDC rate equation as follows:

$$\sum_{\substack{j=1 \\ j\neq i}}^{n} k_{ij}(\bar{X}_j^* - \bar{X}_j) = \sum_{\substack{j=1 \\ j\neq i}}^{n} \bar{k}_{ij}(\bar{Y}_j - \bar{Y}_j^*) \qquad i = 1,....n-1 \qquad (4.10)$$

Eqn. 4.10 shows that there are 2n variables, i.e. $\bar{X}_1^*$, $\bar{Y}_1^*$, $\bar{X}_2^*$, $\bar{Y}_2^*$ ....$\bar{X}_n^*$, $\bar{Y}_n^*$ for n-1 equations, therefore n + 1 equations are required. The supplementary equations are

$$\alpha_n^j = \frac{\bar{Y}_j^* \bar{X}_n^*}{\bar{X}_j^* \bar{Y}_n^*}, \quad j = 1, 2, 3, ...n-1 \qquad (4.11)$$

$$\sum_{j=1}^{n} \bar{X}_j^* = 1 \qquad (4.12)$$

$$\sum_{j=1}^{n} \bar{Y}_j^* = 1 \qquad (4.13)$$

Equations 4.10 - 4.13 can be solved for $\bar{X}_j^*$, $\bar{Y}_j^*$, j = 1,2...n. For binary exchange (n=2) Equations 4.10-4.13 reduce to:

$$k_{12}(\bar{X}_1 - \bar{X}_1^*) = \bar{k}_{12}(\bar{Y}_1^* - \bar{Y}_1) \tag{4.14}$$

$$\alpha_2^1 = \frac{\bar{Y}_1^* \bar{X}_2^*}{\bar{X}_1^* \bar{Y}_2^*} \tag{4.15}$$

$$\bar{X}_1^* + \bar{X}_2^* = 1 \tag{4.16}$$

$$\bar{Y}_1^* + \bar{Y}_2^* = 1 \tag{4.17}$$

Equations 4.14-4.17 are solved for $\bar{Y}_1^*$ to give

$$\bar{Y}_1^{*2} + g\,\bar{Y}_1^* + \ell = 0 \tag{4.18}$$

where

$$g = -\left[\frac{1 + d\alpha_2^1}{d(\alpha_2^1 - 1)} + \frac{\bar{X}_1 + d\bar{Y}_1}{d}\right]$$

$$\ell = \frac{\alpha_2^1(X_1 + dY_1)}{d(\alpha_2^1 - 1)}$$

$$d = \frac{\bar{k}_{12}}{k_{12}}$$

The root of the quadratic, Eqn. 4.18, is chosen to meet the requirement that $0.0 \leq \bar{Y}_1^* \leq 1.0$.

For a ternary system (n=3), Equations 4.10 - 4.13 reduce to

$$k_{12}(\bar{X}_2^* - \bar{X}_2) + k_{13}(\bar{X}_3^* - \bar{X}_3) = \bar{k}_{12}(\bar{Y}_2 - \bar{Y}_2^*) + \bar{k}_{13}(\bar{Y}_3 - \bar{Y}_3^*) \tag{4.19}$$

$$k_{21}(\bar{X}_1^* - \bar{X}_1) + k_{23}(\bar{X}_3^* - \bar{X}_3) = \bar{k}_{21}(\bar{Y}_1 - \bar{Y}_1^*) + \bar{k}_{23}(\bar{Y}_3 - \bar{Y}_3^*) \tag{4.20}$$

$$\bar{X}_1^* = \frac{\alpha_1^3 \bar{Y}_1^*}{\sum_{i=1}^{3} \alpha_i^3 \bar{Y}_i^*} \tag{4.21}$$

$$\bar{X}_2^* = \frac{\alpha_2^3 \bar{Y}_2^*}{\sum_{i=1}^{3} \alpha_i^3 \bar{Y}_i^*} \tag{4.22}$$

$$\bar{X}_1^* + \bar{X}_2^* + \bar{X}_3^* = 1 \tag{4.23}$$

$$\bar{Y}_1^* + \bar{Y}_2^* + \bar{Y}_3^* = 1 \tag{4.24}$$

Equations 4.19 - 4.24 can be solved for $\bar{X}_1^*$, $\bar{X}_2^*$, $\bar{X}_3^*$, $\bar{Y}_1^*$, $\bar{Y}_2^*$, $\bar{Y}_3^*$ as follows:

Step 1 Estimate $\bar{Y}_1^*$ and $\bar{Y}_2^*$; if the grid point (Figure 4.1) is at the top of the bed or the beginning of a new value of ZV, the estimation is done by

$$\bar{Y}_j^* = \frac{\alpha_3^j \bar{X}_j}{\sum_{i=1}^{3} \alpha_3^i \bar{X}_i^*}$$

otherwise the values were taken as those of the previous point.

Step 2 $\bar{Y}_3^*$ is calculated by Eqn. 4.24.

Step 3 $\bar{X}_1^*$, $\bar{X}_2^*$, and $\bar{X}_3^*$ are calculated from Eqns. 4.21-4.23.

Step 4 $\bar{Y}_1^*$, $\bar{Y}_2^*$, and $\bar{Y}_3^*$ are calculated from Eqns. 4.19, 4.20 and 4.24.

Step 5 Test for convergence; compare new values of $\bar{X}_1^*$ and $\bar{X}_2^*$ to their previous values; if the absolute differences are greater than EPSIL (Appendix 4A) go back to Step 3, otherwise the convergence is reached.

It was found that the number of iterations before convergence was about five.

4.6 The Computer Program

Figure 4.3 shows a simplified flow diagram of the digital program developed to compute breakthrough curves from a multi-component fixed-bed ion exchange column. The program is called "GPFIXC" (generalized program for fixed-bed ion exchange columns). A user guide is presented in Appendix 4A. The Fortran listing and sample outputs are shown in Appendices 4B and 4C respectively. The detail of the computer program is shown in Table 4.2.

Routine	Function
MAIN	To organize a breakthrough curve calculation
READ	To read input data
INITL	To set up initial data
DIFFSN	To calculate particle phase self-diffusion coefficients
TITLE	To print heading and input data
VARVOL	To calculate instantaneous bed volume and particle diameter
SELFMT	To calculate parameters for mass transfer coefficient calculations
NERNPL	To calculate mass transfer coefficients
EQUILB	To calculate equilibrium concentrations for a single rate mechanism
VARSEP	To calculate separation factor by linear interpolation method
MIXDIF	To calculate equilibrium concentrations for combined rate mechanism
RATE	To calculate the rate terms
SOLVE	To calculate $\overline{X}_1$ and $\overline{Y}_1$
STEPZV	To increment ZV
OUTPUT	To print output data

Table 4.2: Detail of GPFIXC

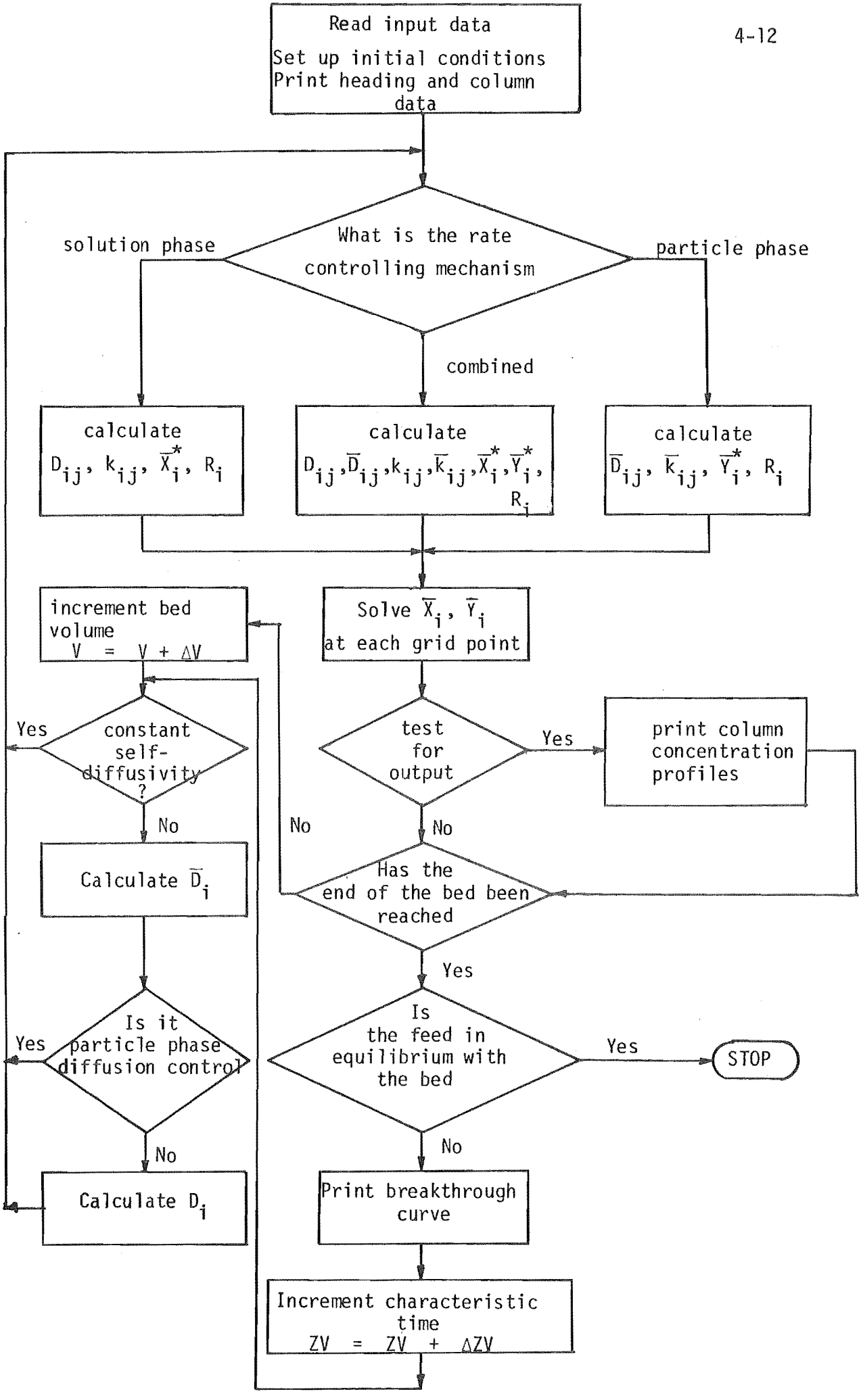

Figure 4.3: Simplified flow diagram of GPFIXC

4.7 Program Verification

This section verifies the numerical method and the numerical integration technique by comparing computed breakthrough curves, generated by GPFIXC, with binary analytical results (J function) and established binary results (Allen, 1973).

The J function solution was derived by Thomas for general expression of binary ion exchange equations with linear equilibrium (Allen, 1973).

Tables 4.3-4.4 show comparisons of GPFIXC results with J functions. The J functions were obtained from Sherwood et al. (1975). Results calculated using the solution phase diffusion model are the same as that from the particle phase diffusion model for the same number of transfer units because for linear equilibrium the rate equations of both models are the same.

Tables 4.5-4.6 show comparisons of GPFIXC results with Allen's results for nonlinear equilibrium cases.

The agreement of GPFIXC results with J functions and Allen's results are clearly shown.

Although binary results were used in the comparison, the verification should also be valid for multicomponent systems since the numerical method and the numerical integration technique, not the equations of the model, were tested.

ΔV (ml) ΔZV(ml)	GPFIXC 1.0 1.0	 2.0 2.0	 4.0 4.0	 10.0 10.0	J Function
Z					
0.2	.0105	.0105	.0105	.0193	.0105
0.4	.0665	.0665	.0669	.0898	.0665
0.6	.1895	.1895	.1901	.2272	.1894
0.8	.3621	.3622	.3625	.4073	.3621
1.0	.5449	.5449	.5449	.5881	.5449
1.2	.7035	.7034	.7032	.7383	.7035
1.4	.8220	.8219	.8216	.8463	.8219
1.6	.9007	.9005	.9002	.9157	.9005
1.8	.9481	.9479	.9477	.9564	.9479
2.0	.9746	.9743	.9741	.9786	.9742
2.2	.9884	.9881	.9879	.9900	.9879
2.4	.9953	.9948	.9946	.9955	.9945
N = 10, $\alpha_2^1 = 1$, $\xi = 0, \infty$					

ΔV (ml) ΔZV(ml)	GPFIXC 0.5 0.5	 1.0 1.0	 2.0 2.0	 4.0 4.0	J Function
Z					
0.5	.0019	.0019	.0024		.0021
0.6	.0139	.0139	.0164	U	.0140
0.7	.0571	.0572	.0641	N	.0573
0.8	.1580	.1581	.1714	S	.1580
0.9	.3222	.3222	.3409	T	.3221
1.0	.5200	.5200	.5398	A	.5200
1.1	.7044	.7043	.7208	B	.7044
1.2	.8420	.8418	.8529	L	.8419
1.3	.9265	.9263	.9324	E	.9263
1.4	.9702	.9699	.9727		.9698
1.5	.9896	.9893	.9902		.9891
1.6	.9972	.9967	.9969		.9965
N = 50, $\alpha_2^1 = 1$, $\xi = 0, \infty$					

Table 4.3: Comparison of GPFIXC results with corresponding J functions.

ΔV (ml) ΔZV(ml)	GPFIXC 1.0 1.0	 2.0 2.0	 4.0 4.0	 10.0 10.0	J Function
Z					
0.2	.0656	.0657	.0658	.0672	.0656
0.4	.1686	.1687	.1689	.1710	.1686
0.6	.2982	.2983	.2985	.3003	.2982
0.8	.4351	.4351	.4352	.4362	.4351
1.0	.5639	.5639	.5639	.5640	.5639
1.2	.6755	.6755	.6754	.6749	.6756
1.4	.7663	.7663	.7662	.7652	.7663
1.6	.8365	.8364	.8363	.8352	.8365
2.0	.9258	.9256	.9255	.9247	.9256
2.2	.9517	.9515	.9514	.9507	.9514
2.6	.9810	.9806	.9804	.9800	.9804
3.0	.9936	.9929	.9927	.9924	.9926
Max. conv. error	.0010	.0003	.0003	.0021	
Computation time (sec.)	99	36	9	2	
N = 10, α_2^1 = 1.0, ξ = 1.0					

ΔV (ml) ΔZV(ml)	GPFIXC 0.5 0.5	 1.0 1.0	 2.0 2.0	 4.0 4.0	J Function
Z					
0.52	.0294	.0294	.0295	.0364	.0295
0.60	.0651	.0651	.0653	.0769	.0651
0.72	.1601	.1602	.1604	.1802	.1601
0.80	.2510	.2510	.2513	.2757	.2510
0.92	.4144	.4144	.4145	.4427	.4144
1.00	.5283	.5283	.5283	.5561	.5283
1.12	.6849	.6848	.6846	.7084	.6848
1.20	.7713	.7711	.7709	.7906	.7712
1.32	.8687	.8685	.8682	.8815	.8685
1.40	.9135	.9133	.9130	.9225	.9132
1.60	.9742	.9738	.9736	.9769	.9736
1.80	.9944	.9938	.9935	.9943	.9934
Max. conv. error	.0010	.0004	.0003	.0278	
Computation time (secs)	220	50	14	5	
N = 50, α_2^1 = 1.0, ξ = 1.0					

Table 4.4: Comparison of GPFIXC results with corresponding J functions.

GPFIXC						Allen Results
Sep. fact.=0.8		Sep. fact.= 2		Sep. fact.= 10		
Z	X	Z	X	Z	X	
0.20	.0264	.59	.0253	.86	.0250	.0245
0.37	.0965	.71	.0914	.89	.1180	.0955
0.54	.2060	.81	.2123	.91	.2166	.2061
0.72	.3437	.89	.3498	.94	.3692	.3455
0.92	.4979	.97	.4987	.97	.5043	.5000
1.15	.6544	1.06	.6496	1.01	.6449	.6545
1.42	.7953	1.17	.7882	1.07	.7890	.7939
1.75	.9049	1.33	.9060	1.16	.9052	.9045
2.23	.9760	1.59	.9778	1.31	.9757	.9755
3.20	1.0000	2.16	1.0000	1.70	1.0000	1.0000
N = 10 particle phase diffusion control						

GPFIXC						Allen Results
Sep. fact.=0.8		Sep. fact.= 2		Sept. fact.= 10		
Z	X	Z	X	Z	X	
0.23	.0250	.46	.0250	.69	.0250	.0245
0.39	.0957	.67	.0950	.84	.0956	.0955
0.55	.2098	.82	.2110	.93	.2118	.2061
0.71	.3436	.93	.3500	.99	.3559	.3455
0.90	.4987	1.02	.4980	1.03	.4975	.5000
1.12	.6510	1.11	.6598	1.06	.6315	.6545
1.40	.7933	1.19	.7900	1.09	.7840	.7939
1.76	.9043	1.29	.9043	1.12	.9240	.9045
2.31	.9762	1.44	.9777	1.14	.9777	.9755
3.45	1.000	1.75	.9999	1.15	.9896	1.0000
N = 10 solution phase diffusion control						

Table 4.5: Comparison of GPFIXC results with Allen's results.

GPFIXC						Allen results
Sep. factor=0.8		Sep. factor=2.0		Sep. factor=10		
Z	X	Z	X	Z	X	
.00		.25	.0251	.59	.0235	.0245
.20	.0935	.48	.0935	.76	.0922	.0955
.39	.2075	.67	.2065	.86	.1955	.2061
.60	.3456	.83	.3461	.94	.3511	.3455
.85	.5006	.98	.4998	1.00	.5008	.5000
1.15	.6549	1.13	.6500	1.06	.6504	.6545
1.52	.7927	1.31	.7943	1.13	.7856	.7939
2.02	.9043	1.53	.9040	1.24	.9090	.9045
2.79	.9759	1.90	.9776	1.41	.9776	.9755
4.50	1.0000	2.71	1.0000	1.82	1.0000	1.0000
N = 10 combined diffusion						

GPFIXC						Allen results
Sep. factor=0.8		Sep. factor=2.0		Sep. factor=10		
Z	X	Z	X	Z	X	
.406	.0247	.786	.0252	.918	0.0261	.0245
.548	.0955	.868	.0945	.952	0.0967	.0955
.676	.2051	.922	.2073	.972	.2032	.2061
.810	.3462	.962	.3418	.988	.3513	.3455
.952	.4990	1.000	.5001	1.000	.4976	.5000
1.114	.6545	1.036	.6509	1.012	.6461	.6545
1.3	.7938	1.078	.7936	1.026	.7831	.7939
1.526	.9044	1.130	.9037	1.048	.9070	.9045
1.84	.9757	1.216	.9763	1.082	.9765	.9755
2.432	1.0000	1.42	.9998	1.164	.9994	1.0000
N = 50 combined diffusion						

Table 4.6: Comparison of GPFIXC results with Allen's results.

4.8 Step Size Selection

Step size selection depends on:

(a) Accuracy: as step size decreases, computed results should tend to become equal to analytical results. This implies that, for the purpose of accuracy, step sizes should be made as small as possible.

(b) Rounding error: consider a column solution phase concentration profile. Then as the bed approaches saturation, $\frac{dX}{dV}$ tends to zero. This causes the difference between the new rate term and the previous one to be very small. Thus as step sizes are decreased, the rounding error becomes significant.

(c) Computation time: computing times decrease as step sizes increase. This suggests that, for economy, step sizes should be made as large as possible provided that stability is maintained and within needed accuracy.

Table 4.4 illustrates the above points.

The following points are noted in studying the effect of step sizes in binary systems.

(1) By defining the convergence error to be |GPFIXC result - analytical results| the maximum convergence error for linear equilibrium case at $\Delta V = \Delta ZV = 2$ are tabulated below.

N	Mechanism parameter	Maximum convergence error
10	0, ∞	0.0003
10	1	0.0003
50	0, ∞	0.0198
50	1	0.0003

(2) For the same value of step size the accuracy for unfavourable is better than favourable ion exchange.

(3) For the same value of step size the accuracy for low number of transfer units is better than for high number of transfer units.

Thus step size selection also depends on the system variables such as separation factor, mass transfer coefficient, bed volume, solution flow rate etc. There is no definite value of step size, their values vary from system to system.

Allen (Section 5.5) suggested a value of $\Delta N = 0.25$ for a system with a value of separation factor less than five. At higher separation factor $\Delta N = 0.125$ was suggested.

The value recommended by Allen is based on the number of transfer units which takes system variables into account. The corresponding ΔV is given by

$$\Delta V = \frac{F}{k} \Delta N = \frac{.25F}{k}$$

It has been found that the range of ΔV employed in this work agreed with the value given by Allen.

4.9 Comparison with Experimental Results

The numerical method and the numerical integration technique have been verified in Section 4.7. The equation of the model should also be verified. Chapter 7 compares computed breakthrough curves with experimental results.

4.10 Conclusion

A computer program has been developed to compute breakthrough curves for multicomponent fixed-bed ion exchange columns.

The numerical method and the method of solution have been verified by comparing GPFIXC results with J functions for linear

equilibrium and with Allen results for non-linear equilibrium. Good agreement was obtained.

APPENDIX 4A

USER GUIDE TO GPFIXC

4A.1 Input Data Symbols

AO(I)-A3(I)	Parameters for computing equivalent conductivity at infinite dilution for counter ion i (section 6.3)
ALPHA (I,N)	Separation factor of counter ion i relative to counter ion n
ATOMWT(I)	Atomic weight of counter ion i
C	Total solution phase concentration, equivalents/ℓ
DELV	Increment in bed volume (V), mls
DELZV	Increment in characteristic time (ZV), mls
DIAP	Particle diameter in Hydrogen form in water, cm
DIACOL	Column diameter, cm
DPARI(I)	Particle phase self-diffusion coefficient of counter ion i, sq.cm/sec.
DSOLI(I)	Solution phase self-diffusion coefficient of counter ion i, sq.cm/sec.
EPSIL	Required computational accuracy for X_i and Y_i
FEED	Solution flow rate, ml/sec.
INV	Print interval in V direction, ml
INZV	Print interval in ZV direction, ml
IPRINT	Output option
MDDFSN	Self-diffusion coefficient option
MDMTCF	Solution phase mass transfer coefficient option
MDRATE	Rate mechanism option
MDSEPF	Separation factor option
NAME	Name of counter ions
N	Number of counter ions
Q	Ion exchange capacity, equivalents/ℓ of packed bed

SEPFAC(I,NP) Separation factor of counter ion i at $\bar{X}_i^*$ equals 0.05(NP-1), where NP is the equally space points ranging from 1 to 21, for a binary system, for example

SEPFAC(1,5) = α_2^1 at $\bar{X}_1^*$ equals 0.2

SEP3(I,J,NP) Separation factor of counter ion i at $\bar{X}_i^*$ equals 0.1(NP-1) and $\bar{X}_{3-i}^*$ equals 0.1(J-1) where NP and J are the equally space points both ranging from 1 to 11, for a ternary system, for example

SEP3(1,1,5) = α_3^1 at $\bar{X}_1^*$ equals 0.4 and $\bar{X}_2^*$ equals 0.0

SEP3(1,3,11) = α_3^1 at $\bar{X}_1^*$ equals 1.0 and $\bar{X}_2^*$ equals 0.2

SEP3(2,5,7) = α_3^2 at $\bar{X}_2^*$ equals 0.6 and $\bar{X}_1^*$ equals 0.4

SEP3(3,J,NP) = α_3^3 = 1

XPZM(I) Normalized feed concentration of counter ion i

XPZN(I) Solution phase normalized concentration at equilibrium with presaturated particle phase normalized concentration

YPZN(I) Presaturated particle phase normalized concentration

VSTART Bed volume at the start of a run, mls

VSTOP Bed volume at final saturation, mls

VOLHW Bed volume in Hydrogen form in water, mls

VOLO(I) Bed volume in counter ion i form in its own solution, mls

VOLIW(I) Bed volume in counter ion i form in water, mls

VOID Voidage

4A.2 Specifying Input Data Option

MDDFSN
- 1 Constant self-diffusion coefficients supplied by user
- 2 Constant self-diffusion coefficients model
- 3 Variable self-diffusion coefficients model

MDRATE	-VE	Particle phase diffusion control
	0	Combined phase diffusion control
	+VE	Solution phase diffusion control
IPRINT	1	Print breakthrough curve only
	2	Print breakthrough curve and column profiles
MDSEPF	1	Constant separation factor
	2	Variable separation factor
MDMTCF	1	Hiester relation
	2	Kataoka relation
EPSIL	The normal range is 0.00001 to 0.001	

APPENDIX 4B

PROGRAM LISTING - GPFIXC

```
                                                                I X
                                                                = =

$ SET $ NEW SEQ
$ SET LONG
C

      REAL   KPAR, KSOL
      COMMON   /A/   KPAR(3,3),KSOL(3,3),PDC, SPDC, SP
      COMMON   /B/   X(3), Y(3),VALENC(3)
      COMMON   /C/   XPZM(3), XPZN(3), YPZM(3), YPZN(3)
      COMMON   /D/   ALPHA(3,3), YSTAR(3), XSTAR(3)
      COMMON   /E/   RSAVE(2,4000)
      COMMON   /F/   R(3)
      COMMON   /G/   YSAVE(2,4000)
      COMMON   /H/   N, FEED, MDDFSN, MDRATE,NSUB1,  MDMIXD
      COMMON   /I/   DELV, DELZV, K, KMAX, KEND, NFLAG
      COMMON   /J/   JPRINT, KPRINT, INZV, INV, IPRINT
      COMMON   /K/   DPARI(3), DSOLI(3), DSOLI0(3), DPAR(3,3), DSOL(3,3)
      COMMON   /L/   KINT, KSTART, ITEST, EPSIL
      COMMON   /M/   J, IJK
      COMMON   /N/   TEMP, DIACOL, Q, C, VOID, VOLHW, DIAP
      COMMON   /O/   ATOMWT(3), CONDUC(3), B(3)
      COMMON   /P/   VOLX, DIAX, MDMTCF,VS, EQBED
      COMMON   /Q/   X0(3), X1(3),  Y1(3)
      COMMON   /R/   SEPFAC(3,21), MDSEPF , SEP3(3,11,11)
      COMMON   /S/   NAME(3)
      COMMON   /T/   VOL0(3), A0(3), A1(3), A2(3), A3(3)
      COMMON   /U/   VSTART, VSTOP, VOLIW(3)
      DIMENSION   XS(3,2000), Z(2000)
C
C     READ INPUT DATA
C     .........
 1000 READ(5,1,END=1001) N

      CALL READ
    1 FORMAT(I2)
C     .........
C     SET UP INITIAL CONDITION & INITIAL CALCULATION
C     ..........
      CALL INITL
C     ..........
C     PRINT INPUT DATA
C     ..........
      CALL TITLE
C     ..........
      L = 0
C
C     COMPUTATION BEGINS
C     ...........
  500 CALL NERNPL
      CALL EQUILB
      CALL RATE
 5000 CALL SOLVE
C     ..........
      IF(K.GT.KMAX) GO TO 3200
      IF(K.NE.KMAX) GO TO 6200
      IF(JPRINT.LT.INZV) GO TO 6200
```

```
C
C
C     STORE THE BREAK-THROUGH CURVES
C
      L = L+1
      GRIDV = K-1
      GRIDZV = J-1
      V = GRIDV*DELV
      ZV = GRIDZV*DELZV
      Z(L) = ZV/V
      DO 6100 I = 1,N
      XS(I,L) = X(I)
 6100 CONTINUE
      WRITE(6,5200) Z(L),X(1),X(2),X(3)

 6200 IF(IPRINT.LE.1) GO TO 6300
      IF(KPRINT.LT.INV) GO TO 6300
      KPRINT = 0
      IF(JPRINT.LT.INZV) GO TO 6300
C     ............
      CALL OUTPUT
C     ............
 6300 CONTINUE
      GO TO (1100,1200,2100), ITEST
 1100 ITEST = 2
      GO TO 2400
C
C     TEST FOR :M: PLATEAU ZONE
C
 1200 DO 1300 I =1,NSUB1
      XX = ABS(X(I)-XPZM(I))
      IF(XX.LE.EPSIL) GO TO 1300
      IF(I.EQ.1) GO TO 2300
      GO TO 2400
 1300 CONTINUE
      KSTART = K
      GO TO 2400
C
C     TEST FOR :N: PLATEAU ZONE
C
 2100 DO 2200 I =1,NSUB1
      XX = ABS(X(I)-XPZN(I))
      IF(XX.GT.EPSIL) GO TO 2400
 2200 CONTINUE
      GO TO 3500
 2300 ITEST = 3
 2400 IF(K-KMAX) 2500,2500,3200
 2500 K = K+1
      KPRINT = KPRINT + 1
      NFLAG = 0
      IJK = J
      GO TO 500
 3200 IF(KSTART - KMAX) 3500,3300,3300
 3300 IF(IJK.LT.0) GO TO 4400
      WRITE(6,6003)
 6003 FORMAT(1H1//)
      WRITE(6,3400)
 3400 FORMAT(1H ,30X,"THE ENTIRE COLUMN IS IN EQUILIBRIUM WITH THE FEED"
     1/)
      WRITE(6,5100)
      DO 5300 J = 1, L
      WRITE(6,5200)       Z(J),(XS(I,J),I=1,3)
 5300 CONTINUE
```

```
C
 5100 FORMAT(27X,"THROUGHPUT RATIO",6X,"X(1)",4X,"X(2)",4X,"X(3)"/)
 5200 FORMAT(1H ,30X,F7.4,10X,3(F6.4,2X))
      GO TO 4400
C
C     MOVE TO J+1 GRID
C
C     ............
 3500 CALL STEPZV
C     ............
      GO TO 5000
 4400 GO TO 1000
 1001 CONTINUE
      STOP
      END
```

```
C
C
      SUBROUTINE     READ
C
C
      COMMON    /B/   X(3), Y(3),VALENC(3)
      COMMON    /C/   XPZM(3), XPZN(3), YPZM(3), YPZN(3)
      COMMON    /D/   ALPHA(3,3), YSTAR(3), XSTAR(3)
      COMMON    /H/   N, FEED, MDDFSN, MDRATE,NSUB1,  MDMIXD
      COMMON    /I/   DELV, DELZV, K, KMAX, KEND, NFLAG
      COMMON    /J/   JPRINT, KPRINT, INZV, INV, IPRINT
      COMMON    /K/   DPARI(3), DSOLI(3), DSOLI0(3), DPAR(3,3), DSOL(3,3)
      COMMON    /L/   KINT, KSTART, ITEST, EPSIL
      COMMON    /N/   TEMP, DIACOL, Q, C, VOID, VOLHW, DIAP
      COMMON    /O/   ATOMWT(3), CONDUC(3), B(3)
      COMMON    /P/   VOLX, DIAX, MDMTCF,VS, EQBED
      COMMON    /R/   SEPFAC(3,21), MDSEPF , SEP3(3,11,11)
      COMMON    /S/   NAME(3)
      COMMON    /T/    VOL0(3), A0(3), A1(3), A2(3), A3(3)
      COMMON    /U/   VSTART, VSTOP, VOLIW(3)
C
      M=N-1
      READ(5,9)  (NAME(I),I=1,N)
      READ(5,3) MDDFSN, INV, INZV, MDRATE, IPRINT, MDSEPF, MDMTCF,MDMIXD
      READ(5,5) DELV, DELZV, EPSIL
      READ(5,5) TEMP,DIACOL,Q,C,VOID,VOLHW,DIAP,FEED
      READ(5,5)   (XPZM(I), I=1,N)
      READ(5,5)   (YPZN(I), I=1,N)
      READ(5,5)   (XPZN(I), I=1,N)
      READ(5,5)  (DPARI(I), I=1,N)
      READ(5,5)  (DSOLI(I), I=1,N)
      READ(5,5)  (ATOMWT(I),I=1,N)
      READ(5,6)  (VALENC(I),I=1,N)
      GO TO (10,20),MDSEPF
   10 READ(5,5)   (ALPHA(I,N), I=1,N)
      GO TO 30
   20 IF(N.NE.2) GO TO 70
      DO 40 I=1,M
      READ(5,7) (SEPFAC(I,NP),NP=1,21)
   40 CONTINUE
      GO TO 30
   70 DO 80 I=1,M
      DO 80 J=1,11
      READ(5,77) (SEP3(I,J,NP),NP=1,11)
   80 CONTINUE
   30 DO 50 I=1,N
      READ(5,8) A0(I),A1(I),A2(I),A3(I)
   50 CONTINUE
      DO 60 I=1,N
      READ(5,5) VOL0(I), VOLIW(I)
   60 CONTINUE
      READ(5,5) VSTART, VSTOP
    3 FORMAT(8I5)
    5 FORMAT(8F10.4)
    6 FORMAT(3F2.0)
    7 FORMAT(16F5.3)
    8 FORMAT(4F20.0)
    9 FORMAT(3A2)
   77 FORMAT(11F5.0)
      RETURN
      END
```

```
C
C
      SUBROUTINE     INITL
C
C
      REAL   KPAR, KSOL
      COMMON    /A/   KPAR(3,3),KSOL(3,3),PDC, SPDC, SP
      COMMON    /B/   X(3), Y(3),VALENC(3)
      COMMON    /C/   XPZM(3), XPZN(3), YPZM(3), YPZN(3)
      COMMON    /D/   ALPHA(3,3), YSTAR(3), XSTAR(3)
      COMMON    /H/   N, FEED, MDDFSN, MDRATE,NSUB1,  MDMIXD
      COMMON    /I/   DELV, DELZV, K, KMAX, KEND, NFLAG
      COMMON    /J/   JPRINT, KPRINT, INZV, INV, IPRINT
      COMMON    /K/   DPARI(3), DSOLI(3), DSOLI0(3), DPAR(3,3), DSOL(3,3)
      COMMON    /L/   KINT, KSTART, ITEST, EPSIL
      COMMON    /M/   J, IJK
      COMMON    /N/   TEMP, DIACOL, Q, C, VOID, VOLHW, DIAP
      COMMON    /O/   ATOMWT(3), CONDUC(3), B(3)
      COMMON    /P/   VOLX, DIAX, MDMTCF,VS, EQBED
      COMMON    /R/   SEPFAC(3,21), MDSEPF , SEP3(3,11,11)
      COMMON    /T/    VOL0(3), A0(3), A1(3), A2(3), A3(3)
      COMMON    /U/   VSTART, VSTOP, VOLIW(3)
C
      J=1
      IJK = 0
      K = 2
      JPRINT = INZV
      KPRINT = 1
      KINT = INV
      KSTART = 1
      ITEST = 2
      KEND = 0
      NFLAG = 0
      ALPHA(N,N) = 1.0
      AREA = (22./7.)*(DIACOL*DIACOL)/4.
      VS = FEED/AREA
      TEMP=TEMP+273.15
      EQBED = Q*VOLHW
      V = (VSTART+VSTOP)/2.0
      Q = EQBED/V
      KMAX = V/DELV + 1.1
      NSUB1 = N-1
C
C     COMPUTE EQUIVALENT CONDUCTIVITY AT INFINITE DILUTION
C
      DELT = TEMP-298.15
      DO 10 I=1,N
      Y1 = A1(I)*DELT
      Y2 = A2(I)*DELT*DELT
      Y3 = A3(I)*DELT*DELT*DELT
      CONDUC(I) = A0(I)+Y1+Y2+Y3
   10 CONTINUE
      DO 8000 I=1,N
      X(I) = XPZM(I)
      Y(I) = YPZN(I)
 8000 CONTINUE
      JJ = MDRATE
      MDRATE = -5
C     ...........
      CALL EQUILB
C     ...........
      DO 222 I = 1,N
      YPZM(I) = YSTAR(I)
```

```
$ SET PAGE
C
C
  222 CONTINUE
      MDRATE = JJ
C     MDDFSN=1 : DIFFUSION COEFFICIENTS ARE GIVEN
C     MDDFSN=2 : DIFFUSION COEFFICIENTS ARE COMPUTED
C                CONSTANT SELF DIFFUSIVITY MODEL
C     MDDFSN=3 : DIFFUSION COEFFICIENTS ARE COMPUTED
C                VARIABLE SELF DIFFUSIVITY MODEL
C
      GO TO (111,1150,1150),MDDFSN
C
C     CALCULATE INFINITE DILUTION CONCENTRATION DIFFUSIVITY
C
 1150 DO 1250 I=1,N
      F1 = TEMP*CONDUC(I)/VALENC(I)
      DSOLI0(I) = 0.0089257lE-07*F1
 1250 CONTINUE
C
      GO TO (111,1450,400),MDDFSN
 1450 SUM1 = 0.0
      SUM2 = 0.0
      DO 1550 I=1,N
      SUM1 = SUM1 + VOLIW(I)*YPZM(I)
      SUM2 = SUM2 + VOLIW(I)*YPZN(I)
 1550 CONTINUE
      VOLX = (SUM1+SUM2)/2.0
C     ............
      CALL DIFFSN
C     ............
      DO 1350 I=1,N
      B(I) = DPARI(I)/DSOLI0(I)
 1350 CONTINUE
      SUM1 = 0.0
      SUM2 = 0.0
      DO 1650 I=1,N
      SUM1 = SUM1 + VOL0(I)*YPZM(I)
      SUM2 = SUM2 + VOL0(I)*YPZN(I)
 1650 CONTINUE
      VOLX = (SUM1+SUM2)/2.0
C     ............
      CALL DIFFSN
  111 P = (V/VOLHW)**(1./3.)
      DDD = DIAP
      DIAP = DIAP*P
      CALL SELFMT
C     ............
      DIAP = DDD
  400 CONTINUE
      RETURN
      END
```

```
C
C
      SUBROUTINE     DIFFSN
C
C
      COMMON    /B/    X(3), Y(3),VALENC(3)
      COMMON    /H/    N, FEED, MDDFSN, MDRATE,NSUB1,  MDMIXD
      COMMON    /K/    DPARI(3), DSOLI(3), DSOLI0(3), DPAR(3,3), DSOL(3,3
      COMMON    /N/    TEMP, DIACOL, Q, C, VOID, VOLHW, DIAP
      COMMON    /O/    ATOMWT(3), CONDUC(3), B(3)
      COMMON    /P/    VOLX, DIAX, MDMTCF,VS, EQBED
      COMMON    /T/     VOL0(3), A0(3), A1(3), A2(3), A3(3)
      COMMON    /U/    VSTART, VSTOP, VOLIW(3)
C
      P = VOLHW/VOLX
      DO 999 I=1,N
      P6 = -(1.392*VALENC(I)*P)
      DPARI(I) = 0.55*EXP(P6)*DSOLI0(I)
  999 CONTINUE
      RETURN
      END
```

```
C
C
      SUBROUTINE     VARVOL
C
C
      COMMON    /B/   X(3), Y(3),VALENC(3)
      COMMON    /H/   N, FEED, MDDFSN, MDRATE,NSUBl,  MDMIXD
      COMMON    /N/   TEMP, DIACOL, Q, C, VOID, VOLHW, DIAP
      COMMON    /P/   VOLX, DIAX, MDMTCF,VS, EQBED
      COMMON    /T/    VOL0(3), A0(3), Al(3), A2(3), A3(3)
      COMMON    /U/   VSTART, VSTOP, VOLIW(3)
C
C     COMPUTE BED VOLUME
C
      SUM=0.0
      DO 100 I=l,N
      SUM = SUM + VOL0(I)*Y(I)
  100 CONTINUE
      VOLX = SUM
C
C     COMPUTE RESIN DIAMETER
C
      P=(VOLX/VOLHW)**(1./3.)
      DIAX=DIAP*P
C
C     COMPUTE BED CAPACITY
C
      Q = EQBED/VOLX
      RETURN
      END
```

```
      SUBROUTINE     TITLE
C
C
      REAL    KPAR, KSOL
      REAL      KPARI, KSOLI
      COMMON    /A/    KPAR(3,3),KSOL(3,3),PDC, SPDC, SP
      COMMON    /C/    XPZM(3), XPZN(3), YPZM(3), YPZN(3)
      COMMON    /D/    ALPHA(3,3), YSTAR(3), XSTAR(3)
      COMMON    /H/    N, FEED, MDDFSN, MDRATE,NSUB1,  MDMIXD
      COMMON    /I/    DELV, DELZV, K, KMAX, KEND, NFLAG
      COMMON    /K/    DPARI(3), DSOLI(3), DSOLI0(3), DPAR(3,3), DSOL(3,3
      COMMON    /N/    TEMP, DIACOL, Q, C, VOID, VOLHW, DIAP
      COMMON    /O/    ATOMWT(3), CONDUC(3), B(3)
      COMMON    /P/    VOLX, DIAX, MDMTCF,VS, EQBED
      COMMON    /R/    SEPFAC(3,21), MDSEPF , SEP3(3,11,11)
      COMMON    /S/    NAME(3)
      COMMON    /T/     VOL0(3), A0(3), A1(3), A2(3), A3(3)
      COMMON    /U/    VSTART, VSTOP, VOLIW(3)
      DIMENSION    KPARI(3), KSOLI(3)
C
      M=N-1
      AREA = (22./7.)*(DIACOL*DIACOL)/4.
      HGHT1= VSTART/AREA
      HGHT2 = VSTOP/AREA
      QH=EQBED/VOLHW
      DO 555 I=1,N
      KPARI(I) = PDC*DPARI(I)
      KSOLI(I) = SPDC*(DSOLI(I)**SP)
  555 CONTINUE
      WRITE(6,6003)
 6003 FORMAT(1H1/)
      WRITE(6,6000) N
 6000 FORMAT(1H ,30X, "MULTI-COMPONENT FIXED-BED ION EXCHANGE COLUMN"//
     120X,  " BY THE METHOD OF CHARACTERISTICS"//
     220X, " NO OF COMPONENT   ",I2)
      WRITE(6,6500) (NAME(I),I=1,N)
      WRITE(6,6600)
 6500 FORMAT(1H0,20X,"THE COUNTER IONS ARE ", 5X,A2,":",A2,":",A2)
 6600 FORMAT(1H0,20X,"THE RESIN IS DOWEX 50W X8")
      WRITE(6,7000) DELV, DELZV
 7000 FORMAT(1H0, 20X, "STEP SIZE IN BED VOLUME   ", F10.4,2X,"ML"//
     120X,  " STEP SIZE IN CHARATERISTIC TIME   ",F10.4,2X,"ML"/)
      WRITE(6,8000) C
 8000 FORMAT(1H ,20X,"TOTAL FEED CONCENTRATION  ",F10.4,2X,"N"/)
      WRITE(6,8500) QH
      WRITE(6,8600) DIACOL
      WRITE(6,8700) HGHT1,HGHT2
 8500 FORMAT(1H ,20X,"RESIN CAPACITY IN H-FORM ",F10.4,2X,"EQ/L.BED"/)
 8600 FORMAT(1H ,20X,"COLUMN DIAMETER  ",F10.4,2X,"CM"/)
 8700 FORMAT(1H ,20X,"BED HEIGHT RANGE ",F10.4,2X,F10.4,2X,"CM"/)
      WRITE(6,9000) VSTART, VSTOP
      WRITE(6,9500) VOID
      WRITE(6,9600) TEMP
      WRITE(6,9700) DIAP
 9000 FORMAT(1H ,20X,"BED VOLUME RANGE ",F10.4,2X,F10.4,2X,"ML"/)
 9500 FORMAT(1H ,20X, "VOIDAGE  ",F10.4,2X,"VOID VOL./BED VOL."/)
 9600 FORMAT(1H ,20X, "OPERATING TEMPERATURE  ",F10.4,2X,"K"/)
 9700 FORMAT(1H ,20X,"PARTICLE DIAMETER IN H-FORM IN WATER   ",F6.4,2X,
     1"CM"/)
      WRITE(6,10000) (XPZM(I),I=1,N)
```

```
$ SET PAGE
C
C
10000 FORMAT(1H ,20X,"NORMALISED FEED CONCENTRATION" ,8X,3F8.4)
      WRITE(6,11000) (YPZN(I),I=1,N)
11000 FORMAT(1H0,20X,"NORMALISED PRESATURATED CONCENTRATION",3F8.4)
      DO 110 I=1,N
      WRITE(6,120)  NAME(I),VOL0(I),VOLIW(I)
  120 FORMAT(1H0,20X,"BED VOL IN ",A2,"-FORM IN ITS OWN SOLN AND IN WA
     1R ",2(F6.1,1X),1X,"ML")
  110 CONTINUE
      WRITE(6,130) VOLHW
  130 FORMAT(1H0,20X,"BED VOLUME IN H-FORM IN WATER  ",F6.1,2X,"ML")
      WRITE(6,12000) FEED
      GO TO(10,20),M
   10 WRITE(6,12999) (DSOLI(I),I=1,N)
      WRITE(6,13999) (DPARI(I),I=1,N)
      WRITE(6,14999) (KSOLI(I),I=1,N)
      WRITE(6,15999) (KPARI(I),I=1,N)
12999 FORMAT(1H0,20X,"SELF DIF COEF IN SOLUTION  ",2(E8.3,1X),1X,"SQ.CM
     A/SEC")
13999 FORMAT(1H0,20X,"SELF DIF COEF IN RESIN     ",2(E8.3,1X),1X,"SQ.CM
     B/SEC")
14999 FORMAT(1H0,20X,"SOLUTION PHASE SELF MASS TRANSFER COEF.  ",2F7.4,
     A2X,"1/SEC")
15999 FORMAT(1H0,20X,"PARTICLE PHASE SELF MASS TRANSFER COEF.  ",2F7.4,
     A2X,"1/SEC")
      GO TO 30
   20 WRITE(6,13000) (DSOLI(I),I=1,N)
      WRITE(6,14000) (DPARI(I),I=1,N)
      WRITE(6,15000) (KSOLI(I),I=1,N)
      WRITE(6,16000) (KPARI(I),I=1,N)
   30 CONTINUE
12000 FORMAT(1H0,20X,"SOLUTION FEED FLOW RATE  ",F10.4,2X,"ML/SEC")
13000 FORMAT(1H0,20X,"SELF DIF COEF IN SOLUTION  ",3(E8.3,1X),1X,"SQ.CM
     A/SEC")
14000 FORMAT(1H0,20X,"SELF DIF COEF IN RESIN     ",3(E8.3,1X),1X,"SQ.CM
     B/SEC")
15000 FORMAT(1H0,20X,"SOLUTION PHASE SELF MASS TRANSFER COEF.  ",3F7.4,
     A2X,"1/SEC")
16000 FORMAT(1H0,20X,"PARTICLE PHASE SELF MASS TRANSFER COEF.  ",3F7.4,
     A2X,"1/SEC")
C
      GO TO (2000,3000),MDSEPF
C
 2000 WRITE(6,2500)
 2500 FORMAT(1H0,20X,"CONSTANT SEPERATION FACTOR MODEL")
      GO TO 500
 3000 WRITE(6,3500)
 3500 FORMAT(1H0,20X,"VARIABLE SEPERATION FACTOR MODEL")
C
  500 IF(MDRATE)600,800,1000
C
  600 WRITE(6,700)
  700 FORMAT(1H0,20X,"THE PARTICLE DIFFUSION RATE MODEL")
      GO TO 1200
  800 WRITE(6,900)
  900 FORMAT(1H0,20X,"COMBINED DIFFUSION RATE MODEL")
      GO TO 1200
 1000 WRITE(6,1100)
 1100 FORMAT(1H0,20X,"SOLUTION DIFFUSION RATE MODEL")
 1200 CONTINUE
      GO TO (40,50,60),MDDFSN
```

```
$ SET PAGE
C
C
   40 GO TO 70
   50 WRITE(6,80)
   80 FORMAT(1H0,20X,"CONSTANT SELF DIFFUSIVITY MODEL")
      GO TO 70
   60 WRITE(6,90)
   90 FORMAT(1H0,20X,"VARIABLE SELF DIFFUSIVITY MODEL")
   70 CONTINUE
C
      GO TO(5100,5200), MDMTCF
C
 5100 WRITE(6,5150)
 5150 FORMAT(1H0,20X,"HIESTER RELATION IS USED TO COMPUTE SOLN. PHASE SE
     1LF MASS TRANSFER COEF."/)
      GO TO 5400
 5200 WRITE(6,5250)
 5250 FORMAT(1H0,20X,"KATAOKA RELATION IS USED TO COMPUTE SOLN. PHASE SE
     1LF MASS TRANSFER COEF."/)
 5400 CONTINUE
      WRITE(6,8991) (NAME(I),I=1,N)
 8991 FORMAT(1H ,20X,"NOTE : COUNTER ION PARAMETERS AER IN THE ORDER ",
     1A2,":",A2,":",A2)
      WRITE(6,95)
   95 FORMAT(1H1)
      RETURN
      END
```

```
C
      SUBROUTINE     SELFMT
C
C
      REAL   KPAR, KSOL
      COMMON    /A/   KPAR(3,3),KSOL(3,3),PDC, SPDC, SP
      COMMON    /B/   X(3), Y(3),VALENC(3)
      COMMON    /H/   N, FEED, MDDFSN, MDRATE,NSUBl,  MDMIXD
      COMMON    /K/   DPARI(3), DSOLI(3), DSOLI0(3), DPAR(3,3), DSOL(3,3)
      COMMON    /N/   TEMP, DIACOL, Q, C, VOID, VOLHW, DIAP
      COMMON    /O/   ATOMWT(3), CONDUC(3), B(3)
      COMMON    /P/   VOLX, DIAX, MDMTCF,VS, EQBED
      COMMON    /T/    VOL0(3), A0(3), Al(3), A2(3), A3(3)
      COMMON    /U/   VSTART, VSTOP, VOLIW(3)
C
      IF(MDRATE)100,100,300
C
C     PARTICLE PHASE DIFFUSION CONTROL
C
  100 Cl=60.0
      C2 = Cl*Q/C
      DD = DIAP*DIAP
      PDC = C2/DD
      IF(MDRATE.GE.0) GO TO 300
      GO TO 400
C
C     SOLUTION PHASE DIFFUSION CONTROL
C
  300 VISCO=0.01
      DENSIY=1.0
      GO TO (1650,200,200),MDDFSN
  200 DO 1550 I = 1,N
      DSOLI(I) = DPARI(I)/B(I)
 1550 CONTINUE
 1650 GO TO (2100,2200),MDMTCF
C
C     HIESTER RELATION
C
 2100 Fl = .5747*6.*VOID*VS/DIAP
      RE=DIAP*VS*DENSIY/(6.*(1.0-VOID)*VISCO)
      SC=VISCO/DENSIY
      RESC=RE*SC
      F2=RESC**0.5
      SP = 0.50
      SPDC = Fl/F2
      GO TO 400
C
C     KATAOKA RELATION
C
 2200 Fl=(1.85*6.0*VS)/(DIAP*VOID)
      F2 =  VOID/(1.0-VOID)
      F3=F2**(1.0/3.0)
      F4=Fl*F3
      RE=DIAP*VS*DENSIY/(1.*(1.0-VOID)*VISCO)
      SC=VISCO/DENSIY
      F5 = (RE*SC)**(2.0/3.0)
      SP = 2.0/3.0
      SPDC = F4/F5
      SPDC = SPDC*(1.0-VOID)
  400 CONTINUE
      RETURN
      END
```

```
C
      SUBROUTINE     NERNPL
C
C
      REAL   KPAR, KSOL
      COMMON    /A/   KPAR(3,3),KSOL(3,3),PDC, SPDC, SP
      COMMON    /B/   X(3), Y(3),VALENC(3)
      COMMON    /H/   N, FEED, MDDFSN, MDRATE,NSUB1,  MDMIXD
      COMMON    /K/   DPARI(3), DSOLI(3), DSOLI0(3), DPAR(3,3), DSOL(3,3
      COMMON    /N/   TEMP, DIACOL, Q, C, VOID, VOLHW, DIAP
      COMMON    /O/   ATOMWT(3), CONDUC(3), B(3)
      COMMON    /P/   VOLX, DIAX, MDMTCF,VS, EQBED
      COMMON    /U/   VSTART, VSTOP, VOLIW(3)
C
      GO TO (300,300,400),MDDFSN
  400 SUM=0.0
      DO 2000 I=1,N
      SUM = SUM + VOLIW(I)*Y(I)
 2000 CONTINUE
      VOLX = SUM
C     ...........
      CALL DIFFSN
C     ...........
      DO 1350 I=1,N
      B(I) = DPARI(I)/DSOLI0(I)
 1350 CONTINUE
C     ...........
      CALL VARVOL
      CALL DIFFSN
C     ...........
      DDD=DIAP
      DIAP=DIAX
C     ...........
      CALL SELFMT
C     ...........
      DIAP=DDD
  300 IF(MDRATE)600,600,800
C
C     PARTICLE PHASE DIFFUSION CONTROL
C
  600 SUM = 0.0
      DO 100 I=1,N
      YMDF = VALENC(I)*Y(I)
      SUM = SUM + YMDF*DPARI(I)
  100 CONTINUE
      DO 200 I=1,NSUB1
      YMDF = VALENC(I)*Y(I)
      SUM1 = SUM-YMDF*DPARI(I)
      DO 200 J =1,N
      IF(I.EQ.J) GO TO 200
      DPAR(I,J) = DPARI(I)*(SUM1+YMDF*DPARI(J))/SUM
      KPAR(I,J) = PDC*DPAR(I,J)
  200 CONTINUE
      IF(MDRATE.GE.0) GO TO 800
      GO TO 999
C
C     SOLUTION PHASE DIFFUSION CONTROL
C
  800 SUM = 0.0
      DO 900 I=1,N
      XMDF = VALENC(I)*X(I)
      SUM = SUM + XMDF*DSOLI(I)
```

```
$ SET PAGE
C
C
  900 CONTINUE
      DO 1000 I=1,NSUB1
      XMDF = VALENC(I)*X(I)
      SUM1 = SUM-XMDF*DSOLI(I)
      DO 1000 J=1,N
      IF(I.EQ.J) GO TO 1000
      DSOL(I,J) = DSOLI(I)*(SUM1+XMDF*DSOLI(J))/SUM
      IF(SP.EQ.0.50) GO TO 910
      KSOL(I,J) = SPDC*(DSOL(I,J)**SP)
      GO TO 1000
  910 KSOL(I,J) = SPDC*SQRT(DSOL(I,J))
 1000 CONTINUE
  999 CONTINUE
      RETURN
      END
```

```
C
C
      SUBROUTINE     EQUILB
C
C
      REAL   KPAR, KSOL
      COMMON   /A/   KPAR(3,3),KSOL(3,3),PDC, SPDC, SP
      COMMON   /B/   X(3), Y(3),VALENC(3)
      COMMON   /D/   ALPHA(3,3), YSTAR(3), XSTAR(3)
      COMMON   /H/   N, FEED, MDDFSN, MDRATE,NSUB1,  MDMIXD
      COMMON   /M/   J, IJK
      COMMON   /N/   TEMP, DIACOL, Q, C, VOID, VOLHW, DIAP
      COMMON   /R/   SEPFAC(3,21), MDSEPF , SEP3(3,11,11)
C
C     MDRATE = -VE : PARTICLE DIFFUSION CONTROL
C     MDRATE =   0 : COMBINED DIFFUSION CONTROL
C     MDRATE = +VE : SOLUTION PHASE DIFFUSION CONTROL
C
      IF(MDSEPF.EQ.2) CALL VARSEP
      IF(MDRATE) 30,40,50
C
C     PARTICLE PHASE DIFFUSION CONTROL
C
   30 SUM = 0.0
      SUM1 = 0.0
      DO 100 I =1,N
      SUM = SUM + X(I)*ALPHA(I,N)
  100 CONTINUE
      DO 200 I = 1,NSUB1
      YSTAR(I) = ALPHA(I,N)*X(I)/SUM
      SUM1 = SUM1 + YSTAR(I)
  200 CONTINUE
      YSTAR(N) = 1. - SUM1
      GO TO 9999
C
C     COMBINED DIFFUSION
C
   40 CALL MIXDIF
      GO TO 9999
C
C     SOLUTION PHASE DIFFUSION CONTROL
C
   50 SUM = 0.0
      SUM1 = 0.0
      DO 300 I = 1,N
      SUM = SUM + Y(I)/ALPHA(I,N)
  300 CONTINUE
      DO 400 I = 1,NSUB1
      XSTAR(I) = (Y(I)/ALPHA(I,N))/SUM
      SUM1 = SUM1 + XSTAR(I)
  400 CONTINUE
      XSTAR(N) = 1. - SUM1
 9999 CONTINUE
      RETURN
      END
```

```
C
C
      SUBROUTINE     VARSEP
C
C
      COMMON    /B/    X(3), Y(3),VALENC(3)
      COMMON    /D/    ALPHA(3,3), YSTAR(3), XSTAR(3)
      COMMON    /H/    N, FEED, MDDFSN, MDRATE,NSUB1,  MDMIXD
      COMMON    /M/    J, IJK
      COMMON    /R/    SEPFAC(3,21), MDSEPF , SEP3(3,11,11)
C
      IF(MDRATE) 10,20,20
   10 DO 30 I=1,NSUB1
      XSTAR(I) = X(I)
   30 CONTINUE
      GO TO 100
   20 IF(IJK.EQ.J) GO TO 100
      DO 40 I=1,NSUB1
      XSTAR(I) = X(I)
   40 CONTINUE
  100 IF(N.NE.2) GO TO 400
C     ............
C     BINARY DATA
C     ............
      DO 200 I=1,NSUB1
      IK= XSTAR(I)/0.05 + 1
      IF(IK.GE.21) GO TO 300
      P = (XSTAR(I)-(IK-1)*0.05)/0.05
      ALPHA(I,N) = (1.0-P)*SEPFAC(I,IK)+ P*SEPFAC(I,IK+1)
      GO TO 200
  300 ALPHA(I,N) = SEPFAC(I,21)
  200 CONTINUE
      GO TO 2000
C     ............
C     TERNARY DATA
C     ............
  400 DO 1000 I=1,NSUB1
      IK = XSTAR(I)/0.1 + 1.0
      PIK = (XSTAR(I)-((IK-1)*0.1))/0.1
C     FIND IJ & PIJ
      IF(I.EQ.1) GO TO 500
      IJ = XSTAR(1)/0.1 + 1
      PIJ = (XSTAR(1)-((IJ-1)*0.1))/0.1
      GO TO 600
  500 IJ = XSTAR(2)/0.1 + 1.0
      PIJ = (XSTAR(2)-((IJ-1)*0.1))/0.1
  600 IF(IK.LT.11) GO TO 700
      ALPHA(I,N) = SEP3(I,1,11)
      GO TO 1000
  700 IF(IJ.LT.11) GO TO 800
      ALPHA(I,N) = SEP3(I,11,1)
      GO TO 1000
  800 HOR1=((1.0-PIK)*SEP3(I,IJ,IK))+(PIK*SEP3(I,IJ,IK+1))
      HOR2=((1.0-PIK)*SEP3(I,IJ+1,IK))+(PIK*SEP3(I,IJ+1,IK+1))
      ALPHA(I,N) = (1.0-PIJ)*HOR1 + (PIJ*HOR2)
 1000 CONTINUE
 2000 CONTINUE
      RETURN
      END
```

```
C
C
      SUBROUTINE     MIXDIF
C
C
      REAL      KEQ
      REAL    KPAR, KSOL
      COMMON    /A/    KPAR(3,3),KSOL(3,3),PDC, SPDC, SP
      COMMON    /B/    X(3), Y(3),VALENC(3)
      COMMON    /D/    ALPHA(3,3), YSTAR(3), XSTAR(3)
      COMMON    /H/    N, FEED, MDDFSN, MDRATE,NSUB1,  MDMIXD
      COMMON    /L/    KINT, KSTART, ITEST, EPSIL
      COMMON    /M/    J, IJK
      COMMON    /N/    TEMP, DIACOL, Q, C, VOID, VOLHW, DIAP
      COMMON    /R/    SEPFAC(3,21), MDSEPF , SEP3(3,11,11)
C
      IF(N.GT.2) GO TO 1000
C
C     BINARY PROBLEM
C
      KEQ = ALPHA(1,2)
      XX = X(1)
      YY = Y(1)
      ZETA = KPAR(1,2)/KSOL(1,2)
  600 IF(KEQ.EQ.1) GO TO 700
      RZETA = 1.0/ZETA
      ALFA = XX+ZETA*YY
      FAC1 = (1.0+KEQ*ZETA)/ZETA/(KEQ-1.0)
      FAC2 = KEQ/ZETA/(KEQ-1.0)
      B = -(ALFA*RZETA+FAC1)
      CC = ALFA*FAC2
      PAR = -B/2.0
      DIS = SQRT(B*B-4.0*CC)/2.0
      ROOT1 = PAR+DIS
      IF(PAR.LT.0.0) ROOT1=PAR-DIS
      ROOT2 = CC/ROOT1
      E1 = ABS(0.5-ROOT1)
      E2 = ABS(0.5-ROOT2)
      YS = ROOT1
      IF(E2.LT.E1) YS = ROOT2
      XS = (YS/KEQ)/(YS/KEQ + 1.0 - YS)
      GO TO 800
  700 YS = (XX+ZETA*YY)/(1.0+ZETA)
      XS = YS
  800 CONTINUE
      YSTAR(1) = YS
      XSTAR(1) = XS
      YSTAR(2) = 1.0-YS
      XSTAR(2) = 1.0-XS
      GO TO 999
C
C     TERNARY PROBLEM
C
 1000 MM = MDRATE
      MDS=MDSEPF
      NLOOP = 0
      IF(MDMIXD.GT.1) GO TO 1100
      AA = KPAR(1,2)*Y(2) + KPAR(1,3)*Y(3)
      BB = KPAR(2,1)*Y(1) + KPAR(2,3)*Y(3)
      A1 = KSOL(1,2)*X(2) + KSOL(1,3)*X(3)
      B1 = KSOL(2,1)*X(1) + KSOL(2,3)*X(3)
      G = (KPAR(1,2)-KPAR(1,3))/KPAR(1,3)
      IF(KPAR(2,1).EQ.KPAR(2,3)) GO TO 1250
```

```
$ SET PAGE
C
C
      H = KPAR(2,3)/(KPAR(2,1)-KPAR(2,3))
 1250 CONTINUE
C
C     ESTIMATE YSTAR(I),I=1,3
C
      IF(IJK.EQ.J) GO TO 4000
      MDRATE = -5
      MDSEPF=1
      CALL EQUILB
      MDRATE = MM
      MDSEPF=MDS
 4000 NLOOP = NLOOP+1
      IF(NLOOP.GT.500)GO TO 909
      SUM=0.0
      SUM1 = 0.0
      DO 4200 I=1,N
      SUM = SUM + YSTAR(I)/ALPHA(I,N)
 4200 CONTINUE
      DO 4400 I=1,NSUB1
      XSTAR(I) = (YSTAR(I)/ALPHA(I,N))/SUM
      SUM1 = SUM1 + XSTAR(I)
 4400 CONTINUE
      XSTAR(N) = 1. - SUM1
      A = A1-(KSOL(1,2)*XSTAR(2) + KSOL(1,3)*XSTAR(3))
      B = B1-(KSOL(2,1)*XSTAR(1)+KSOL(2,3)*XSTAR(3))
      CC=A+AA
      D = B+BB
      E=CC-KPAR(1,3)
      F = D-KPAR(2,3)
      IF(KPAR(2,1).EQ.KPAR(2,3)) GO TO 1350
      YY2=(E/KPAR(1,3)+F/(KPAR(2,1)-KPAR(2,3)))/(G-H)
      GO TO 1450
 1350 YY2 = -(F/KPAR(2,3))
 1450 YY1 = G*YY2-(E/KPAR(1,3))
      YYY1 = ABS(YY1-YSTAR(1))
      YYY2 = ABS(YY2-YSTAR(2))
      YSTAR(1) = YY1
      YSTAR(2) = YY2
      YSTAR(3) = 1.0-YY1-YY2
      IF(YYY1.GT.EPSIL)  GO TO 4000
      IF(YYY2.GT.EPSIL)  GO TO 4000
      GO TO 909
 1100 ICNVGE=0
      AA = KSOL(1,2)*X(2) + KSOL(1,3)*X(3)
      BB = KSOL(2,1)*X(1) + KSOL(2,3)*X(3)
      A1 = KPAR(1,2)*Y(2) + KPAR(1,3)*Y(3)
      B1 = KPAR(2,1)*Y(1) + KPAR(2,3)*Y(3)
      G = (KSOL(1,2)-KSOL(1,3))/KSOL(1,3)
      IF(KSOL(2,1).EQ.KSOL(2,3)) GO TO 1550
      H = KSOL(2,3)/(KSOL(2,1)-KSOL(2,3))
 1550 CONTINUE
C
C
 2000 SUM = 0.0
      SUM1 = 0.0
      DO 100 I =1,N
      SUM = SUM + XSTAR(I)*ALPHA(I,N)
  100 CONTINUE
      DO 200 I = 1,NSUB1
      YSTAR(I) = ALPHA(I,N)*XSTAR(I)/SUM
      SUM1 = SUM1 + YSTAR(I)
```

```
$ SET PAGE
C
C
  200 CONTINUE
      YSTAR(N) = 1. - SUM1
      IF(ICNVGE.GE.1) GO TO 909
      NLOOP=NLOOP+1
      IF(NLOOP.GT.500)GO TO 909
      A = A1-(KPAR(1,2)*YSTAR(2) + KPAR(1,3)*YSTAR(3))
      B = B1-(KPAR(2,1)*YSTAR(1)+KPAR(2,3)*YSTAR(3))
      CC=A+AA
      D = B+BB
      E=CC-KSOL(1,3)
      F = D-KSOL(2,3)
      IF(KSOL(2,1).EQ.KSOL(2,3)) GO TO 1650
      XX2=(E/KSOL(1,3)+F/(KSOL(2,1)-KSOL(2,3)))/(G-H)
      GO TO 1750
 1650 XX2 = -(F/KSOL(2,3))
 1750 XX1 = G*XX2 - E/KSOL(1,3)
      XXX1 = ABS(XX1-XSTAR(1))
      XXX2 = ABS(XX2-XSTAR(2))
      IF(XXX1.GT.EPSIL) GO TO 2100
      IF(XXX2.GT.EPSIL) GO TO 2100
      ICNVGE = 1
 2100 XSTAR(1) = XX1
      XSTAR(2) = XX2
      XSTAR(3) = 1.0-XX1-XX2
      GO TO 2000
  909 CONTINUE
      DO 919 I=1,N
      IF(ABS(YSTAR(I)-0.5).LE.0.501) GO TO 929
      WRITE(6,2) YSTAR(1),YSTAR(2),YSTAR(3)
  929 IF(ABS(XSTAR(I)-0.5).LE.0.501) GO TO 919
      WRITE(6,3) XSTAR(1),XSTAR(2),XSTAR(3)
  919 CONTINUE
    2 FORMAT(1H ,10X,"YSTAR(1) =",F10.4,2X,"YSTAR(2) =",F10.4,2X,
     1 "YSTAR(3) =",F10.4/)
    3 FORMAT(1H ,10X,"XSTAR(1) =",F10.4,2X,"XSTAR(2) =",F10.4,2X,
     1 "XSTAR(3) =",F10.4/)
  999 CONTINUE
      RETURN
      END
```

```
C
C
      SUBROUTINE     RATE
C
C
C     MDRATE = -VE : PARTICLE DIFFUSION CONTROL
C     MDRATE =   0 : COMBINED DIFFUSION CONTROL
C     MDRATE = +VE : SOLUTION PHASE DIFFUSION CONTROL
C
C
      REAL   KPAR, KSOL
      COMMON   /A/   KPAR(3,3),KSOL(3,3),PDC, SPDC, SP
      COMMON   /B/   X(3), Y(3),VALENC(3)
      COMMON   /D/   ALPHA(3,3), YSTAR(3), XSTAR(3)
      COMMON   /F/   R(3)
      COMMON   /H/   N, FEED, MDDFSN, MDRATE,NSUB1,  MDMIXD
C
      IF(MDRATE) 500,500,1000
C
C     PARTICLE PHASE DIFFUSION CONTROL
C
  500 DO 200 I = 1,NSUB1
      SUM = 0.0
      DO 100 J = 1,N
      IF(I.EQ.J) GO TO 100
      P = KPAR(I,J)/FEED
      SUM = SUM + P*Y(J) - P*YSTAR(J)
  100 CONTINUE
      R(I) = SUM
  200 CONTINUE
      GO TO 999
C
C     SOLUTION PHASE DIFFUSION CONTROL
C
 1000 DO 250 I = 1,NSUB1
      SUM = 0.0
      DO 150 J = 1,N
      IF(I.EQ.J) GO TO 150
      P = KSOL(I,J)/FEED
      SUM = SUM + P*XSTAR(J) - P*X(J)
  150 CONTINUE
      R(I) = SUM
  250 CONTINUE
  999 CONTINUE
      RETURN
      END
```

```
C
C
      SUBROUTINE     SOLVE
C
C
      REAL    KPAR, KSOL
      COMMON    /A/   KPAR(3,3),KSOL(3,3),PDC, SPDC, SP
      COMMON    /B/   X(3), Y(3),VALENC(3)
      COMMON    /C/   XPZM(3), XPZN(3), YPZM(3), YPZN(3)
      COMMON    /D/   ALPHA(3,3), YSTAR(3), XSTAR(3)
      COMMON    /E/   RSAVE(2,4000)
      COMMON    /F/   R(3)
      COMMON    /G/   YSAVE(2,4000)
      COMMON    /H/   N, FEED, MDDFSN, MDRATE,NSUB1,  MDMIXD
      COMMON    /I/   DELV, DELZV, K, KMAX, KEND, NFLAG
      COMMON    /K/   DPARI(3), DSOLI(3), DSOLI0(3), DPAR(3,3), DSOL(3,3
      COMMON    /L/   KINT, KSTART, ITEST, EPSIL
      COMMON    /M/   J, IJK
      COMMON    /N/   TEMP, DIACOL, Q, C, VOID, VOLHW, DIAP
      COMMON    /O/   ATOMWT(3), CONDUC(3), B(3)
      COMMON    /P/   VOLX, DIAX, MDMTCF,VS, EQBED
      COMMON    /Q/   X0(3), X1(3),  Y1(3)
      COMMON    /R/   SEPFAC(3,21), MDSEPF , SEP3(3,11,11)
      COMMON    /T/    VOL0(3), A0(3), A1(3), A2(3), A3(3)
      COMMON    /U/   VSTART, VSTOP, VOLIW(3)
C
      IF(NFLAG-1) 500,547,500
  500 SUM = 0.0
      DO 520 I =1,NSUB1
      RSAVE(I,K-1) = R(I)
      YSAVE(I,K-1) = Y(I)
      X0(I) = X(I)
      X(I) = X0(I) - R(I)*DELV
      X1(I) = X(I)
      SUM = SUM + X(I)
  520 CONTINUE
      X(N) = 1. - SUM
      IF(K.GT.KMAX) GO TO 999
      IF(K-KEND)547,535,535
C
  535 DO 540 I = 1,N
      Y(I) = YPZN(I)
  540 CONTINUE
C
C     ...........
      CALL NERNPL
      CALL EQUILB
      CALL RATE
C     ...........
C
  525 SUM = 0.0
      DO 530 I = 1,NSUB1
      X(I) = X0(I) - R(I)*DELV
      X(I) = (X(I)+X1(I))*0.5
      SUM = SUM + X(I)
  530 CONTINUE
      X(N) = 1. - SUM
      IF(K-KEND)555,999,999
C
  547 SUM = 0.0
      DO 550 I = 1,NSUB1
      Y(I) = YSAVE(I,K) + RSAVE(I,K)*DELZV
      Y1(I) = Y(I)
```

```
$ SET PAGE
C
C
      SUM = SUM + Y(I)
  550 CONTINUE
      Y(N) = 1. -SUM
C
C     ...........
      CALL NERNPL
      CALL EQUILB
      CALL RATE
C     ...........
C
      IF(NFLAG.EQ.1) GO TO 555
      GO TO 525
C
  555 SUM = 0.0
      DO 560 I = 1,NSUB1
      Y(I) = YSAVE(I,K) + R(I)*DELZV
      Y(I) = (Y(I)+Y1(I))*0.5
      SUM = SUM + Y(I)
  560 CONTINUE
      Y(N) = 1.-SUM
  999 CONTINUE
      DO 600 I=1,NSUB1
      IF(ABS(X(I)-0.5).LE.0.5015) GO TO 610
      WRITE(6,1) (X(I),I=1,N)
      WRITE(6,2) J,K
      K=KMAX+1
      KSTART=K
      IJK=-5
      GO TO 9999
  610 IF(ABS(Y(I)-0.5).LE.0.5015) GO TO 600
      WRITE(6,3) (Y(I),I=1,N)
      WRITE(6,2) J,K
      K=KMAX+1
      KSTART=K
      IJK=-5
      GO TO 9999
  600 CONTINUE
    1 FORMAT(1H0,20X,"SOLUTION PHASE CONCENTRATION NOT IN SUITABLE RANGI
     1"/20X,3F10.4)
    2 FORMAT(20X,I4,2X,I4)
    3 FORMAT(1H0,20X,"PARTICLE PHASE CONCENTRATION NOT IN SUITABLE RANGI
     1"/20X,3F10.4)
 9999 RETURN
      END
```

```
C
C
      SUBROUTINE     STEPZV
C
C
      COMMON   /B/   X(3), Y(3),VALENC(3)
      COMMON   /C/   XPZM(3), XPZN(3), YPZM(3), YPZN(3)
      COMMON   /H/   N, FEED, MDDFSN, MDRATE,NSUB1,  MDMIXD
      COMMON   /I/   DELV, DELZV, K, KMAX, KEND, NFLAG
      COMMON   /J/   JPRINT, KPRINT, INZV, INV, IPRINT
      COMMON   /L/   KINT, KSTART, ITEST, EPSIL
      COMMON   /M/   J, IJK
C
      J=J+1
      KEND = K
      K = KSTART
      KPRINT =  INV
      JPRINT = JPRINT + 1
      IF(JPRINT-INZV) 4200,4200,4100
 4100 JPRINT = 1
 4200 ITEST = 1
      DO 4300 I = 1,N
      X(I) = XPZM(I)
 4300 CONTINUE
      NFLAG = 1
      RETURN
      END
```

```
C
C
      SUBROUTINE     OUTPUT
C
C
      REAL   KPAR, KSOL
      COMMON   /A/   KPAR(3,3),KSOL(3,3),PDC, SPDC, SP
      COMMON   /B/   X(3), Y(3),VALENC(3)
      COMMON   /D/   ALPHA(3,3), YSTAR(3), XSTAR(3)
      COMMON   /H/   N, FEED, MDDFSN, MDRATE,NSUB1,  MDMIXD
      COMMON   /I/   DELV, DELZV, K, KMAX, KEND, NFLAG
      COMMON   /M/   J, IJK
      DIMENSION   PAR(3)
C
      GRIDV = K-1
      GRIDZV = J-1
      V = GRIDV*DELV
      ZV = GRIDZV*DELZV
      IF(IJK.EQ.J) GO TO 50
      WRITE(6,20) ZV
   20 FORMAT(1H1,30X,"ZV  = ",F7.2//11X,"V",8X,
     1 "X(1)",4X,"X(2)",4X,"Y(1)",4X,"Y(2)",4X,"X*(1)",3X,"X*(2)",3X,
     2"Y*(1)",3X,"Y*(2)",8X,"MECHANISM PARAMETER"/)
   50 DO 100I=1,N
      IF(N.GT.2) GO TO 400
      PAR(I)=KPAR(1,2)/KSOL(1,2)
      GO TO 100
  400 YY = YSTAR(I)-Y(I)
      IF(YY.NE.0.0) GO TO 200
      YY = 0.0000000001
  200 PAR(I)=(X(I)-XSTAR(I))/YY
  100 CONTINUE
      WRITE(6,300) V,(X(I),I=1,2),(Y(I),I=1,2),(XSTAR(I),I=1,2)
     1,(YSTAR(I),I=1,2),(PAR(I),I=1,N)
  300 FORMAT(1H ,7X,F7.2,4X,8(F6.4,2X),3(F10.4,2X))
      RETURN
      END
```

APPENDIX 4C

SAMPLE OUTPUT

MULTI-COMPONENT FIXED-BED ION EXCHANGE COLUMN

BY THE METHOD OF CHARACTERISTIC

NO OF COMPONENT 2

THE COUNTER IONS ARE NA: H:

THE RESIN IS DOWEX 50W X8

STEP SIZE IN BED VOLUME 3.2000 ML

STEP SIZE IN CHARATERISTIC TIME 6.4000 ML

TOTAL FEED CONCENTRATION 1.0000 N

RESIN CAPACITY IN H-FORM 2.1280 EQ/L.BED

COLUMN DIAMETER 3.0600 CM

BED HEIGHT RANGE 86.9906 86.9906 CM

BED VOLUME RANGE 640.0000 640.0000 ML

VOIDAGE 0.3900 VOID VOL./BED VOL.

OPERATING TEMPERATURE 298.1500 K

PARTICLE DIAMETER IN H-FORM IN WATER 0.0809 CM

NORMALISED FEED CONCENTRATION 1.0000 0.0000

NORMALISED PRESATURATED CONCENTRATION 0.0000 1.0000

BED VOL IN NA-FORM IN ITS OWN SOLN AND IN WATER 640.0 640.0 ML

BED VOL IN H-FORM IN ITS OWN SOLN AND IN WATER 640.0 640.0 ML

BED VOLUME IN H-FORM IN WATER 640.0 ML

SOLUTION FEED FLOW RATE 0.8600 ML/SEC

SELF DIF COEF IN SOLUTION .133E-04 .931E-04 SQ.CM /SEC

SELF DIF COEF IN RESIN .182E-05 .127E-04 SQ.CM /SEC

SOLUTION PHASE SELF MASS TRANSFER COEF. 0.1397 0.3689 1/SEC

PARTICLE PHASE SELF MASS TRANSFER COEF. 0.0356 0.2483 1/SEC

CONSTANT SEPARATION FACTOR MODEL

COMBINED DIFFUSION RATE MODEL

CONSTANT SELF DIFFUSIVITY MODEL

HIESTER RELATION IS USED TO COMPUTE SOLN. PHASE SELF MASS TRANSFER COEF

NOTE : COUNTER ION PARAMETERS ARE IN THE ORDER NA: H:

THE ENTIRE COLUMN IS IN EQUILIBRIUM WITH THE FEED

THROUGHPUT RATIO	X(1)	X(2)	X(3)
0.3200	0.0001	0.9999	0.0000
0.3400	0.0002	0.9998	0.0000
0.3600	0.0004	0.9996	0.0000
0.3800	0.0006	0.9994	0.0000
0.4000	0.0009	0.9991	0.0000
0.4200	0.0013	0.9987	0.0000
0.4400	0.0019	0.9981	0.0000
0.4600	0.0026	0.9974	0.0000
0.4800	0.0035	0.9965	0.0000
0.5000	0.0047	0.9953	0.0000
0.5200	0.0061	0.9939	0.0000
0.5400	0.0080	0.9920	0.0000
0.5600	0.0102	0.9898	0.0000
0.5800	0.0130	0.9870	0.0000
0.6000	0.0164	0.9836	0.0000
0.6200	0.0205	0.9795	0.0000
0.6400	0.0254	0.9746	0.0000
0.6600	0.0313	0.9687	0.0000
0.6800	0.0382	0.9618	0.0000
0.7000	0.0463	0.9537	0.0000
0.7200	0.0558	0.9442	0.0000
0.7400	0.0669	0.9331	0.0000
0.7600	0.0797	0.9203	0.0000
0.7800	0.0943	0.9057	0.0000
0.8000	0.1111	0.8889	0.0000
0.8200	0.1302	0.8698	0.0000
0.8400	0.1518	0.8482	0.0000
0.8600	0.1762	0.8238	0.0000
0.8800	0.2034	0.7966	0.0000
0.9000	0.2338	0.7662	0.0000
0.9200	0.2675	0.7325	0.0000
0.9400	0.3045	0.6955	0.0000
0.9600	0.3451	0.6549	0.0000
0.9800	0.3891	0.6109	0.0000
1.0000	0.4365	0.5635	0.0000
1.0200	0.4872	0.5128	0.0000
1.0400	0.5407	0.4593	0.0000
1.0600	0.5965	0.4035	0.0000
1.0800	0.6538	0.3462	0.0000
1.1000	0.7113	0.2887	0.0000
1.1200	0.7677	0.2323	0.0000
1.1400	0.8210	0.1790	0.0000
1.1600	0.8690	0.1310	0.0000
1.1800	0.9097	0.0903	0.0000
1.2000	0.9416	0.0584	0.0000
1.2200	0.9645	0.0355	0.0000
1.2400	0.9795	0.0205	0.0000
1.2600	0.9886	0.0114	0.0000
1.2800	0.9939	0.0061	0.0000
1.3000	0.9968	0.0032	0.0000
1.3200	0.9984	0.0016	0.0000
1.3400	0.9992	0.0008	0.0000
1.3600	0.9997	0.0003	0.0000
1.3800	1.0000	0.0000	0.0000

MULTI-COMPONENT FIXED-BED ION EXCHANGE COLUMN

BY THE METHOD OF CHARACTERISTIC

NO OF COMPONENT 3

THE COUNTER IONS ARE K:NA: H

THE RESIN IS DOWEX 50W X8

STEP SIZE IN BED VOLUME 4.0000 ML

STEP SIZE IN CHARATERISTIC TIME 4.0000 ML

TOTAL FEED CONCENTRATION 0.1000 N

RESIN CAPACITY IN H-FORM 1.8671 EQ/L.BED

COLUMN DIAMETER 4.9300 CM

BED HEIGHT RANGE 93.8643 89.9736 CM

BED VOLUME RANGE 1792.5000 1718.2000 ML

VOIDAGE 0.3800 VOID VOL./BED VOL.

OPERATING TEMPERATURE 297.0000 K

PARTICLE DIAMETER IN H-FORM IN WATER 0.0759 CM

NORMALISED FEED CONCENTRATION 0.6000 0.2000 0.2000

NORMALISED PRESATURATED CONCENTRATION 0.0000 1.0000 0.0000

BED VOL IN K-FORM IN ITS OWN SOLN AND IN WATER 1667.7 1670.6 ML

BED VOL IN NA-FORM IN ITS OWN SOLN AND IN WATER 1755.4 1759.2 ML

BED VOL IN H-FORM IN ITS OWN SOLN AND IN WATER 1908.0 1913.7 ML

BED VOLUME IN H-FORM IN WATER 1913.7 ML

SOLUTION FEED FLOW RATE 1.7425 ML/SEC

SELF DIF COEF IN SOLUTION .190E-04 .129E-04 .910E-04 SQ.CM /SEC

SELF DIF COEF IN RESIN .226E-05 .154E-05 .108E-04 SQ.CM /SEC

SOLUTION PHASE SELF MASS TRANSFER COEF. 0.1661 0.1370 0.3636 1/SEC

PARTICLE PHASE SELF MASS TRANSFER COEF. 0.5068 0.3449 2.4280 1/SEC

VARIABLE SEPARATION FACTOR MODEL

COMBINED DIFFUSION RATE MODEL

CONSTANT SELF DIFFUSIVITY MODEL

HIESTER RELATION IS USED TO COMPUTE SOLN. PHASE SELF MASS TRANSFER COEF

NOTE : COUNTER ION PARAMETERS ARE IN THE ORDER K:NA: H

THE ENTIRE COLUMN IS IN EQUILIBRIUM WITH THE FEED

THROUGHPUT RATIO	X(1)	X(2)	X(3)
0.6735	-.0000	0.9999	0.0001
0.6849	-.0000	0.9992	0.0008
0.6963	0.0000	0.9963	0.0037
0.7078	0.0000	0.9881	0.0119
0.7192	0.0000	0.9688	0.0312
0.7306	0.0000	0.9372	0.0628
0.7420	0.0000	0.9048	0.0952
0.7534	0.0000	0.8800	0.1200
0.7648	0.0000	0.8578	0.1422
0.7763	0.0000	0.8389	0.1611
0.7877	0.0000	0.8235	0.1765
0.7991	0.0000	0.8116	0.1884
0.8105	0.0000	0.8026	0.1974
0.8219	0.0000	0.7957	0.2043
0.8333	0.0000	0.7897	0.2103
0.8447	0.0000	0.7844	0.2156
0.8562	0.0000	0.7798	0.2202
0.8676	0.0000	0.7758	0.2242
0.8790	0.0000	0.7725	0.2275
0.8904	0.0000	0.7698	0.2302
0.9018	0.0000	0.7675	0.2325
0.9132	0.0000	0.7655	0.2345
0.9247	0.0000	0.7640	0.2360
0.9361	0.0000	0.7628	0.2372
0.9475	0.0000	0.7619	0.2381
0.9589	0.0000	0.7612	0.2387
0.9703	0.0000	0.7608	0.2391
0.9817	0.0001	0.7605	0.2394
0.9932	0.0001	0.7603	0.2396
1.0046	0.0002	0.7600	0.2398
1.0160	0.0003	0.7598	0.2399
1.0274	0.0005	0.7596	0.2399
1.0388	0.0009	0.7592	0.2399
1.0502	0.0016	0.7586	0.2399
1.0616	0.0028	0.7575	0.2398
1.0731	0.0048	0.7557	0.2395
1.0845	0.0084	0.7525	0.2391
1.0959	0.0145	0.7471	0.2384
1.1073	0.0249	0.7379	0.2371
1.1187	0.0422	0.7226	0.2351
1.1301	0.0699	0.6980	0.2321
1.1416	0.1116	0.6607	0.2278
1.1530	0.1697	0.6085	0.2218
1.1644	0.2417	0.5436	0.2147
1.1758	0.3188	0.4717	0.2095
1.1872	0.3903	0.4052	0.2045
1.1986	0.4473	0.3507	0.2020
1.2100	0.4944	0.3046	0.2011
1.2215	0.5336	0.2679	0.1985
1.2329	0.5590	0.2423	0.1987
1.2443	0.5750	0.2258	0.1992
1.2557	0.5849	0.2155	0.1996
1.2671	0.5910	0.2092	0.1998
1.2785	0.5947	0.2054	0.1999
1.2900	0.5970	0.2030	0.2000
1.3014	0.5984	0.2016	0.2000
1.3128	0.5993	0.2008	0.2000

CHAPTER 5

BINARY AND TERNARY ION EXCHANGE EQUILIBRIA

5.1 Introduction

Ion exchange equilibrium data are required for the prediction of ion exchange breakthrough curves. Binary ion exchange equilibrium data have been established for a number of counter ions for many ion exchange resins.

In practice, ion exchange operations usually involve multicomponent systems. Equilibrium data for multicomponent systems are even less common due to difficulties and accuracies in measuring ionic concentrations.

Equilibria in ternary systems have been measured by a few workers (Dranoff and Lapidus, 1957; Glaski 1960; Pieroni and Dranoff, 1963). The object of these studies was to investigate the feasibility of representing ternary equilibrium data with binary equilibrium data. They concluded that equilibria for any two ions were the same in binary and ternary systems.

The object of this chapter is to obtain equilibrium data for K-H, Na-H and K-Na-H systems in Dowex 50W X8.

Theory of ion exchange equilibria

The condition for the equilibrium distribution of ionic species i between the resin and the solution is

$$\Gamma_i = \overline{\Gamma}_i \qquad (5.1)$$

where Γ_i and $\overline{\Gamma}_i$ are the electrochemical potentials of species i in solution and particle phases respectively, $\Gamma_i = \mu_i + Z_i f\phi$ and $\overline{\Gamma}_i = \overline{\mu}_i + Z_i f\overline{\phi}$. Eqn. 5.1 becomes

$$\mu_i + Z_i f\phi = \overline{\mu}_i + Z_i f\overline{\phi} \qquad (5.2)$$

where $\bar{\mu}_i$ is the chemical potential of species i in particle phase and $\bar{\phi}$ is the electric potential in particle phase.

The chemical potentials μ_i and $\bar{\mu}_i$ can be written as (Appendix 2B):

$$\mu_i = \mu_i^{\phi}(T,P_s) + RT\ell n\gamma_i C_i \qquad (5.3A)$$

$$\bar{\mu}_i = \mu_i^{\phi}(T,P_r) + RT\ell n\bar{\gamma}_i q_i \qquad (5.3B)$$

where $\bar{\gamma}_i$ is the molar activity coefficient in particle phase, q_i is the weight equivalent concentration of species i in particle phase, P_s is the pressure in the external solution, P_r is the pressure in the resin.

The term $\mu_i^{\phi}(T,P_r)$ can be written as (Helfferich, 1962)

$$\mu_i^{\phi}(T,P_r) = \mu_i^{\phi}(T,P_s) + (P_r - P_s)V_i \qquad (5.4)$$

where V_i is the partial equivalent volume of species i.

Combining Eqn. 5.4 with Eqn. 5.3B gives:

$$\bar{\mu}_i = \mu_i^{\phi}(T,P_s) + (P_r - P_s)V_i + RT\ell n\bar{\gamma}_i q_i \qquad (5.5)$$

Eqn. 5.5 can be further simplified by combining the pressure difference term with the resin activity coefficient.

$$\bar{\mu}_i = \mu_i^{\phi}(T,P_s) + RT\ell nf_i q_i \qquad (5.6)$$

where f_i is the effective resin activity coefficient.

Equations 5.2, 5.3A and 5.6 are solved for $\bar{\phi} - \phi$

$$\bar{\phi} - \phi = \frac{RT}{Z_i f}\ell n\left(\frac{\gamma_i C_i}{f_i q_i}\right) \qquad (5.7)$$

Eqn. 5.7 can be applied to any component in the system, therefore

$$\frac{RT}{Z_i f}\ell n\left(\frac{\gamma_i C_i}{f_i q_i}\right) = \frac{RT}{Z_j f}\ell n\left(\frac{\gamma_j C_j}{f_j q_j}\right) = \frac{RT}{Z_n f}\ell n\left(\frac{\gamma_n C_n}{f_n q_n}\right) \qquad (5.8)$$

Considering species i and n, both are homo-valent ions, and using Eqn. 5.8 it can be shown that

$$\frac{Y_i \, X_n}{X_i \, Y_n} = \frac{f_n \, \gamma_i}{\gamma_n \, f_i} \qquad (5.9)$$

A separation factor for species i with respect to species n has been defined (Section 2.4)

$$\alpha_n^i = \frac{\bar{Y}_i^* \, \bar{X}_n^*}{\bar{X}_i^* \, \bar{Y}_n^*}$$

Eqn. 5.9 can be written as

$$\alpha_n^i = \frac{\bar{Y}_i^* \, \bar{X}_n^*}{\bar{X}_i^* \, \bar{Y}_n^*} = \frac{f_n \gamma_i}{\gamma_n f_i} \qquad (5.10)$$

Ion exchange equilibrium data can be obtained either by experiments or from theoretical predictions. The theoretical predictions involve calculating activity coefficients of counter ions in both solution and resin phases. Activity coefficients in the solution phase have been established (Robinson and Stokes, 1959; Bates, 1973). There is no well established method for predicting activity coefficients in the resin phase. Various empirical approaches have been used in obtaining activity coefficients in the resin phase (Myers and Boyd, 1956; Rao and David, 1957; Marinsky, 1973; Bajpai et al., 1973), but the predicted separation factors do not agree with experimental values.

Helfferich (1962) has discussed the prediction of ion exchange equilibrium in detail and concluded that, at the present state of equilibrium theory, reliable equilibrium data can only be obtained experimentally.

5.2 Experimental Method

System description

A column method was used in the equilibrium determinations. The column was constructed from a 100 ml burette, 1.5 cm in diameter, with a sintered glass disc to support the resin. The column volume was calibrated by series of weight measurements of distilled water.

Dowex 50W X8 ion exchange resin with mesh size range of 18# - 25# was used in the experiments. The resin volume was 26.1 ml in H form, 24.5 ml in Na form and 23.0 ml in K form. The resin was pretreated with 1.0 M NaOH and 1.0 M HCl for several cycles.

Standard KNO_3 and $NaNO_3$ solutions were made from Analar crystal, oven dried for 2-3 days at 110°C. Standard HNO_3 solution was made by dilution of concentrated commercial Baker HNO_3 solution. Equilibrating solutions, to a total normality of 0.1, were made by weight combination of KNO_3, $NaNO_3$ and HNO_3 0.1 N solutions.

The feed flow rates for binary and ternary runs were chosen by computer simulation. At high flow rates the breakthrough curves were wide, requiring excessive equilibrating solution. At low flow rates, the time required for the operation was long. It was concluded that the flow rates of 6.8 ml/sq.cm min. and 5.1 ml/sq.cm min. were a reasonable compromise for binary and ternary exchanges respectively.

The column capacity was repeatedly measured during the experiments (Appendix 5B). Experimental evidence (Kelly, 1966; Omatete, 1971) has shown that electrolyte sorption at a total

solution concentration of 0.1 N is negligible. At a total solution concentration 0.1 N, the measured capacity was due to ion exchange only and was therefore constant. Consequently, only n-1 of the n components concentrations needed to be measured.

Equilibrium data were obtained by passing a solution of known composition through the ion exchange bed via a micropump until equilibrium was obtained, i.e. when the feed concentration equalled the effluent concentration. The bed was then quickly rinsed with deionized water to minimize the change in the resin concentration. The equilibrium composition of the bed was obtained by passing 0.1 N $NaNO_3$ solution through the bed until sodium ions displaced all counter ions in the bed. The concentrations of the effluents were analysed. The experimental procedure is presented in Appendix 5C.

All runs were made at room temperature (22-25°C). The effect of temperature on equilibrium data has been shown to be negligible for a small range of temperature (Section 6.3).

Concentration measurements

For binary component systems, K-H and Na-H, hydrogen ion concentrations were measured by a titration method. Potassium (K) and sodium (Na) ion concentrations were obtained by material balance. The titration method involved titrating samples, each containing 50 ml of the effluent solution, with 0.1 N NaOH. A pH measurement system was used as an indicator, and consisted of an Orion model 91-02 combination pH electrode and an Orion 701A ionalyzer, capable of measuring millivolt signals with a resolution of 0.1 mV.

For the ternary component system, K-Na-H, H^+ and K^+ were measured and Na^+ were obtained by material balance.

Potassium ion concentrations were measured by a system consisting of an Orion 93-19 potassium electrode, an Orion 90-01 single junction reference electrode and the Orion 701A digital meter. Measurements were made directly by dipping the electrodes into the samples. The measured potentials and the potassium ion concentrations were related by the modified Nernst equation.

$$E_K = E_o - E_j + ST\ell n\left(\frac{A_K + K_{NaK}A_{Na} + K_{HK}A_H}{A_o}\right) \qquad (5.11)$$

E_K potential of potassium ion concentration

E_o standard potential

E_j liquid junction potential

S a constant with a theoretical value of $\frac{R}{Z_K f}$

T absolute temperature

A_K, A_{Na}, A_H activity of potassium, sodium and hydrogen ions respectively

K_{NaK}, K_{HK} selectivity constants of Na, H ions relative to K ion respectively

A_o zero potential activity of potassium ion

The manufacturer's values (Orion, 1979) for K_{NaK} and K_{HK} were 0.0002 and 0.01 respectively. These values indicate that the potassium ion selective electrode was 5000 times more sensitive toward potassium ion than sodium ion and 100 times more sensitive toward potassium ion than hydrogen ion. In these experiments the solution which contained the highest level of Na ions had the composition C_K:0.004 M, C_{Na}:0.0942 M and C_H:0.0018 M. The error caused by dropping the term $K_{NaK}A_{Na}$ from Eqn. 5.11 is

$$\text{Percentage error} = \frac{K_{NaK}A_{Na}100}{A_K}$$

For the above mixture

$$\text{Percentage error} \doteqdot \frac{0.0002 \times 0.0942 \times 100}{0.004} \doteqdot 0.5\%$$

This sample calculation suggested that the term $K_{NaK}A_{Na}$ could be dropped from Eqn. 5.11, i.e.

$$E_K = E_o - E_j + ST\ell n\left(\frac{A_K + K_{HK}\,A_H}{A_o}\right) \qquad (5.12)$$

The error caused by dropping the term $K_{HK}A_H$ is

$$\text{Percentage error} = \frac{K_{HK}\,A_H\,100}{A_K} = \frac{A_H}{A_K}$$

Therefore if A_H is kept less than A_K the percentage error for dropping the hydrogen ion interference term would be less than one, thus Eqn. 5.12 becomes

$$E_K = E_o - E_j + ST\ell n\left(\frac{A_K}{A_o}\right) \qquad (5.13)$$

The column effluent samples and the calibrating standard solutions were measured within an hour so that electrode drift was negligible and it could be assumed that both the samples and the calibrating solution were at the same temperature.

The magnitude of liquid junction potentials, E_j, depended on:

- total ionic strengths of the measured solution and a reference filling solution;
- individual concentrations of the measured solution and a reference filling solution;
- temperature.

The filling solution was 0.12 M NaCl saturated with $AgNO_3$. The values of liquid junction potentials for various compositions of KNO_3, $NaNO_3$ and HNO_3 at a total ionic strength of 0.1 M were computed by the Henderson equation (Section 6.3) and the results are shown in Table 5.1. Two observations could be made from the

results shown. Firstly, the changes of E_j should not be ignored since fluctuations of ±0.1 mV corresponded to ±0.4% in concentration. Secondly, the magnitude of E_j depended almost entirely on the levels of hydrogen ion concentrations. This was because hydrogen ion had a high value of equivalent ionic conductivity (λ^o_H = 349.82, λ^o_{Na} = 50.11 and λ^o_K = 73.52 sq.cm/ohm gm.equivalent).

Therefore, to obtain meaningful concentration measurements, E_j of the samples and the calibrating standard solutions must be approximately the same. This was done by making the levels of hydrogen ion concentrations and total ionic strengths of both samples and calibrating solutions the same, i.e. by multicomponent calibrations. Eqn. 5.13 reduces to

$$E_K = E_\phi + ST\ell n\left(\frac{A_K}{A_o}\right)$$

$$E_K = E_\phi + ST\ell n\gamma_K C_K \qquad (5.14)$$

The validity of Eqn. 5.14 was tested with three standard solutions, two being used to obtain E_ϕ and ST, and the third being used to check the accuracy of Eqn. 5.14. The results, Table 5.2, showed that the Nernst equation has yielded a reliable method for measuring potassium ion concentrations, even for the difficult case of C_H greater than C_K, System 4. Multicomponent calibrations effectively corrected for hydrogen ion interference.

Solution Composition			
KNO_3 (M)	$NaNO_3$ (M)	HNO_3 (M)	E_j (mV)
.03	.05	.02	11.8
.041	.0426	.0164	9.7
.045	.05	.005	6.4
.045	.054	.001	4.3
.0219	.0775	.0006	3.2
.0	.10	.0	2.0

Liquid junction potentials, E_j, calculated from the Henderson equation. The junction is solution/0.12 M NaCl saturated with $AgNO_3$.

The error in using the Henderson equation could be up to ±20% (Orion, 1969).

Table 5.1

System	Solution 1	Solution 2	E_ϕ & ST	Solution 3	C_K computed from Eqn. 5.14 (M)	Percentage error in C_K
1	C_K = 0.003 M C_{Na} = 0.09523 M C_H = 0.00177 M E_1 = -140.6 mV	C_K = 0.015 C_{Na} = 0.08323 C_H = 0.00177 E_2 = -100.2	E_ϕ = 5.22071 ST = 25.10193	C_K = 0.01 C_{Na} = 0.08823 C_H = 0.00177 E_3 = -110.1	C_K = 0.01011	1.1
2	C_K = 0.014 C_{Na} = 0.08429 C_H = 0.00171 E_1 = -100.7	C_K = 0.02 C_{Na} = 0.07829 C_H = 0.00171 E_2 = -91.7	E_ϕ = 7.01231 ST = 25.23306	C_K = 0.017 C_{Na} = 0.08129 C_H = 0.00171 E_3 = -95.6	C_K = 0.01714	0.8
3	C_K = 0.004 C_{Na} = 0.0927 C_H = 0.0033 E_1 = -132.0	C_K = 0.02 C_{Na} = 0.0767 C_H = 0.0033 E_2 = -92.2	E_ϕ = 4.54093 ST = 24.72913	C_K = 0.01 C_{Na} = 0.0867 C_H = 0.0033 E_3 = -109.1	C_K = 0.01010	1.0
4	C_K = 0.004 C_{Na} = 0.0911 C_H = 0.0049 E_1 = -131.95	C_K = 0.018 C_{Na} = 0.0771 C_H = 0.0049 E_2 = -94.5	E_ϕ = 5.52877 ST = 24.89898	C_K = 0.01 C_{Na} = 0.0851 C_H = 0.0049 E_3 = -109.1	C_K = 0.01001	0.1

This table shows the accuracies of using Eqn. 5.14 to determine potassium ion concentrations from electrode potential measurements.

Table 5.2

5.3 Results

Binary equilibria

The experimental results of binary ion exchange equilibrium for the K-H and Na-H systems in Dowex 50W X8 are shown in Figures 5.1 and 5.2 respectively. The mean values of the separation factors from this work and the published values are shown below.

System	Mean value of separation factor ($\bar{\alpha}$); $\log \bar{\alpha}_n^i = \int_0^1 \log \alpha_n^i \, dX_i$			
	This Work	Bonner et. al. 1954	Myers & Boyd 1956	Kelly 1966
K-H	2.0	2.09	2.16	2.2
Na-H	1.41	1.49	1.40	1.48

Ternary equilibria

Ternary equilibrium experimental data of K-Na-H system in Dowex 50W X8 are shown in Figures 5.3 and 5.4. Figure 5.3 shows α_H^K vs X_K^* at various levels of sodium ion concentration. Figure 5.4 shows α_H^{Na} vs X_{Na}^* at various levels of potassium ion concentration.

Error analysis

A separation factor for a species i with respect to a species n is given by:

$$\alpha_n^i = \frac{Y_i^* X_n^*}{X_i^* Y_n^*}$$

By taking logarithms and differentiating, the above equation becomes:

$$\frac{\Delta\alpha_n^i}{\alpha_n^i} = \frac{\Delta Y_i^*}{Y_i^*} + \frac{\Delta X_i^*}{X_i^*} + \frac{\Delta Y_n^*}{Y_n^*} + \frac{\Delta X_n^*}{X_n^*} \qquad (5.15)$$

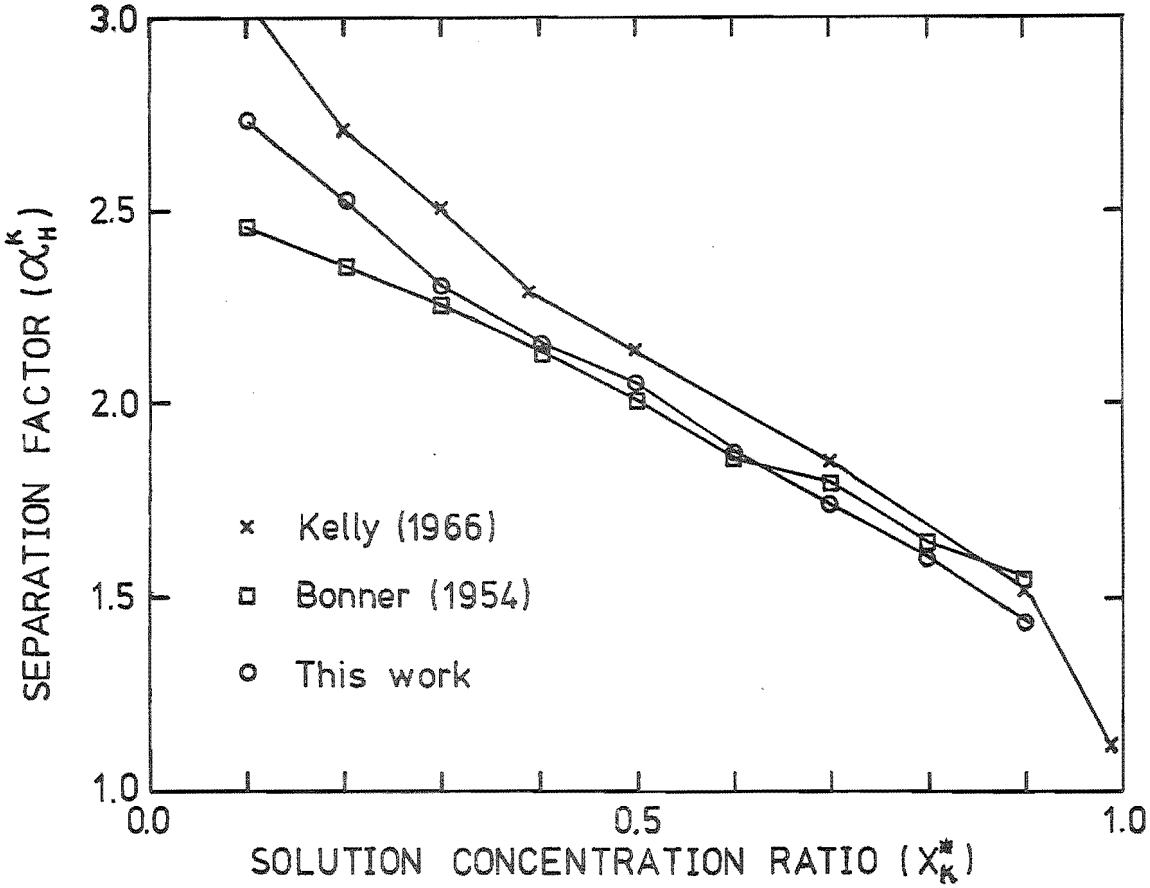

FIGURE 5.1 EQUILIBRIUM EXPRESSION FOR THE K-H/DOWEX 50W X8 SYSTEM AT 0.1N TOTAL SOLUTION CONCENTRATION

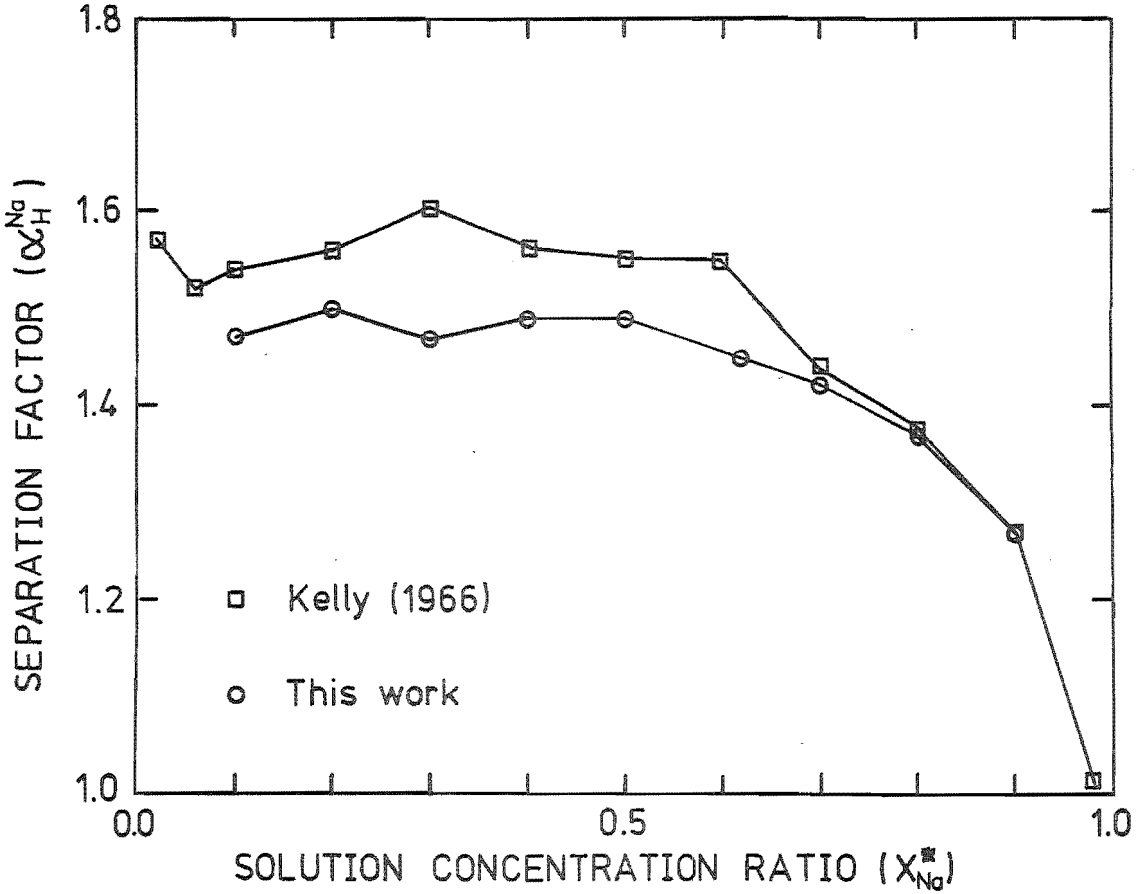

FIGURE 5.2 EQUILIBRIUM EXPRESSION FOR THE Na-H/DOWEX 50W X8 SYSTEM AT 0.1 N TOTAL SOLUTION CONCENTRATION

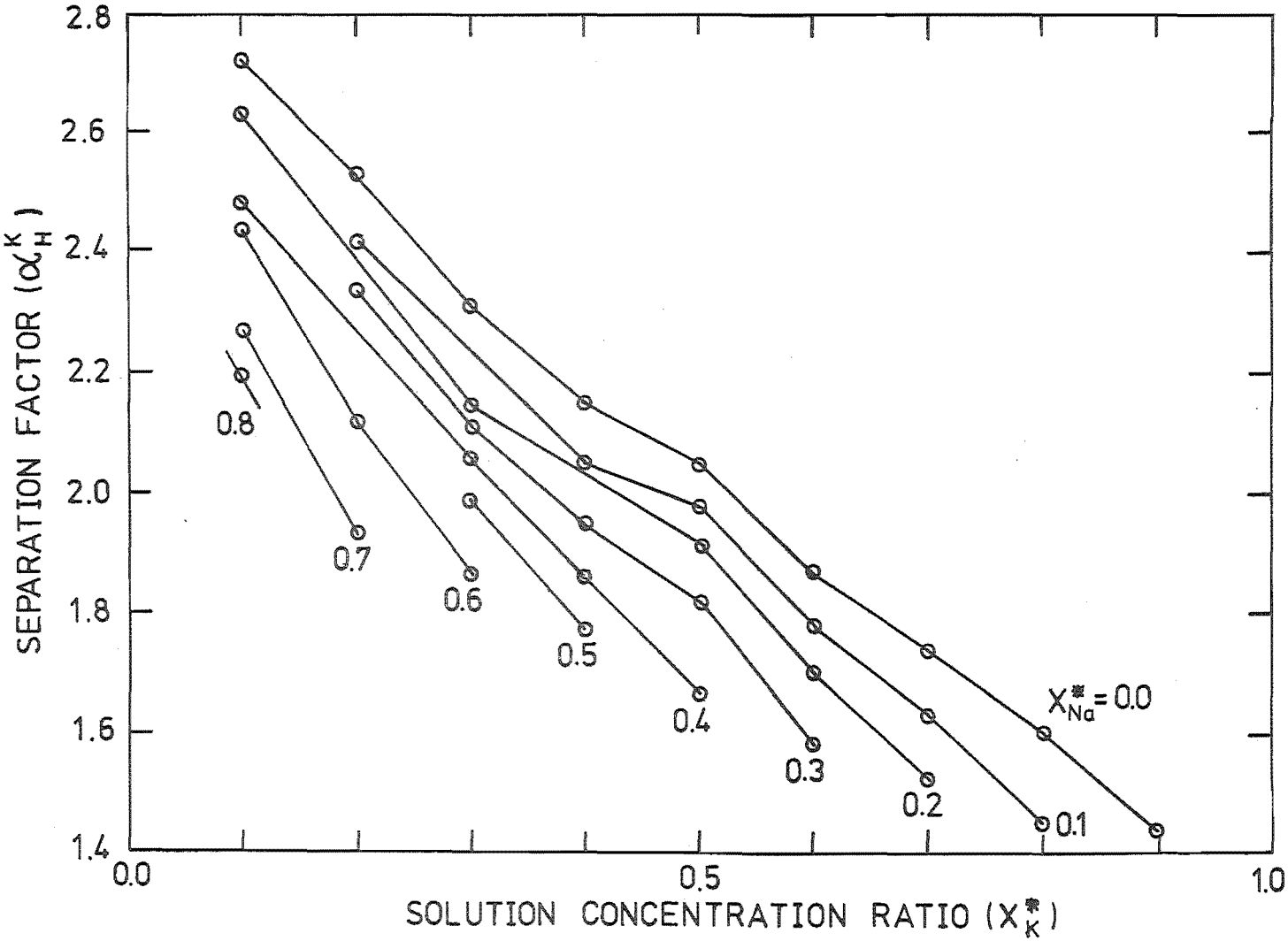

FIGURE 5.3 EQUILIBRIUM EXPRESSION FOR THE K-Na-H/DOWEX 50W X8 SYSTEM AT 0.1N TOTAL SOLUTION CONCENTRATION

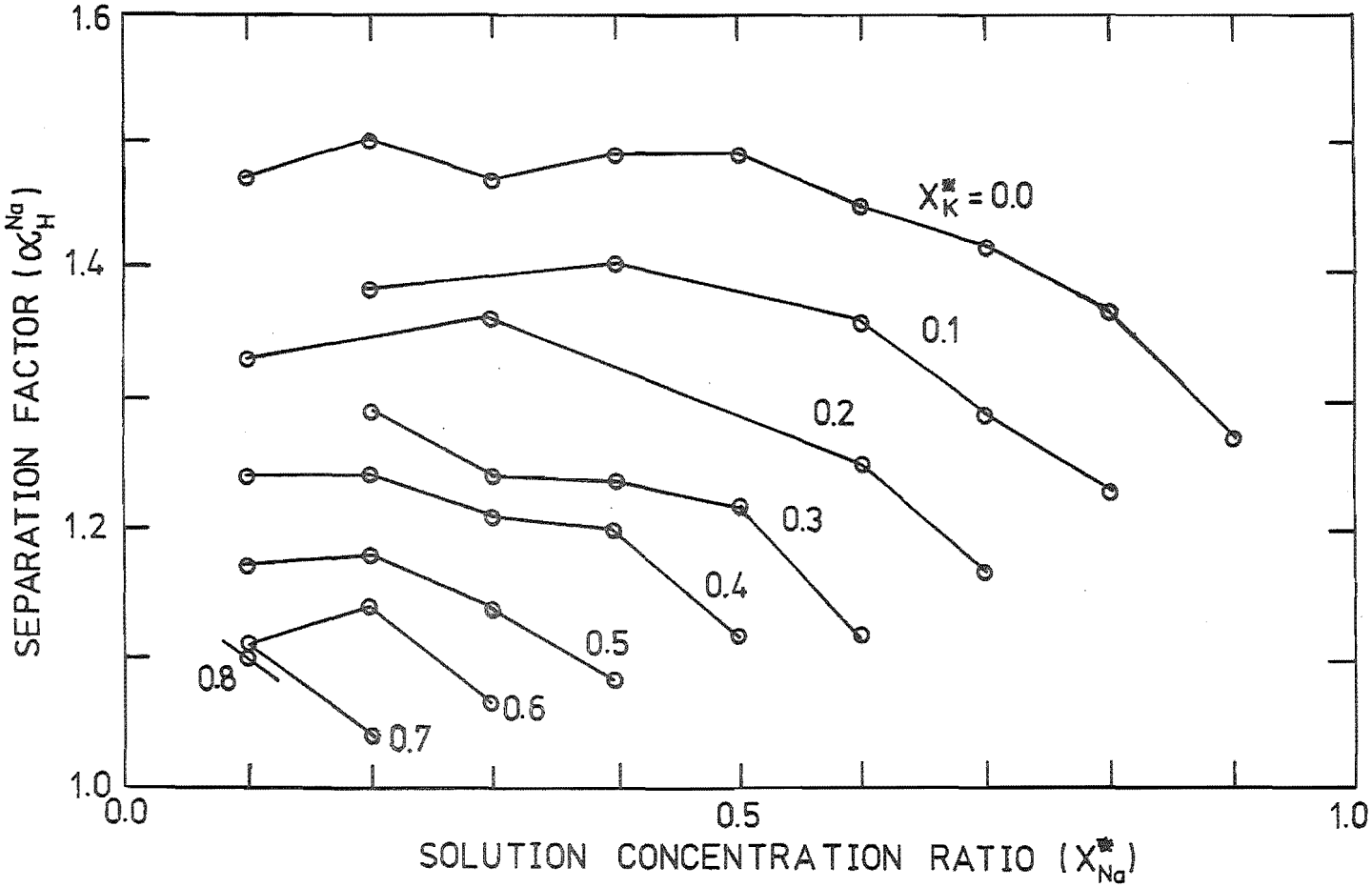

FIGURE 5.4 EQUILIBRIUM EXPRESSION FOR THE K-Na-H/DOWEX 50W X8 SYSTEM AT 0.1 N TOTAL SOLUTION CONCENTRATION

An error of α_n^i calculated by Eqn. 5.15 is called a predicted error. The predicted errors in separation factors of various systems are shown below. The details are given in Appendix 5D.

System	i-n	Concentration level	$\frac{100\Delta Y_i^*}{Y_i^*}$	$\frac{100\Delta Y_n^*}{Y_n^*}$	$\frac{100\Delta X_i^*}{X_i^*}$	$\frac{100\Delta X_n^*}{X_n^*}$	$\frac{100\Delta\alpha_n^i}{\alpha_n^i}$
K-H	K-H	X_K/X_H 0.5/0.5	1.85	1.85	0.45	0.55	4.7
Na-H	Na-H	X_{Na}/X_H 0.5/0.5	1.73	1.73	0.45	0.55	4.5
K-Na-H	K-H	$X_K/X_{Na}/X_H$ 0.3/0.4/0.3	1.76	1.55	1.26	1.36	5.93
K-Na-H	Na-H	$X_K/X_{Na}/X_H$ 0.3/0.4/0.3	3.31	1.55	1.19	1.36	7.41

5.4 Discussion

Experimental method

Results of repeated runs indicated that the column method gave consistent results provided that the following conditions were met:-

- quick rinsing
- negligible electrolyte sorption
- equilibrium was attained

The quick rinsing was necessary so that the change of the equilibrating solution concentrations was minimised. The column method can still be used to obtain equilibrium data when electrolyte sorption is not negligible. In this case the column capacity is given by:

$$Q = Q_{IX} + Q_{ES}$$

Q_{IX} ion exchange capacity

Q_{ES} electrolyte sorption capacity

Q_{IX} and Q_{ES} must be measured separately, and whereas Q_{IX} is

constant, Q_{ES} is not necessarily constant.

Experimental errors can arise from random errors in making up the equilibrating solutions, column capacity, concentration measurements. The magnitude of these errors compared with the predicted errors are shown in Table 5.3.

Item	Parameter	Experimental random error (%)	Average Predicted error (%)
Equilibrating solutions	C_K	-	0.6
"	C_{Na}	-	0.6
"	C_H	-	0.7
Column capacity	EQ	0.28	0.7
Concentrations	C_K	0.7	1.0
"	C_H	0.2	0.9

Table 5.3

For successful measurement of potassium ion concentration, each term in the Nernst equation must be considered in detail.

Binary ion exchange equilibrium

Data for binary ion exchange equilibrium have been well established. The results obtained here agree, within experimental error, with published values.

Ion exchange equilibrium mainly depends on solution concentrations, equivalent fractions of counter ions, valence of counter ions, solvated volumes of counter ions, swelling pressure, ion-pair formations and temperature. In short, an ion exchange resin prefers a counter ion which forms a lower energy state with the fixed ionic group.

The results obtained here showed that the average separation factor of the counter ions are in the following sequence:-

$$\alpha_H^K > \alpha_H^{Na} > \alpha_H^H$$

The corresponding measured solvated bed volumes are:-

$$V_K(23\ ml) < V_{Na}(24.5\ ml) < V_H(25.1 ml)$$

The plots of α_H^K vs X_K^* and α_H^{Na} vs X_{Na}^*, Figures 5.1 and 5.2, show a discontinuity at either X_K^* and X_{Na}^* equal 0.5. Both α_H^K and α_H^{Na} decreased as X_H^* decreased. This was clear for the K-H system, for the Na-H system the decrease was clear at X_H^* less than 0.5. Reichenberg (Helfferich, 1962) obtained similar experimental results. This phenomena could not be due to experimental errors even though as X_H^* decreased the errors in titration increased. Table 5.4 shows the predicted errors in α_H^{Na} for X_{Na}^* ranges from 0.1 to 0.9.

X_{Na}^*	$\frac{\Delta X_{Na}^*}{X_{Na}^*}$	$\frac{\Delta X_H^*}{X_H^*}$	$\frac{\Delta Y_H^*}{Y_H^*}$	$\frac{\Delta \alpha_H^{Na}}{\alpha_H^{Na}} \times 100$
0.1	.0070	.0057	.0145	4.2
0.2	.0080	.0070	.0149	4.5
0.3	.0074	.0074	.0155	4.6
0.4	.0068	.0074	.0162	4.7
0.5	.0045	.0055	.0173	4.5
0.6	.0070	.0086	.0188	5.3
0.7	.0069	.0091	.0212	5.8
0.8	.0067	.0102	.0257	6.8
0.9	.0040	.0074	.0383	8.8

Table 5.4

The predicted error analysis showed that the lowest value of α_H^{Na} at X_{Na}^* equals 0.1 ($\alpha_H^{Na} = 1.47 \pm 0.06$) was outside the range of the highest value of α_H^{Na} at X_{Na}^* equals 0.9 ($\alpha_H^{Na} = 1.27 \pm 0.11$). The experimental values of α_H^{Na} at X_{Na}^* equals 0.9 for five repeated runs were 1.27, 1.27, 1.27, 1.27 and 1.28.

Ternary ion exchange equilibrium

Experimental results for ternary components, Figures 5.3 and 5.4, showed that α_H^K and α_H^{Na} depended on X_K^*, X_{Na}^*, and X_H^*. The presence of the third component decreased the values of the separation factors.

The shapes of the curves for ternary equilibrium followed the shapes of the binary equilibrium closely.

The separation factors calculated here were based on hydrogen ion since it was the least preferred of the counter ions considered. For a binary K-H system, at the feed $X_K^* = 0.5$ and $X_H^* = 0.5$, at equilibrium the resin composition was $Y_K^* = 0.672$ and $Y_H^* = 0.328$ ($\alpha_H^K = 2.05$) as was expected since potassium was preferred to hydrogen. Considering the feed at $X_K^* = 0.5$, $X_{Na}^* = 0.4$ and $X_H^* = 0.1$, at equilibrium the resin composition was $Y_K^* = 0.610$, $Y_{Na}^* = 0.317$ and $Y_H^* = 0.073$ ($\alpha_H^K = 1.672$) indicating that the presence of sodium ions decreased the separation factor of potassium ions (α_H^K). This was also found in the Na-H system in which the presence of potassium ions decreased α_H^{Na} for the same level of sodium ion concentration.

The results of the ternary equilibrium could be related to the results of binary equilibrium. The separation factors, α_H^K and α_H^{Na}, for both binary and ternary systems decreased as hydrogen ion concentration decreased.

The results obtained here were in contrast with Dranoff and Lapidus (1957), Glaski (1960) and Pieroni and Dranoff (1963) who concluded that α_n^i for any two ions were the same in binary and ternary mixtures.

In section 5.1 it was shown that the separation factor is given by:

$$\alpha_n^i = \frac{\gamma_i \, f_n}{f_i \, \gamma_n}$$

Activity coefficients in the solution phase can be assumed to be constant since the total ionic strength is constant and equal to 0.1 M. Thus the variations in the separation factor indicate that activity coefficients in the resin phase, f_i and f_n, are not constant. This can be explained if the resin is considered to be a strong electrolyte having a concentration equal to its capacity, i.e. about 2 M. At this high concentration, there will be ion associations which will affect the values of the activity coefficients. It was concluded earlier that α_H^i decreased as X_H^* decreased. Accordingly, X_H^* decreases as f_H/f_i decreases. For a given ion its activity coefficient decreases when its ion association increases (Robinson and Stokes, 1959). Therefore, as X_H^* decreases, either the H^+ ions in the resin phase interact more with the fixed ionic groups or counter ions i interact less with the fixed ionic groups, or both happen together.

APPENDIX 5A

EXPERIMENTAL EQUILIBRIUM DATA

Tables 5A.1 and 5A.2 show binary ion exchange equilibrium data for K-H and Na-H systems respectively.

Tables 5A.3 and 5A.4 show ternary ion exchange equilibrium data for α_H^K in K-Na-H system and α_H^{Na} in K-Na-H system respectively.

X_K^*	Run	Y_K^*	Average Value of Y_K^*	α_H^K
0.1	1	0.2361		
	2	0.2319	0.2322	2.72
	3	0.2308		
	4	0.2298		
0.2	1	0.3863	0.3861	2.52
	2	0.3859		
0.3	1	0.4977	0.4970	2.31
	2	0.4962		
0.4	1	0.5891	0.5891	2.15
	2	0.5891		
0.5	1	0.6720		
	2	0.6733	0.6720	2.05
	3	0.6731		
	4	0.6695		
0.6	1	0.7382	0.7379	1.87
	2	0.7376		
0.7	1	0.8038	0.8025	1.74
	2	0.8011		
0.8	1	0.8646	0.8644	1.60
	2	0.8642		
0.9	1	0.9281	0.9283	1.44
	2	0.9283		
	3	0.9283		
	4	0.9283		

Ion exchange equilibrium data of K-H/Dowex 50W X8 system at 0.1 N total solution concentration.

Table 5A.1

X^*_{Na}	Run	Y^*_{Na}	Average Value of Y^*_{Na}	α^{Na}_{H}
0.1	1	0.1384		
	2	0.1406		
	3	0.1409	0.1401	1.47
	4	0.1409		
	5	0.1399		
0.2	1	0.2725	0.2727	1.50
	2	0.2728		
0.3	1	0.3871	0.3870	1.47
	2	0.3868		
0.4	1	0.4995	0.4987	1.49
	2	0.4978		
0.5	1	0.5992		
	2	0.6010		
	3	0.5991	0.5988	1.49
	4	0.5958		
	5	0.5987		
0.6	1	0.6868	0.6852	1.45
	2	0.6836		
0.7	1	0.7692	0.7684	1.42
	2	0.7675		
0.8	1	0.8455	0.8453	1.37
	2	0.8451		
0.9	1	0.9196		
	2	0.9196		
	3	0.9196	0.9197	1.27
	4	0.0196		
	5	0.9206		

Ion exchange equilibrium data of Na-H/Dowex 50W X8 system at 0.1 N total solution concentration.

Table 5A.2

X^*_{Na}	α^K_H							
	0.1	0.2	0.3	0.4	0.5	0.6	0.7	0.8
X^*_K								
0.1		2.633		2.480		2.432	2.267	2.192
0.2	2.417		2.325			2.115	1.931	
0.3		2.153	2.109	2.061	1.992	1.872		
0.4	2.043	2.037	1.946	1.864	1.776			
0.5	1.968	1.913	1.815	1.672				
0.6	1.777	1.701	1.578					
0.7	1.625	1.520						
0.8	1.444							

Ion exchange equilibrium data of K-Na-H/Dowex 50W X8 system at 0.1 N total solution concentration.

Table 5A.3

X_K^*	α_H^{Na}							
	0.1	0.2	0.3	0.4	0.5	0.6	0.7	0.8
X_{Na}^*								
0.1		1.332		1.240	1.174	1.106	1.112	1.103
0.2	1.384		1.294	1.242	1.180	1.137	1.038	
0.3		1.361	1.244	1.206	1.143	1.065		
0.4	1.405		1.241	1.198	1.085			
0.5			1.222	1.115				
0.6	1.359	1.250	1.118					
0.7	1.294	1.167						
0.8	1.230							

Ion exchange equilibrium data of K-Na-H/Dowex 50W X8 system at 0.1 N total solution concentration.

Table 5A.4

APPENDIX 5B

CAPACITY MEASUREMENT

The capacity of an ion exchange resin is defined as the number of exchangeable ions in a specific quantity of the resin and may be measured in a number of units. In this work, the basis used is number of equivalents in the bed used. The column method was used for capacity measurement. The total solution concentration was 0.1 N, ensuring that electrolyte sorption was negligible.

The capacity of the Dowex 50W X8 resin in hydrogen form was determined since hydrogen concentration was accurately and easily analysed.

The experimental procedure was:-

(1) the resin was in H form in water;

(2) 0.1 N $NaNO_3$ was passing through the bed until the resin was totally converted to Na form;

(3) the effluent collected was determined by titration for hydrogen equivalents.

The capacity runs were obtained randomly between equilibrium runs. Results are shown in Tables 5B.1 and 5B.2.

Run Number	Number of equivalents (meq)	Average number of equivalents (meq)	Experimental random error (%)	Predicted error (%)
1	47.325			
2	47.200	47.26	0.13	0.7
3	47.250			

Capacity results for the bed used in the binary equilibrium experiments.

Table 5B.1

Run Number	Number of equivalents (meq)	Average number of equivalents (meq)	Experimental random error (%)	Predicted error (%)
1	46.78			
2	47.04	46.91	0.28	0.7
3	46.94			

Capacity results for the bed used in the ternary equilibrium experiments.

Table 5B.2

APPENDIX 5C

EXPERIMENTAL PROCEDURE IN EQUILIBRIUM MEASUREMENTS

The following procedure was used in the determination of separation factors α_H^K and α_H^{Na}:-

(1) The resin was in Na form in water.

(2) An equilibrating solution X_K^*, X_{Na}^* and X_H^* was passed through the bed until the bed was in equilibrium with the feed.

(3) The bed was quickly rinsed with deionized water until there was no traces of the equilibrating solution.

(4) 0.1 N sodium nitrate solution was passed through the bed until the resin was converted to Na form.

(5) The effluent collected was analysed for number of equivalents of potassium and hydrogen.

(6) α_H^K and α_H^{Na} were calculated from

$$Y_K^* = \frac{\text{number of potassium equivalents}}{\text{bed capacity}}$$

$$Y_H^* = \frac{\text{number of hydrogen equivalents}}{\text{bed capacity}}$$

$$Y_{Na}^* = 1 - Y_K^* - Y_{Na}^*$$

$$\alpha_H^K = \frac{Y_K^* X_H^*}{X_K^* Y_H^*} ; \qquad \alpha_H^{Na} = \frac{Y_{Na}^* X_H^*}{X_{Na}^* Y_H^*}$$

APPENDIX 5D

ERROR ANALYSIS-EQUILIBRIUM DETERMINATION

5D.1 Introduction

The design of the apparatus and experimental method was based on the error analysis in this appendix.

For each derived measurement, an error estimate has been made in terms of the error in each fundamental measurement, for example the error in the volume of a block (the derived measurement) would have been estimated from the errors in the measurements of the sides (the fundamental measurements).

The error in a fundamental measurement was taken from the instruments specification (Table 5D.1) or determined by comparison against a local standard (Table 5D.2).

The errors in equilibrium experiment can arise from errors in:-

- making up standard solutions (Table 5D.3)
- making up equilibrating solutions (Section 5D.2)
- capacity measurement (Section 5D.3)
- hydrogen concentration measurement (Section 5D.4)
- potassium concentration measurement (Section 5D.5)

Instrument	Range	Error
Burette	50 ml	±0.05 ml
701A Ionalyzer	±1999.9 mV	±0.1 mV
Mettler P1200	1200 gm	±0.01 gm
Avery scale	10 kg	±2.5 gm
Platform balance	100 kg	±50 gm

Instrument errors from manufacturer's specification.

Table 5D.1

Instrument	Size	Error
Pipette	50 ml	±0.1 ml
Volumetric flask A	1000 ml	±1.23 ml
" " B	1000 ml	±1.5 ml
" " C	1000 ml	±0.56 ml
" " D	2000 ml	±2.05 ml
" " E	2000 ml	±1.55 ml
" " F	2000 ml	±0.10 ml

Instrument errors determined by comparison against a local standard.

Table 5D.2

Standard Solution	Method Used	Equation used for Estimating the Error	Percentage Estimate Error
0.1 N NaOH	Ampoule	$\frac{\Delta C}{C} = \frac{\Delta \text{number of equivalents}}{\text{number of equivalents}} + \frac{\Delta \text{solution volume}}{\text{solution volume}}$	0.2
0.02N NaOH	Ampoule	$\frac{\Delta C}{C} = \frac{\Delta \text{number of equivalents}}{\text{number of equivalents}} + \frac{\Delta \text{solution weight}}{\text{solution weight}}$	0.15
0.1 N KNO_3	Gravimetric	$\frac{\Delta C}{C} = \frac{\Delta KNO_3 \text{ crystal weight}}{KNO_3 \text{ crystal weight}} + \frac{\Delta \text{solution weight}}{\text{solution weight}}$	0.1
0.1 N $NaNO_3$	Gravimetric	$\frac{\Delta C}{C} = \frac{\Delta NaNO_3 \text{ crystal weight}}{NaNO_3 \text{ crystal weight}} + \frac{\Delta \text{solution weight}}{\text{solution weight}}$	0.1
0.1 N HNO_3	Dilution	$\frac{\Delta C}{C} = \text{Error in conc. solution} + \frac{\Delta 0.1N\ HNO_3 \text{ solution weight}}{0.1N\ HNO_3 \text{ solution weight}} + \frac{\Delta \text{concentrated solution weight}}{\text{concentrated solution weight}}$	0.2

Table 5D.3 Estimated Standard Solution Error

5D.2 Equilibrating Solution Error

Binary Component

Equilibrating solutions, to a total normality of 0.1, were made by weight combination of KNO_3 and HNO_3, 0.1N solutions or $NaNO_3$ and HNO_3 0.1N solutions.

The error in the equilibrating solutions can be estimated as:-

$$\frac{\Delta X_i^*}{X_i^*} = \frac{\Delta C_i}{C_i} + \frac{\Delta C_o}{C_o} \qquad (5D.1)$$

$$\frac{\Delta C_i}{C_i} = \frac{\Delta C_i^o}{C_i^o} + \frac{\Delta W_i}{W_i} + \frac{\Delta W_i + W_j}{W} \qquad (5D.2)$$

$$\frac{\Delta C_o}{C_o} = \frac{\Delta C_i + \Delta C_j}{C_o} \qquad (5D.3)$$

where C_i, C_i^o, C_o, W_i, W are the concentration of component i in the equilibrating solution, the concentration of component i in the standard solution (C_i^o = 0.1 N), the total solution concentration of the equilibrating solution (C_o = 0.1 N), the weight of component i in the equilibrating solution, the total weight of the equilibrating solution respectively.

Considering the K-H system, the errors in the calibrating solution at X_K^*/X_H^* = 0.5/0.5 were estimated from Equations 5D.1-5D.3 to be

$$\frac{\Delta X_K^*}{X_K^*} = 0.0045$$

$$\frac{\Delta X_H^*}{X_H^*} = 0.0055$$

For the Na-H system, the errors in the calibrating solutions at X^*_{Na} range from 0.1 to 0.9, as shown below.

X^*_{Na}	W_{Na} (gm)	W_H (gm)	$\frac{\Delta C_{Na}}{C_{Na}}$	$\frac{\Delta C_H}{C_H}$	$\frac{\Delta X^*_{Na}}{X^*_{Na}}$	$\frac{\Delta X^*_H}{X^*_H}$
0.1	1004	9014	.004	.0028	.007	.0057
0.2	1004	4006	.0045	.0036	.008	.007
0.3	1506	3505	.0037	.0037	.0074	.0074
0.4	2008	3005	.0032	.0038	.0068	.0074
0.5	5020	5008	.002	.003	.0045	.0055
0.6	2410	1603	.0032	.0048	.0070	.0086
0.7	2811	1201	.0031	.0053	.0069	.0091
0.8	3213	801	.0030	.0063	.0067	.0102
0.9	8132	901	.0018	.0053	.004	.0074

Ternary Component

For a ternary system the error in the equilibrating solution can be shown to be:-

$$\frac{\Delta X^*_i}{X^*_i} = \frac{\Delta C_i}{C_i} + \frac{\Delta C_o}{C_o} \qquad (5D.4)$$

$$\frac{\Delta C_i}{C_i} = \frac{\Delta C^o_i}{C^o_i} + \frac{\Delta W_i}{W_i} + \frac{\sum_{j=1}^{3} \Delta W_j}{W} \qquad (5D.5)$$

$$\frac{\Delta C_o}{C_o} = \frac{\sum_{j=1}^{3} \Delta C_j}{C_o} \qquad (5D.6)$$

Considering the mixture at $X^*_K/X^*_{Na}/X^*_H = 0.3/0.4/0.3$, the errors in the calibrating solution were estimated from Equations 5D.4 - 5D.6 to be:-

$$\frac{X^*_K}{X^*_K} = 0.0126, \quad \frac{X^*_{Na}}{X^*_{Na}} = 0.0119 \quad \text{and} \quad \frac{X^*_H}{X^*_H} = 0.0136$$

5D.3 Capacity Measurement Error

The error in the capacity measurement can be estimated from:-

$$\frac{\Delta EQ}{EQ} = \frac{\Delta C_H}{C_H} + \frac{\Delta Vef}{Vef} \qquad (5D.7)$$

$$\frac{\Delta C_H}{C_H} = \frac{\Delta C_{NaOH}}{C_{NaOH}} + \frac{\Delta V_{NaOH}}{V_{NaOH}} + \frac{\Delta V_H}{V_H} \qquad (5D.8)$$

where EQ, C_H, Vef, C_{NaOH} and V_H are the total number of equivalents in the bed used for equilibrium measurement, hydrogen concentration in the effluent, effluent volume, concentration of sodium hydroxide used for titration, volume of sodium hydroxide and volume of an effluent sample used for titration.

The following data was used to estimate capacity measurement error:-

C_{NaOH} = 0.1 ± 0.02 N (Table 5D.3)

V_{NaOH} = 23.4 ± 0.05 ml (Table 5D.1)

V_H = 50 ± 0.1 ml (Table 5D.2)

Vef = 1000 ± 1 ml (Table 5D.2)

Substituting the above data in Equations 5D.7 and 5D.8 gave

$$\frac{\Delta EQ}{EQ} = 0.007$$

5D.4 Hydrogen Concentration Measurement Error

Hydrogen concentration was determined by titration with sodium hydroxide solution. The error in the measurement can be estimated from:-

$$\frac{\Delta C_H}{C_H} = \frac{\Delta C_{NaOH}}{C_{NaOH}} + \frac{\Delta V_{NaOH}}{V_{NaOH}} + \frac{\Delta V_H}{V_H} \qquad (5D.9)$$

$$\frac{\Delta Y_H^*}{Y_H^*} = \frac{\Delta C_H}{C_H} + \frac{\Delta Vef}{Vef} + \frac{\Delta EQ}{EQ} \qquad (5D.10)$$

For the K-H and Na-H systems, the concentration of sodium hydroxide was 0.1 N. The values $\Delta Y_H^*/Y_H^*$ for the Na-H system at X_{Na}^* ranges from 0.1 to 0.9 is shown below.

X_{Na}^*	V_{NaOH}	$\frac{Y_H^*}{Y_H}$
0.1	20.30	.0145
0.2	17.20	.0149
0.3	14.48	.0155
0.4	11.85	.0162
0.5	9.50	.0173
0.6	7.40	.0188
0.7	5.45	.0212
0.8	3.66	.0257
0.9	1.90	.0383

For the K-Na-H system, the concentration of sodium hydroxide was 0.02 N and $\Delta Y_H^*/Y_H^*$ at $X_K^*/X_{Na}^*/X_H^*$ = 0.3/0.4/0.3 was estimated to be:-

$$\frac{\Delta Y_H^*}{Y_H^*} = 0.0155$$

5D.5 Potassium Concentration Measurement Error

Potassium concentration was derived from the Nernst equation:-

$$E = E_o + \frac{RT}{Z_K f} \ln C_K$$

By taking logarithms and differentiating and substitute values of R, Z_K, f and T at 25°C, it can be shown that:-

$$\frac{\Delta C_K}{C_K} = \frac{\Delta E + \Delta E_o}{25.69} \qquad (5D.11)$$

ΔE_o is found from electrode calibrations, i.e.

$$\Delta E_o = \Delta E + 25.69 \frac{\Delta C_K'}{C_K'} \qquad (5D.12)$$

where $\Delta C_K'/C_K'$ is the calibrating solution error and given by Eqn. 5D.5.

$$\frac{\Delta C_K'}{C_K'} = \frac{\Delta C_K^o}{C_K^o} + \frac{\Delta W_K}{W_K} + \frac{\Delta W_K + \Delta W_{Na} + \Delta W_H}{W}$$

For an average case, $X_K^*/X_{Na}^*/X_H^* = 0.3/0.4/0.3$, $\Delta C_K'/C_K'$ was found to be 0.0018, thus from Eqn. 5D.12, $\Delta E_o = 0.1462$ millivolt. The error in potassium concentration measurement was, Eqn. 5D.11, then equalled to 0.0096.

$\Delta Y_K^*/Y_K^*$ can be determined from:-

$$\frac{\Delta Y_K^*}{Y_K^*} = \frac{\Delta C_K}{C_K} + \frac{\Delta Vef}{Vef} + \frac{\Delta EQ}{EQ}$$

$$= 0.0096 + 0.001(\text{Table 5D.2}) + 0.007(\text{Section 5D.3})$$

$$\frac{\Delta Y_K^*}{Y_K^*} = 0.0176$$

5D.6 Conclusion

The result of the analysis showed that the errors in the equilibrium measurement were in an acceptable range (4.5% to 7.4%; Section 5.3).

CHAPTER 6

COLUMN EXPERIMENTS

6.1 Introduction

Objective

A computer program to simulate multicomponent fixed-bed ion exchange columns has been developed, and its numerical method and numerical integration technique have been verified. A comparison between calculated and experimentally measured breakthrough curves will now confirm the equations of the model.

In the past, the effluent concentration from a fixed-bed ion exchange column has been determined by collecting effluent fractions, and analysing them by standard methods, for example, titration. With the availability of advanced instrumentation, these measurements can be done continuously with ion selective electrodes and recording results with a data logging system.

This chapter presents an experimental method for measuring experimental breakthrough curves.

Ion Exchange Resin

Dowex 50W X8 ion exchange resin was used because it is a common commercially available cation exchanger and its physical and chemical data are available (Table 6.1). The commercial resin was wet screened by sieving under deionized water. The screened particles (18# - 25# Na form) were analysed for average diameter and this was found to be 0.074 cm.

The wet resin was transferred into a two inch column, back-washed to remove air bubbles and dirt, and pretreated with 1N NaOH, deionized water and 1N HNO_3 for several cycles.

Type	Strongly acidic cation exchanger
Active group	sulfonic acid
Cross linking (%)	8.0
Form supplied	Na and H
Mesh size (wet)	16-52# (.3-1.0 mm diameter)
Physical form	spheres
Shipping density (lb/cu.ft)	53 (Na):50.0 (H)
Shipping moisture content (%)	44-47 (Na):51-54 (H)
Volume change (%)	Na → H 8%
Effective pH range	0-14
Order of selectivity for	Ba > Sr > Ca > Mg > Be
common ions	Ag>Cs>Rb>K>NH_4>Na>H>Li
Sphericity (%)	>95
Maximum operating temp (^{o}C)	150

From "A laboratory ion exchange manual" Dow Chemical Company (1971)

Table 6.1: Properties of Dowex 50W X8 ion exchange resin.

Solution Flow Rate

The solution flow rate is an important factor in an ion exchange operation. Its effect on a breakthrough curve shape is profound for favourable equilibrium. A flow rate should be selected such that a plateau zone is developed in a reasonable amount of time. Generally a low flow rate (3.0-10.0 ml/min sq.cm) is employed, but if too low the column can be in equilibrium at all points. A high flow rate (>10 ml/min sq.cm) is used when the process solution is very dilute. Some previously used flow

rates and the flow rates used in this work are:-

Flow rate (ml/min sq.cm)	Authors
3.0 - 10.0	Samuelson (1963)
2.0 - 7.0	Kelly (1966)
4.5	Clazie (1966)
6.1	Omatete (1971)
3.0 - 15.0	This work

With the availability of GPFIXC any flow rate can be simulated to study its effect on the computed breakthrough curve.

Water Quality

Large amounts of water are required in ion exchange operations for making up process solutions and washing the bed. With such large amounts of water, the presence of polyvalent ions even in trace concentrations would poison the bed because of their high selectivities at low concentrations.

The analysis of local tap water showed an average hardness of 40 mg/litre. The hardness was due to the presence of calcium carbonate (30 mg/litre) and magnesium carbonate (10 mg/litre). The corresponding normalities of $CaCO_3$ and $MgCO_3$ were 0.0006 and 0.00024 respectively. For one ion exchange operation, the amount of water required was approximately 100 litres, and the amount of hardness in this 100 litres was 0.084 equivalents. Since the ion exchange bed contained 3.573 equivalents of exchanging ions, the resin poisoned would be 2.35% of the bed.

Thus the tap water needed to be purified and a two bed system, with Dowex 50W X8 and Dowex 21K, was used to deionize the tap water.

Process Solutions

Feed and calibrating solutions were made up as in the equilibrium experiment (Chapter 5).

6.2 Concentration Measurement

Concentration measurement for potassium and hydrogen ions was carried out using ion selective electrodes. The Nernst equation (Appendix 6B) was used to convert measured electrical signals to corresponding concentrations.

Parameters that had to be considered were activity coefficients, liquid junction potentials, electrode interferences, electrode driftings, reference filling solution, electrode calibrations and multicomponent calibrating solutions.

In equilibrium experiments, the filling solution used for the reference electrode was 0.12N sodium chloride saturated with silver nitrate solution as was recommended by Orion (1979). At this level of ionic strength the filling solution did not interfere with potassium electrode. A disadvantage was that since the filling solution concentration was low, liquid junction potentials generated at the reference electrode would vary with the change in hydrogen ion concentration from one sample to another. However, in the equilibrium experiments, concentration measurement was batchwise and therefore the levels of hydrogen ion concentration in the calibrating solutions were made similar to those in the samples. In column experiments, the levels of hydrogen ion concentration were changing throughout the breakthrough curve, thus prohibited the use of the above technique. Consequently, the filling solution used in the column experiments was Orion 900001 equitransferent solution containing Na, K, NO_3 and Cl ions saturated with Ag ions (Orion, 1969). Orion (1979)

recommended against the use of this filling solution because of its release of potassium ions into the solution being measured. However, as shown in Section 6.4, by placing the reference electrode at the downstream end of the cell chamber, the filling solution could not diffuse back to the potassium electrode which was placed at the entry to the chamber.

K-Na System

The Orion 93-19 potassium ion selective electrode was used to monitor potassium ion concentrations for the K-Na system. The form of the Nernst equation used was:-

$$E_i = E_o + ST \ln \left(\frac{\gamma_i C_i}{A_o}\right)$$

The solutions used to calibrate the electrodes were:-

- calibrating solution 1; 0.1N KNO_3
- calibrating solution 2; 0.01N KNO_3 and 0.09N $NaNO_3$

The total ionic strengths of the calibrating solutions were made to be the same as that of the effluent solution so that the activity coefficient of potassium ions can be assumed to be constant for all of the solutions being measured.

Na-H System

The Orion 91-01 pH electrode was used to determine hydrogen ion concentrations. The levels of hydrogen ion concentration in the effluents varied from 0.0N to 0.1N, suggesting that the liquid junction potential term had to be included in the Nernst equation. The form of the Nernst equation used was:-

$$E_i = E_o - E_j + ST \ln \left(\frac{\gamma_i C_i}{A_o}\right)$$

The Henderson equation (Appendix 6B) was used to estimate E_j. The calibrating solutions used were:-

- calibrating solution 1; 0.1N HNO_3
- calibrating solution 2; 0.01N HNO_3 and 0.09N $NaNO_3$

K-Na-H System

The Orion 93-19 potassium and the Orion 91-01 hydrogen ion selective electrodes were used to measure potassium and hydrogen ion concentrations respectively. The experiment was planned so that the simplified form of the Nernst equation:-

$$E_i = E_o + ST \ln \left(\frac{\gamma_i C_i}{A_o}\right)$$

would apply for both electrodes. The composition of the feeds and the presaturated beds were arranged so that:-

(1) Liquid junction potentials of the effluents did not vary significantly during the run. Table 6.2 shows liquid junction potentials of the K-Na-H system at various compositions with Orion equitransferent solution as a junction.

(2) Potassium nitrate concentrations were greater than or equal to the nitric acid concentrations, therefore interferences by hydrogen ions at the potassium electrode were negligible (Chapter 5).

Multicomponent solutions used for calibrating the electrodes are presented in Table 6.3

The programs, written in BASIC, to compute points on experimental breakthrough curves, are shown in Appendix 6C.

Concentration ratio ($X_K/X_{Na}/X_H$)	E_j (mV)
.01/.98/.01	1.5
.1/.8/.1	1.9
.2/.6/.2	2.3
.02/.96/.02	1.6
.3/.4/.3	2.7
.5/.3/.2	2.4
.05/.92/.03	1.6
.4/.5/.1	2.0
.04/.95/.01	1.5

Notes:

(1) The junction is Orion 900001 equitransferent solution.

(2) Total solution of the samples = 0.1N.

(3) The Henderson equation was used to compute E_j.

Table 6.2: Liquid junction potential

Run numbers	Effluent concentration ratio ($X_K/X_{Na}/X_H$)		Calibrating Solution 1	Calibrating Solution 2
	Beginning of run	End of run	($X_K/X_{Na}/X_H$)	($X_K/X_{Na}/X_H$)
15:17 & 37:39	0.0/1.0/0.0	0.3/0.5/0.2	0.03/0.95/0.02	0.3/0.5/0.2
16:18 & 38:40	0.3/0.5/0.2	0.0/1.0/0.0	0.03/0.95/0.02	0.3/0.5/0.2
19:21	0.0/1.0/0.0	0.3/0.3/0.4	0.03/0.93/0.04	0.3/0.3/0.4
20:22	0.3/0.3/0.4	0.0/1.0/0.0	0.03/0.93/0.04	0.3/0.3/0.4
23:31 & 33:35	0.0/1.0/0.0	0.6/0.2/0.2	0.06/0.92/0.02	0.6/0.2/0.2
24:32 & 34:36	0.6/0.2/0.2	1.0/0.0/0.0	0.06/0.92/0.02	0.6/0.2/0.2
25:28	1.0/0.0/0.0	0.7/0.2/0.1	0.97/0.02/0.01	0.7/0.2/0.1
26:29	0.7/0.2/0.1	0.4/0.4/0.2	0.7/0.2/0.1	0.4/0.4/0.1
27	0.4/0.4/0.2	1.0/0.0/0.0	0.4/0.4/0.2	0.94/0.04/0.02
30	0.4/0.4/0.2	0.0/1.0/0.0	0.35/0.60/0.05	0.07/0.92/0.01

Multicomponent calibrating solutions were used to determine E_o and S, which were constants in the Nernst equations, the requirements for the solutions were:

(1) the compositions were in the ranges of the effluent solutions;

(2) the total ionic strengths were the same as those of the effluent solutions.

Table 6.3: Calibrating Solutions

6.3 Effect of Temperature on Column Experiments

In an ion exchange operation, temperature has effects on:

- ion exchange rate
- ion exchange equilibrium
- concentration measurement.

This section investigates the dependence of the above parameters on the temperature.

Effect of temperature on ion exchange rate

For an exchanging species i in a solution passing through a fixed-bed ion exchange column, its self mass transfer coefficients are given by (Chapter 3):-

$$k_i = \frac{3.4482 F\varepsilon}{A d_p} \left(\frac{Re\mu}{\rho D_i}\right)^{-0.5}$$ for solution phase diffusion

$$\bar{k}_i = \frac{60 \bar{D}_i Q}{d_p^2 C_o}$$ for particle phase diffusion

For a small change in temperature ($\pm 2.5^{o}C$), ε and d_p can be assumed to be constant and thus for a constant feed operation:-

$$k_i \alpha D_i^{0.5}$$

$$\bar{k}_i \alpha \bar{D}_i$$

The diffusion coefficient of species i in the solution phase at infinite dilution is given by (Robinson and Stokes, 1959):-

$$D_i^o = \frac{RT\lambda_i^o}{|Z_i| f^2} \qquad (6.1)$$

where λ_i^o is the ionic equivalent conductivity of species i at infinite dilution.

The ionic equivalent conductivity at infinite dilution is a function of temperature. Its variation with temperature can

be expressed by a cubic equation (Harn and Owen, 1957):-

$$\lambda_i^o = \lambda_i^o(\text{at } 25^oC) + A_1(T - 298.15) + A_2(T-298.15)^2 + A_3(T-298.15)^3 \quad (6.2)$$

Values of A_1, A_2, A_3 and λ_i^o (at 25°C) for H, Na and K ions are:-

Species	λ^o at 25°C (sq.cm/ohm gm equiv.)	A_1	$A_2 10^2$	$A_3 10^4$
H	349.85	4.81595	-1.03125	-0.7670
Na	50.15	1.09160	0.47150	-0.1150
K	73.50	1.43260	0.40563	-0.3183

Table 6.4 tabulates diffusion coefficients of K, Na and H ions in aqueous solution at various temperatures.

Average changes of D_i^o per degree centigrade of K, Na and H ions are 2.5%, 2.7% and 1.9% respectively, over the 15-25°C interval.

In the column experiments, temperature fluctuations were within ±1°C, average values of the diffusion coefficients were used, and the effects of temperature on the ion exchange rates were assumed negligible.

Effect of temperature on ion exchange equilibrium

The thermodynamic equilibrium constant, K_B^A, is related to temperature by the relationship (Helfferich, 1962):-

$$\ell n\ K_B^A = -\frac{\Delta G^o}{RT} \quad (6.3)$$

where ΔG^o is the standard free energy of an ion exchange operation.

By differentiating Eqn. 6.3 with respect to temperature it is shown (Perry, 1963)

Temp. (^{o}C)	D^{o}_{K} ($m\ s^{-1}$)10^{9}	D^{o}_{Na} ($m\ s^{-1}$)10^{9}	D^{o}_{H} ($m\ s^{-1}$)10^{9}
0	0.9923	0.6461	5.4857
5	1.1594	0.7523	6.2093
15	1.5329	1.0210	7.7311
18	1.6606	1.1122	8.1859
25	1.9560	1.3333	9.3089
35	2.4259	1.6916	10.9195
45	2.9363	2.0929	12.5344
55	3.4914	2.5394	14.1500
100	6.4947	4.8294	20.9828

Solution phase self diffusion coefficients at infinite dilution at various temperatures.

Table 6.4

$$\left[\frac{d\ell nK_B^A}{dT}\right]_p = \frac{H^o_{product} - H^o_{reactant}}{RT^2} = \frac{\Delta H^o}{RT^2} \qquad (6.4)$$

where ΔH^o is the standard enthalpy change of an ion exchange operation.

Ion exchange is not a chemical reaction process, thus it is expected that there will be little heat involved in the exchange reaction.

Kraus and Raridon (1959) studied the temperature dependence of ion exchange equilibrium for a number of systems with Dowex 50W X12 at 1.0 M total solution concentration. For Na-H, K-H and K-Na systems, ΔH^o at 25°C was -1.11 kcal/eq., -2.14 kcal/eq. and -0.90 kcal/eq. respectively. The results obtained agreed well with the calorimetric data of Cruickshank and Meares (1957, 1958) which were -1.25, -2.05 and -0.73 kcal/eq. for Na-H, K-H and K-Na systems respectively at 25°C.

Eqn. 6.4 can be rearranged to give:-

$$\frac{\Delta K_B^A}{K_B^A \Delta T} = \frac{\Delta H^o}{RT^2} \qquad (6.5)$$

Substituting the enthalpy values from Kraus and Raridon (1959), R = 1.987 kcal/°K mole and T = 298.15°K in Eqn. 6.5 gives:

Na-H; $\dfrac{\Delta K_H^{Na}}{K_H^{Na} \Delta T} = 0.6\%$ per °C

K-H; $\dfrac{\Delta K_H^{K}}{K_H^{K} \Delta T} = 1.2\%$ per °C

K-Na; $\dfrac{\Delta K_{Na}^{K}}{K_{Na}^{K} \Delta T} = 0.5\%$ per °C

The equilibrium constant used by Kraus and Raridon was

$$K_B^A = \frac{\gamma_B \, Y_A^* \, X_B^*}{\gamma_A \, X_A^* \, Y_B^*} \qquad (6.6)$$

where γ_i is the solution phase activity coefficient of species i.

Combining Eqn. 6.6 with the definition of a separation factor:-

$$K_B^A = \frac{\gamma_B}{\gamma_A} \alpha_B^A \qquad (6.7)$$

Eqn. 6.7 can be rearranged to give:

$$\frac{\Delta K_B^A}{K_B^A} = \frac{\Delta \gamma_B}{\gamma_B} + \frac{\Delta \gamma_A}{\gamma_A} + \frac{\Delta \alpha_B^A}{\alpha_B^A}$$

For a small change in temperature the change in activity coefficient can be assumed to be negligible (Table 6.5) thus:

$$\frac{\Delta K_B^A}{K_B^A \Delta T} \doteq \frac{\Delta \alpha_B^A}{\alpha_B^A \Delta T} \qquad (6.8)$$

Therefore for a small change in temperature it can be assumed that the percentage change in separation factors are negligible.

Effect of temperature on concentration measurement

The effect of temperature on concentration measurement is shown by the Nernst equation:-

$$E = E_o - E_j + \frac{RT}{Z_i f} \ell n\left(\frac{A_i}{A_o}\right) \qquad (6.9)$$

where E_o is the electrode constant, A_o is the activity of the filling solution and E_j is the liquid junction potential relating to temperature by (Appendix 6B):-

$$E_j = \frac{\Sigma \lambda_i / Z_i (C_{Si} - C_{Ri}) \; RT}{\Sigma \lambda_i (C_{Si} - C_{Ri}) \quad f} \ell n \left(\frac{\Sigma C_{Si} \lambda_i}{\Sigma C_{Ri} \lambda_i}\right) \qquad (6.10)$$

C_{Si} solution concentration of species i in a sample

C_{Ri} solution concentration of species i in the filling solution of the reference electrode.

The summation is carried out for all ions present.

Therefore, with temperature monitoring of the effluent from a fixed-bed ion exchange column and by assuming that activity coefficients are constant for a small change of temperature (Table 6.5), Equations 6.9 and 6.10 were used to compensate for the effect of temperature change on concentration measurement.

Temperature (^{o}C)	γ_K	γ_{Na}	γ_H
10	.7576	.7806	.8285
15	.7564	.7794	.8271
20	.7547	.7776	.8258
25	.7530	.7764	.8251
30	.7513	.7746	.8244

Activity coefficients of K, Na and H ions in aqueous solution. The Debye-Huckel equation (Appendix 6B) was used to compute the activity coefficients. For a temperature range of 20-25^{o}C, the percentage change of activity coefficient per degree centigrade of K, Na and H ions are 0.045%, 0.031% and 0.017% respectively.

Table 6.5

6.4 On-Line Monitoring

Previously, experimental breakthrough curves were typically obtained by titrations of samples collected from the fixed-bed ion exchange columns. This proved to be tedious and time-consuming. This section discusses on-line monitoring of breakthrough curves.

Parameters that must be considered for on-line monitoring are lag (concentration and time), electrode response time and cell design.

Concentration and time lags

Considering the figure shown, the obvious place to monitor an effluent is at the bottom of the bed (at A). However to ensure a proper flow of the filling solution from the reference electrode it is necessary to monitor at atmospheric pressure (at B). However, monitoring at B would cause time and concentration lags. The time lag can be corrected with the equation:-

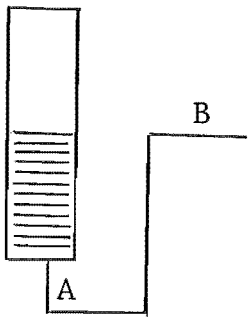

$$Z = \frac{C_o}{QV}(Ft - V\varepsilon - FT_L)$$

where T_L, the time lag, can be computed from the volume between A and B and the flow rate used. At the smallest flow rate ($F = 1\ ml\ s^{-1}$):-

$$T_L = \frac{V_{AB}}{F} \doteq 18\ s.$$

The problem caused by the concentration lag can be understood by considering species i with concentration C_A at A at time zero. At time 18 secs it would expect the concentration to be C_A at B. However concentration gradients between A and B will cause the species i to diffuse during this lag time. For example, consider a case in which sodium ions were replacing hydrogen ions in the bed (Runs 12:14, Chapter 7), the steepest part of the experimental breakthrough curve can be shown to be:-

$$\frac{\Delta X_H}{\Delta t} = 7.10^{-4} \qquad (6.11)$$

The concentration gradient between A and B is obtained by substituting the time lag in Eqn. 6.11:-

$$\Delta C_H = 1.26.10^{-3} \text{ N}$$

The flux between A and B is

$$J_H = - \frac{D_H \Delta C_H}{L_{AB}}$$

where L_{AB} is the distance between A and B (L_{AB} = 86 cms), D_H is the diffusion coefficient of hydrogen ions ($D_H = 2.5.10^{-5}$ sq.cm/sec) substituting the values of D_H, ΔC_H and L_{AB} in the above equation gives:-

$$J_H = 3.6.10^{-6} \text{ eq/sq.cm sec}$$

The flux of hydrogen ions diffusing during the lag time can be computed by combining J_H with the tube cross section area and the time lag, this was found to be $1.8.10^{-7}$ equivalents. By comparing this value ($1.8.10^{-7}$ eq.) with the bed capacity (3.573 eq.) it was assumed that the concentration lag was negligible

Electrode response time

The electrode response time is the time required for the electrode to produce a potential corresponding to a new level of concentration. The response time is one factor in deciding whether a particular electrode can be employed for a particular analytical measurement. The 93-19 potassium electrode was chosen in preference to sodium electrode because its response time is faster. The response times of the hydrogen and the potassium electrodes from equilibrium experiments were 2-5 secs and 10-20 secs respectively. However, it was observed that the response times during continuous flows were faster, 2-3 secs for the hydrogen electrode and 5-10 secs for the potassium electrode. The effect of the electrode response time on breakthrough curves can be examined by considering

the breakthrough curve with the steepest slope, Eqn. 6.11,

$$\frac{\Delta X_H}{\Delta t} = 7.10^{-4} \text{ per second}$$

with the electrode response time of 10 secs, the error in the concentration ratio is:

$$\Delta X_H = 0.007$$

Since this is the worse case it can then be concluded that the rate of change of concentration is slower than the electrode response rates.

Cell design

The on-line monitoring was accomplished by passing the effluent solution from the fixed-bed ion exchange column through the cell chamber in which were mounted the electrodes and a temperature sensor. The criteria for the cell design were:-

(1) No dead space or air bubbles in the cell during the concentration monitorings. To achieve this the following conditions were necessary:-

(A) The chamber entrance must be smooth, the angle of the cell chamber to the horizontal is suggested to be 20^{o} (Whitfield, 1971).

(B) Flat membrane electrodes should be used and mounted such that they do not produce resistance to the flow, however, if bulb type electrodes have to be used it is recommended that the diameter of the cell chamber is at least twice the electrode diameter (Eisenman, 1967).

(2) The filling solution from the reference electrode must not interfere with the measuring electrode. If the flow in the

cell chamber is turbulent, the filling solution from the reference electrode may flow back to the measuring electrode due to eddy diffusion, thus interfering with the potential output. Therefore the flow in the chamber must be laminar. However, even if the flow is laminar there will be eddy diffusion caused by the reduction of flow velocity coming from the inlet tube. This suggests that the reference electrode should be placed far down the stream where the laminar flow is fully developed. The entrance length, Le, required for a laminar flow to be fully developed was estimated from (Perry, 1963):-

$$\frac{Le}{D} = \beta Re \qquad (6.12)$$

where D is the cell diameter, β is a constant with a value from 0.05 to 0.065, Re is a Reynolds number given by:

$$Re = \frac{4\rho F}{\mu \pi D}$$

For ρ = 1 gm/cm^3, F = 2 cm^3/sec, μ = 0.01 gm/cm sec and D = 2.5 cms, Reynolds number was calculated to be 101.8 and the entrance length, Le, was estimated to be from 12.7 cms to 16.5 cms.

The cell was designed accordingly. However, flow around the electrodes themselves causes some turbulence. A simple test was carried out by passing deionized water through the cell in which were mounted a potassium electrode and a reference electrode filled with 4.0 N potassium chloride solution. The output potential from the potassium electrode system was monitored for three hours. Results indicated that the filling solution from the reference electrode did not flow back to the potassium electrode.

6.5 The Apparatus

The experimental apparatus and components are shown in Figures 6.1 - 6.7. Each component will now be described.

Column (Figure 6.3)

The design requirements for a fixed-bed ion exchange column were:-

- sufficient free space above the resin for bed expansion during backwashing
- a flow distributor
- a bed supporter

The column was constructed of a 2 inch diameter 80 inch long QVF glass tube, connected at the top to a 2 inch diameter tee for backwashing and further connected to a flow distributor and a 6 inch long QVF glass tube.

The bed was supported by a stainless steel screen with glass wool enclosed in polythene rings below. The dead volume occupied in the bed support was determined by passing 0.1 N nitric acid into the column and adjusted so that the solution occupied only the bed support,then rinsed with deionized water until clear of the nitric acid. The effluent was analysed for hydrogen equivalents from which the dead volume was found to be 46.28 mls.

Scalefix (self adhesive P.V.C. transparent scale) was attached outside the column. The volume between each 10 cm graduation was measured by filling the column with water and draining between each point. The effluent volume was then determined by weight measurement. The procedure was repeated until duplicate results were obtained. The average bed diameter from the bed support up to 100 cm level was found to be 4.93 cms.

Electrode calibrating column (Figure 6.4)

A solution flowing past a reference electrode generates a streaming potential. The magnitude of the streaming potential depends on the ionic strength, the solution flow rate and the position of the reference electrode with respect to the sensing electrode (Whitfield, 1971). To ensure that the streaming potential generated by the calibrating solution was the same as that of the effluent solution, the calibrating solution flow rate had to be the same as the effluent solution flow rate. A column, constructed from a 2 inch diameter and 12 inch long QVF glass tube, was used for this purpose.

Cell chamber (Figure 6.5)

The electrodes and a temperature sensor were screwed tightly into the perspex cell chamber. The order of the sensors in the cell were potassium ion selective electrode, pH electrode, temperature probe and reference electrode in the direction of flow.

Pumps (Figure 6.6)

Two 6 mls^{-1} DCL metering pumps were used, one for delivering feed solutions and deionized water for rinsing and the other for delivering calibrating solutions and deionized water for back-washing. Both pumps were calibrated, with micro-meter adjustment, to give the same flow rate. Because the metering pumps produced pulsating flows, flow distributors were put between the pumps and the columns for uniform flow.

Data logging system (Figure 6.7)

The components of the data logging system were:-

(1) Ion selective electrode system. An Orion potassium ion selective electrode model 93-19, Orion pH electrode model 91-01 and a single junction reference electrode model 90-01 were used.

(2) Temperature probe. A National Semiconductor LX5700 temperature sensor was enclosed in a 10 mm diameter 100 mm long glass tube for protection showing a time constant of 6-8 secs.

(3) Orion 701A Ionalyzer. The model 701A digital pH/mV meter covered a range of ±1999.9 mV with a parallel BCD digital output permitting the 701A to be interfaced directly to a microcomputer. It has an input impedance of 10^{13} ohms and drift less than 60 $\mu V/^{o}C$.

(4) Electrode switch. A self-contained single-pole double position switch, used in conjunction with 701A ionalyzer for selecting between two electrodes under manual or microcomputer control, was designed with an isolation resistance of 10^{15} ohms to prevent interference from the inactive electrode. Under program control, a channel was selected by a digital signal from the microcomputer:-

Digital signal	Channel	Electrode
low	0	Potassium
high	1	Hydrogen

(5) Data acquisition system. Appendix 6D contains details of the data acquisition system. It is the central control of the data logging system. A program, written in Assembler, controlled and manipulated sampling time, electrode settling time, input data from the 701A ionalyzer and the A/D converter, and punched measured values onto paper tape with a ASR-33 teletype. Final results were processed in a PDP-11 computer.

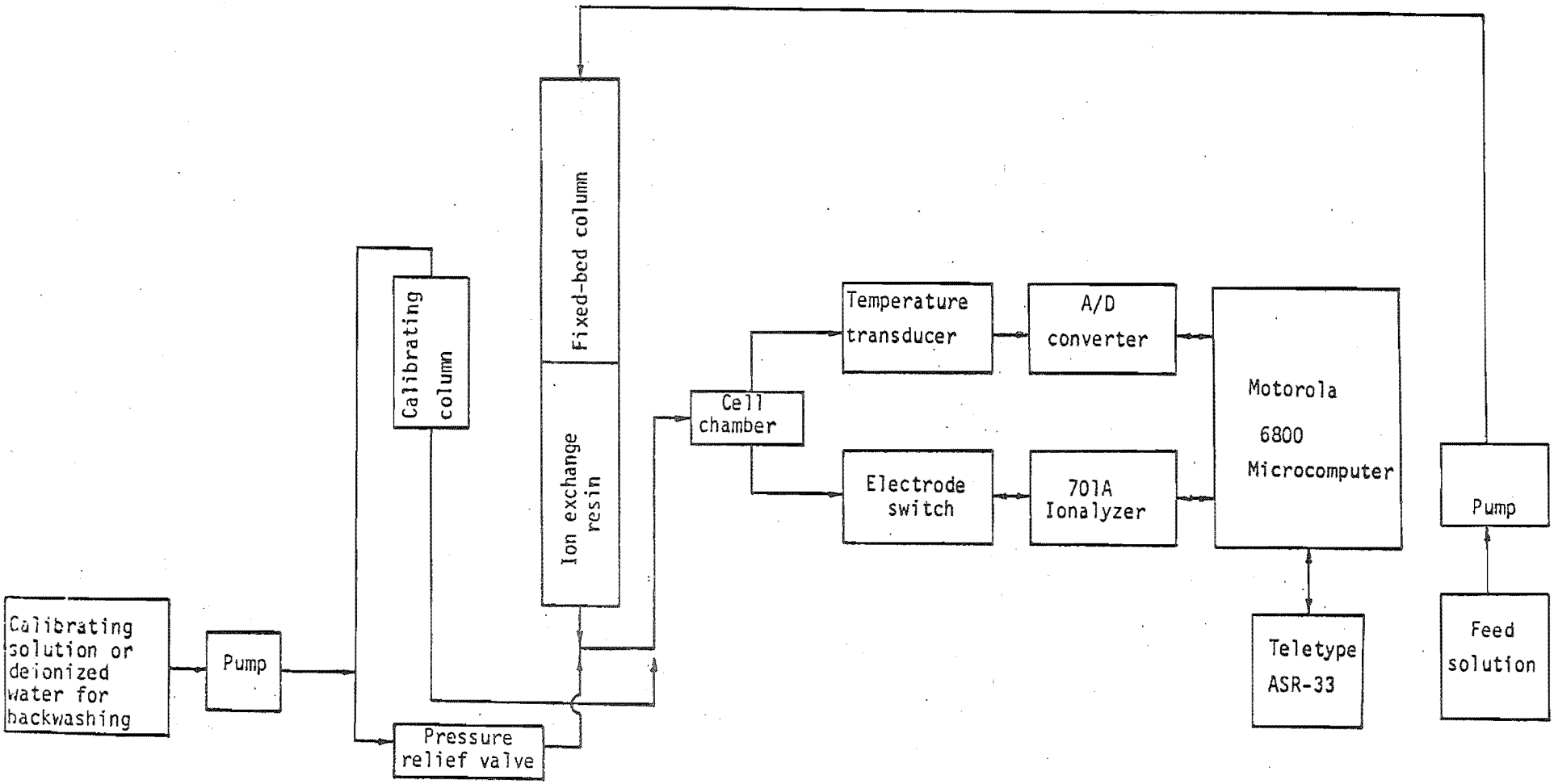

Figure 6.1: Simplified block diagram of the experimental apparatus.

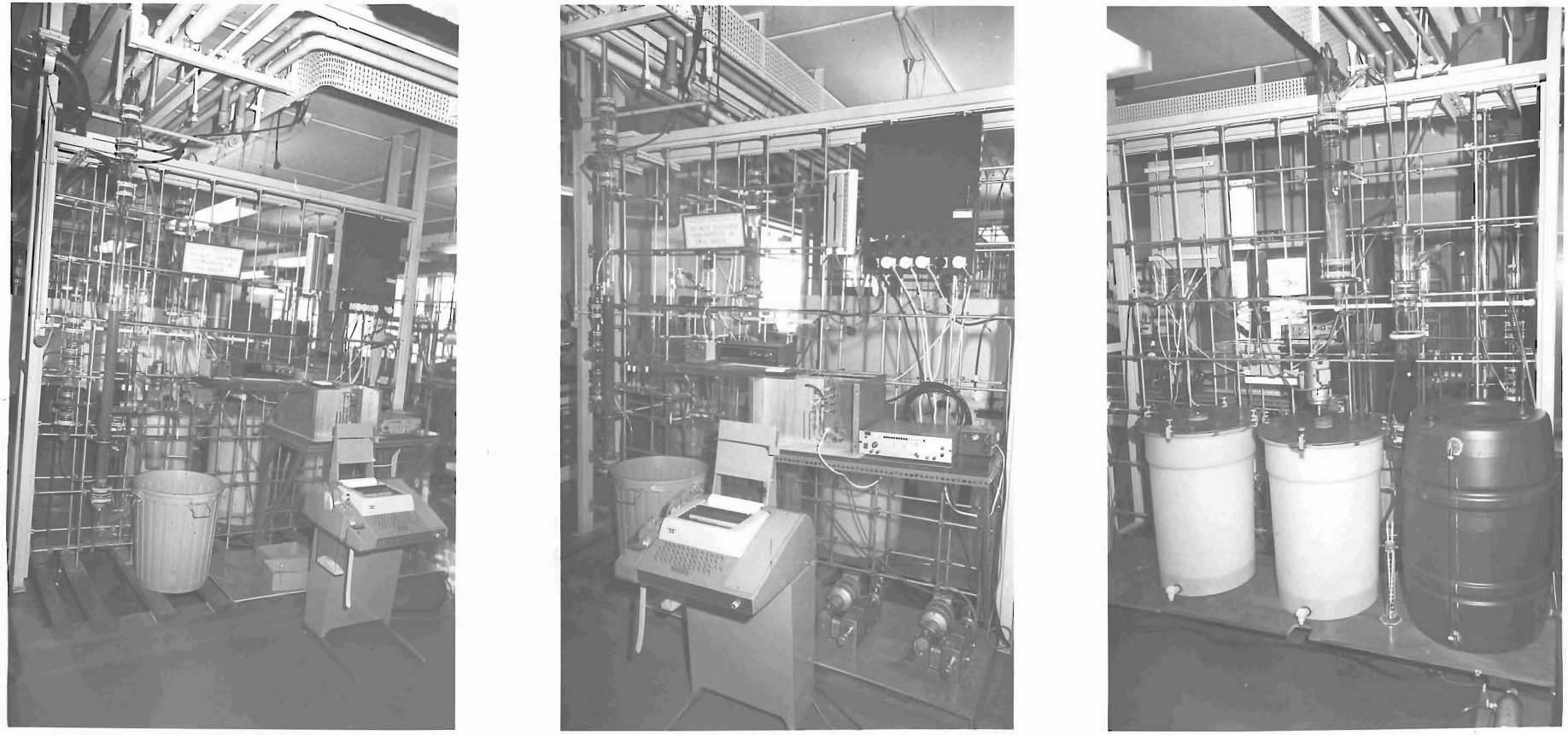

FIGURE 6.2 OVERALL VIEW OF APPARATUS

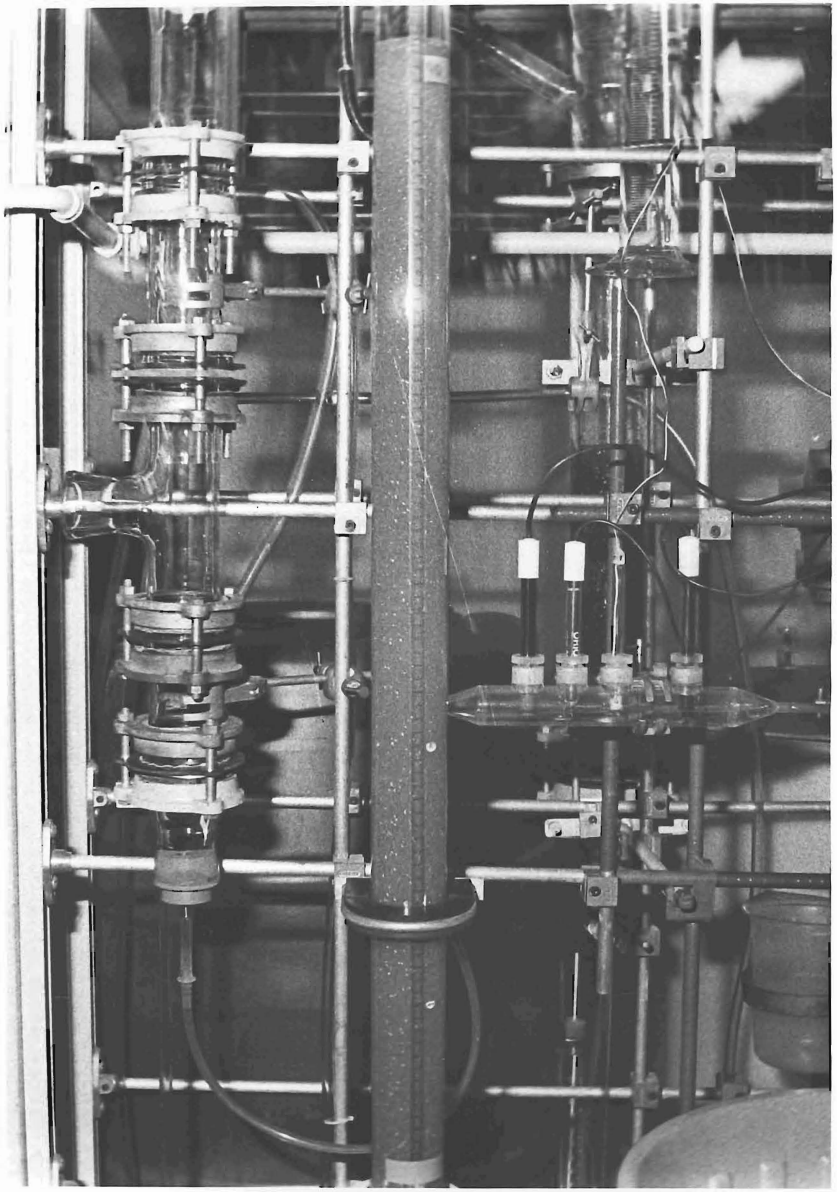

FIGURE 6.3 COLUMN USED FOR RATE EXPERIMENTS

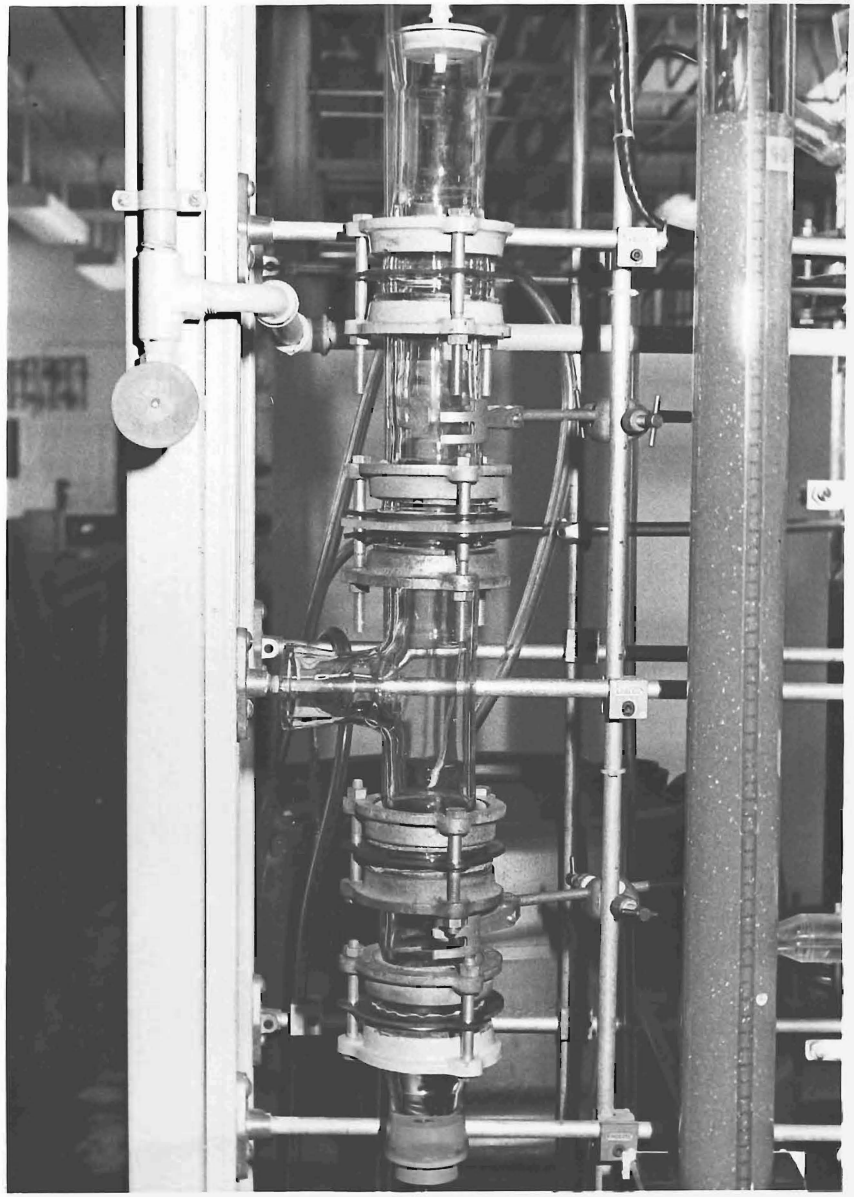

FIGURE 6.4 COLUMN USED FOR CALIBRATING ELECTRODES

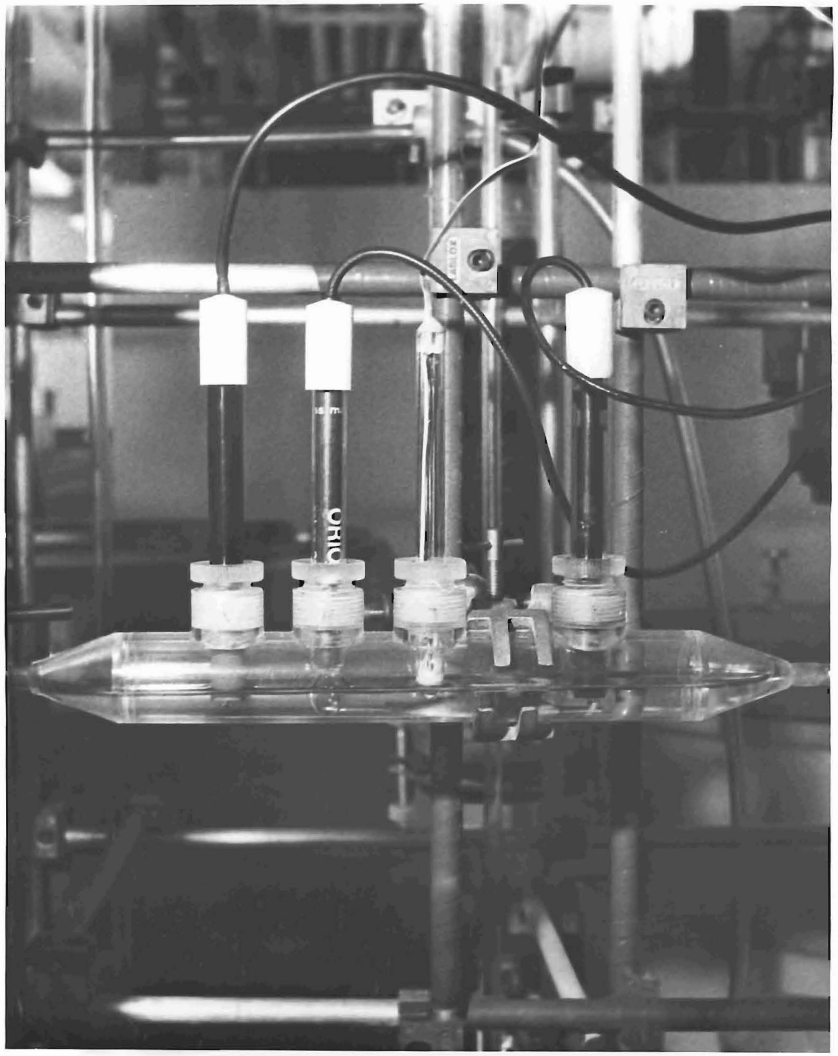

FIGURE 6.5 CELL CHAMBER

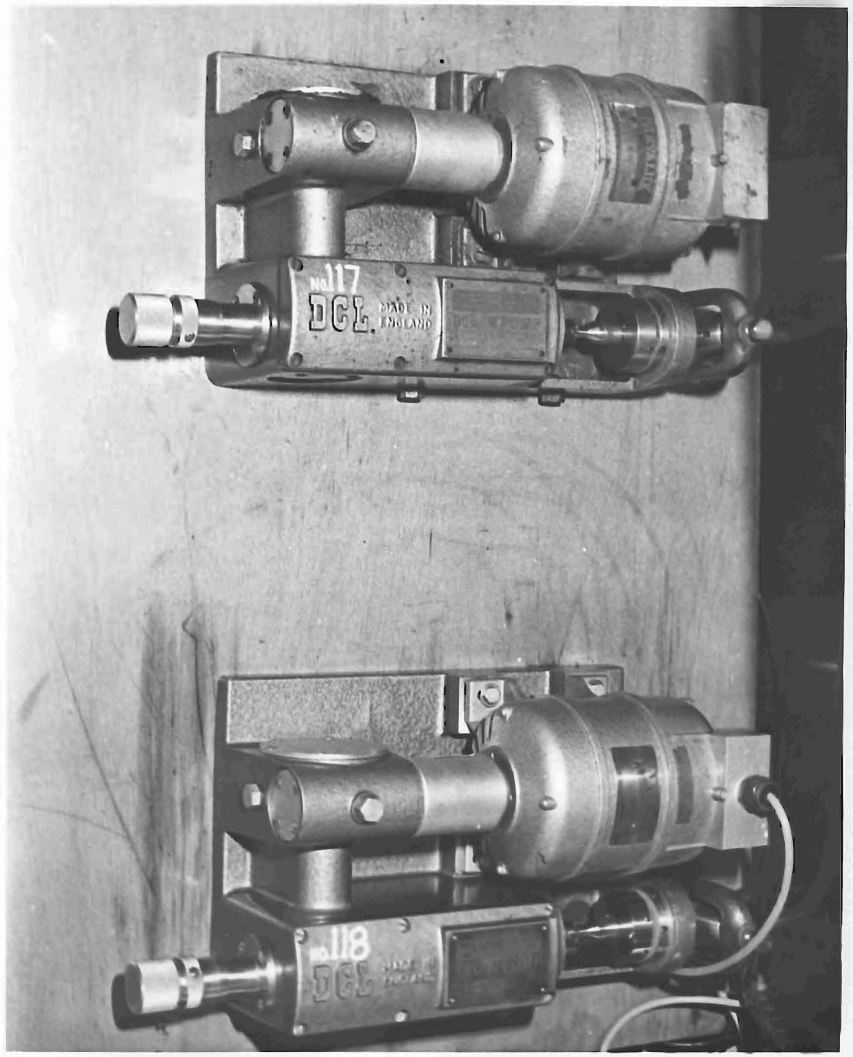

FIGURE 6.6 DCL METERING PUMPS

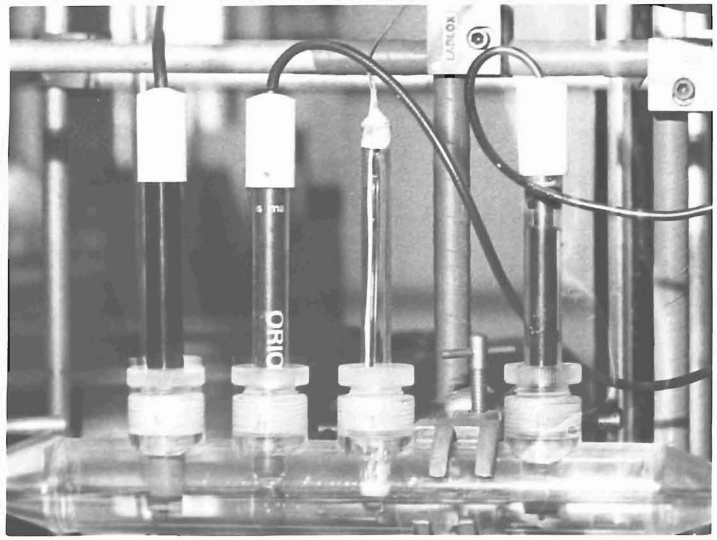

A. ION SELECTIVE ELECTRODES AND TEMPERATURE PROBE

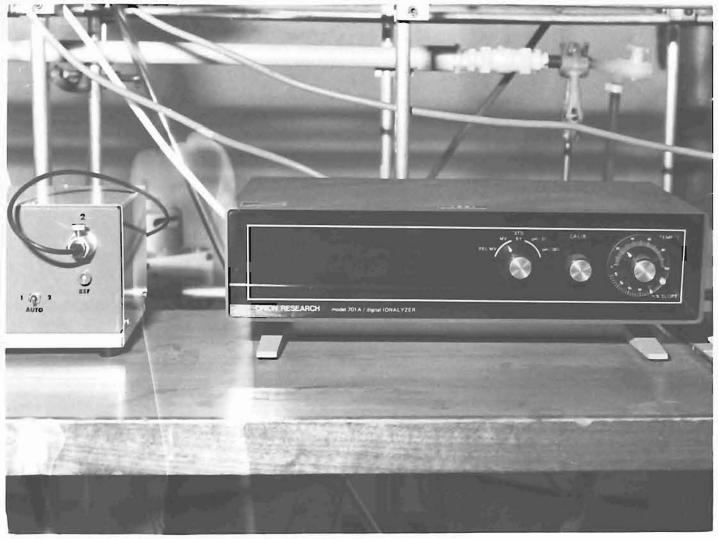

B. ORION 701A IONALYZER AND ELECTRODE SWITCH

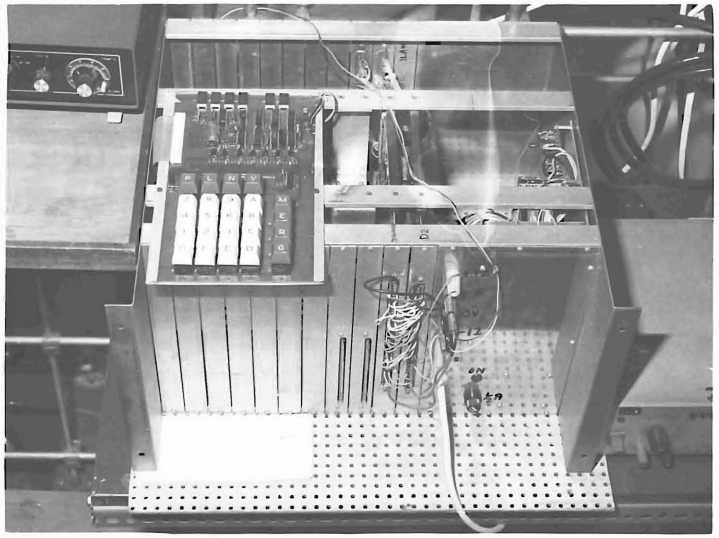

C. MOTOROLA MEK 6800D2 EVALUATION BOARD

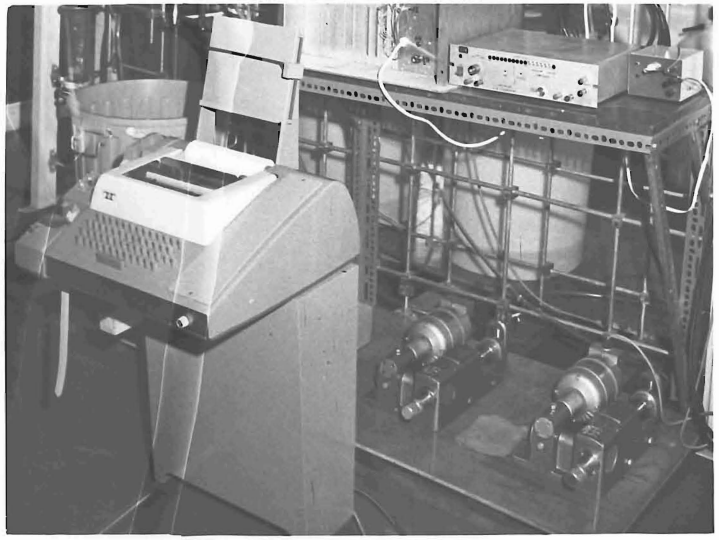

D. TELETYPE, A/D CONVERTER AND TEMPERATURE TRANSDUCER

FIGURE 6.7 DATA LOGGING SYSTEM

APPENDIX 6A

COLUMN EXPERIMENTAL PROCEDURE

6A.1 Breakthrough Curve Measurement

The following procedure was used in breakthrough curve measurement.

(1) Check pump settings, making sure that both pumps produce the same flow rate.

(2) Electrode preparation

(i) Soak hydrogen electrode in 0.1N HCl for 2-3 mins then store in water.

(ii) Soak potassium electrode in water for 10 mins then store in 0.01N KCl.

(3) Equipment preparation

(i) Calibrate temperature sensor at $0^{o}C$ and room temperature.

(ii) Calibrate A/D converter using a programmable voltage regulator.

(iii) Zero 701A by connecting a shorting strap between the input and reference jack, turning the function switch to mV, and adjusting to 000.0 ± 0.1 with the zero adjust on the rear panel.

(iv) Fill the reference electrode with Orion 90 00 01 equitransferent solution, making sure there are no air bubbles inside the reference electrode.

(4) Put the electrodes and the temperature probe in the cell chamber, making sure there are no air bubbles in the cell chamber.

(5) Electrode calibrations

(i) Pass calibrating solution 1 into the calibrating column then through the cell chamber, record E_1 for

potassium and hydrogen electrodes and temperature T_1.

(ii) Rinsing the calibrating column and the cell chamber.

(iii) The same as in 5(i) with calibrating solution 2, obtains E_2 and T_2 for both electrodes.

(iv) Rinsing.

(6) Data logger preparation

(i) Start up the data acquisition system.

(ii) Type in sampling time.

(iii) Type in electrode settling time.

(7) Prepare for a start of a run

(i) Record the bed volume.

(ii) Deliver the feed into the column, turn on valve at the bottom of the column and hit any key of the teletype to start the data logging cycle.

(iii) Collect the effluent in a 110 litre container.

(8) End of the run

(i) Record the bed volume

(ii) Electrode calibrations

(iii) Rinse pumps and electrodes and store electrodes in their buffers.

(9) The flow rate is determined from the volume of the effluent in the container and the operating time.

(10) Rinsing and backwashing the bed.

6A.2 Voidage Measurement

The following procedure was used in voidage measurement.

(1) The bed is in hydrogen form in 0.1N HNO_3 solution.

(2) Passing deionized water through the column, collecting the effluent in a container, until pH of the effluent is greater than 5.5.

(3) The number of hydrogen equivalents in the effluent is determined by titrating with 0.1N NaOH standard solution.

(4) Void volume + volume of bed support = $\frac{\text{No. of hydrogen equivs.}}{HNO_3 \text{ conc. (0.1N)}}$

APPENDIX 6B

THE NERNST EQUATION AND ITS USE WITH ION SELECTIVE ELECTRODES

6B.1 Introduction

Potassium and hydrogen ion selective electrodes were used to monitor effluent concentrations from the fixed-bed ion exchange column. The Nernst equation was used to convert electrode potential measurements into corresponding concentrations. For accurate concentration measurement, the Nernst equation was considered in detail, including:-

- electrode potentials (Section 6B.2)
- activity coefficient (Section 6B.3)
- liquid junction potentials (Section 6B.4)
- temperature dependence of E_o (Section 6B.5)

6B.2 Electrode Potentials

Fig. 6B.1 illustrates the potentials developed in an ion selective electrode measurement system. The measured potential, E, is given by:-

$$E = (E_{RM} + E_D + E_{ASYM} - E_{REF} + E_M) - (E_J + E_{RR}) \quad (6B.1)$$

The values of E_D and E_{ASYM} are characteristic of the measuring electrode, and therefore if there is no change in the electrode (for example if there is no scratching at the membrane, no thermal or mechanical shock to the electrode) then E_D and E_{ASYM} can be assumed to be constant for period up to 24 hours and its variation due to membrane drift only.

The relationship between electrode potentials and ionic concentrations is given by the Nernst equation:-

$$E_i = E_\Delta + \frac{RT}{Z_i f} \ln A_i \quad (6B.2)$$

where A_i and E_Δ are the activity and the electrode potential at unit activity respectively.

Using Eqn. 6B.2 to expand E_{REF} and E_M in Eqn. 6B.1

$$E = (E_D + E_{ASYM}) + (E_{RM} - E_{RR}) - E_j + \frac{RT}{Z_i f}\ell n(\frac{A_i}{A_o}) \qquad (6B.3)$$

where A_o is the activity of the reference solution in the measuring electrode.

Eqn. 6B.3 can be further simplified by assuming that E_D, E_{ASYM}, E_{RM} and E_{RR} are constant with their values depending on the characteristic of the measuring and reference electrodes being used, thus:-

$$E = E_o - E_j + \frac{RT}{Z_i f}\ell n(\frac{A_i}{A_o}) \qquad (6B.4)$$

where E_o is the sum of E_D, E_{ASYM}, E_{RM} and E_{RR}.

Eqn. 6B.4 is derived under the condition that the solution being measured contains no ions which might interfere with the measuring electrode. For a solution containing interfering ions, Eqn. 6B.4 has to be modified (Mohan and Bates, 1977):-

$$E = E_o - E_j + \frac{RT}{Z_i f}\ell n(\frac{A_i + \sum_{j\neq i} K_{ji}(A_j)^{Z_i/Z_j}}{A_o}) \qquad (6B.5)$$

where K_{ji} and A_j are the selectivity constant of j relative to i and the activity of an interfering ion j in the sample solution respectively.

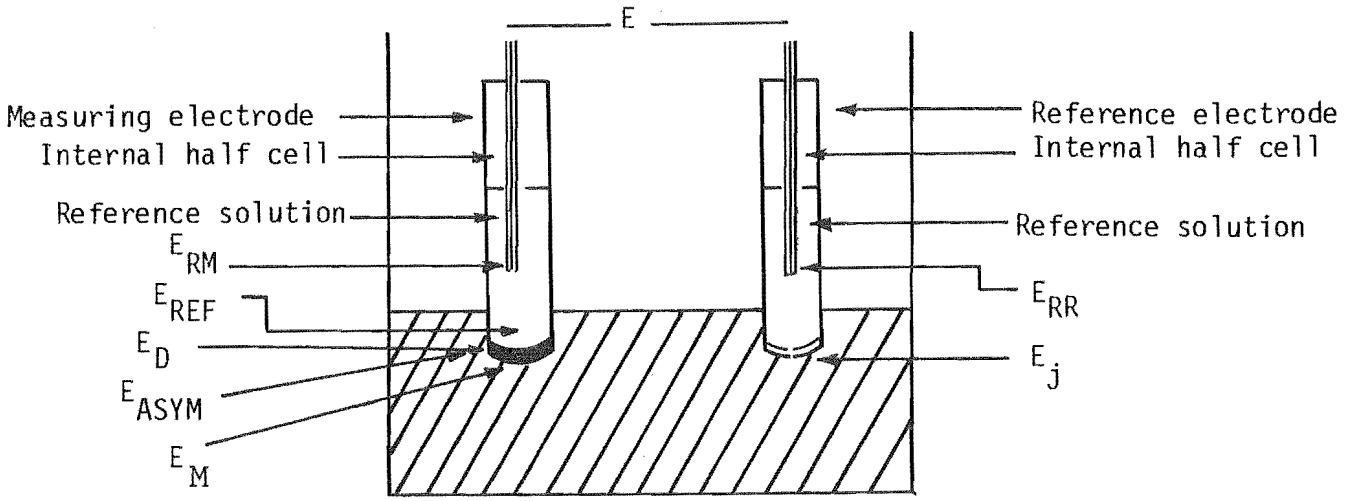

E_{RM} potential of the internal half cell of the measuring electrode

E_{REF} potential developed at the inside of the membrane

E_D potential developed across the membrane due to ion exchange across the membrane (diffusion potential)

E_{ASYM} potential developed due to different kinds of surfaces in the membrane (asymmetrical potential)

E_M potential developed at the outside of the membrane

E_{RR} potential of the internal half cell of the reference electrode

E_j liquid junction potential

Figure 6B.1

6B.3 Activity Coefficient

If one equivalent of an electrolyte XY dissociates into a number of equivalents consisting of a positive equivalents and b negative equivalents, the thermodynamics of electrolyte solution gives that (Robinson and Stokes, 1959):-

$$\gamma_{XY}^{a+b} = \gamma_X^a \cdot \gamma_Y^b \qquad (6B.6)$$

where γ_{XY}, γ_X and γ_Y are the mean ionic activity coefficient of electrolyte XY, individual activity coefficient of positive ion X and individual activity coefficient of negative ion Y respectively.

The mean ionic activity coefficient can be predicted successfully at low ionic strength by the limiting Debye-Huckel law (Whitfield, 1971):-

$$\log_{10}(\gamma_{XY}) = -A|Z_+Z_-|\sqrt{I} \qquad (6B.7)$$

where A is the Debye-Huckel constant; its value as a fraction of temperature is available in Robinson and Stokes (1959). I is the total ionic strength of the solution, related to solution concentration by:-

$$I = \tfrac{1}{2} \Sigma Z_i^2 M_i \qquad (6B.8)$$

where M_i is the molar concentration of species i in the solution and the summation is carried out for all ions present.

Equation 6B.7 applies at a total ionic strength of less than 0.1M. Values of γ_{XY} at higher ionic strengths are published in Whitfield (1971).

There is no reliable method to measure individual ionic activity coefficients, and methods are needed to estimate them. Four conventional activity scales used for estimating individual ionic activity coefficients are described:-

- Debye-Huckel convention
- MacInnes convention
- pH convention
- Hydration convention

Debye-Huckel Convention

The Debye-Huckel convention predicts the individual ionic activity coefficient, γ_i, in aqueous solution (Bates, 1973):-

$$\log_{10}(\gamma_i) = - \frac{A\, Z_i^2\, \sqrt{I}}{1 + BA\sqrt{I}} \qquad (6B.9)$$

A,B the Debye-Huckel constants, available as functions of temperature in Bates (1973)

$\dot{A}$ an ion-size parameter, ranging from 2.5 to 9 $\dot{A}$

The Debye-Huckel equation gives good results up to 0.1M provided one of the ions in the compound is singly charged (Whitfield, 1971). Large discrepancies may occur due to ion association in multiplely-charged ions, because the Debye-Huckel equation is based on the charge, radius and distribution of the ions and the dielectric constant of the medium, but not on the chemical properties of the ions.

MacInnes Convention

The MacInnes convention states that for a given total ionic strength then

$$\gamma_K = \gamma_{CL} = \gamma_{KCL} \qquad (6B.10)$$

and also γ_K and γ_{Cl} are assumed to have the same values in other solutions, provided that the total ionic strengths are the same. For example, for sodium chloride solution at a total ionic strength of I, γ_{NaCl} can be obtained (Robinson and Stokes, 1959) and γ_{Na} and γ_{Cl} can be related to γ_{NaCl} by (Eqn. 6B.6):-

$$\gamma_{Na}\,\gamma_{Cl} = \gamma^2_{NaCl}$$

The MacInnes convention gives that $\gamma_{Cl} = \gamma_{KCl}$, and thus γ_{Na} can be computed from:

$$\gamma_{Na} = \frac{\gamma^2_{NaCl}}{\gamma_{KCl}}$$

pH Convention

The pH convention (Bates and Alfenaar in Durst, 1969) states that the activity coefficient (Molality scale) of chloride ion at a total ionic strength of 0.1m or less is given by:

$$\log_{10}(\gamma_{Cl}) = -\frac{A\sqrt{I}}{1 + 1.5\sqrt{I}} \qquad (6B.11)$$

For example, for sodium nitrate solution at a total ionic strength of I, the following procedure can be used to estimate γ_{Na} and γ_{NO_3}:-

(i) compute γ_{Cl} from Eqn. 6B.11

(ii) obtain γ_{NaCl} from Bates (1973) at ionic strength I

(iii) compute γ_{Na} from $\gamma_{Na} = \frac{\gamma^2_{NaCl}}{\gamma_{Cl}}$

(iv) obtain γ_{NaNO_3} from Bates (1973) at ionic strength I

(v) compute γ_{NO_3} from $\gamma_{NO_3} = \frac{\gamma^2_{NaNO_3}}{\gamma_{Na}}$

Bates and Alfenaar (1969) compared the three conventions (Debye-Huckel, MacInnes and pH conventions) and concluded that

all three conventions gave closely comparable results at total ionic strengths of 0.1m or less.

Hydration Convention

The first three conventions are not suitable at high ionic strengths (Bates, Staples and Robinson, 1970) and therefore another convention is required to estimate individual ionic activity coefficients at high ionic strengths.

The Hydration convention was based on the work of Stokes and Robinson (1948) who showed that the mean activity coefficient of unassociated electrolytes can be determined up to an ionic strength of 6.0 m by an equation involving ionic strength, osmotic coefficient (σ) and a parameter called the hydration number (h_i).

Based on the above work, Bates, Staples and Robinson (1970) showed that for a uni-univalent electrolyte MX:-

$$\log_{10}(\gamma_M) = \log_{10}(\gamma_{MX}) + 0.00782(h_M - h_X)m\sigma \quad (6B.12)$$

$$\log_{10}(\gamma_X) = \log_{10}(\gamma_{MX}) - 0.00782(h_M - h_X)m\sigma \quad (6B.13)$$

Individual ionic activity coefficients in mixed electrolytes

Based on the work of Bagg and Rechnitz (1973), Leyendekkers (1971), Mohan and Bates (1975, 1977) and Shatkay (1967), the following assumptions are made regarding individual ionic activity coefficients in mixed electrolytes:-

(A) For a mixture of electrolytes in which its total ionic strength is 0.1M or less, then γ_i in this mixture equals γ_i in a single electrolyte of the same ionic strength.

(B) If the total ionic strength of the mixture is constant then γ_i in the mixture is also constant.

6B.4 Liquid Junction Potential

When two electrolyte solutions are brought into contact, ions in both solutions will diffuse into one another due to concentration potentials. The rates of diffusion depend on the types of the ions and the solution concentrations. The interdiffusions of these ions result in liquid junction potentials.

Liquid junction potentials, E_j, can be computed from the Henderson equation (Bates, 1973):

$$E_j = \frac{\Sigma\, \lambda_i/Z_i\, (C_{Si} - C_{Ri})}{\Sigma\, \lambda_i\, (C_{Si} - C_{Ri})} \frac{RT}{f} \ell n\left(\frac{\Sigma\, C_{Si}\, \lambda_i}{\Sigma\, C_{Ri}\, \lambda_i}\right) \qquad (6B.14)$$

λ_i equivalent ionic conductivity of species i

Z_i charge of species i

C_{Si} solution concentration of species i in sample

C_{Ri} solution concentration of species i in filling solution

The summations are carried out over all the ions present.

If all the ions present are uni-valent ions, Eqn. 6B.14 can be written as:

$$E_j = \frac{(U_S - V_S) - (U_R - V_R)}{(U_S + V_S) - (U_R + V_R)} \frac{RT}{f} \ell n\left(\frac{U_S + V_S}{U_R + V_R}\right) \qquad (6B.15)$$

$U_S = \Sigma C_+\lambda_+$ of the sample

$V_S = \Sigma C_-\lambda_-$ of the sample

$U_R = \Sigma C_+\lambda_+$ of the filling solution

$V_R = \Sigma C_-\lambda_-$ of the filling solution

In choosing the filling solution for the reference electrodes the following points should be considered:-

(A) The total ionic strength of the filling solution should be much greater than that of the sample solution.

When this is the case, the Henderson equation reduces to

$$E_j \doteq - \frac{U_R - V_R}{U_R + V_R} \frac{RT}{f} \ell n(U_R + V_R) \qquad (6B.16)$$

showing E_j is constant.

(B) The filling solution should be equitransferrent, i.e.

$$\Sigma|Z_+|C_+\lambda_+ = \Sigma|Z_-|C_-\lambda_-$$

Using the above relation Eqn. 6B.16 becomes

$$E_j = 0$$

(C) The ions in the filling solution should not react with ions in the sample solution.

(D) The ions in the filling solution should not interfere with the measuring electrode.

When the above four conditions are fulfilled then the liquid junction potentials can be assumed to be constant. However, in a solution in which values of pH change significantly, the liquid junction potential cannot be assumed to be constant because of the high conductivity of H and OH ions.

Table 6B.1 shows some common values of equivalent ionic conductivity at infinite dilution at 25°C.

Species	λ_i^o (sq.cm/eq. ohm)	Species	λ_i^o (sq.cm/eq. ohm)
Ag^+	61.9	Br^-	78.14
Ba^{++}	63.64	$CO_3^=$	69.20
Ca^{++}	59.5	Cl^-	76.35
Cs^+	77.3	I^-	76.8
Cu^+	53.6	NO_3^-	71.42
H^+	349.82	OH^-	198.6
K^+	73.52		
Na^+	50.11		

Table 6B.1

6B.5 Temperature Dependence of E_o

Eqn. 6B.4 can be written as

$$E = E_o - E_j + ST\ell n(\frac{A_i}{A_o}) \qquad (6B.17)$$

where S is a constant with a theoretical value of $\frac{R}{Z_i f}$.

The terms E_j and $ST\ell n(\frac{A_i}{A_o})$ are temperature dependent and can be compensated. Since there is no equation available at present to correlate E_o with temperature, the values of E_o at various temperatures were investigated. The concentration measurement system used was an Orion 91-02 combination pH electrode and 701A ionalyzer.

E_o and S were measured at various temperatures and the results were:-

Temp. (^oC)	$E = E_o - E_j + ST\ell n(\frac{A_i}{A_o})$		$E = E_o + ST\ell n (\frac{A_i}{A_o})$	
	S ($mV/^oK$)	E_o (mV)	S ($mV/^oK$)	E_o (mV)
19.5	0.0884	-29.95	0.0815	-8.60
24.5	0.0882	-29.57	0.0815	-8.83
32.5	0.0870	-29.54	0.0807	-8.66

The above results indicate that within experimental errors the parameters E_o and S can be assumed to be constant over this small temperature range. At a higher temperature range, other factors such as activity coefficients, solution density and electrode material must be considered.

Due to electrode drift, E_o and S are functions of time and therefore frequent electrode calibrations are essential.

APPENDIX 6C

PROGRAM LISTINGS FOR COMPUTING EXPERIMENTAL BREAKTHROUGH CURVES

6C.1 Binary System

Equations used for computing experimental points on breakthrough curves for the binary systems, K-Na and Na-H, were:-

$$C_i = \left(\frac{A_o}{\gamma_i}\right) \mathrm{EXP}\left(\frac{E - E_o + E_j}{ST}\right)$$

$$S = \frac{(E + E_j)_1 - (E + E_j)_2}{T_1 \ell n\left(\frac{\gamma_i C_1}{A_o}\right) - T_2 \ell n\left(\frac{\gamma_i C_2}{A_o}\right)}$$

$$E_o = (E + E_j)_1 - ST_1 \ell n\left(\frac{\gamma_i C_1}{A_o}\right)$$

$$X_i = \frac{C_i}{C_o}$$

$$Z = \frac{C_o}{QV}(Ft - V\varepsilon - V_D)$$

where the subscripts 1 and 2 refer to the calibrating solutions 1 and 2 respectively, and V_D is the volume occupied by the effluent solution between the bed and the measuring point.

The values of A_o and γ_i used for potassium and hydrogen ion selective electrodes were 1 N and 0.7633, and 10^{-7} N and 0.8155 respectively. For the K-Na system, the liquid junction potential term was not included.

```
 INPUT C1, E1, T1, C2, E2, T2
20 INPUT G, F
30 INPUT L, C0
40 INPUT P3
50 J0=0
60 A9=.8155
70 T1=T1+273.15
80 T2=T2+273.15
90 C=.1
100 A0=1.00000E-07
110 REM COMPUTE LIQUID JUNCTION POTENTIAL
120 IF L=0 GO TO 220
130 T=T1
140 H=C1
150 GOSUB 2000
160 E1=E1+J0
170 T=T2
180 H=C2
190 GOSUB 2000
200 E2=E2+J0
210 REM COMPUTE NERNST SLOPE
220 P1=T1*LOG(A9*C1/A0)
230 P2=T2*LOG(A9*C2/A0)
240 S=(E1-E2)/(P1-P2)
250 REM COMPUTE E0
260 E0=E2-(S*P2)
270 S1=S*T2*2.303
280 REM CREAT FILES FOR INPUT&OUTPUT
290 OPEN "PC:" FOR INPUT AS FILE #1
300 OPEN "LP:" FOR OUTPUT AS FILE #2
310 PRINT #2, TAB(10), "S = ", S1
320 PRINT #2, TAB(10), "E0 = ", E0
330 PRINT #2, "TIME", "TEMP", "E", "Z", "X"
340 PRINT #2, "(MIN)", "(C)", "(MV)", "(-)", "(-)"
350 INPUT #1, A$, E, E, T
360 IF END #1 THEN 9999
370 J=2
380 I=POS(A$, CHR$(10), 1)
390 IF I=0 THEN J=1
400 B$=SEG$(A$, J, 80)
410 A=VAL(B$)
420 A=A*P3
460 A=A*60
470 T=ABS(T)
480 T=(T/10)+273.15
490 E=(E/10)
500 X0=(A0/A9)*EXP((E-E0+J0)/(S*T))
510 X2=X0
520 IF L=0 GO TO 720
530 REM WEGSTEIN ITERATIVE METHOD
540 H=X0
550 GOSUB 2000
560 X1=(A0/A9)*EXP((E-E0+J0)/(S*T))
570 IF X0<>X1 GO TO 600
580 X2=X1
590 GO TO 720
600 FOR J=1 TO 1000
610 H=X1
620 GOSUB 2000
630 Y=(A0/A9)*EXP((E-E0+J0)/(S*T))
```

```
640 P=(Y-X1)/(X1-X0)
650 Q=1/(1-P)
660 X2=Q*(Y-X1)+X1
670 REM FOR 0.01%ERROR
680 IF ABS(X2-X1)<=(1.00000E-04*X2) GO TO 720
690 X0=X1
700 X1=X2
710 NEXT J
720 H=X2
730 H=H-(1.00000E-14/H)
740 X=H/C
750 Z=G*A-F
760 A=A/60
770 T=T-273.15
780 PRINT #2, A, T, E, Z, X
1140 GO TO 350
2000 REM THIS IS SUBROUTINE TO COMPUTE LIQ. JUNC. POTENTIAL
2010 R=8.31439
2030 S0=R*T/96.4853
2040 D=T-298.15
2080 REM FOR POTASSIUM ION
2100 G0=73.5
2110 G1=1.43262*D
2120 G2=4.05630E-03*D*D
2130 G3=-3.18300E-05*D*D*D
2140 G4=G0+G1+G2+G3
2150 U1=G4*C0
3000 REM FOR CHORIDE ION
3010 G0=76.35
3020 G1=1.54037*D
3030 G2=4.65000E-03*D*D
3040 G3=-1.28500E-05*D*D*D
3050 G4=G0+G1+G2+G3
3060 V1=G4*C0
4000 REM FOR NITRATE ION
4010 G0=71.42
4020 G4=G0+G1+G2+G3
4030 V9=.1*G4
5000 REM FOR COUNTER ION
5010 H0=349.85
5020 H1=4.01595*D
5030 H2=-.0103125*D*D
5040 H3=-7.67000E-05*D*D*D
5050 H4=H0+H1+H2+H3
5060 M0=50.15
5070 M1=1.0915*D
5080 M2=4.71500E-03*D*D
5090 M3=-1.15000E-05*D*D*D
6000 M4=M0+M1+M2+M3
6010 U9=(H*H4)+((.1-H)*M4)
6020 F1=U9-V9
6030 F2=U1-V1
6040 F3=U9+V9
6050 F4=U1+V1
6060 F5=(F1-F2)/(F3-F4)
6070 F6=LOG(F3/F4)
6080 J0=S0*F5*F6
7000 RETURN
9999 CLOSE #1 \ CLOSE #2 \ STOP
```

6C.2 Ternary System

Equations used for computing points on breakthrough curves from experimental measurements for the K-Na-H system were:-

$$C_K = \left(\frac{1}{0.7633}\right)EXP\left(\frac{E_K - E_{KO}}{S_K T}\right)$$

$$C_H = \left(\frac{10^{-7}}{0.8155}\right)EXP\left(\frac{E_H - E_{HO}}{S_H T}\right)$$

$$S_K = \frac{E_{K1} - E_{K2}}{T_1 \ln\left(\frac{0.7633C_{K1}}{1}\right) - T_2 \ln\left(\frac{0.7633C_{K2}}{1}\right)}$$

$$S_H = \frac{E_{H1} - E_{H2}}{T_1 \ln\left(\frac{0.8155C_{H1}}{10^{-7}}\right) - T_2 \ln\left(\frac{0.8155C_{H2}}{10^{-7}}\right)}$$

$$E_{KO} = E_{K1} - S_K T_1 \ln\left(\frac{0.7633C_{K1}}{1}\right)$$

$$E_{HO} = E_{H1} - S_H T_1 \ln\left(\frac{0.8155C_{H1}}{10^{-7}}\right)$$

$$X_K = \frac{C_K}{C_o}$$

$$X_H = \frac{C_H}{C_o}$$

$$Z = \frac{C_o}{QV}(Ft - V\varepsilon - V_D)$$

where subscripts 1 and 2 are used to indicate calibrating solutions 1 and 2 respectively.

```
10 REM
20 REM A PROGRAM TO COMPUTE K-ION& H-ION CONCENTRATION
30 REM
40 REM
50 REM INPUT DATA FOR K-ION
60 REM
70 INPUT C1, E1, T1, C2, E2, T2
80 REM
90 REM INPUT DATA FOR H-ION CONCENTRATION
100 REM
110 INPUT C3, E3, T3, C4, E4, T4
120 INPUT G, F
130 INPUT PS
140 A8=.7633
150 A9=.8155
160 T1=T1+273.15
170 T2=T2+273.15
180 T3=T3+273.15
190 T4=T4+273.15
200 C=.1
210 A1=1
220 A3=1.00000E-07
230 REM COMPUTE NERNST SLOPE
240 P1=T1*LOG(A8*C1/A1)
250 P2=T2*LOG(A8*C2/A1)
260 P3=T3*LOG(A9*C3/A3)
270 P4=T4*LOG(A9*C4/A3)
280 S1=(E1-E2)/(P1-P2)
290 S3=(E3-E4)/(P3-P4)
300 REM COMPUTE E0
310 K1=E1-(S1*P1)
320 K3=E3-(S3*P3)
330 S2=S1*T2*2.303
340 S4=S3*T4*2.303
350 REM CREAT FILES FOR INPUT&OUTPUT
360 OPEN "PC:" FOR INPUT AS FILE #1
370 OPEN "LP:" FOR OUTPUT AS FILE #2
380 PRINT #2, TAB(10), "S =  ", S2, TAB(5), S4
390 PRINT #2, TAB(10), "E0 =  ", K1, TAB(5), K3
400 PRINT #2, "TIME", "TEMP", "Z", "X1", "X2"
410 PRINT #2, "(MIN)", "(C)", "(-)", "(-)", "(-)"
420 INPUT #1, A$, E1, E3, T
430 IF END #1 THEN 9999
440 J=2
450 I=POS(A$, CHR$(10), 1)
460 IF I=0 THEN J=1
470 B$=SEG$(A$, J, 80)
480 A=VAL(B$)
490 A=A*PS
500 A=A*60
510 T=ABS(T)
520 T=(T/10)+273.15
530 E1=E1/10
535 E3=E3/10
540 C1=(A1/A8)*EXP((E1-K1)/(S1*T))
550 C3=(A3/A9)*EXP((E3-K3)/(S3*T))
560 C3=C3-(1.00000E-14/C3)
570 X1=C1/C
580 X3=C3/C
590 Z=G*A-F
```

```
600 A=A/60
610 T=T-273.15
620 PRINT #2, A, T, Z, X1, X3
630 GO TO 420
9999 CLOSE #1 \ CLOSE #2 \ STOP
```

APPENDIX 6D

6800-BASED DATA ACQUISITION SYSTEM

This work was carried out by Dr G. Wilson (October, 1979).

A simple data acquisition system was constructed from available integrated circuits. Its principal features were:-

- Motorola MEK 6800D2 Evaluation board with J-bug monitor
- 2K x 8 random access memory (RAM)
- Two 8-bit parallel ports
- One serial port
- ASR-33 teletype
- 2K x 8 UV-erasable programmable read-only memory (EPROM)
- 10-bit A/D converter.

The microprocessor program development was done in the PDP-11 with a locally developed cross-assembler and down-load program. The system was programmed to collect data from the A/D converter and the ORION 701A ionalyzer, and punch the data on papertape. A block diagram of the system is shown in Figure 6D.1.

Timing of all operations is based on a 0.5 Hz clock interrupting through the parallel port. The clock is derived from the 50 Hz signal on the mains.

The program was assembled and burnt into the EPROM at memory location hexadecimal C000($C000). The program is started by executing a GO TO $C000 command. On power up the system must be initialized by pressing the reset button.

Operating the system is relatively self-explanatory:

(i) the sample time can be set as any integer number of minutes from 0 (continuous sampling) up to 99 mins (interrogation

from teletype key board);

(ii) the settling time for the second selected electrode is ranged from 0-99 secs (interrogation from the teletype key board);

(iii) the format of the logged output is:-

Sample number,	ORION channel 0,	ORION channel 1,	temperature
(4 digits)	(±4 digits)	(±4 digits)	(4 digits)

The 0-10 V output of the temperature transducer has been scaled so that 0-100^{o}C corresponds to a count of 0-1000 on the A/D unit.

A sample output is shown in Fig. 6D.2.

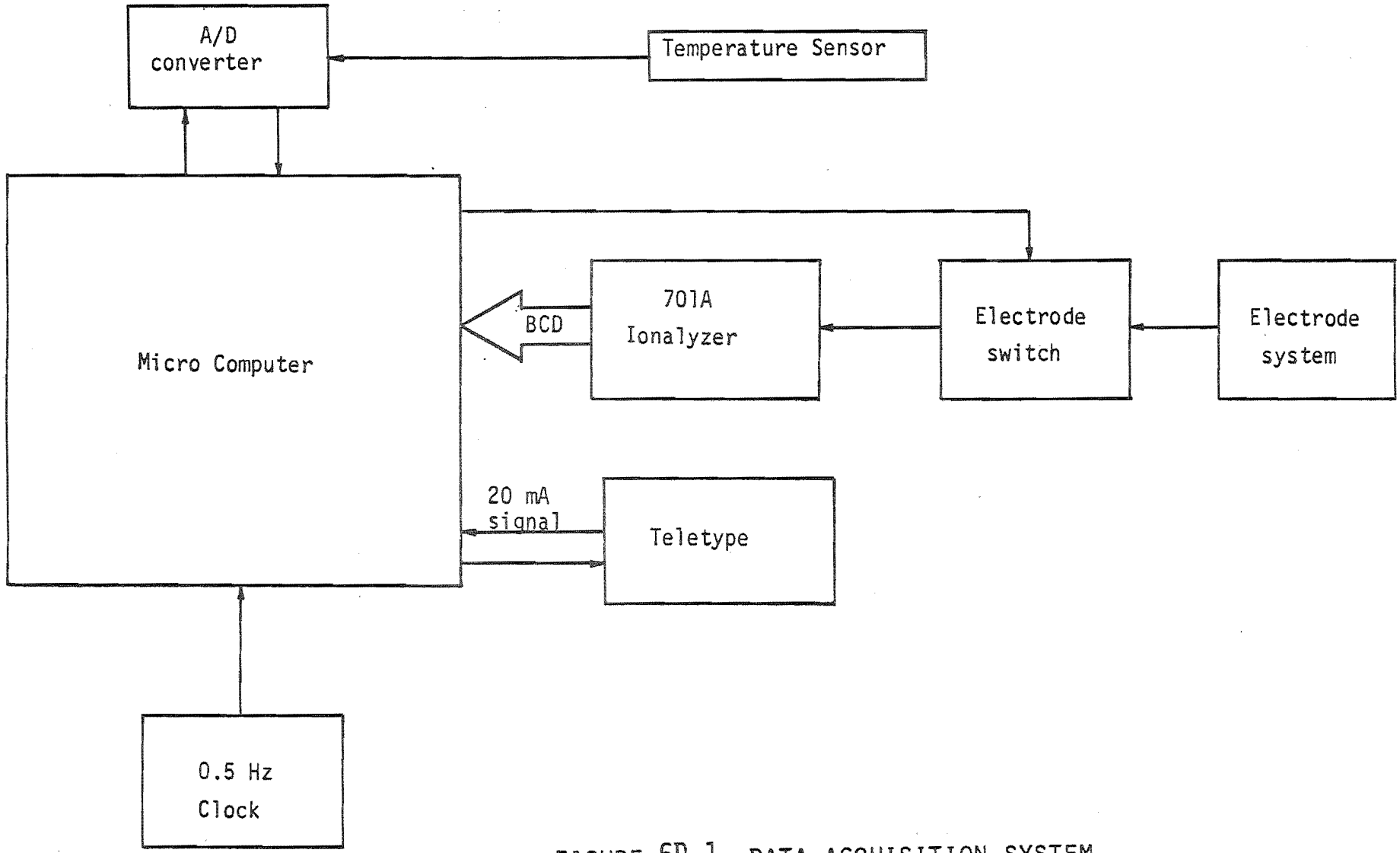

FIGURE 6D.1 DATA ACQUISITION SYSTEM

```
DATA ACQUISTION SYSTEM

ENTER SAMPLE PERIOD (MINUTES) - 04

ENTER SETTLING PERIOD (SECONDS) - 10

TURN ON PUNCH AND HIT ANY KEY TO START
0000,-2043,+0370,0244
0001,-2056,+0375,0243
0002,+0001,+2456,0244
0003,+0062,+2517,0244
0004,+0066,+2520,0246
0005,+0067,+2522,0245
0006,+0068,+2522,0245
0007,+0068,+2521,0244
0008,+0069,+2521,0244
0009,+0068,+2521,0243
0010,+0069,+2520,0243
0011,+0070,+2521,0243
0012,+0070,+2520,0243
0013,+0070,+2521,0243
0014,+0070,+2520,0243
0015,+0070,+2520,0243
0016,+0070,+2520,0243
0017,+0070,+2520,0243
0018,+0070,+2520,0243
0019,+0070,+2520,0243
0020,+0070,+2520,0243
0021,+0070,+2520,0243
0022,+0070,+2520,0243
0023,+0071,+2520,0243
0024,+0071,+2520,0243
0025,+0071,+2520,0243
0026,+0071,+2520,0243
0027,+0071,+2520,0243
0028,+0071,+2520,0243
0029,+0071,+2519,0243
0030,+0071,+2520,0243
0031,+0072,+2520,0243
0032,+0072,+2520,0243
```

Data acquisition sample output

Figure 6D.2

PROGRAM LISTING OF DATA ACQUISITION SYSTEM

```
                        *       DATA BASE
                        *
                4030    ACIACS  EQU     $4030
                4032    ACIAD   EQU     $4032
                        *       TIMER PIA
                4024    PIATD   EQU     $4024
                4026    PIACTS  EQU     $4026
                        *       A/D PIA
                402A    ADCSA   EQU     $402A
                402B    ADCSB   EQU     $402B
                4028    ADDAA   EQU     $4028
                4029    ADDAB   EQU     $4029
                        *       ORION PIA
                4026    OCSA    EQU     $4026
                4027    OCSB    EQU     $4027
                4024    ODA     EQU     $4024
                4025    ODB     EQU     $4025
                        *       IRQ VECTOR
                A000    IRQVEC  EQU     $A000           IRQ VECTOR
                0010            ORG     $10
0010            0002    WORD    RMB     2               BINARY DATA
0012            0001    MSD     RMB     1               TEMPORARY STORAGE
0013            0002    TEMP    RMB     2
0015            0002    XREG    RMB     2
0017            0002    COUNT   RMB     2               TIMER COUNT
0019            0002    ADWORD  RMB     2               A/D DATA
001B            0002    TIMER1  RMB     2               TIMER 1 REGISTER
001D            0001    TIMER2  RMB     1               TIMER 2 REGISTER
001E            0001    SETTLE  RMB     1               ORION SETTLING TIME
001F            0001    ECHO    RMB     1               FLAG FOR INPUT ROUTINE
                        *
                        *       MAIN PROGRAM
                        *
                        *       INITIALISATION
                        *
                C000            ORG     $C000
C000              86    START   LDAA    #3              RESET TTY ACIA
C001              03
C002              B7            STAA    ACIACS
C003              40
C004              30
C005              86            LDAA    #1              SET TTY ACIA CLOCK
C006              01
C007              B7            STAA    ACIACS
C008              40
C009              30
                        *       INITIALISE THE ORION PIA
                        *       PA,PB=INPUTS , CA1=TIMER INPUT
                        *       CA2=ELECTRODE SELECT
                        *       CB1=DATA READY (INPUT) , CB2=HOLD (OUTPUT)
C00A              86            LDAA    #$34
C00B              34
C00C              B7            STAA    OCSA
C00D              40
C00E              26
```

```
C00F  86 3E       LDAA   #$3E
C011  B7 40 27    STAA   OCSB
C014  4F          CLRA
C015  B7 40 24    STAA   ODA
C018  B7 40 25    STAA   ODB
C01B  86 30       LDAA   #$30
C01D  B7 40 26    STAA   OCSA
C020  86 3A       LDAA   #$3A
C022  B7 40 27    STAA   OCSB
C025  4F          CLRA
C026  B7 40 24    STAA   ODA
C029  B7 40 25    STAA   ODB
C02C  86 35       LDAA   #$35          IRQ ENAVLED ON CA1
C02E  B7 40 26    STAA   OCSA
C031  86 3E       LDAA   #$3E
C033  B7 40 27    STAA   OCSB
                  *
                  *      INITIALISE THE A/D PIA
                  *      PA,PB=INPUTS , CA2=EOC (INPUT)
                  *      CB2=START(OUTPUT)
C036  96 14       LDAA   #$14
C038  B7 40 2A    STAA   ADCSA
C03B  86 34       LDAA   #$34
C03D  B7 40 2B    STAA   ADCSB
C040  4F          CLRA
C041  B7 40 28    STAA   ADDAA
```

```
C044  B7 40 29    STAA   ADDAB
C047  86 10       LDAA   #$10
C049  B7 40 2A    STAA   ADCSA
C04C  86 30       LDAA   #$30
C04E  B7 40 28    STAA   ADCSB
C051  4F          CLRA
C052  B7 40 28    STAA   ADDAA
C055  B7 40 29    STAA   ADDAB
C058  86 14       LDAA   #$14
C05A  B7 40 2A    STAA   ADCSA
C05D  86 34       LDAA   #$34
C05F  B7 40 28    STAA   ADCSB
                  *
                  *      STARTUP SEQUENCE
                  *
C062  CE C2 C1    LDX    #STMSG
C065  BD C2 72    JSR    PMSG          PRINT HEADER
C068  BD E1 C2 55 JSR    CRLF
C06B  CE C2 DB    LDX    #SAMP         SAMPLE TIME INPUT
C06E  BD C2 72    JSR    PMSG
C071  7F 00 1F    CLR    ECHO          ENABLE ECHO
C074  BD C2 81    JSR    INPUT         GET FIRST DIGIT
```

```
C077  81 FF       CMPA  #$FF        VALID DIGIT ?
C079  27 ED       BEQ   E1          NO
C07B  16          TAB
C07C  BD C2 81    JSR   INPUT       GET SECOND DIGIT
C07F  81 FF       CMPA  #$FF        VALID DIGIT ?
C081  27 E5       BEQ   E1          NO
C083  BD C1 FC    JSR   BCDBIN      CONVERT TO BINARY
C086  C6 1E       LDAB  #30
C088  36          PSHA
C089  86 08       LDAA  #8
C08B  36          PSHA              SET UP DATA ON STACK
C08C  30          TSX
C08D  4F          CLRA
C08E  56          RORB
C08F  24 02 MT    BCC   MF
C091  AB 01       ADDA  1,X
C093  46 MF       RORA
C094  56          RORB
C095  6A 00       DEC   0,X
C097  26 F6       BNE   MT          RESULT IS IN A,B
C099  31          INS
C09A  31          INS               CLEAN UP STACK
C09B  B7 00 17    STAA  COUNT       STORE SAMPLE TIME
C09E  F7 00 18    STAB  COUNT+1
C0A1  BD C2 65    JSR   CRLF
C0A4  BD C2 65 E2 JSR   CRLF
C0A7  CE C2 FC    LDX   #SETT       GET SETTLING TIME
C0AA  BD C2 72    JSR   PMSG
```

```
C0AD  BD C2 91     JSR   INPUT     GET FIRST DIGIT
C0B0  81 FF        CMPA  #$FF      VALID ?
C0B2  27 F0        BEQ   E2        NO
C0B4  16           TAB
C0B5  BD C2 81     JSR   INPUT     GET SECOND DIGIT
C0B8  81 FF        CMPA  #$FF      VALID ?
C0BA  27 E8        BEQ   E2        NO
C0BC  BD C1 FC     JSR   BCDBIN    CONVERT TO BINARY
C0BF  44           LSRA            DIVIDE BY TWO
C0C0  B7 00 1E     STAA  SETTLE    STORE SETTLING TIME
C0C3  BD C2 65     JSR   CRLF
C0C6  BD C2 65     JSR   CRLF
C0C9  CE C3 1F     LDX   #GO       START MESSAGE
C0CC  BD C2 72     JSR   PMSG
C0CF  BD C2 65     JSR   CRLF
C0D2  7C 00 1F     INC   ECHO      DISABLE ECHO
C0D5  BD C2 81     JSR   INPUT     WAIT FOR ANY INPUT
                   *
                   *   SET UP TIMER INTERRUPTS
                   *
C0D8  CE C1 8C     LDX   #TIMER
C0DB  FF A0 00     STX   IRQVEC    SET UP INT VECTOR
C0DE  7F 00 18     CLR   TIMER1    CLEARS REGISTERS
```

```
C0E1  7F 00 1C      CLR   TIMER1+1
C0E4  7F 00 1D      CLR   TIMER2
C0E7  0E            CLI
                *
                *   MAIN PROGRAM
                *
C0E8  CE FF FF      LDX   #$FFFF          INITIALISE TIMER
C0EB  FF 00 15      STX   XREG            SAVE TIMER
C0EE  B6 00 18 ST1  LDAA  TIMER1          GET TIMER REG
C0F1  B1 00 17      CMPA  COUNT           TIME TO LOG ?
C0F4  25 F8         BCS   ST1             NO
C0F6  22 08         BHI   ST2             SAMPLE NOW
C0F8  B6 00 1C      LDAA  TIMER1+1        UPPER BYTES EQUAL
C0FB  B1 00 18      CMPA  COUNT+1         CHECK LOWER BYTES
C0FE  25 EE         BCS   ST1             NO TIMER1+1<COUNT+1
C100  7F 00 18 ST2  CLR   TIMER1          RESET TIMER
C103  7F 00 1C      CLR   TIMER1+1
C106  FE 00 15      LDX   XREG            PRINT TIME INTERVAL
C109  08            INX                   INCREMENT TIMER COUNT
C10A  FF 00 15      STX   XREG            AND SAVE IT
C10D  FF 00 10      STX   WORD            SET UP BINARY WORD
C110  BD C2 07      JSR   BINBCD          CONVERT TO BCD
C113  CE 00 13      LDX   #TEMP           SET UP FOR PRBCD
```

```
C115  C6 04     LDAB   #4              NO. OF DIGITS = 4
C118  BD C2 39  JSR    PRBCD           PRINT TIME
C11B  BD C2 5F  JSR    COMMA           PRINT COMMA
                *
                *      GET DATA FROM ORION IONANALYSER
                *
                *      CHANNEL 0
C11E  BD C1 A3  JSR    OMC             GATHER DATA
                *      SELECT CHANNEL 1
C121  86 3D     LDAA   #$3D
C123  B7 40 25  STAA   OCSA            SELECT CH1
                *      PROCESS CH0 DATA
C126  BD C1 CF  JSR    OMP             PRINT
C129  BD C2 5F  JSR    COMMA           PRINT
                *      DELAY FOR ORION TO SETTLE
C12C  7F 00 1D  CLR    TIMER2          RESET TIMER
C12F  B6 00 1D  OR1    LDAA   TIMER2
C132  B1 00 1E  CMPA   SETTLE
C135  25 F8     BCS    OR1             TIMER2<SETTLE
                *      COLLECT AND PROCESS CH1 DATA
C137  BD C1 A3  JSR    OMC
C13A  BD C1 CF  JSR    OMP
C13D  BD C2 5F  JSR    COMMA           PRINT ,
                *      RESELECT CH0
C140  86 35     LDAA   #$35
C142  B7 40 26  STAA   OCSA
```

```
                *
                *       GET DATA FROM TEMPERATURE PROBE VIA A/D
                *       CONVERT TO BCD WITH BINBCD
                *       PRINT WITH PRBCD
                *
C145  86        ADC1    LDAA    #$3C            START CONVERSION
      3C
C147  B7                STAA    ADCSB           SET CB2 HI
      40
      2B
C14A  01                NOP
C14B  01                NOP
C14C  86                LDAA    #$34            SET CB2 LO
      34
C14E  B7                STAA    ADCSB
      40
      2B
C151  CE                LDX     #$FFF           WATCHDOG COUNTER
      0F
      FF
C154  B6                LDAA    ADCSA           GET STATUS
      40
      2A
C157  09                DEX                     DEC COUNTER
C158  27                BEQ     ADCE            TOO LONG - ERROR
      25
C15A  85                BITA    #%01000000      EOC ?
      40
C15C  27                BEQ     ADC1            NO
      F6
C15E  B6                LDAA    ADDAB           YES - GET MSB
      40
      29
C161  84                ANDA    #$03            STRIP OFF BITS
      03
C163  B7                STAA    ADWORD
      00
      19
C166  B6                LDAA    ADDAA           GET LSB
      40
      28
C169  B7                STAA    ADWORD+1
      00
      1A
C16C  FE                LDX     ADWORD          CONVERT
      00
      19
C16F  FF                STX     WORD            TO BCD
      00
      10
C172  BD                JSR     BINBCD
      C2
      07
C175  CE                LDX     #TEMP
      00
      13
```

```
C178  C6 04     LDAB   #4
C17A  BD C2 39  JSR    PRBCD          PRINT ON TTY
C17D  20 06     BRA    ADC2
C17F  CE C2 A5  ADCE   LDX    #ADERR   A/D ERROR
C182  BD C2 72  JSR    PMSG           PRINT MESSAGE
C185  01        ADC2   NOP
                *
                *      SAMPLE LOOP COMPLETE
                *
C186  BD C2 65  JSR    CRLF
C189  7E C0 EE  JMP    ST1
                *
                *      TIMER INTERRUPT ROUTINE
                *
C18C  7C 00 1D  TIMER  INC    TIMER2   INC TIMER REGS
C18F  B6 00 1C  LDAA   TIMER1+1
C192  F6 00 1B  LDAB   TIMER1
C195  8B 01     ADDA   #1
C197  C9 00     ADCB   #0
C199  B7 00 1C  STAA   TIMER1+1
C19C  F7 00 1B  STAB   TIMER1
C19F  B6 40 24  LDAA   ODA            CLEAR INTERRUPT
C1A2  3B        RTI
                *
                *      ROUTINE TO COLLECT DATA FROM ORION METER
                *
C1A3  86 36     OMC    LDAA   #$36
```

```
C1A5  B7          STAA   OCSB          SET HOLD ON (LO)
      40
      27
C1A8  CE          LDX    #$FFF         WATCHDOG TIMER
      0F
      FF
C1AB  B6  OM1     LDAA   OCSB          STATUS
      40
      27
C1AE  09          DEX                  DECR TIMER
C1AF  27          BEQ    OME           ERROR
      17
C1B1  B6          LDAA   OCSB          GET STATUS
      40
      27
C1B4  2A          BPL    OM1
      F5
C1B6  B6          LDAA   ODB
      40
      25
C1B9  B7          STAA   TEMP          STORE DATA
      00
      13
C1BC  B6          LDAA   ODA
      40
      24
C1BF  B7          STAA   TEMP+1
      00
      14
C1C2  96  OM2     LDAA   #$3E
      3E
C1C4  B7          STAA   OCSB          RELEASE HOLD (HI)
      40
      27
C1C7  39          RTS
C1C8  86  OME     LDAA   #$FF          ORION METER ERROR
      FF
C1CA  B7          STAA   TEMP          STORE FLAG
      00
      13
C1CD  20          BRA    OM2
      F3
            *
            *     ROUTINE TO PRINT ORION METER DATA
            *
C1CF  B6  OMP     LDAA   TEMP          ERROR FLAG SET ?
      00
      13
C1D2  81          CMPA   #$FF          SET TO $FF FOR ERROR
      FF
C1D4  27          BEQ    OMP1          YES
      1F
            *     PRINT SIGN (=BIT 7 IN ODB)
C1D6  F6          LDAB   TEMP
      00
      13
```

```
C1D9  2A 07     BPL   OMP2    NEGATIVE SIGN
C1DB  86 2B     LDAA  #'+     POSITIVE
C1DD  BD C2 4F  JSR   DIGIT3  PRINT +
C1E0  20 05     BRA   OMP3
C1E2  86 2D     LDAA  #'-     NEGATIVE
C1E4  BD C2 4F  JSR   DIGIT3  PRINT -
C1E7  C4 7F     ANDB  #$7F    CLEAR SIGN
C1E9  F7 00 13  STAB  TEMP    AND SAVE
C1EC  CE 00 13  LDX   #TEMP   ADDRESS OF DATA
C1EF  C6 04     LDAB  #4      4 DIGITS
C1F1  BD C2 39  JSR   PRBCD   PRINT DIGITS
C1F4  39        RTS
C1F5  CE C2 AF  OMP1  LDX   #OMERR  ERROR MESSAGE
C1F8  BD C2 72  JSR   PMSG  PRINT IT
C1FB  39        RTS
                *
                *     ROUTINE TO CONVERT
                *     2 BCD DIGITS INTO BINARY
                *     MSD IN B , LSD IN A
                *     RESULT IS AN 8 BIT BYTE IN A (0-99)
                *
C1FC  36  BCDBIN  PSHA          SAVE LSD
C1FD  17          TBA           B->A
C1FE  58          ASLB
C1FF  58          ASLB
C200  58          ASLB          B*8
C201  48          ASLA          A*2
C202  1B          ABA           =A*10
C203  16          TAB           A ->   B
C204  32          PULA          GET LSD
C205  1B          ABA           FORM SUM
C206  39          RTS
                *
                *     S/R TO CONVERT BINARY TO BCD
```

```
                *       5 DIGITS IN MSD.  TEMP, TEMP+1
                *
C207    CE      BINBCD  LDX     #16             SET LOOP COUNT
        00
        10
C20A    5F              CLRB                    CLEAR DECIMAL
C20B    7F              CLR     TEMP            ...
        00
        13
C20E    7F              CLR     TEMP+1          MAX 6 DIGITS USE 5
        00
        14
                *       ROTATE 16 BITS LEFT CIRCULARLY
C211    77      BI1     ASR     WORD            DUPLICATE MSB
        00
        10
C214    79              ROL     WORD            SHIFT INTO CARRY
        00
        10
C217    79              ROL     WORD+1          ROTATE INTO LOW BYTE
        00
        11
C21A    79              ROL     WORD            ROTATE INTO HIGH BYTE
        00
        10
C21D    B6              LDAA    TEMP+1          DOUBLE DECIMAL
        00
        14
C220    B9              ADCA    TEMP+1
        00
        14
C223    19              DAA
C224    B7              STAA    TEMP+1          ...
        00
        14
C227    B6              LDAA    TEMP            PROPAGATE 5 DIGITS
        00
        13
C22A    B9              ADCA    TEMP            ...
        00
        13
C22D    19              DAA                     ...
C22E    B7              STAA    TEMP            ...
        00
        13
C231    59              ROLB                    IGNORE SIXTH DIGIT
C232    09              DEX                     DECREMENT COUNT
C233    26              BNE     BI1             TOTAL 16 BITS
        DC
C235    F7              STAB    MSD
        00
        12
C238    39              RTS
```

```
                        *
                        *       I/O SUBROUTINES
                        *
                        *       PRBCD   PRINTS A STRING OF BCD NUMBERS
                        *
C233    57      PRBCD   ASRB                    GET NO. OF BYTES
C23A    A6      PR1     LDAA    0,X             GET BYTE
        00
C23C    8D              BSR     DIGIT1          PRINT MSD
        09
C23E    A6              LDAA    0,X             GET BYTE
        00
C240    8D              BSR     DIGIT2          PRINT LSD
        03
C242    08              INX                     INCREMENT POINTER
C243    5A              DECB                    DECREMENT COUNTER
C244    26              BNE     PR1
        F4
C246    39              RTS
                        *
                        *       OUTPUT ROUTINES
                        *
C247    44      DIGIT1  LSRA                    GET MSD
C248    44              LSRA
C249    44              LSRA
C24A    44              LSRA
C24B    84      DIGIT2  ANDA    #$0F            STRIP UPPER NIBBLE
        0F
C24D    8A              ORAA    #'0             CONVERT TO ASCII
        30
C24F    8D      DIGIT3  BSR     RDV             TTY READY ?
        04
C251    B7              STAA    ACIAD           YES - PRINT
        40
        32
C254    39              RTS
                        *
C255    36      RDV     PSHA                    SAVE A
C256    B6      RD1     LDAA    ACIACS          GET STATUS
        40
        30
C259    95              BITA    #$2             BUSY ?
        02
C25B    27              BEQ     RD1             YES
        F9
C25D    32              PULA                    NO
C25E    39              RTS
                        *
                        *       SUBROUTINE TO PRINT A COMMA
                        *
C25F    86      COMMA   LDAA    #',
        2C
C261    BD              JSR     DIGIT3
        C2
        4F
```

```
C264  39          RTS
                  *
                  *       SUBROUTINE TO PRINT CR,LF
                  *
C265  36    CRLF  PSHA                        SAVE A
C266  86          LDAA    #$0D                CR
      0D
C268  BD          JSR     DIGIT3
      C2
      4F
C26B  86          LDAA    #$0A                LF
      0A
C26D  BD          JSR     DIGIT3
      C2
      4F
C270  32          PULA                        RESTORE A
C271  39          RTS
                  *
                  *       ROUTINE TO PRINT ASCII MESSAGE
                  *       POINTED TO BY X ON THE TTY.
                  *       THE STRING IS TERMINATED
                  *       BY AN EOT($04).
                  *
C272  36    PMSG  PSHA
C273  A6    PM1  LDAA    0,X
      00
C275  81          CMPA    #$04                END OF STRING ?
      04
C277  27          BEQ     PM2                 YES
      06
C279  BD          JSR     DIGIT3              NO
      C2
      4F
C27C  08          INX                         INCR POINTER
C27D  20          BRA     PM1
      F4
C27F  32    PM2   PULA
C280  39          RTS
                  *
                  *       ROUTINE TO INPUT A DECIMAL
                  *       DIGIT FROM THE TTY.
                  *
C281  37    INPUT PSHB                        SAVE B
C282  F6    IN1  LDAB    ACIACS              GET STATUS
      40
      30
C285  57          ASRB                        RDRF INTO C
C286  24          BCC     IN1                 NO DATA AVAILABLE
      FA
C288  B6          LDAA    ACIAD               GET BYTE
      40
      32
C28B  84          ANDA    #$7F                STRIP BIT 8
      7F
```

```
C28D  7D 00 1F      TST     ECHO            ECHO ?
C290  26 03         BNE     IN2             NO
C292  BD C2 4F      JSR     DIGIT3          YES
C295  80 30 IN2     SUBA    #'0             CONVERT TO BCD
C297  81 00         CMPA    #0
C299  25 06         BCS     INE             <0
C29B  81 09         CMPA    #9
C29D  22 02         BHI     INE             >9
C29F  33            PULB
C2A0  39            RTS
C2A1  86 FF INE     LDAA    #$FF            ERROR INDICATION
C2A3  33            PULB
C2A4  39            RTS
                *
                *   ERROR MESSAGES
                *
C2A5  41 2F ADERR   FCC     !A/D ERROR!
C2A6  2F
C2A7  44
C2A8  20
C2A9  45
C2AA  52
C2AB  52
C2AC  4F
C2AD  52
C2AE  04            FCB     $04
C2AF  4F OMERR      FCC     !ORION METER ERROR!
C2B0  52
C2B1  49
C2B2  4F
C2B3  4E
C2B4  20
C2B5  4D
C2B6  45
C2B7  54
C2B8  45
C2B9  52
C2BA  20
C2BB  45
C2BC  52
C2BD  52
C2BE  4F
C2BF  52
```

```
C2C0    04              FCB     $04
                *
                *       MESSAGES
                *
C2C1    44      STMSG   FCC     /DATA ACQUISITION SYSTEM/
C2C2    41
C2C3    54
C2C4    41
C2C5    20
C2C6    41
C2C7    43
C2C8    51
C2C9    55
C2CA    49
C2CB    53
C2CC    49
C2CD    54
C2CE    49
C2CF    4F
C2D0    4E
C2D1    20
C2D2    53
C2D3    59
C2D4    53
C2D5    54
C2D6    45
C2D7    4D
C2D8    0D              FCB     $D, $A, $4
C2D9    0A
C2DA    04
C2DB    45      SAMP    FCC     /ENTER SAMPLE PERIOD (MINUTES) - /
C2DC    4E
C2DD    54
C2DE    45
C2DF    52
C2E0    20
C2E1    53
C2E2    41
C2E3    4D
C2E4    50
C2E5    4C
C2E6    45
C2E7    20
C2E8    50
C2E9    45
C2EA    52
C2EB    49
C2EC    4F
C2ED    44
C2EE    20
C2EF    28
C2F0    4D
C2F1    49
C2F2    4E
```

```
C2F3    55
C2F4    54
C2F5    45
C2F6    53
C2F7    29
C2F8    20
C2F9    2D
C2FA    20
C2FB    04          FCB     $4
C2FC    45  SETT    FCC     /ENTER SETTLING PERIOD (SECONDS) - /
C2FD    4E
C2FE    54
C2FF    45
C300    52
C301    20
C302    53
C303    45
C304    54
C305    54
C306    4C
C307    49
C308    4E
C309    47
C30A    20
C30B    50
C30C    45
C30D    52
C30E    49
C30F    4F
C310    44
C311    20
C312    28
C313    53
C314    45
C315    43
C316    4F
C317    4E
C318    44
C319    53
C31A    29
C31B    20
C31C    2D
C31D    20
C31E    04          FCB     $4
C31F    54  GO      FCC     /TURN ON PUNCH AND HIT ANY KEY TO START
C320    55
C321    52
C322    4E
C323    20
C324    4F
C325    4E
C326    20
C327    50
C328    55
```

```
C329    4E
C32A    41
C32B    48
C32C    20
C32D    41
C32E    4E
C32F    44
C330    20
C331    48
C332    49
C333    54
C334    20
C335    41
C336    4E
C337    59
C338    20
C339    48
C33A    45
C33B    59
C33C    20
C33D    54
C33E    4F
C33F    20
C340    53
C341    54
C342    41
C343    52
C344    54
C345    20
C346    04          FCB     $4
                    END

ERRORS DETECTED   0
```

SYMBOL TABLE

ACIACS	4030	ACIAD	4032	PIATD	4024	PIACTS	4026
ADCSA	402A	ADCSB	402B	ADDRA	4028	ADDRB	4029
DCSA	4026	DCSB	4027	DDA	4024	DDB	4025
IRQVEC	A000	WORD	0010	MSD	0012	TEMP	0013
XREG	0015	COUNT	0017	ADWORD	0019	TIMER1	001B
TIMER2	001D	SETTLE	001E	ECHO	001F	START	C000
STMSG	C2C1	PMSG	C272	E1	C068	CRLF	C265
SAMP	C2DB	INPUT	C281	BCDBIN	C1FC	MT	C08F
MF	C093	E2	C0A4	SETT	C2FC	GO	C31F
TIMER	C18C	ST1	C0EE	ST2	C100	BINBCD	C207
PRBCD	C239	COMMA	C25F	OMC	C1A3	OMP	C1CF
DR1	C12F	ADC1	C154	ADCE	C17F	ADC2	C185
ADERR	C2A5	OM1	C1AB	OME	C1C8	OM2	C1C2
OMP1	C1F5	OMP2	C1E2	DIGIT3	C24F	OMP3	C1E7
OMERR	C2AF	BI1	C211	PR1	C23A	DIGIT1	C247
DIGIT2	C24B	RDV	C255	RD1	C256	PM1	C273
PM2	C27F	IN1	C282	IN2	C295	INE	C2A1

CHAPTER 7

RESULTS AND DISCUSSION OF COLUMN EXPERIMENTS

Experimental techniques were detailed in Chapter 6. In this chapter, experimental results for binary and ternary breakthrough curves are presented and compared to theoretical predictions from the computer program GPFIXC.

7.1 Experimental Method

To confirm experimental reproducibility, the breakthrough curve for each set of experimental conditions was repeated.

The basic data required by the computer simulations are presented in Table 7.1. Each presented value represents the average of a number of measurements.

Difficulties were experienced with earth loops associated with the concentration measurements. The effluent from the measuring cell passed to drain. Consequently the measuring solution was connected to earth. Since the reference electrode was also connected to earth via the Orion metal case, a loop existed between the reference electrode and the measuring solution. The problem was solved by isolating the solution from earth by collecting the effluent in a large plastic vessel.

Electrodes were calibrated at the start and the finish of each run to compensate for drift. Table 7.2 shows values of electrode drift for some runs.

Contrary to expectation, the positive displacement metering pumps employed did not produce absolutely constant flow rates with change in feed solution levels. The flow rate variations during a run were in some cases up to 2%. Computer analysis

showed that these flow rate variations had negligible effect on the breakthrough curve shapes.

Material balances for each run were performed by comparing the bed capacity from experimental breakthrough curves to that from capacity measurement. The results were shown in Table 7.3. The discrepancies in the percentage deviations were due to both of the experimental breakthrough curves and the column capacity measurements.

The sampling time for each run was not the same. For steeper transition zones, a shorter sampling time was used. Sampling times of one to four minutes were employed.

One conclusion to be drawn from this work is that ion selective electrodes can be accurately used in monitoring ionic concentrations from fixed-bed ion exchange columns. The knowledge of activity coefficients, liquid junction potentials, electrode interferences, electrode drift, reference filling solutions, Nernst equation and multicomponent calibrating solutions is necessary for the successful application of ion selective electrodes. The availability of new ion selective electrodes and better qualities in existing ones will allow ion selective electrodes to become a common concentration measurement tool.

Total solution concentration	0.1 N
Column equivalents	3573.04 meq.
Voidage	0.38
Particle diameter in hydrogen form in water	0.076 cm
Column diameter	4.93 cm
Bed volume of K form in water	1670.6 ml
Bed volume of K form in 0.1 N KNO_3	1667.7 ml
Bed volume of Na form in water	1759.2 ml
Bed volume of Na form in 0.1 N $NaNO_3$	1755.4 ml
Bed volume of H form in water	1913.7 ml
Bed volume of H form in 0.1 N HNO_3	1908.0 ml

Table 7.1: Column Data

Run No.	Time interval (hr)	Potassium electrode				Hydrogen electrode			
		S ($mV/^oK$)		E_o (mV)		S ($mV/^oK$)		E_o (mV)	
		Begin	End	Begin	End	Begin	End	Begin	End
16	14	.1909	.1904	68.2486	69.2503	.1927	.1935	-36.5760	-38.0886
20	13	.1873	.1876	95.6381	98.1209	.1904	.1904	- 6.7062	- 4.4288
26	8	.1942	.1976	80.2622	81.9351	.1988	.2010	-39.6430	-42.8618
28	7	.1972	.1989	79.7411	82.5366	.1985	.1989	-36.8106	-37.8106
30	12	.1920	.1924	80.1122	80.6050	.1952	.1946	-33.0687	-32.3352
31	8	.1881	.1880	77.2265	77.9088	.1925	.1919	-29.4947	-28.5521
34	11	.1921	.1969	70.1304	72.6343	.1975	.1975	-48.1028	-48.3466
37	4	.1925	.1925	72.2386	72.6386	.1949	.1942	-44.3071	-42.5647
40	5	.1926	.1931	72.8666	73.1470	.1943	.1945	-42.3072	-43.3130

Notes:

(1) Electrodes drift according to Nernst equation:

$$E = E_o - E_j + ST\ell n(\frac{\gamma_i C_i}{A_o})$$

(2) The theoretical value of S = 0.2166 $mV/^oK$

(3) 0.1 mV corresponds to 0.4% in concentration.

Table 7.2

Run No.	Potassium ion mass balance		Hydrogen ion mass balance	
	Bed capacity (meq.)	% deviation from capacity measurement	Bed capacity (meq.)	% deviation from capacity measurement
7	3596.1	-0.6	-	-
8	3622.8	-1.4	-	-
13	-	-	3564.7	0.2
14	-	-	3615.4	-1.2
17	3610.4	-1.0	3443.3	3.6
18	3613.0	-1.1	3366.5	5.8
19	3607.5	-1.0	3492.5	2.3
22	3716.8	-4.0	3480.8	2.6
31	3576.3	-0.1	3462.2	3.1
32	3622.5	-1.4	3538.0	1.0
28	3611.6	-1.1	3407.7	4.6
26	3508.7	1.8	3526.2	1.3
27	3500.3	2.0	3501.4	2.0
30	3676.5	-2.9	3487.3	2.4
33	3586.7	0.4	3479.0	2.6
37	3599.6	-0.7	3421.7	4.2
38	3605.0	-0.9	3590.4	-0.5

The equation used for computing bed capacity from experimental breakthrough curve was:-

$$C_o\bar{X}_i^o Ft + QV\bar{Y}_i^o = FC_o\int_o^t \bar{X}_i\,dt + QV\bar{Y}^\infty + C_o\bar{X}_i^o(V\varepsilon + V_D)$$

$C_o\bar{X}_i^o Ft$ the number of equivalents of i added to the column during time t

$QV\bar{Y}_i^o$ the number of equivalents of i in the resin at time zero

$FC_o\int_o^t \bar{X}_i\,dt$ the number of equivalents of i in the effluent at time t

$QV\bar{Y}_i^\infty$ the number of equivalents of i in the resin at time t

$C_o\bar{X}_i^o(V\varepsilon+V_D)$ the number of equivalents of i in the void at time t

Table 7.3

7.2 Results of Binary Experiments

Although the aim of this work was to study multicomponent fixed-bed ion exchange behaviour, the program developed should be able to predict breakthrough curves for any number of components, thus binary systems K-Na and Na-H were studied.

A summary of the binary runs is shown in Table 7.4 and the breakthrough curves (plots of normalized solution concentrations against throughput ratios) are shown in Figures 7.1-7.4.

Unless specified, the computer predictions were based on combined diffusion mechanism, constant self-diffusion coefficients and Hiester relation for computing solution phase mass transfer coefficients.

Figure 7.1 shows experimental and predicted breakthrough curves of runs 7 and 9. In these two runs, 0.1 N KNO_3 solution was passed through the bed of ion exchange resin initially in Na form. The bed volume changed from 1770.6 ml to 1671.4 ml .

The shapes of these breakthrough curves indicate constant pattern conditions as might be expected for a deep bed ion exchange operation under a favourable equilibrium condition.

Binary equilibrium data (Kelly, 1966) showed that the K-Na is a variable separation factor system, yet the use of a constant separation factor in the breakthrough curve prediction gives good agreement with the experimental result. This supports the common view that with favourable equilibrium, the shape of the breakthrough curve is determined more by rate than by equilibrium.

The effective diffusion coefficients are not constant but vary with concentration from that of the self-diffusion coefficient of sodium ion alone to that of the potassium ion in accordance with the Nernst-Planck equation. Thus the number of solution phase transfer units in the column is not constant but ranges from 131-108. The range is small because the self-diffusion coefficient of potassium and sodium ions are similar ($D_K = 1.8.10^{-5}$ sq.cm/sec and $D_{Na} = 1.2.10^{-5}$ sq.cm/sec).

The range of number of transfer units and the average value of separation factor for this system indicates that the breakthrough curve attained a constant pattern (Allen, 1973).

Figure 7.2 shows the experimental and predicted breakthrough curves of runs 8 and 10. If runs 7 and 9 are to be considered as exhaustions then runs 8 and 10 are the corresponding regenerations. The experimental results show a proportionate pattern shape as the exchange were under unfavourable equilibrium conditions.

There are two predictions; one is based on a constant separation factor (CSF) and the other based on variable separation factors (VSF). The prediction based on VSF fits the experimental results better than that of CSF. The classical argument is that because the exchange is under an unfavourable equilibrium condition and the number of transfer units is relatively high (108-131), then concentration gradients at the solution-particle interface are small, bulk concentrations tend to be in equilibrium and the exchange is under equilibrium control.

Figure 7.3 shows the experimental and predicted results of runs 11 and 13. The pH electrode became unreliable towards the end of run 13 and was replaced. In these runs, 0.1 N HNO_3 was passed through the sodium bed, since α_{Na}^{H} is 0.71, less than one, the breakthrough curve shape is proportionate pattern. The number of transfer units is 113-303. The range is more than that of K-Na system because the self-diffusion coefficient of hydrogen ion is higher than those of the potassium and sodium ions.

The reverse exchanges of runs 11 and 13 are shown in Figure 7.4. In these runs (12 and 14), 0.1 N $NaNO_3$ solution was passed through the bed of H-form. From the number of transfer units (308-114) and the average separation factor (α_{H}^{Na} = 1.41) a constant pattern was attained in the runs.

Comparisons of runs 7 and 9 with runs 12 and 14 reveal three points. Firstly, runs 7 and 9 reached the end of the runs slower than runs 12 and 14 even though the separation factors of runs 7 and 9 (α_{H}^{K}) were greater than those of runs 12 and 14 (α_{H}^{Na}), thus showing the effect of mass transfer control since the number of transfer units of runs 7 and 9 was less than that of runs 12 and 14. Secondly, the shape of the breakthrough curves of runs 7 and 9 is rotationally symmetric with a pivot point at Z equals one whereas for runs 12 and 14 the first part of the curves (Z from zero to one) is less steep (i.e. it has a larger radius of curvature) than the second part (Z from one to the end of the runs). Thirdly, for runs 7 and 9 Z = 1.0 at X $\doteqdot$ 0.5, but for runs 12 and 14 Z = 1.0 at X $\doteqdot$ 0.58.

The last two points can be explained by considering intra-diffusion coefficients. For runs 7 and 9 the intra-diffusion coefficient is given by (Eqn. 2.9):-

$$D_{KNa} = \frac{D_K D_{Na}(Z_K X_K + Z_{Na} X_{Na})}{Z_K X_K D_K + Z_{Na} X_{Na} D_{Na}}$$

$$= \frac{D_K D_{Na}}{X_K D_K + X_{Na} D_{Na}}$$

since self-diffusion coefficients of potassium and sodium ions are similar:

$$D_{KNa} \doteqdot D_K \doteqdot D_{Na}$$

Thus, for these runs, the mass transfer coefficient was approximately constant for the entire breakthrough curve, explaining the observed behaviour of Z = 1.0 at X ≒ 0.5 and rotationally symmetric about point Z = 1.0. For runs 12 and 14 the intra-diffusion coefficient is given by:

$$D_{NaH} = \frac{D_{Na} D_H}{X_{Na} D_{Na} + X_H D_H}$$

The above expression cannot be further simplified in the same manner as the K-Na system because $D_H >> D_{Na}$. Thus, for these runs, the mass transfer coefficient was not constant but would vary throughout the runs as the resin changed from hydrogen form to sodium form. This explains why the breakthrough curves were not rotationally symmetric about Z = 1.0.

To confirm this explanation, the computer calculations for runs 12 and 14 were repeated but with the exception of holding the intra-diffusion coefficient constant. The results show rotational symmetry and that the point Z = 1, X = 0.5 lies on the breakthrough curve. Consequently, these results show that the Nernst-Planck model, allowing variable intra-diffusion coefficients, is necessary to accurately represent ion exchange column behaviour.

Verification of constant and proportionate patterns can be confirmed by plotting computed concentrations ($\bar{X}_i$, $\bar{X}_i^*$, $\bar{Y}_i$ and $\bar{Y}_i^*$) against throughput ratio (Z). Figure 7.5 shows such plots for runs 11 and 13 and runs 12 and 14. The plot of runs 12 and 14, sodium ions replacing hydrogen ions, i.e. favourable equilibrium condition, shows that the concentrations of sodium ion in both solution phase and particle phase are approximately the same ($\bar{X}_{Na} \doteqdot \bar{Y}_{Na}$), a condition for a constant pattern. The plot of runs 11 and 13, hydrogen ions replacing sodium ions i.e. unfavourable equilibrium condition, shows that the concentrations of hydrogen ions in solution and particle phases approximately equal their corresponding interphase concentrations respectively ($\bar{X}_H = \bar{X}_H^*$ and $\bar{Y}_H = \bar{Y}_H^*$), a condition for a proportionate pattern.

Figure 7.5 also shows plots of mechanism parameter against throughput ratio. The plot for runs 12 and 14 shows the mechanism parameter varying from 2.0 to 5.4, whereas for runs 11 and 13 it varies from 5.4 to 2.0. Thus, for these runs, the mass transfer is predominantly under solution phase diffusion control and the number of transfer units are not constant.

Run Number	Feed composition	Bed Form		Bed volume (ml)		Flow rate (ml s^{-1})	Mean separation factor	No. of solution phase mass transfer unit
		Beginning	End	Beginning	End			
7&9	0.1 N KNO_3	Na	K	1770.6	1673.4	2.9835	1.45	131 - 108
8&10	0.1 N $NaNO_3$	K	Na	1678.7	1705.8	2.9775	1.45	108 - 131
11&13	0.1 N HNO_3	Na	H	1764.0	1837.2	2.9613	1.41	113 - 303
12&14	0.1 N $NaNO_3$	H	Na	1906.7	1752.5	2.9825	1.41	308 - 114

Summary of parameters for experimental breakthrough curves of binary systems

Table 7.4

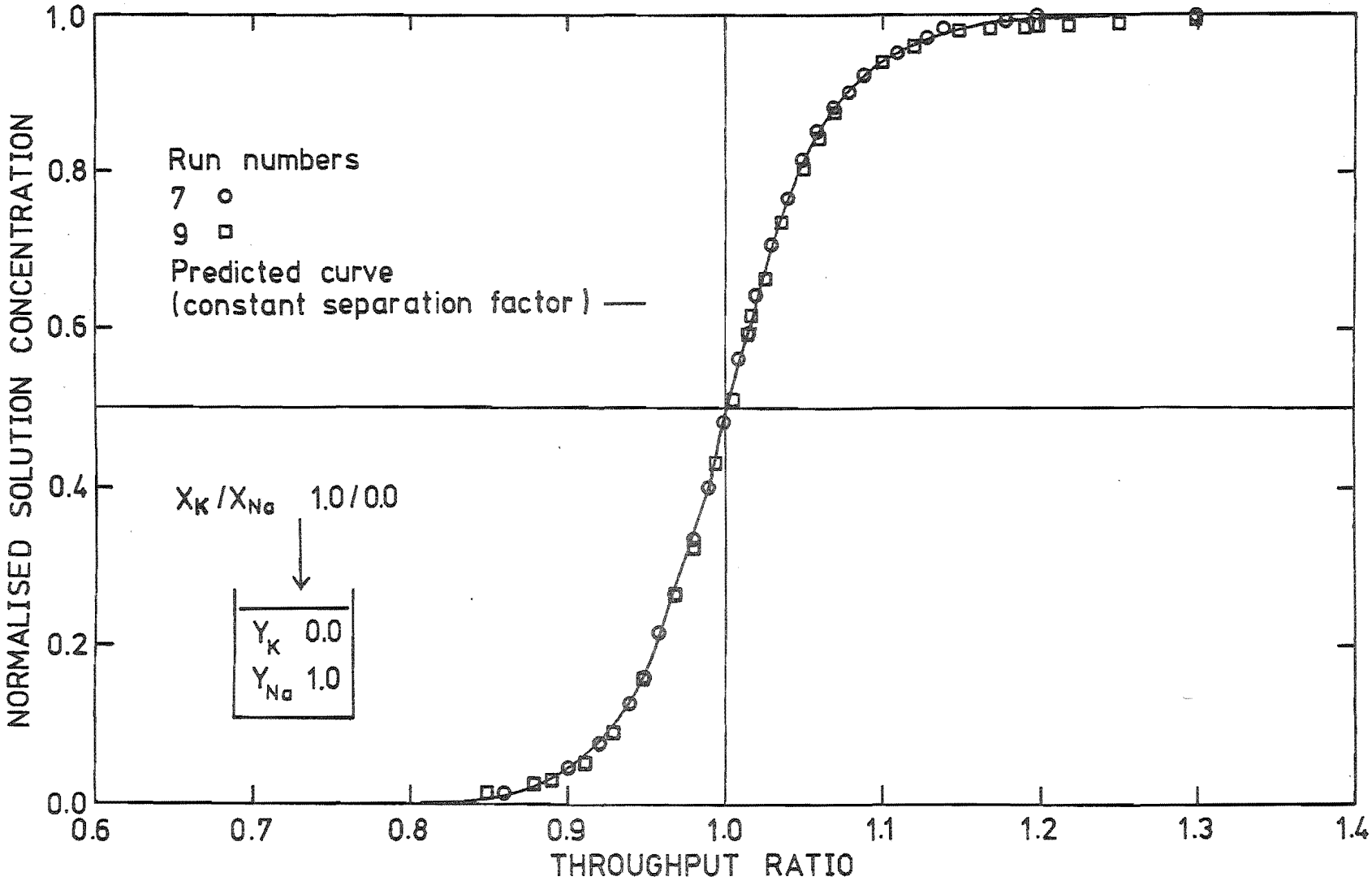

FIGURE 7.1 COMPUTED AND EXPERIMENTAL BREAKTHROUGH CURVES

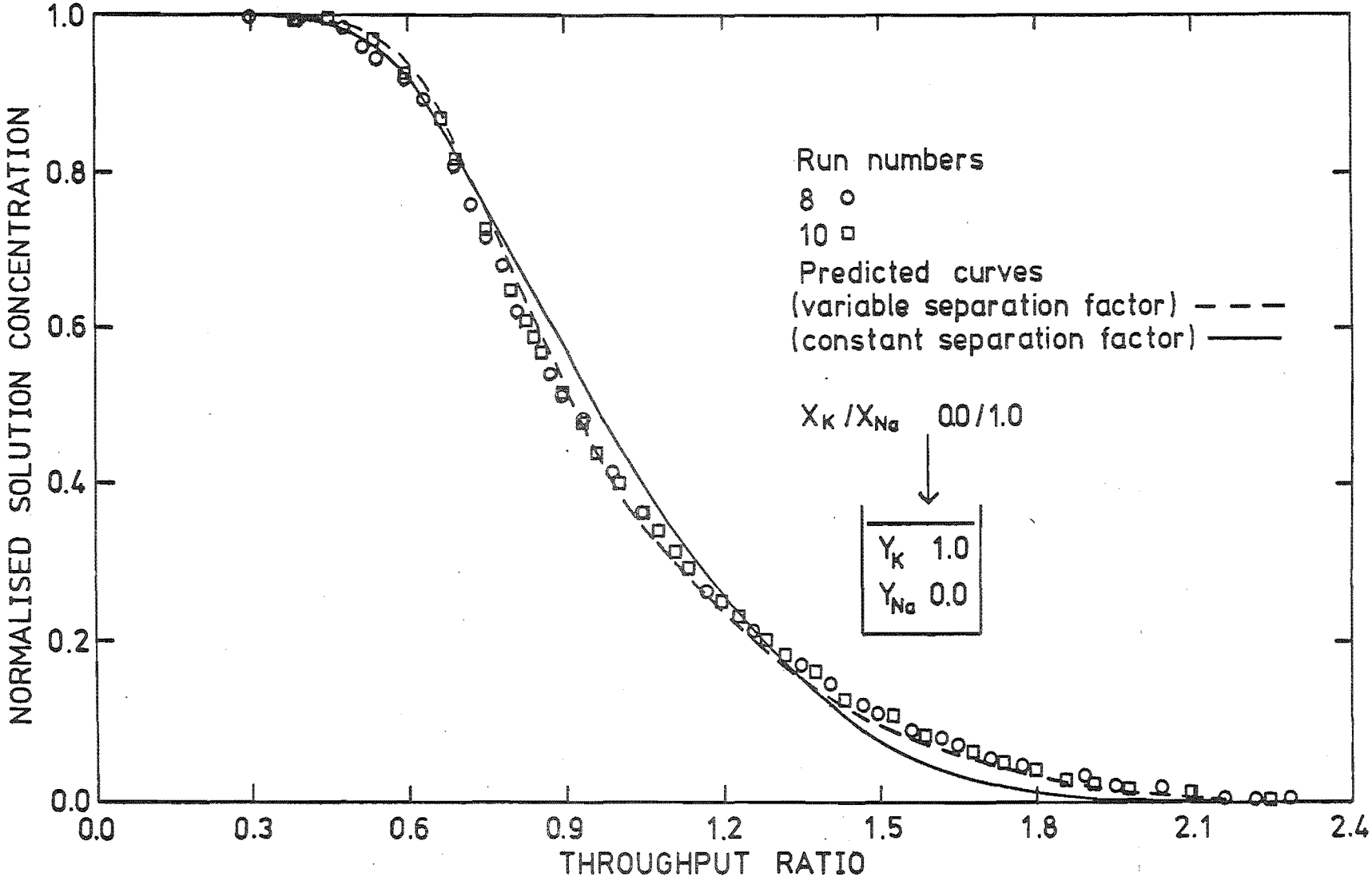

FIGURE 7.2 COMPUTED AND EXPERIMENTAL BREAKTHROUGH CURVES

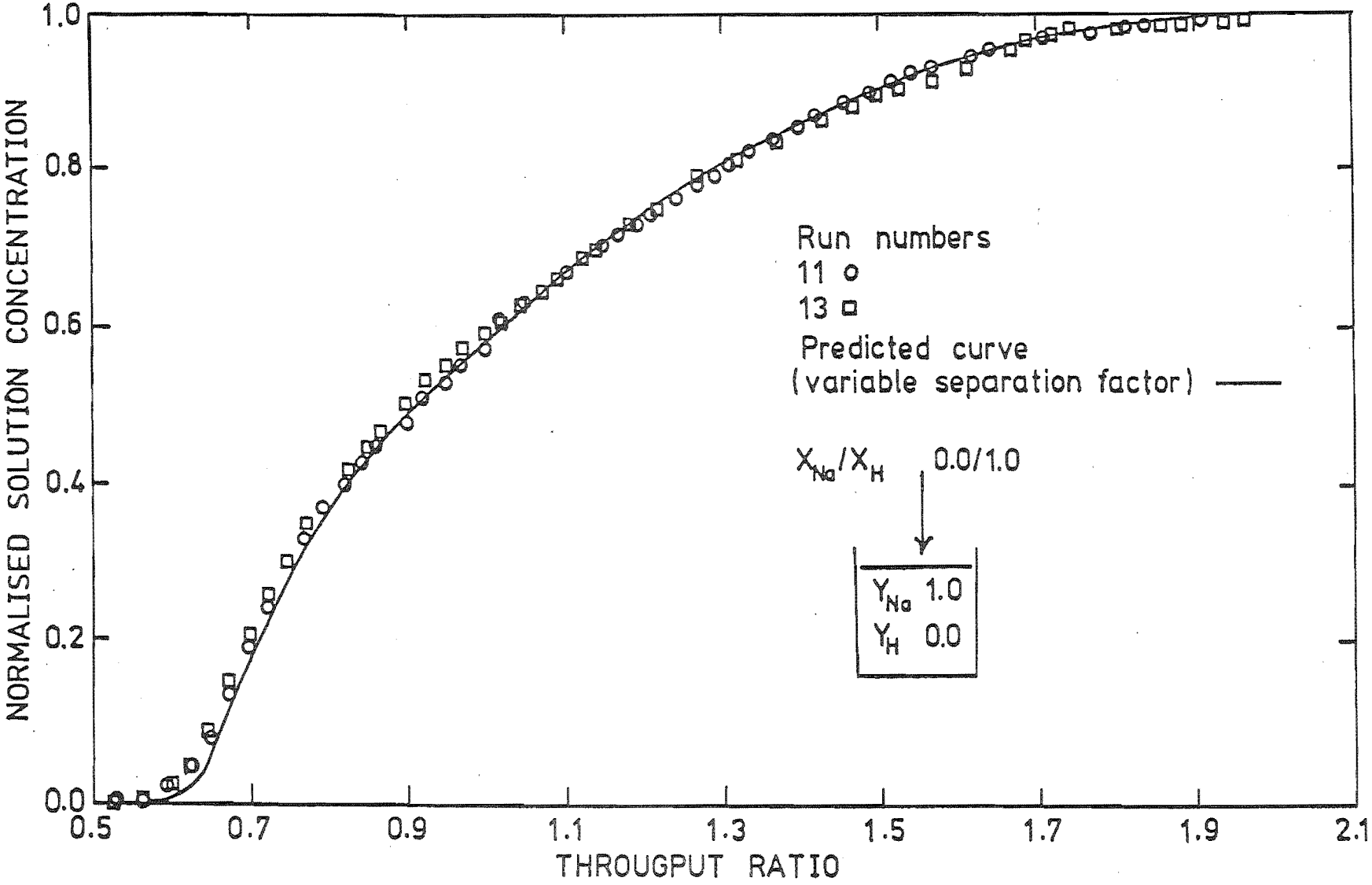

FIGURE 7.3 COMPUTED AND EXPERIMENTAL BREAKTHROUGH CURVES

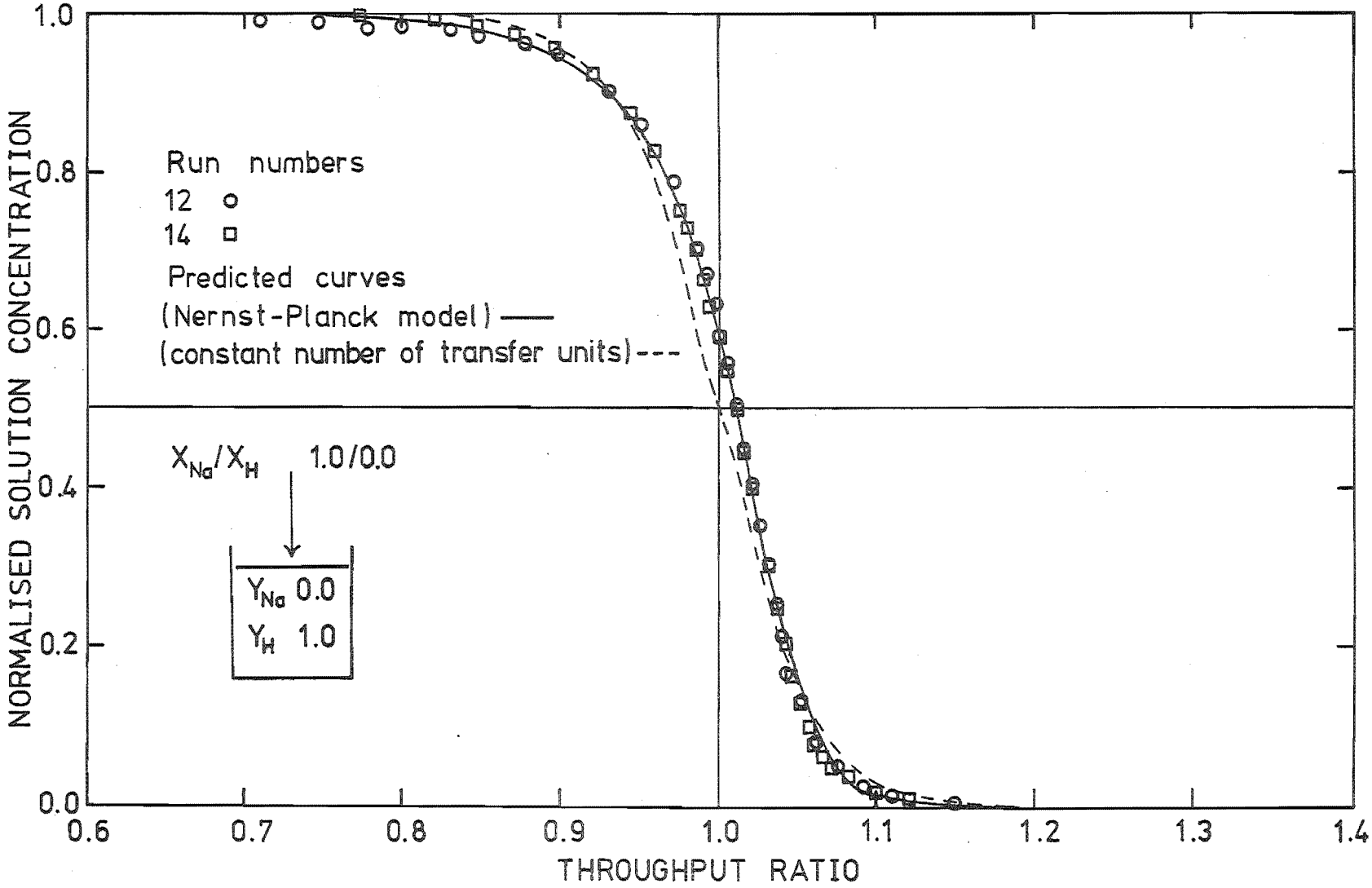

FIGURE 7.4 COMPUTED AND EXPERIMENTAL BREAKTHROUGH CURVES

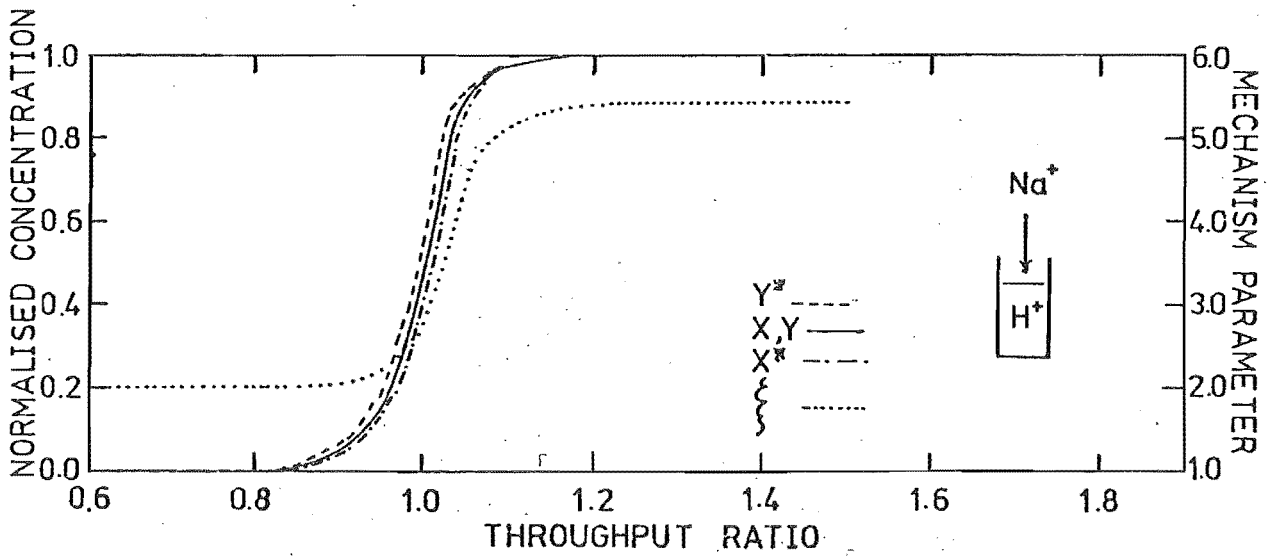

(A) RUNS 12,14

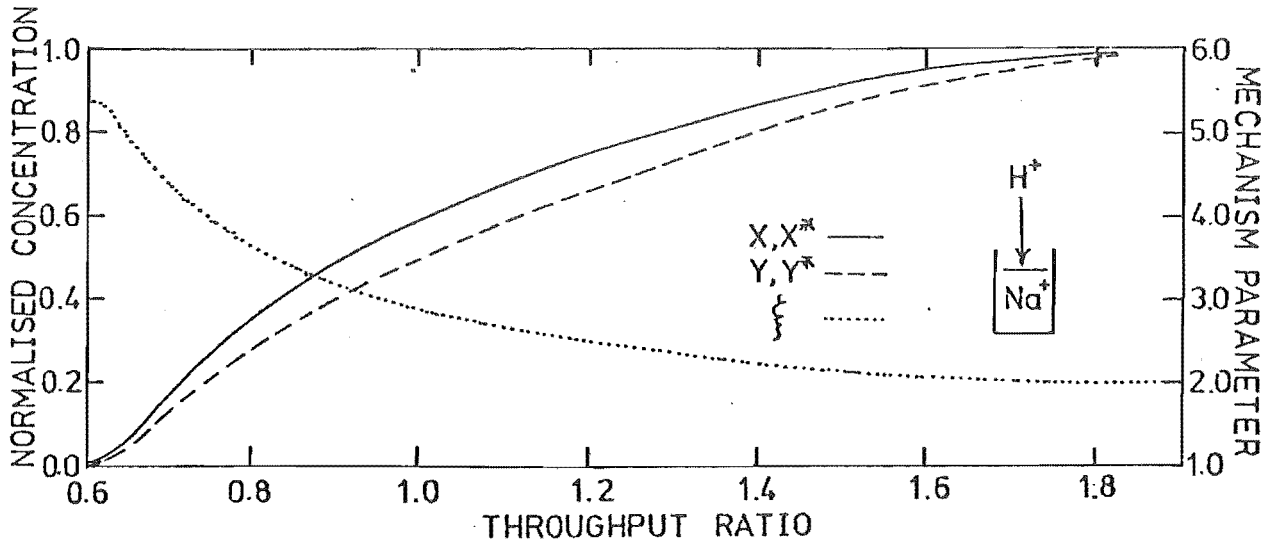

(B) RUNS 11,13

FIGURE 7.5 VERIFICATION OF CONSTANT AND PROPORTIONATE PATTERNS

7.3 Results of Ternary Experiments

Twenty-six breakthrough curves for the ternary component system, K/Na/H, were measured. The experimental runs were gathered under varying conditions so as to test the generality of the equations of the model developed here. These included a range of flow rates from 0.9 to 5.2 ml s^{-1}, various operating temperatures (from 22 to 28°C) and a range of composition for both feed and column presaturation.

In the development of the column material balance equation (Chapter 2), the effect of axial dispersion was not included. Usually this effect becomes important at low flow rates. Since low flow rates ($F \doteq 1$ ml s^{-1}) were employed in four runs (runs 33 to 36), it was necessary to verify that this effect was negligible by comparing average mass transfer coefficients for the particle phase, for the solution phase and for the axial dispersion. Axial dispersion in a fixed-bed ion exchange column originates from molecular diffusion and uneven velocity profiles in the bed. The mass transfer coefficient reflecting the axial dispersion is given by (Perry, 1963):

$$k_d A_p = \frac{F}{AL}$$

where L, the axial mixing length, is given by

$$L = \frac{d_p}{P_d} + \frac{D}{\sqrt{2}(F/A)}$$

P_d is the Peclet number having a value of 0.5 for a laminar liquid flow and 2.0 for a turbulent liquid flow.

F flow rate

A column cross sectional area

d_p particle diameter

D solution phase diffusion coefficient

Comparisons of the mass transfer coefficients based on axial effects to those of solution phase and particle phase, shown in Table 7.5, indicate that the effect of axial mixing can be ignored for the experiments here.

Run Number	Flow Rate ($ml\ s^{-1}$)	Temperature (^{o}C)	Average mass transfer coeff. (s^{-1})		
			Axial Effect	Particle phase	Solution phase
34&36	0.9559	24.6	0.3524	0.0031	0.0074
15&17	1.7877	21.7	0.6619	0.0231	0.0086
37&39	5.1793	27.7	1.9245	0.0263	0.0158

As temperature increases, diffusion coefficient increases and thus particle phase mass transfer coefficient increases (runs 15 & 17 and runs 37 & 39). Further, as the flow rates increase, solution phase mass transfer coefficients come closer to particle phase mass transfer coefficients.

Table 7.5

In a binary system, ion exchange takes place under favourable or unfavourable equilibrium conditions. In a ternary system however, ion exchange may take place under a mixture of both favourable and unfavourable equilibrium conditions from ion to ion. This fact is shown in many of ternary runs for example, runs 16 & 18 where the hydrogen curve displays a constant pattern shape (favourable displacing) and the potassium curve displays a proportionate pattern shape (unfavourable displacing).

A summary of the ternary runs is shown in Table 7.7. The number of transfer units presented in the table needs explanation. In binary ion exchange column, the number of

transfer units is given by N = kV/F and a range of N may be computed from the individual mass transfer coefficients corresponding to the beginning and the end of the exchange. In a ternary system, however, at each point of the breakthrough curve there are three individual mass transfer coefficients. Thus the number of transfer units for a ternary system are not the same as the binary case. Notwithstanding, it is useful to have a guideline for a range of number of transfer units for multicomponent systems. For a solution phase diffusion, a combined solution phase mass transfer coefficient k_{ef}, has been defined (Perry, 1963)

$$\frac{1}{k_{ef}} = \frac{1}{k_s} + \frac{1}{k_p} + \frac{1}{k_d}$$

where k_s, k_p and k_d are the mass transfer coefficient for film diffusion, pore diffusion and axial dispersion respectively. Analogously, the film diffusion mass transfer coefficient, k_s, can be defined as:

$$\frac{1}{k_s} = \Sigma \frac{\bar{X}_i}{k_i}$$

where k_i is the mass transfer coefficient of species i. The above equation was used purely as an indication for the number of transfer units in multicomponent systems and it has not been used in the theoretical development of this work.

All predicted breakthrough curves are based on (except when indicated):-

- constant self diffusion coefficient
- variable separation factor (VSF)
- combined diffusion mechanism
- Hiester relation, for computing solution phase mass transfer coefficients.

The Hiester relation has been employed instead of Kataoka relation because:-

(i) it is based on experimental data

(ii) its validity has been verified by Vanichseni (1970)

(iii) it has been used successfully for binary ion exchange by Allen (1973)

(iv) its computing time is much less than that for Kataoka relation because

$$k_{ij} = f(\sqrt{D_{ij}}); \quad \text{Hiester relation}$$

$$k_{ij} = f(D_{ij}^{2/3}); \quad \text{Kataoka relation}$$

The equilibrium data of K/Na/H/Dowex 50W X8 at 0.1N total solution concentration (Chapter 5) shows that it is a variable separation factor system. Thus VSF has been employed in the computer simulation.

Overall, the breakthrough curves generated from GPFIXC fit and reflect the experimental breakthrough curves well (Figures 7.6-7.22). In some runs, however, there are some discrepancies between GPFIXC and experimental results. A number of factors contribute to these discrepancies; the equations of the model (Chapters 2, 3 and 4), equilibrium data (Chapter 5) and experimental technique (Chapter 6). The discrepancy due to equilibrium data and experimental technique can be indicated by considering mass balances (Table 7.3). The computer calculations (GPFIXC) used the bed capacity from independent capacity measurements. This suggests that if the discrepancies were due to mass balances, the area differences between the predicted and experimental breakthrough curves would be comparable to the differences between the bed capacities from independent capacity measurements and the experimental breakthrough curve providing

that the slopes in transition zones of both predicted and experimental breakthrough curves are similar. Considering, for example, run 22, the bed capacities from the experimental breakthrough curves were calculated from (Table 7.3):-

$$QV = \frac{FC_o \int_o^Z \bar{X}_i \, dZ}{\bar{Y}_i^o}$$

i.e. the areas under the experimental breakthrough curves were used to compute the bed capacities which are 3716.8 and 3480.8 meq. for potassium and hydrogen ions respectively. The bed capacity from independent capacity measurement is 3573 meq. Figure 7.10 shows that for the potassium breakthrough curve, the area under the experimental breakthrough curve is greater than under the predicted curve, and for the hydrogen breakthrough curve, the area under the experimental breakthrough curve is smaller than under the predicted curve, showing that mass balance errors contribute to the discrepancies. Table 7.6 illustrates the above point for some other breakthrough curves.

Figure 7.6 shows the experimental and predicted breakthrough curves of runs 15 & 17. As shown in Table 7.7, in these runs, a mixture of potassium nitrate, sodium nitrate and nitric acid with equivalent fractions of 0.3, 0.5 and 0.2 respectively was passed through the bed initially in sodium form. The experimental results show that there were three plateau zones and two transition zones. The first plateau zone contains only sodium ions with throughput ratio from zero to 0.65. The first transition zone has sodium and hydrogen ions with throughput ratio from 0.65 to 0.9. The intermediate plateau zone has sodium and hydrogen ions with throughput ratio from 0.9 to 1.26. The second transition zone has all counter ions with throughput

ratio from 1.26 to 1.6. The third plateau zone contains the feed with throughput ratio from 1.6 onward.

This behaviour can be explained by considering the potassium and hydrogen column concentration profiles at a particular time. At this particular time some solution has been passed through the bed but not enough that equilibrium has been attained. Resin phase concentration profiles show five zones.

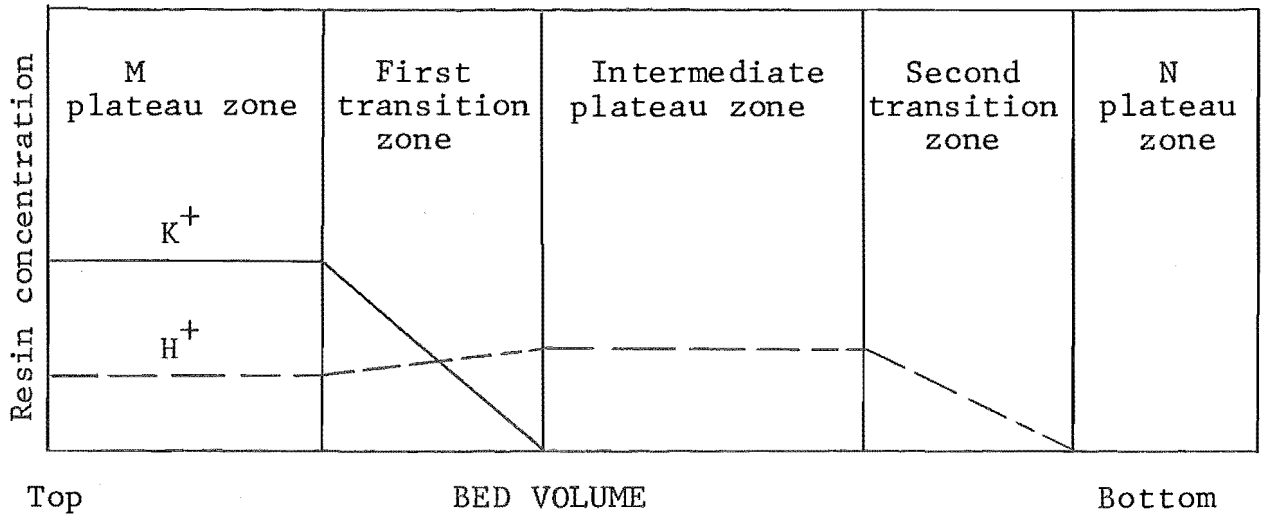

In zone 1, the bed is in equilibrium with the feed. Resin concentrations in this zone resulted from equilibrium with the feed; $\overline{Y}_K = 0.4242$ and $\overline{Y}_H = 0.1420$, i.e. more potassium ions have been exchanged than hydrogen ions. This zone is known as a plateau zone M.

In zone 2, little potassium ions have been left in the solution since most has been exchanged in zone 1. Thus, in this zone, $\overline{Y}_K$ goes from .4242 to 0.0. This is in a contrary to $\overline{Y}_H$ which goes up from 0.1420 to a new value. This zone is known as the 1st transition.

Since all potassium ions have been exchanged in zone 1 and zone 2, there are only sodium and hydrogen ions left in the feed solution in the beginning of zone 3. Therefore from this zone onward the system can be considered as a binary system. Zones 3, 4 and 5 are known as intermediate plateau, second transition and N plateau respectively.

The agreement between the multicomponent equilibrium theory (Chapter 1), which predicts that there will be three plateau zones and two transition zones for ternary components, and the experimental results is noted here. This indicates that in these two runs the number of transfer units is sufficient for the concentration profiles to fully develop.

Predicted results of both constant and variable separation factor models show that the variable separation factor model fits the experimental data much better than the constant separation factor model. Apparent contradiction in the areas above the predicted curves is due to the different amount of the ions said to be left in the resin by the two models.

Figure 7.7 shows the reverse exchange of runs 15 & 17. In these two runs (16 & 18) the feed solution, 0.1N $NaNO_3$, was passed through the bed having been in equilibrium with the feed solution of runs 15 & 17. The experimental results show that there was no intermediate plateau zone and there was a maximum on the potassium breakthrough curve. This behaviour can be explained as follows: as sodium nitrate solution was passed through the bed ($\bar{Y}^o_K/\bar{Y}^o_{Na}/\bar{Y}^o_H$ = 0.4242/0.4338/0.1420), due to concentration effect, the top of the bed was converted to sodium form. The solution, leaving this part of the bed, contained mostly potassium and hydrogen ions and which were exchanged in

the next layer of the bed. Due to selectivity effect, potassium ions from the solution displaced hydrogen ions in the resin. This caused the level of potassium ions in the resin to be greater than its presaturated value. This maximum moved down the bed and appeared in the potassium breakthrough curve (Figures 7.7 and 7.8).

If the feed to the column is potassium nitrate solution (as in runs 24 & 32 and 27) rather than sodium nitrate solution, the maximum would be less well established because of the lower selectivity α_H^{Na} as compared to α_H^K. Experimental results of runs 24 & 32 (Figure 7.12) and run 27 (Figure 7.15) support this argument. In these runs, potassium nitrate solution was passed through the beds presaturated with potassium, sodium and hydrogen ions. The maximum of sodium breakthrough curves of runs 24 & 32 is not clearly apparent and that of run 27 is just evident.

Figure 7.9 shows the experimental and predicted breakthrough curves of runs 19 & 21 showing the effect of increasing hydrogen ion equivalent fraction in the feed from 0.2 (runs 15 & 17) to 0.4 (runs 19 & 21). The pH electrode was unstable during part of run 21. This was not due to aging effect since it was a new electrode. During this malfunction the pH electrode took longer than the allowed ten seconds to settle.

Figure 7.10 shows the experimental and predicted breakthrough curves of runs 20 & 22 which are the regenerations of runs 19 & 21. There are similarities between the experimental results of runs 16 & 18 and runs 20 & 22. Both have maximums for the potassium breakthrough curves and the hydrogen breakthrough curves are steep and short.

The maximum of runs 20 & 22 ($\overline{X}_K$ = 0.44) is greater than that of runs 16 & 18 ($\overline{X}_K$ = 0.35). There are two reasons for this occurrence. Firstly, and less importantly, the presaturated value of potassium ions in the bed of runs 20 & 22 ($\overline{Y}_K$ = 0.45) was greater than that of runs 16 & 18 ($\overline{Y}_K$ = 0.4242). The second reason is the nature of the exchange. In runs 20 & 22, the solution which left the top part of the bed consisting mainly of potassium and hydrogen ions, with a lower proportion of potassium ($\overline{X}_K/\overline{X}_H$ = 0.75) than runs 16 & 18 ($\overline{X}_K/\overline{X}_H$ = 1.5). This caused the resin to have more affinity for potassium ions in runs 20 & 22 (α_H^K = 2.1) than in runs 16 & 18 (α_H^K = 1.85). Subsequently, the maximum of the potassium breakthrough curves of runs 20 & 22 was greater than that of runs 16 & 18.

For both sets of runs, 16 & 18 and 20 & 22, although the predicted breakthrough curves reflect the experimental breakthrough curves well, there are some discrepancies between them. One of the contributions to the discrepancies is the mass balance errors (Table 7.6).

Figure 7.11 shows the experimental and predicted breakthrough curves of runs 23 & 31. These runs were carried out to study the effect of increasing potassium equivalent fractions from 0.3 (runs 15 & 17) to 0.6 (runs 23 & 31). As in runs 15 & 17, the experimental breakthrough curves of runs 23 & 31 show fully developed concentration profiles (3 plateau zones and 2 transition zones). The computer results fit the experimental data well.

Figure 7.12 shows the experimental and predicted curves of runs 24 & 32. In these runs, potassium nitrate solution was used to regenerate the bed, whereas sodium nitrate solution was used in runs 16 & 18 and runs 20 & 22.

In runs 16 & 18 and runs 20 & 22, there are maximums on the potassium breakthrough curves and so one would expect to find a maximum on the sodium breakthrough curve for runs 24 & 32. The sodium curve shows that it does have a maximum but barely evident as previously discussed. Only a part of the sodium curve was plotted, since it was not measured, but calculated

GPFIXC results fit experimental data of runs 24 & 32 well. A small discrepancy between the computed and experimental results of hydrogen ions is due to mass balance error (Table 7.6). For potassium breakthrough curve, however, the discrepancy is partly due to mass balance error, but the slope of the experimental breakthrough curve is slightly greater than that of the predicted curve, especially when approaching the end of the breakthrough curve indicating that either mass transfer model or equilibrium data (or perhaps both) contribute to the discrepancy.

Figure 7.13 shows the experimental and predicted breakthrough curves of runs 25 & 28. Unlike runs 15 & 17 and runs 19 & 21 where the beds were in the sodium form, in runs 25 & 28 the beds were in the potassium form. In runs 15 & 17 and runs 19 & 21, there were two transition zones and an intermediate plateau zone whereas in runs 25 & 28 there was no intermediate plateau zone and thus one transition zone. The width of the hydrogen breakthrough curve in the transition (Figure 7.13) is shorter than others. Since hydrogen is the least preferred ions of the ternary system one might expect that the hydrogen breakthrough curve would show a proportionate pattern. In a binary system, both counter ions have the same number of transfer units, but this is not so in a ternary system in which each counter ion can have a different number of transfer units. If, as in runs 25 & 28, the exchange were under mass transfer control and if

the hydrogen ions possessed higher number of transfer units than potassium and sodium ions due to its high diffusion coefficient, then the hydrogen breakthrough curve would be steeper and narrower as it would be in binary ion exchange.

The agreement between GPFIXC and the experimental results is similar to those of runs 24 & 32 as previously discussed.

Figure 7.14 shows the experimental and predicted curves of runs 26 & 29. These runs were carried out to test GPFIXC with a mixed feed passed through a mixed partially presaturated bed. Experimental results agree well with GPFIXC results.

The widths of the first plateau zones of both potassium and hydrogen experimental breakthrough curves are the same. However, the width of the transition zone of the hydrogen breakthrough curve is narrower than that of the potassium breakthrough curve. The above behaviour is also found in runs 24 & 32, runs 25 & 28 and run 27. Therefore, it can be concluded that the width of the transition zone for each ion is not necessarily the same.

Figure 7.15 shows the experimental and predicted results of run 27. This run is similar to runs 24 & 32 in that potassium nitrate solution was the feed for both sets of runs. The difference is that the presaturated bed of run 27 had more sodium content than runs 24 & 32. The experimental breakthrough curves of run 27 and 24 & 32 are similar except that the maximum of the sodium curve of run 27, which had more sodium content in the presaturated bed, is more evident.

Figure 7.16 shows the experimental and predicted results of run 30. The experimental result of run 30 is of the same

form as those of runs 16 & 18 and runs 20 & 22 in which the potassium breakthrough curve has a maximum and the hydrogen breakthrough curve is steep and short.

Figure 7.17 shows the experimental and predicted results of runs 33 & 35. These runs were carried out to study the effect of decreasing solution flow rate from 1.7426 ml s^{-1} (runs 23 & 31) to 0.9504 ml s^{-1} (runs 33 & 35). The average number of transfer units based on solution phase diffusion of runs 23 & 31 and runs 33 & 35 are 168 and 232 respectively. There is very little difference between the results of runs 33 & 35 and runs 23 & 31. The breakthrough curves of runs 33 & 35 are slightly steeper than those of runs 23 & 31. This is to be expected since the number of transfer units of runs 33 & 35 is higher.

GPFIXC results fit experimental data of runs 33 & 35 well.

Figure 7.18 shows the experimental and predicted results of runs 34 & 36. These runs were performed to study the effect of decreasing solution flow rate from 1.7889 ml s^{-1} (runs 24 & 32) to 0.9559 ml s^{-1} (runs 34 & 36). As with runs 33 & 35 and runs 23 & 31, there is little difference between the results of runs 34 & 36 and runs 24 & 32.

Figure 7.19 shows the experimental and predicted results of runs 37 & 39. The feed mixture and the presaturated bed of runs 37 & 39 were the same as those of runs 15 & 17, the differences between them were:

	Runs 37&39	Runs 15&17
- solution flow rate (ml s^{-1})	5.1793	1.7877
- average number of transfer units	101	158
- no. of transfer units of hydrogen ion	239	380
- no. of transfer units of potassium ion	110	172

A comparison of runs 37 & 39 with runs 15 & 17 shows that the hydrogen curve in the first transition zone of runs 15 & 17 is slightly steeper and the potassium curve in the second transition zone of runs 15 & 17 is significantly steeper. The above results indicate that, unlike binary ion exchange where both counter ions display the same breakthrough curve since both have the same number of transfer units, in multicomponent ion exchange, the change in a solution flow rate has different effect on the breakthrough curve of each counter ion depending on its number of transfer units.

The existence of an intermediate plateau zone depends on the availability of hydrogen ions after a transition zone. It follows that if the transition zone were steeper then there would be more hydrogen ions available for the intermediate plateau zone. The above argument indicates that when there are few transfer units (very high flow rates or very shallow beds) the spread of the transition zone will be such that there will be no intermediate plateau zone. To demonstrate this point, computer simulations of the same feed mixture and presaturated bed as runs 15 & 17 were obtained. These are shown in Figure 7.20 where hydrogen breakthrough curves at various flow rates were plotted. As can be seen, solution flow rates have to be very high before the intermediate plateau zone disappears, i.e. intermediate plateau zones are only weakly dependent on rate effects.

Figure 7.21 shows the experimental and predicted results of runs 38 & 40. These runs were carried out to study the effect of increasing solution flow rate from 1.7901 ml s^{-1} (runs 16 & 18) to 5.1775 ml s^{-1} (runs 38 & 40). The breakthrough curves of both sets of the runs are quite similar. Runs 16 & 18

with a greater number of transfer units rises more steeply to the maximum in the potassium curve, and is somewhat faster to complete regeneration. This implies that the maximum may disappear if the exchange takes place under very low number of transfer units. Figure 7.22 shows computer simulations of the same feed mixture and presaturated bed as runs 38 & 40 at various flow rates for potassium breakthrough curves. It is clearly shown that at very high solution flow rates (very low number of transfer units) the maximum disappears.

From the results shown, the breakthrough curves generated by GPFIXC reflect the experimental breakthrough curves well.

Run Number	Species	Comparison between bed capacities from experimental breakthrough curve and capacity measurement	Is area used to compute bed capacity under or above the breakthrough curve	Comparison between areas of experimental breakthrough curve and predicted breakthrough curve
17	H	3443 < 3573	above (Figure 7.6)	$A_{expt} < A_{computed}$
18	K	3613 > 3573	under (Figure 7.7)	$A_{expt} > A_{computed}$
18	H	3367 < 3573	under (Figure 7.7)	$A_{expt} < A_{computed}$
22	K	3718 > 3573	under (Figure 7.10)	$A_{expt} > A_{computed}$
22	H	3481 < 3573	under (Figure 7.10)	$A_{expt} < A_{computed}$
32	K	3623 > 3573	above (Figure 7.12)	$A_{expt} \doteqdot A_{computed}$
32	H	3538 < 3573	under (Figure 7.12)	$A_{expt} < A_{computed}$
28	K	3612 > 3573	under (Figure 7.13)	$A_{expt} \doteqdot A_{computed}$
28	H	3408 < 3573	above (Figure 7.13)	$A_{expt} < A_{computed}$
26	K	3509 < 3573	under (Figure 7.14)	$A_{expt} < A_{computed}$
27	K	3500 < 3573	above (Figure 7.15)	$A_{expt} < A_{computed}$
27	H	3501 < 3573	under (Figure 7.15)	$A_{expt} < A_{computed}$
30	K	3677 > 3573	under (Figure 7.16)	$A_{expt} > A_{computed}$
30	H	3487 < 3573	under (Figure 7.16)	$A_{expt} < A_{computed}$
36	K	3555 ≒ 3573	above (Figure 7.18)	$A_{expt} \doteqdot A_{computed}$
36	H	3470 < 3573	under (Figure 7.18)	$A_{expt} < A_{computed}$

Average value of independent capacity measurement = 3573.04 meq.

A_{expt} is the area under or above experimental breakthrough curve

$A_{computed}$ is the area under or above predicted breakthrough curve

Table 7.6: Relationships between mass balances and breakthrough curve areas.

Run Nos.	Feed composition $\bar{X}^o_K/\bar{X}^o_{Na}/\bar{X}^o_H$	Bed form $\bar{Y}^o_K/\bar{Y}^o_{Na}/\bar{Y}^o_H$		Bed volume (ml)		Temperature (^oC)	Flow rate (ml s^{-1})	No. of transfer units	
		Beginning	End	Beginning	End			Solution phase	Particle phase
15&17	0.3/0.5/0.2	0.0/1.0/0.0	.4242/.4338/.1420	1770.6	1726.8	21.7	1.7877	173-142	488-356
16&18	0.0/1.0/0.0	.4242/.4338/.1420	0.0/1.0/0.0	1726.8	1736.3	22.0	1.7901	141-171	357-488
19&21	0.3/0.3/0.4	0.0/1.0/0.0	.4500/.2655/.2845	1780.1	1751.5	22.8	1.8007	208-145	656-367
20&22	0.0/1.0/0.0	.4500/.2655/.2845	0.0/1.0/0.0	1753.4	1734.4	22.2	1.7828	143-205	365-652
23&31	0.6/0.2/0.2	0.0/1.0/0.0	.7048/.1570/.1382	1792.5	1718.2	23.9	1.7426	191-144	600-382
24&32	1.0/0.0/0.0	.7048/.1570/.1382	1.0/0.0/0.0	1732.5	1685.9	24.2	1.7889	143-186	361-566
25&28	0.7/0.2/0.1	1.0/0.0/0.0	.7757/.1514/.0729	1685.8	1675.4	23.3	1.7484	173.171	519-527
26&29	0.4/0.4/0.2	.7757/.1514/.0729	.5233/.3363/.1404	1714.4	1716.4	23.6	1.7550	179-177	529-537
27	1.0/0.0/0.0	.5233/.3363/.1404	1.0/0.0/0.0	1730.6	1681.1	23.5	1.7443	174-178	539-523
30	0.0/1.0/0.0	.5233/.3363/.1404	0.0/1.0/0.0	1764.9	1753.4	24.3	1.7834	148-183	381-543
33&35	0.6/0.2/0.2	0.0/1.0/0.0	.7048/.1570/.1382	1800.0	1723.0	24.2	0.9504	263-202	1110-707
34&36	1.0/0.0/0.0	.7048/.1570/.1382	1.0/0.0/0.0	1723.0	1683.0	24.6	0.9559	237-254	1000-1069
37&39	0.3/0.5/0.2	0.0/1.0/0.0	.4242/.4338/.1420	1799.6	1754.9	27.7	5.1793	111-91	194-143
38&40	0.0/1.0/0.0	.4242/.4338/.1420	0.0/1.0/0.0	1771.6	1761.1	27.3	5.1775	90-110	142-193

Table 7.7: Summary of parameters for experimental breakthrough curves of ternary system.

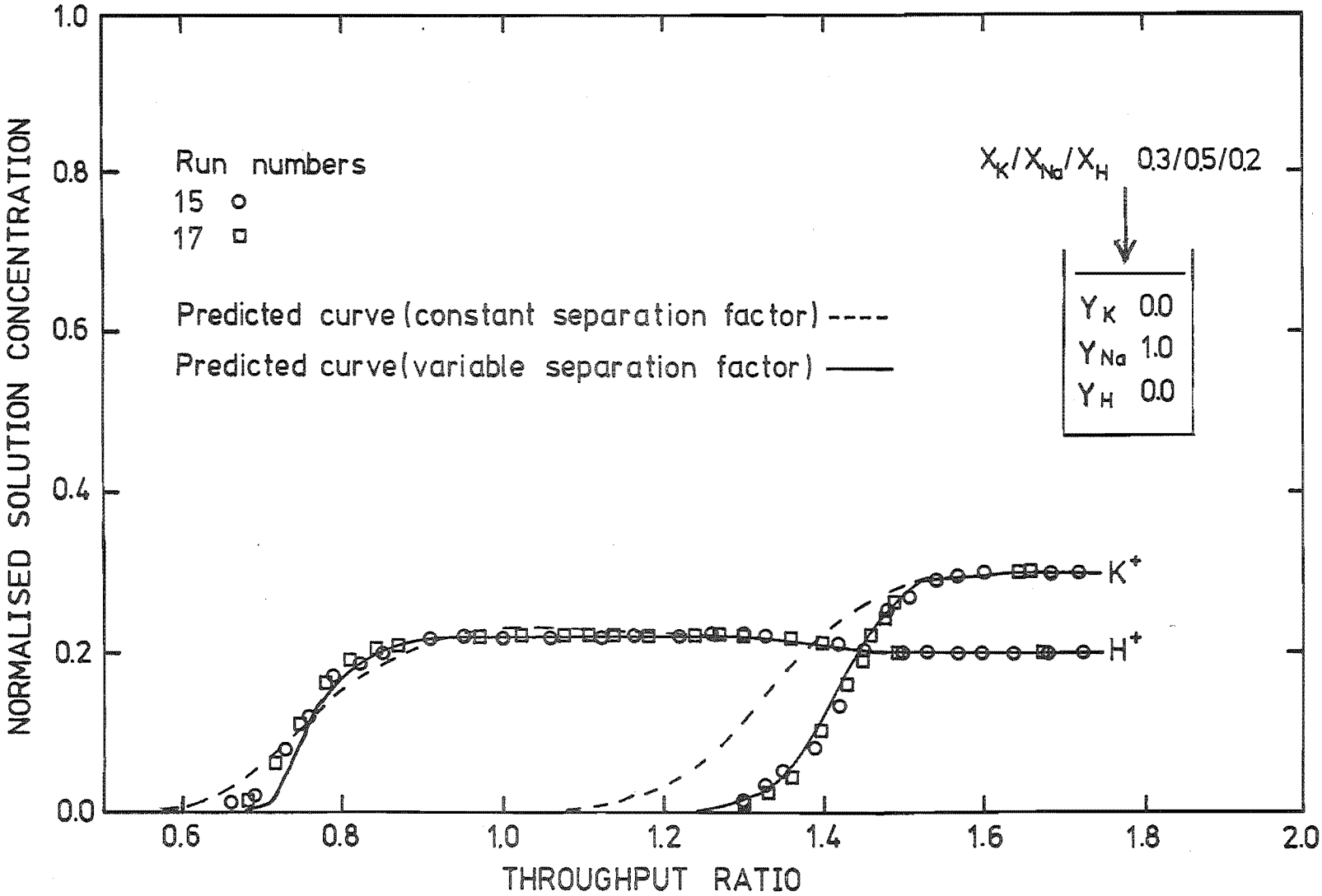

FIGURE 7.6 COMPUTED AND EXPERIMENTAL BREAKTHROUGH CURVES

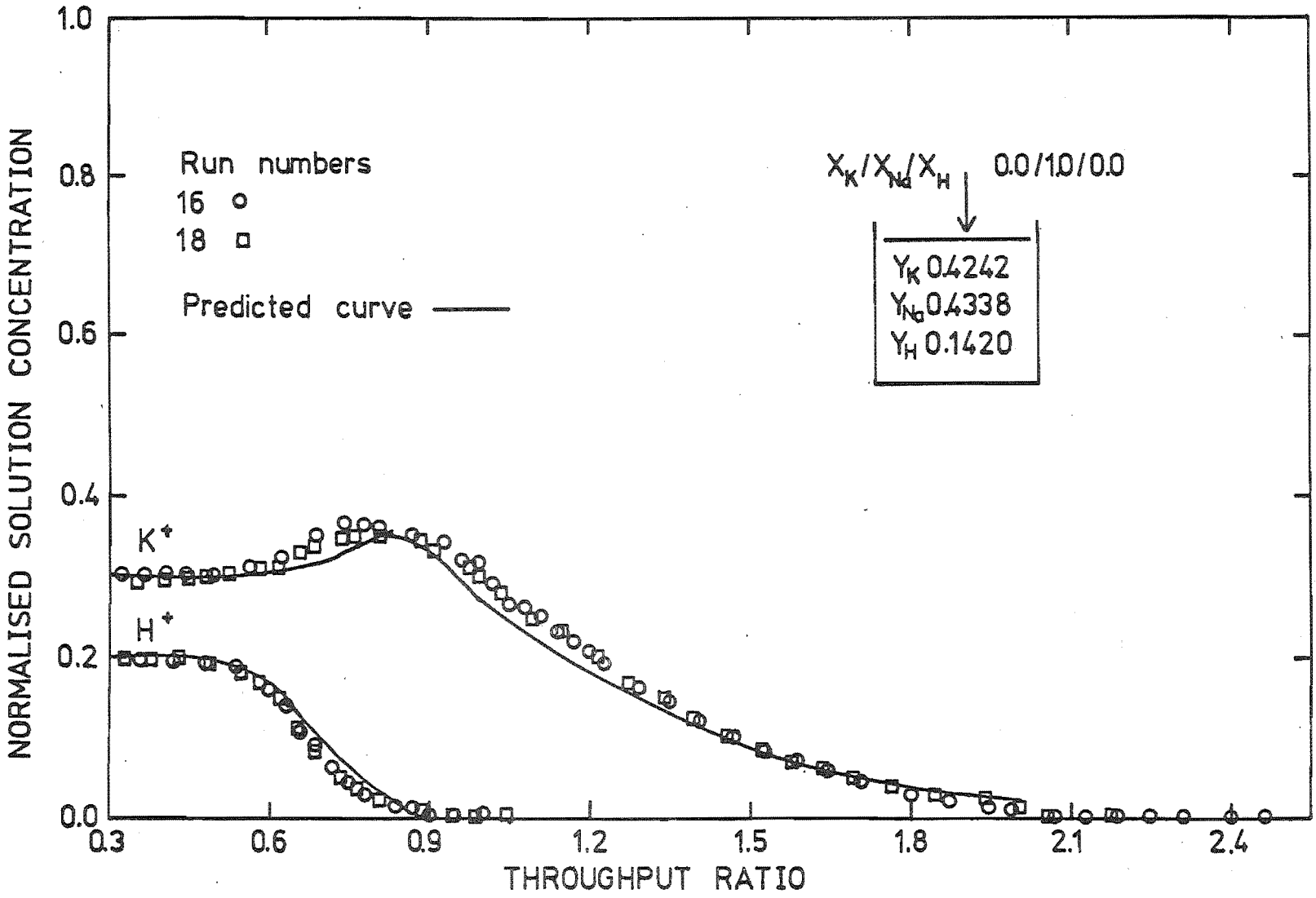

FIGURE 7.7 COMPUTED AND EXPERIMENTAL BREAKTHROUGH CURVES

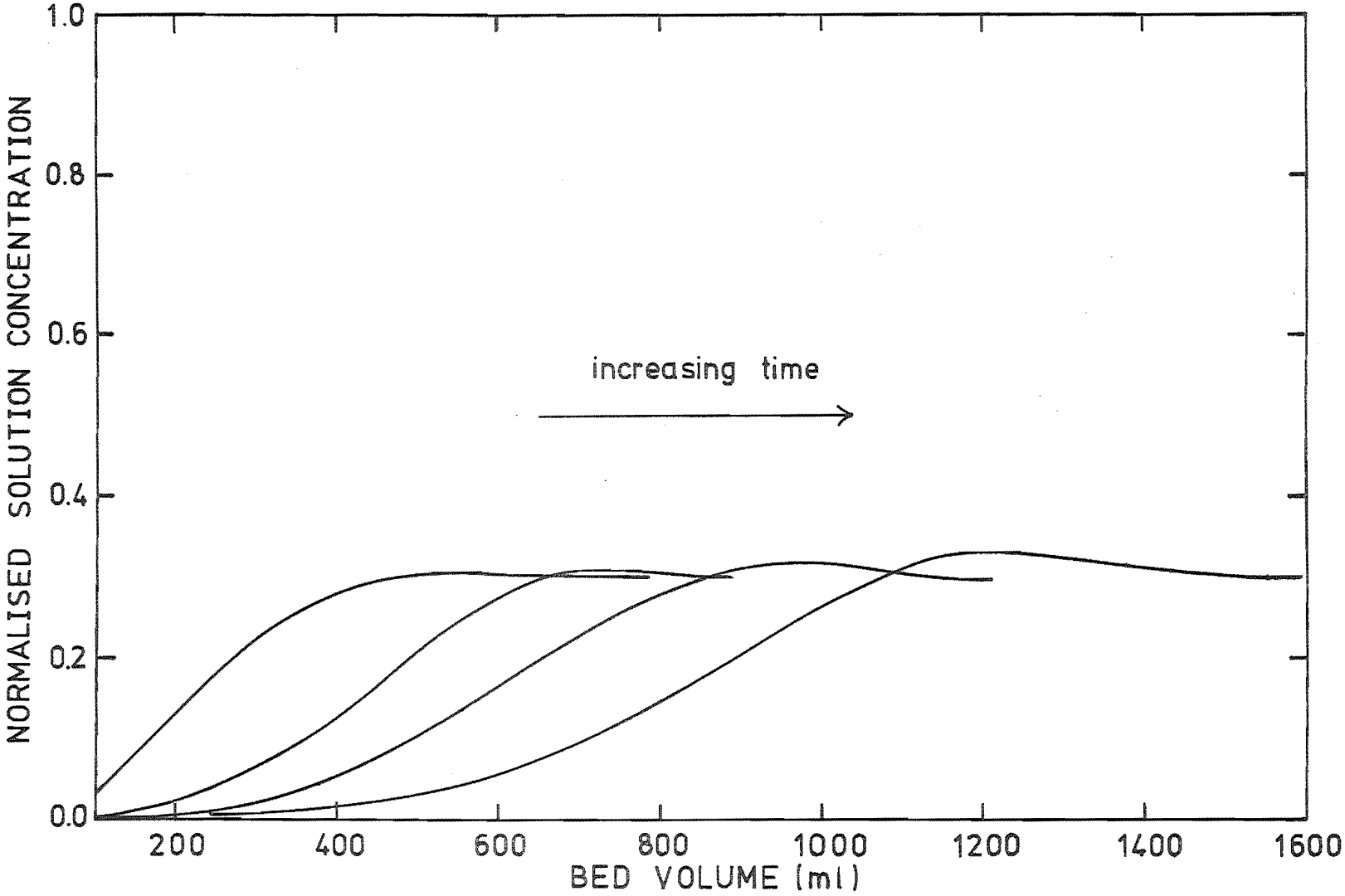

FIGURE 7.8 POTASSIUM CONCENTRATION PROFILES

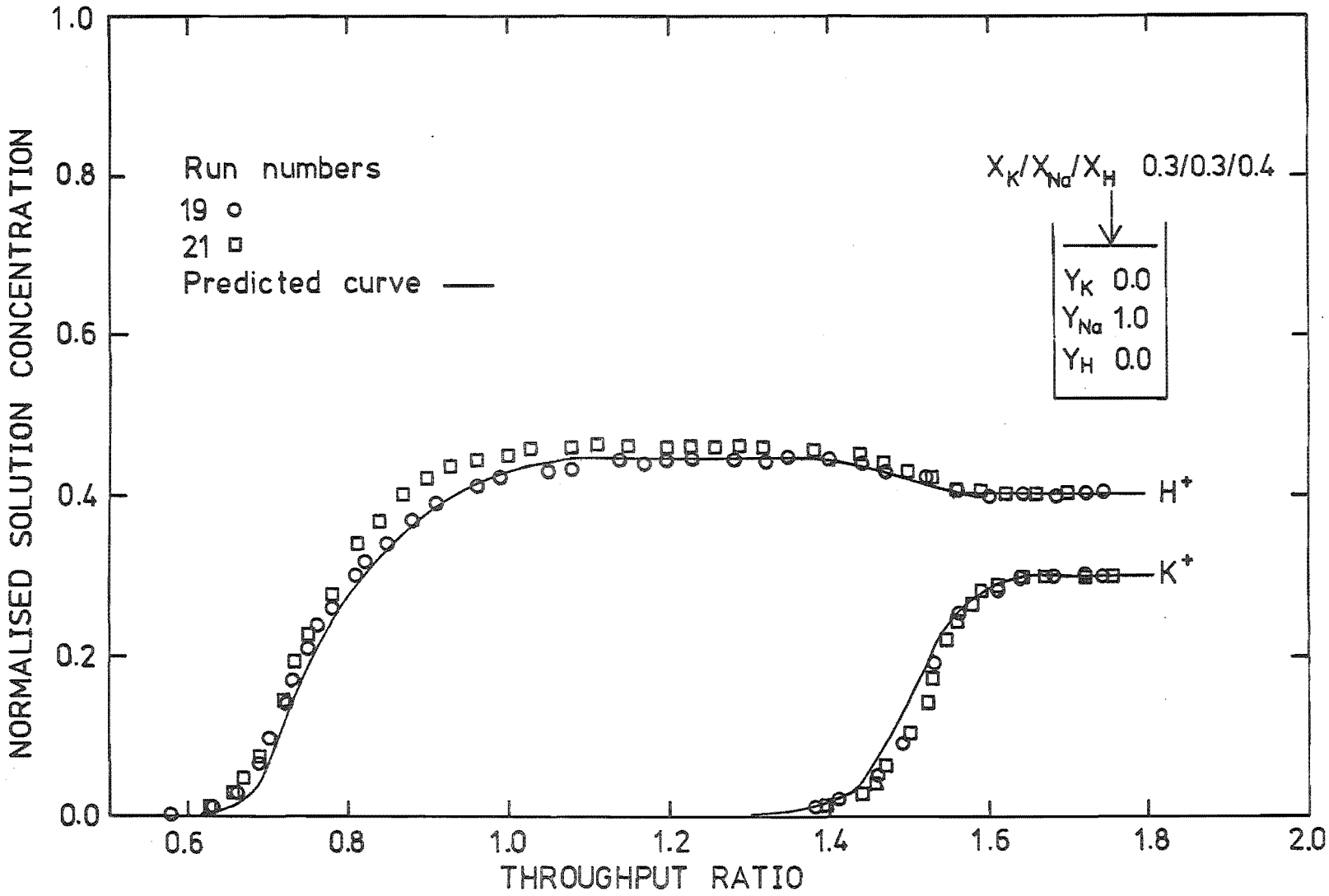

FIGURE 7.9 COMPUTED AND EXPERIMENTAL BREAKTHROUGH CURVES

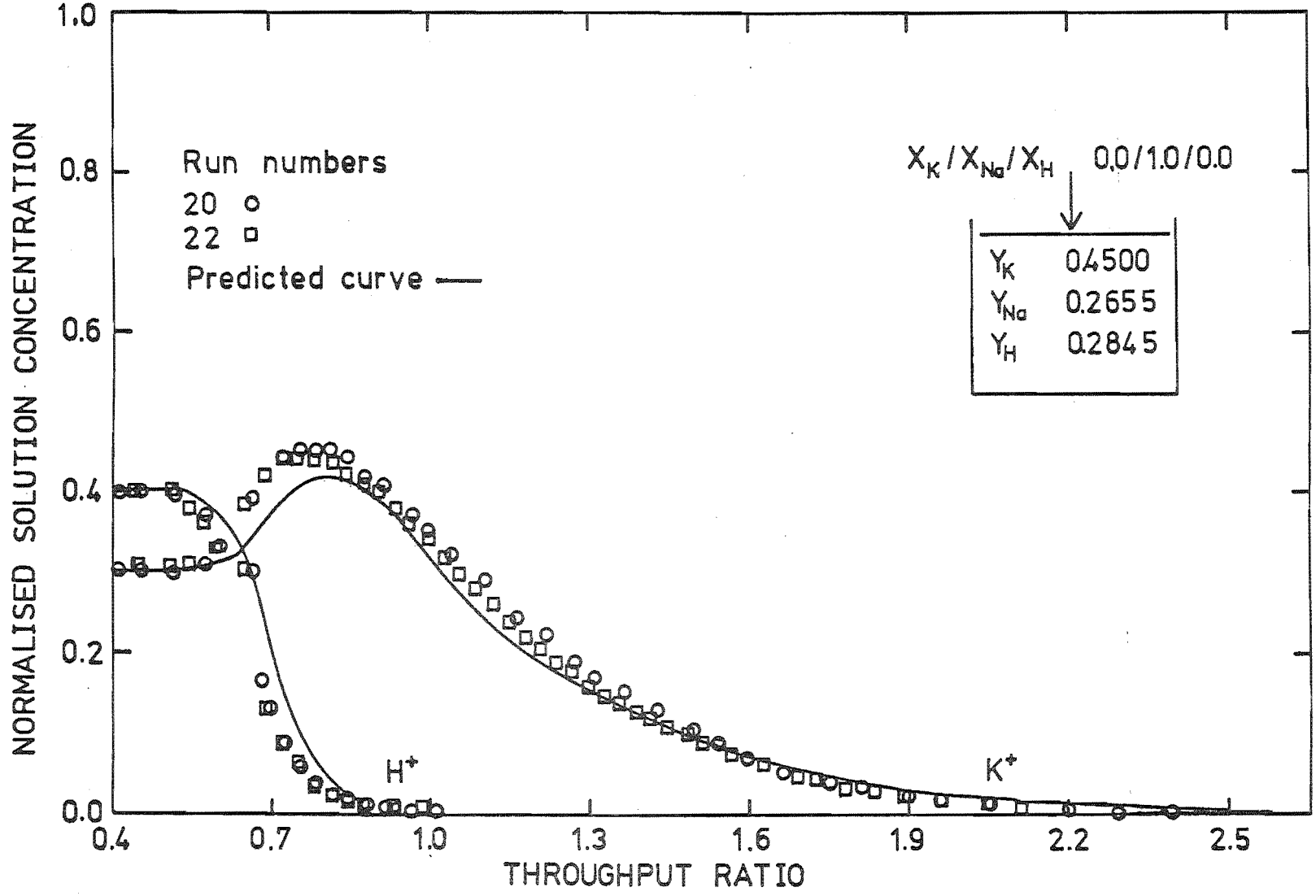

FIGURE 7.10 COMPUTED AND EXPERIMENTAL BREAKTHROUGH CURVES

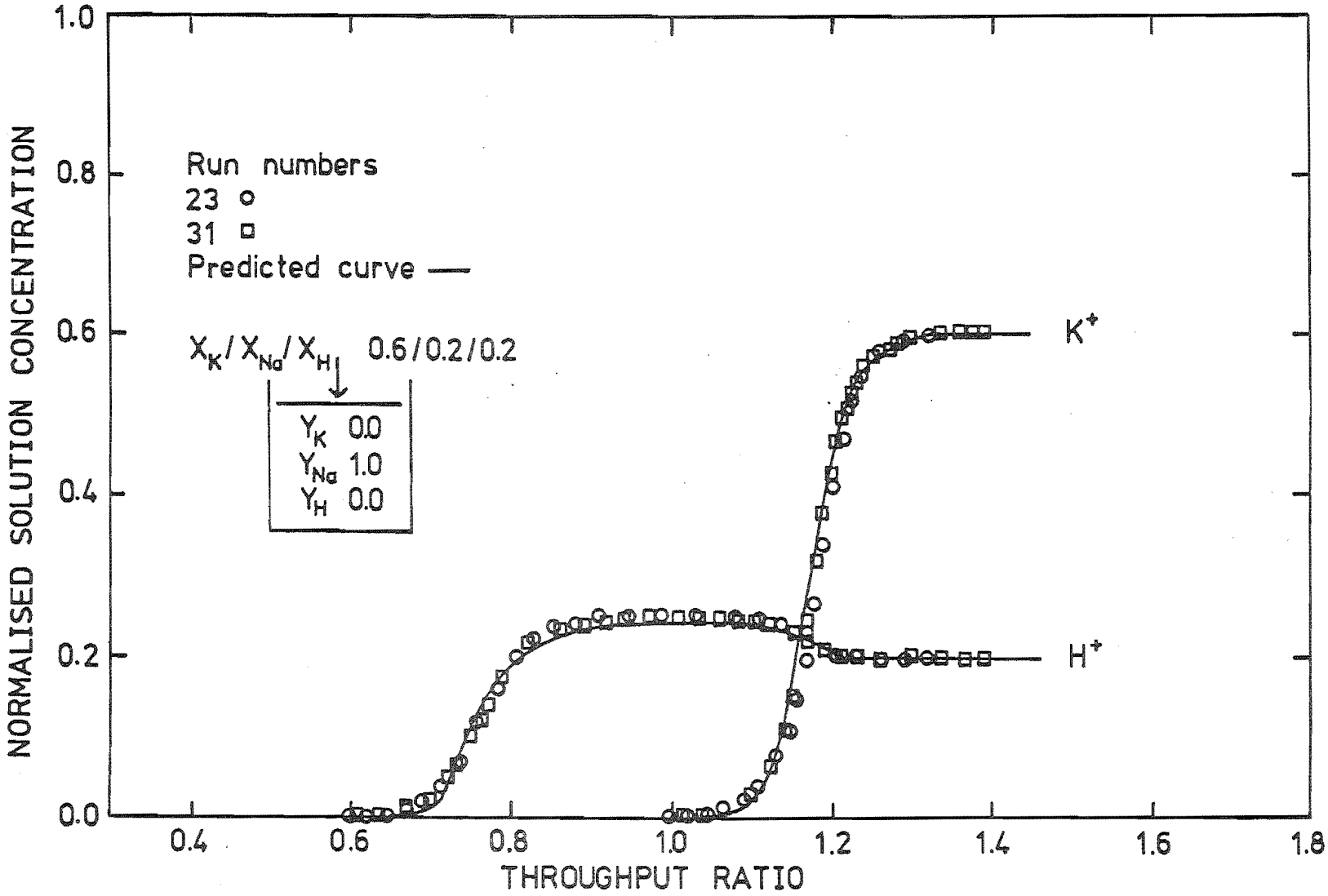

FIGURE 7.11 COMPUTED AND EXPERIMENTAL BREAKTHROUGH CURVES

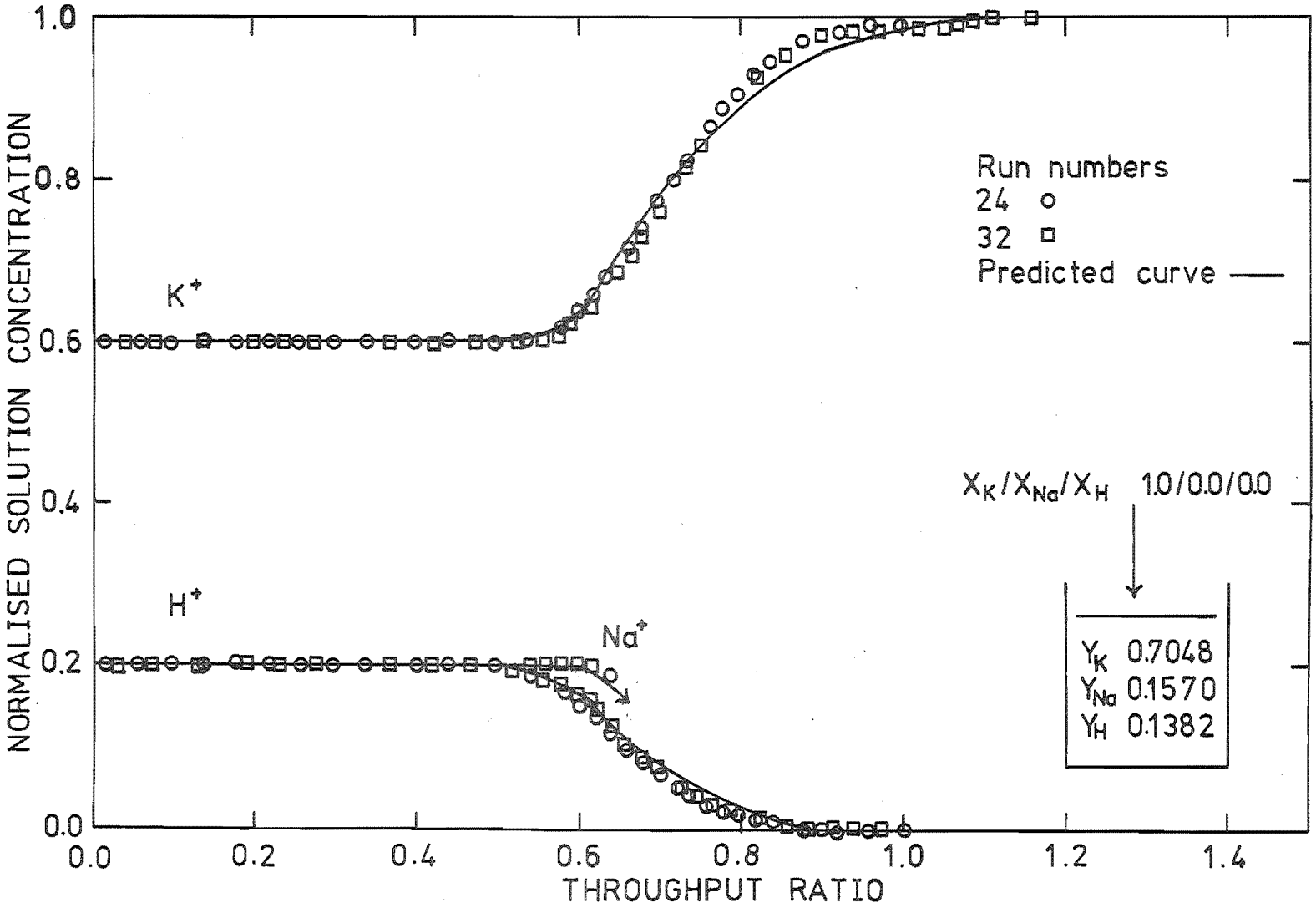

FIGURE 7.12 COMPUTED AND EXPERIMENTAL BREAKTHROUGH CURVES

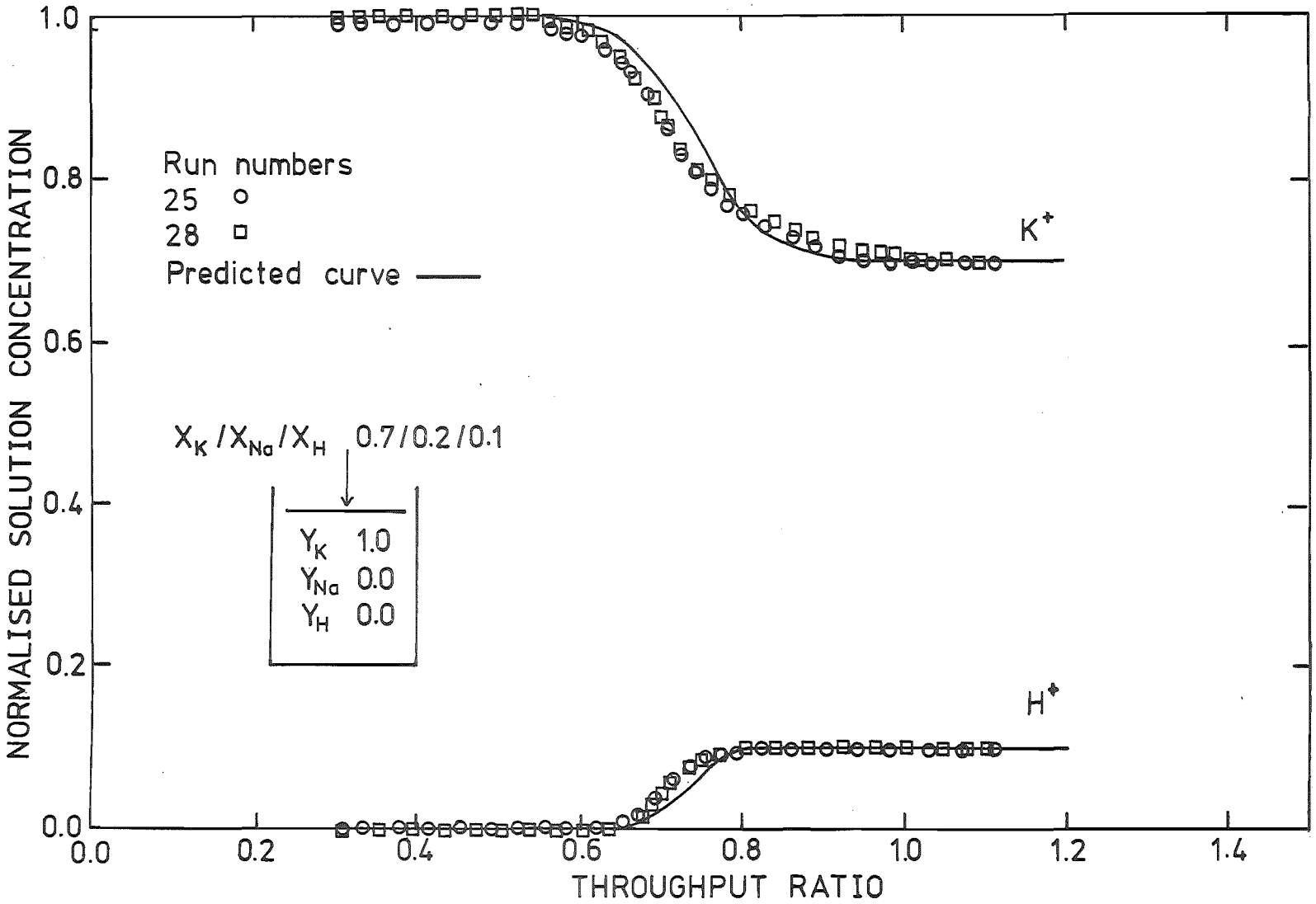

FIGURE 7.13 COMPUTED AND EXPERIMENTAL BREAKTHROUGH CURVES

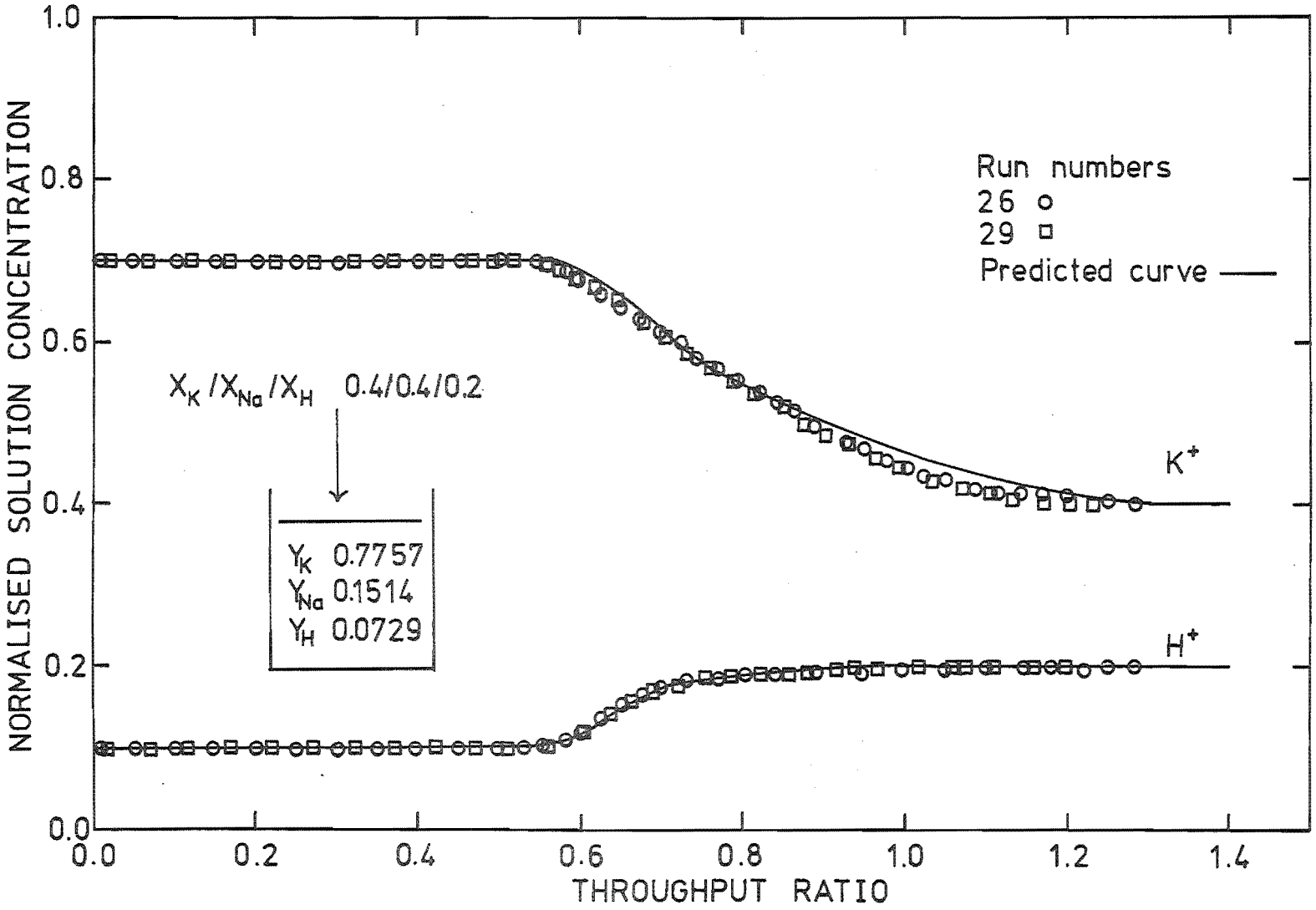

FIGURE 7.14 COMPUTED AND EXPERIMENTAL BREAKTHROUGH CURVES

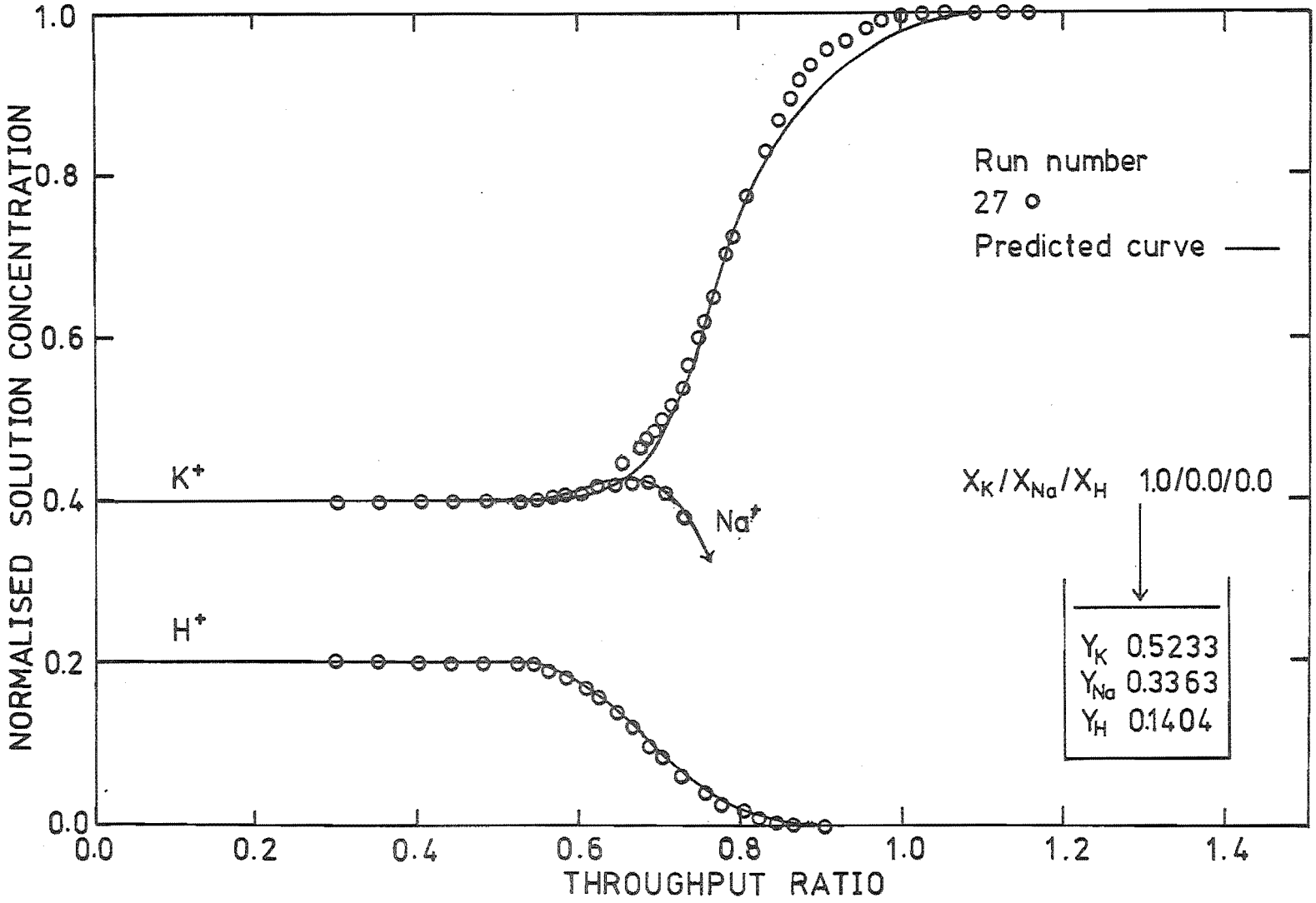

FIGURE 7.15 COMPUTED AND EXPERIMENTAL BREAKTHROUGH CURVES

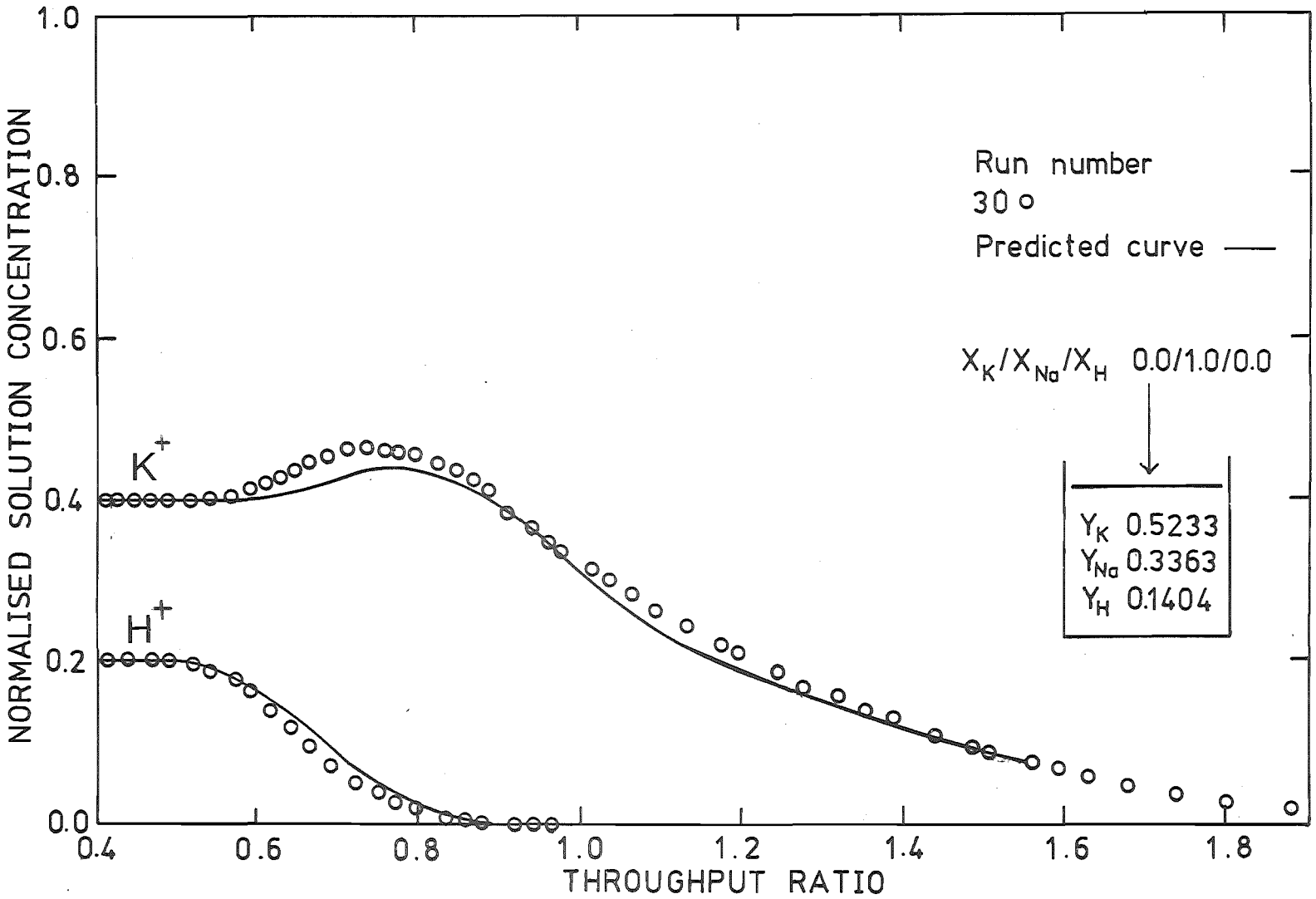

FIGURE 7.16 COMPUTED AND EXPERIMENTAL BREAKTHROUGH CURVES

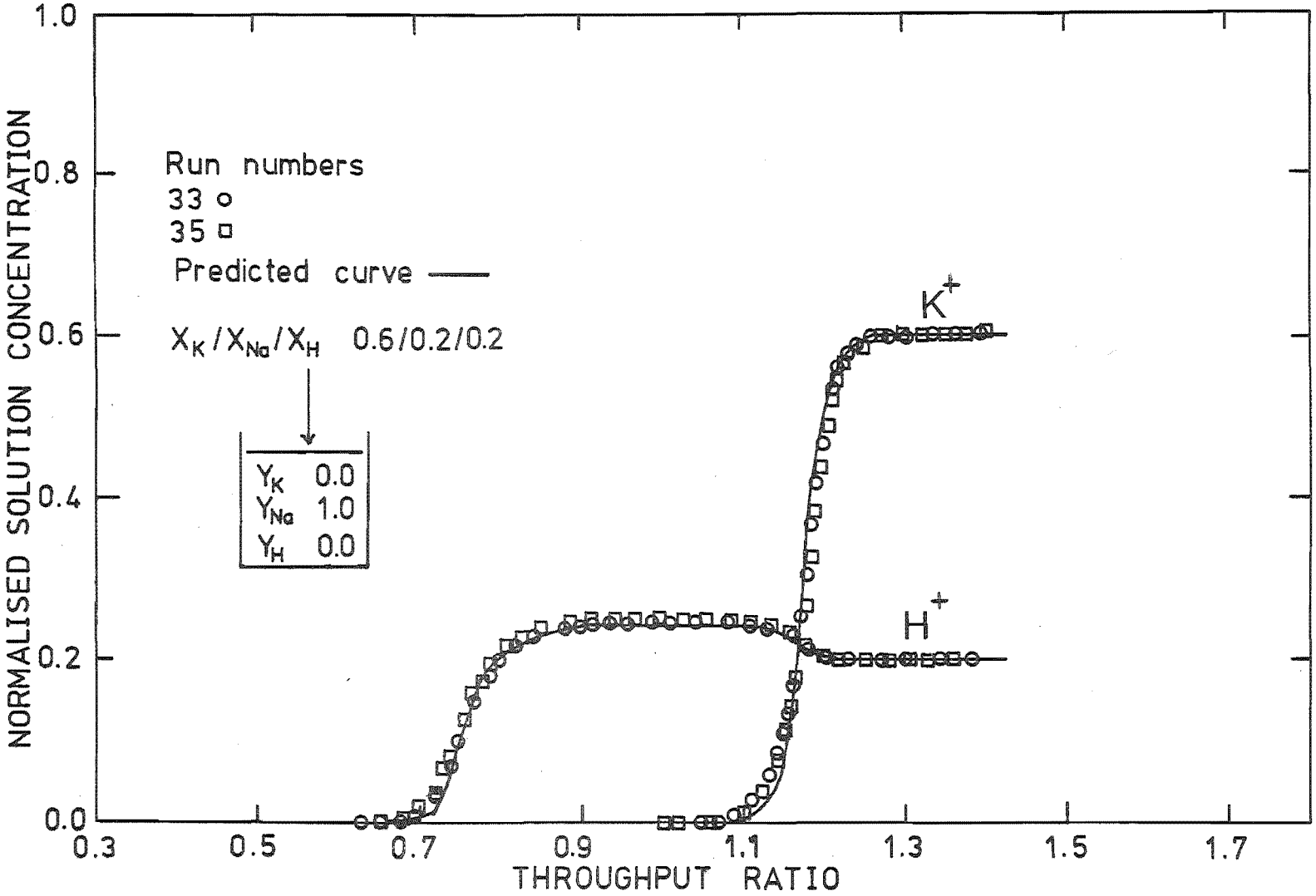

FIGURE 7.17 COMPUTED AND EXPERIMENTAL BREAKTHROUGH CURVES

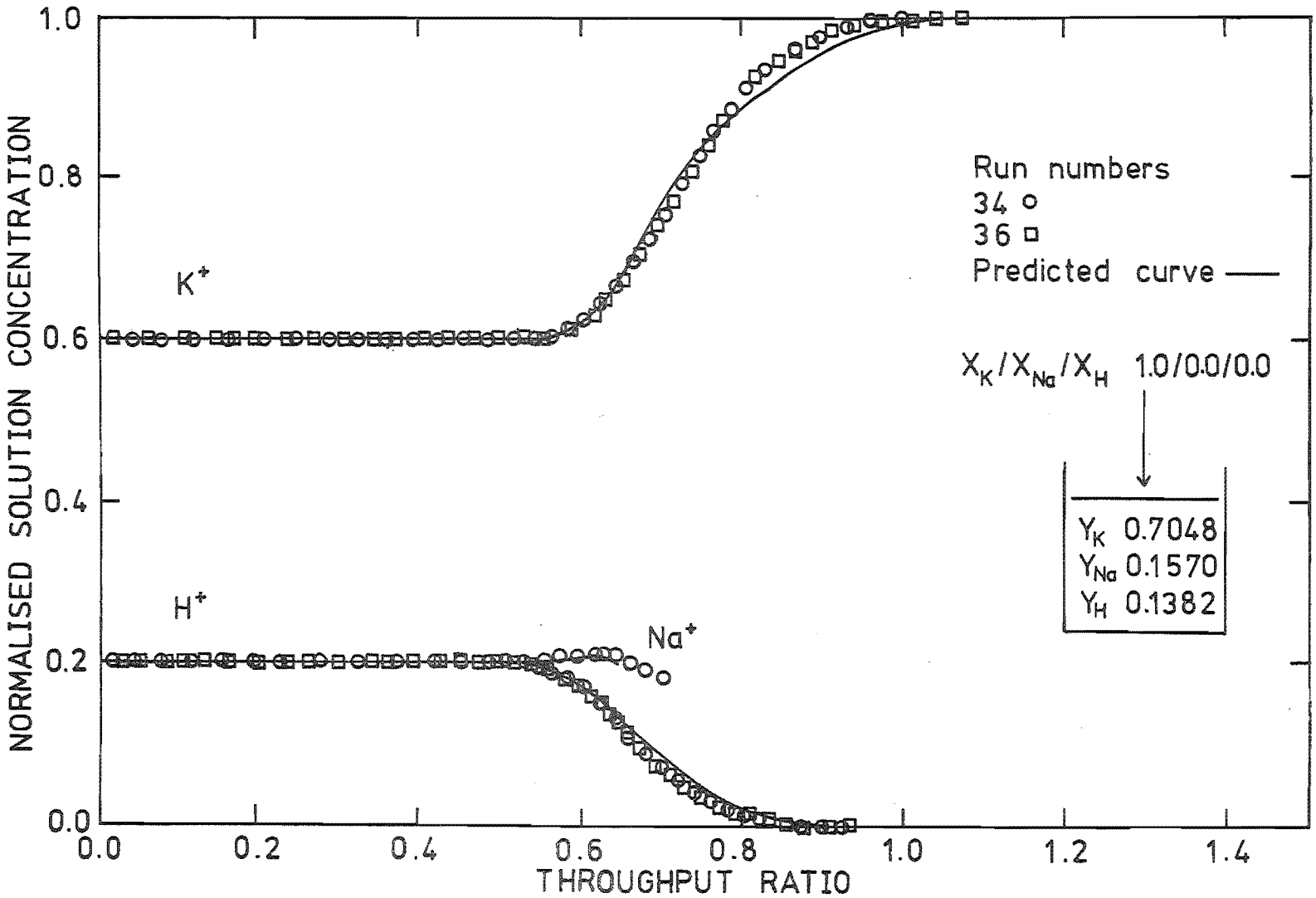

FIGURE 7.18 COMPUTED AND EXPERIMENTAL BREAKTHROUGH CURVES

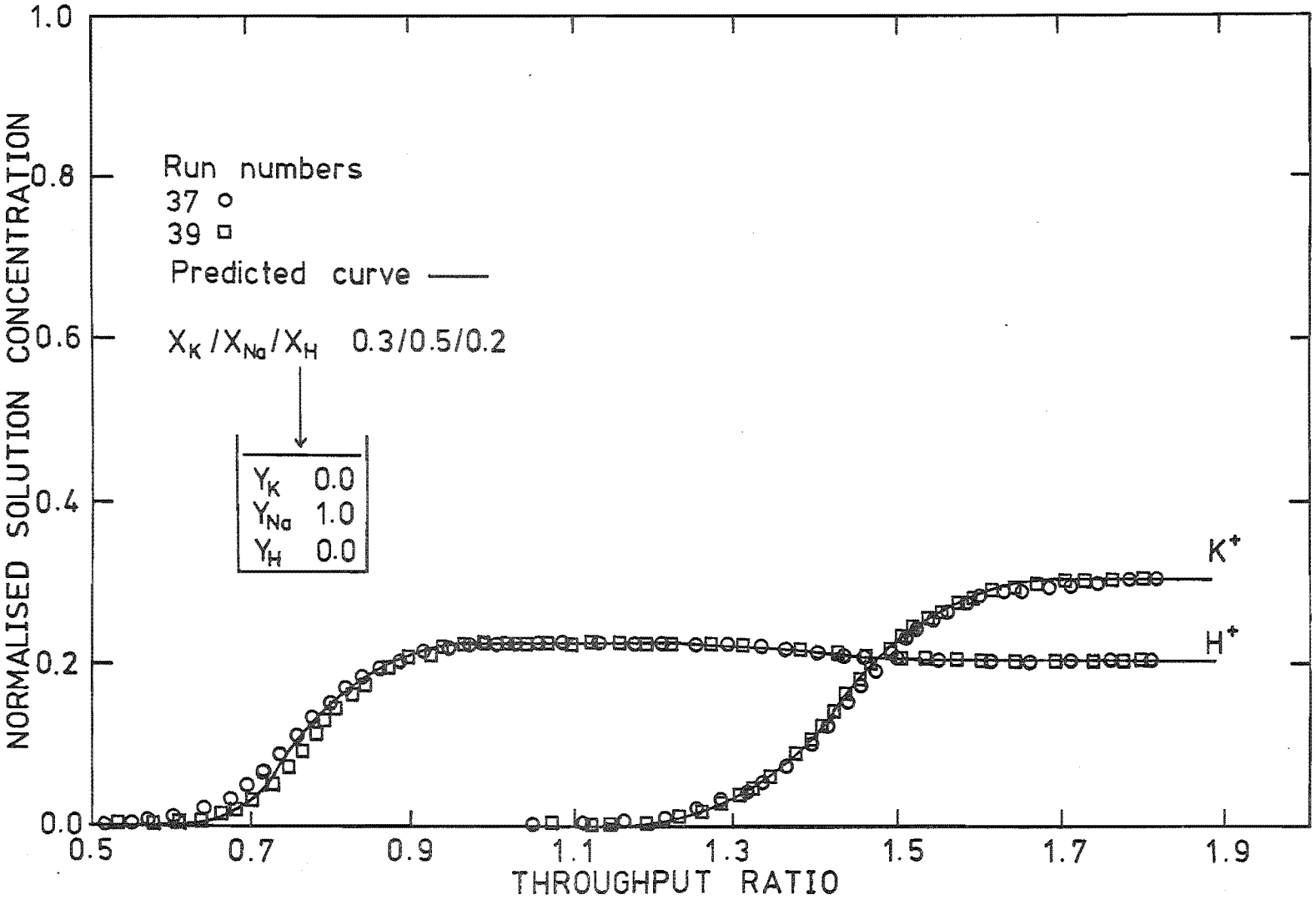

FIGURE 7.19 COMPUTED AND EXPERIMENTAL BREAKTHROUGH CURVES

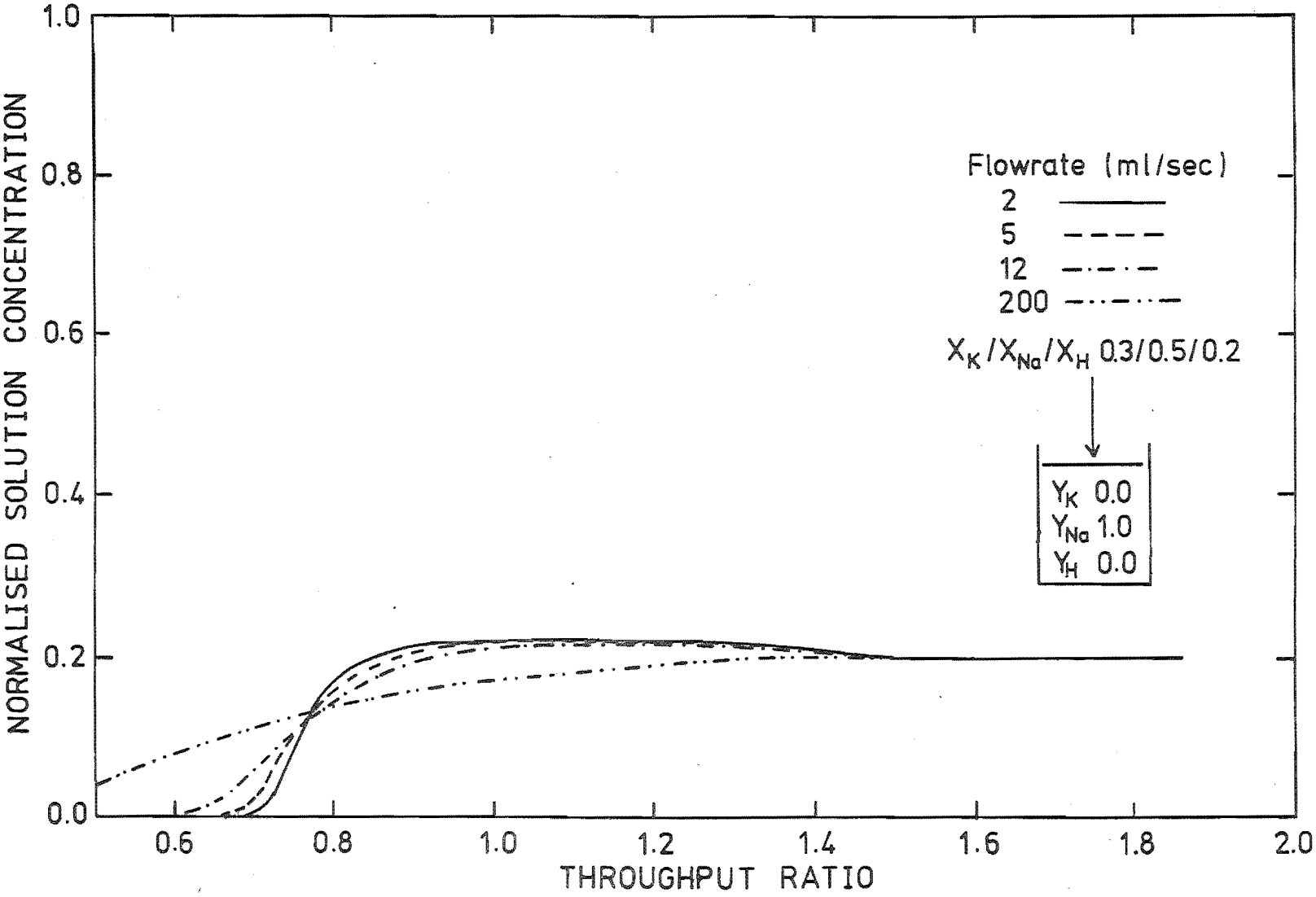

FIGURE 7.20 COMPUTED BREAKTHROUGH CURVES AT VARIOUS FLOWRATES

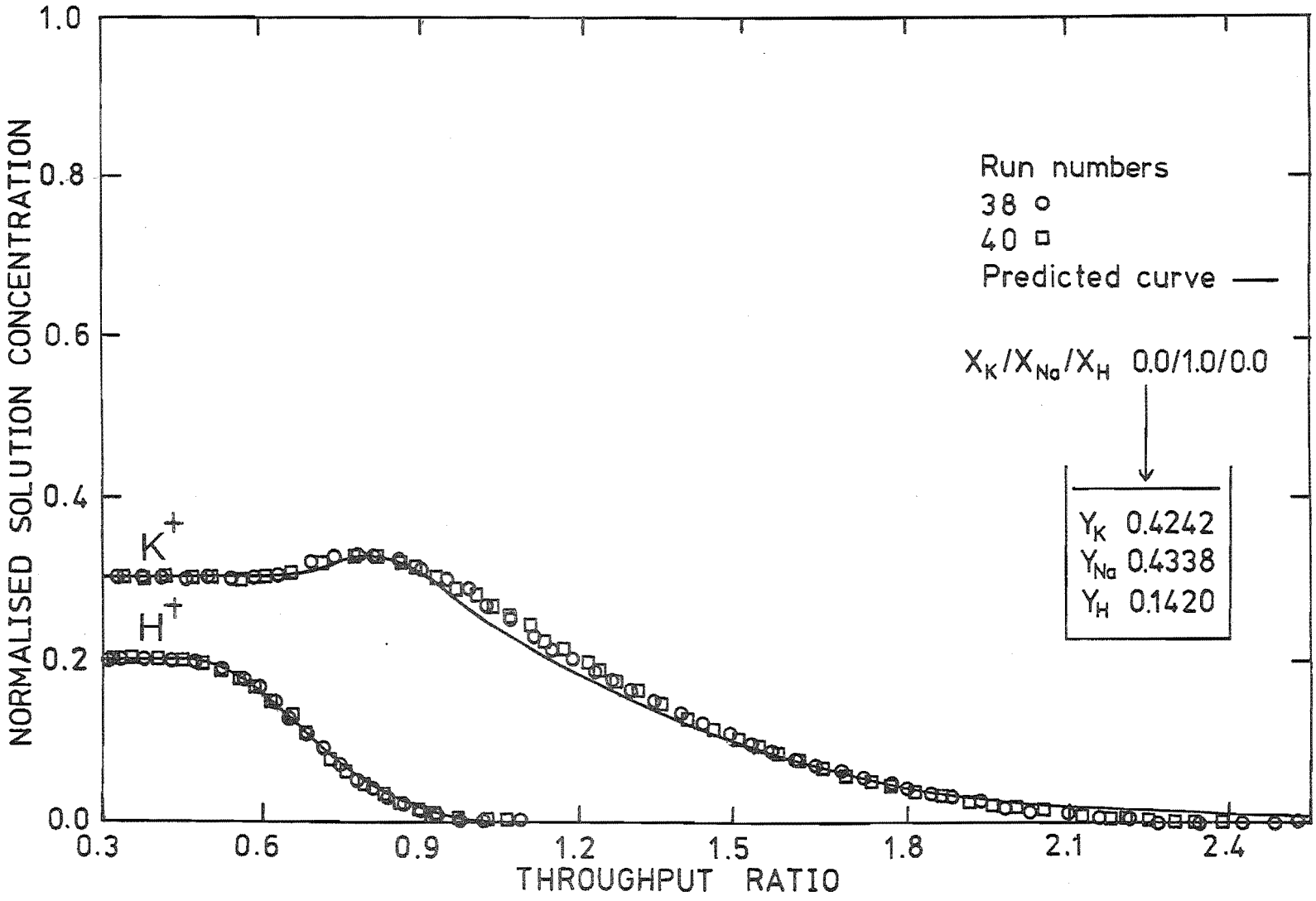

FIGURE 7.21 COMPUTED AND EXPERIMENTAL BREAKTHROUGH CURVES

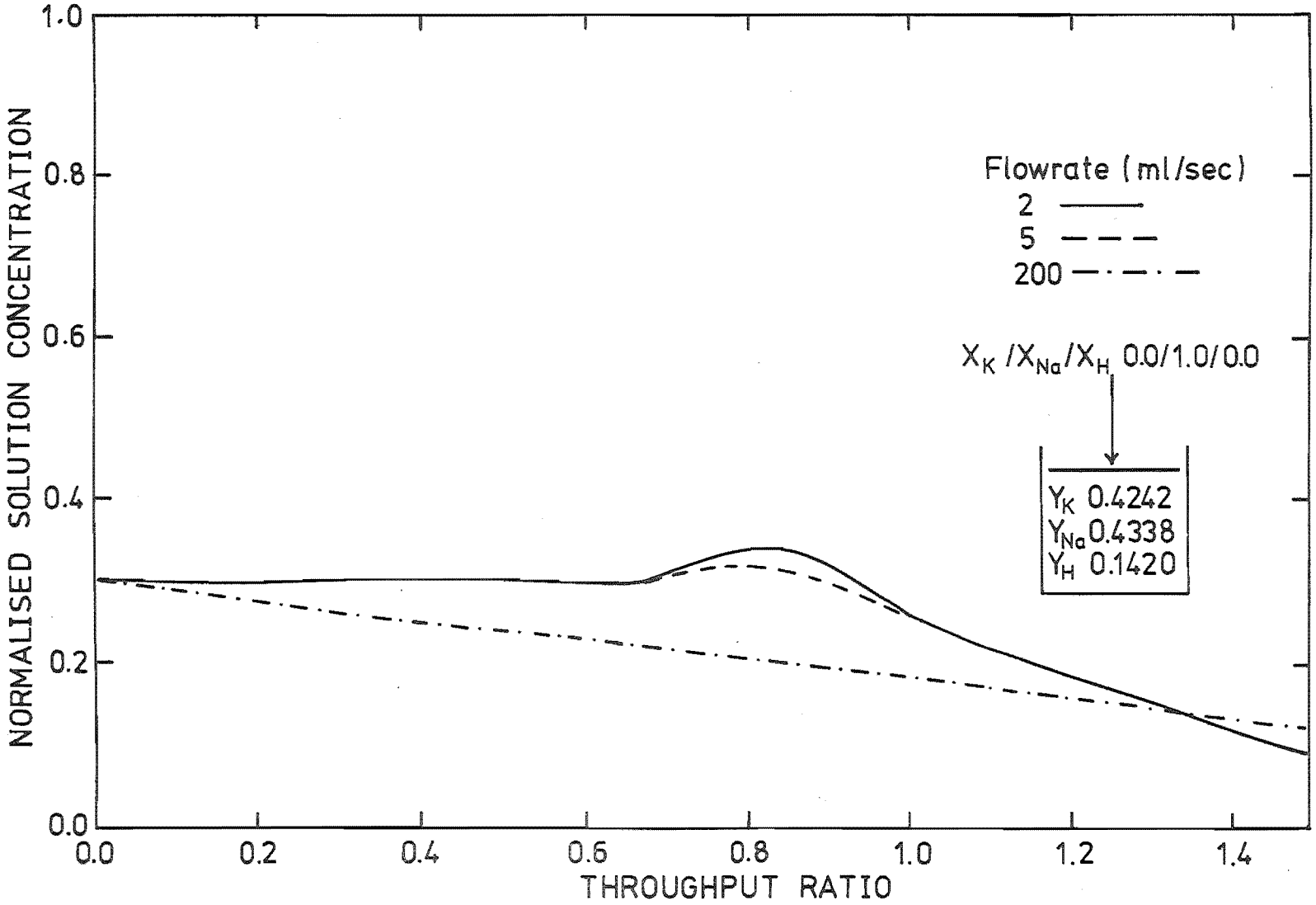

FIGURE 7.22 COMPUTED BREAKTHROUGH CURVES AT VARIOUS FLOWRATES

CHAPTER 8

CONCLUSIONS

The study of multicomponent fixed-bed ion exchange column behaviour is far from complete. The contribution of this work has been the prediction of breakthrough curves for multicomponent ion exchange fixed-bed columns. The data required by GPFIXC are equilibrium information and the fundamental physical properties of the system.

The numerical method and the method of solution have been verified by comparing GPFIXC results with J functions and Allen's results. The equations of the model have been verified in comparison with experimental breakthrough curves. The results show that GPFIXC can be used successfully to predict multicomponent fixed-bed ion exchange column behaviour.

Eight breakthrough curves of binary, K-Na and Na-H, systems were obtained. Under favourable equilibrium conditions, the exchange was under mass transfer control and the constant separation factor model was used to predict the breakthrough curves. For unfavourable equilibrium, exchange was under equilibrium control and the variable separation factor model was used. The experimental evidences indicated that the Nernst-Planck model, allowing variable intra-diffusion coefficients, represents ion exchange column behaviour well.

Twenty-six experimental breakthrough curves of ternary, K-Na-H, system were obtained. The following conclusions can be made from the experimental results.

(1) Intermediate plateau zones were not found for all runs. For intermediate plateaus to exist, there must be a sufficient number of transfer units in the column and the equilibrium must be unfavourable for some counter ions.

(2) Intermediate plateaus are weakly dependent on rate effects.

(3) The width of the transition zone for each counter ion is not necessarily the same.

The future directions of this research should be:-

(1) Further testing of the rate model under particle phase diffusion control. This can be accomplished by employing high solution flow rates.

(2) Using GPFIXC to study multicomponent fixed-bed ion exchange column behaviour.

(3) Formulate multicomponent ion exchange equilibrium data.

(4) Although, the counter ions used in the experimental work were univalent, one would expect that GPFIXC would predict column behaviour for non equi-valent exchange (for example Ca^{++}-K^{+}-Na^{+}) equally well. However, it would be desirable to test this expectation.

(5) The Kataoka equation, with a strong theoretical basis, but involving long computer times, should be considered as another option for determining solution phase mass transfer coefficients.

(6) Improved numerical methods should be sought for solving the hyperbolic partial differential equations of fixed-bed ion exchange.

NOMENCLATURE

A,B,a,b	Constants
A	Column free cross-sectional area (L^2)
A_p	Mass transfer area (L^2/L^3)
A_i	Activity of species i, equivalents/litre
A_o	Activity of a reference solution in a measuring electrode, equivalents/litre
B	Correction term for mixed diffusion, Eqn. 3.20
B_i	Diffusivity ratio, Eqn. 3.45
C	Solution concentration, equivalents/litre
C_o	Total solution concentration, equivalents/litre
C_i	Solution concentration of species i, equivalents/litr
d_p	Particle diameter (L)
D_i	Solution phase self-diffusion coefficient of species i (L^2/T)
$\bar{D}_i$	Resin phase self-diffusion coefficient of species i (L^2/T)
D, $\bar{D}$	Effective diffusion coefficient in solution phase, in resin phase, Eqns. 3.11 and 3.12 (L^2/T)
D_i^o, $\bar{D}_i^o$	D_i, $\bar{D}_i$ at infinite dilution (L^2/T)
D_{ij}	Multicomponent solution phase diffusion coefficient (L^2/T)
$\bar{D}_{ij}$	Multicomponent resin phase diffusion coefficient ($L^2/$
D	Column diameter (L)
EQ	Number of equivalents in the bed
E	Equivalent weight of ion, Eqn. 3.41
E	Electrode potential, MV
E_i	Electrode potential of species i, MV
E_j	Liquid junction potential, MV
E_o, E_Δ, E_ϕ	Electrode constants, MV
F	Solution feed rate to column (L^3/T)
f	Faraday's constant

f_i	Effective resin activity coefficient of species i, Eqn. 5.6
ΔG^o	Standard free energy, Eqn. 6.3
ΔH^o	Standard enthalpy change, Eqn. 6.4
H	Hydrogen
h	Bed height (L)
h_i	Hydration number, Eqn. 6B.12
I	Total ionic strength
J	The J function
j	The j factor, Eqn. 3.33
J_i	Weight equivalent flux of species i relative to weight equivalent average frame velocity in solution phase (equivalents/L^2 T)
$\bar{J}_i$	Weight equivalent flux of species i relative to weight equivalent average frame velocity in resin phase (equivalents/L^2 T)
K	Potassium
k	Mass transfer coefficient (1/T)
k_s	Mass transfer coefficient for film diffusion (1/T)
k_p	Mass transfer coefficient for pore diffusion (1/T)
k_d	Mass transfer coefficient for axial dispersion (1/T)
k_r	Mass transfer coefficient for reaction kinetics (1/T)
k^*	Mass transfer coefficient used in Kataoka equation, Eqn. 3.33
k_i	Solution phase self mass transfer coefficient of species i (1/T)
$\bar{k}_i$	Particle phase self mass transfer coefficient of species i (1/T)
k_{ij}	Multicomponent solution phase mass transfer coefficient (1/T)
$\bar{k}_{ij}$	Multicomponent particle phase mass transfer coefficient (1/T)
K_{ij}	Selectivity constant of ion j with respect to ion i
K_B^A	Thermodynamic equilibrium constant, Eqn. 6.3
L_e	Entrance length (L)
L	Axial mixing length (L)

L_{ij}	Weight equivalent phenomenological coefficient for diffusion
M	Molarity, moles/litre
M_i	Molar concentration of species i, moles/litre
m	Molality, moles/kg
N	Normality, equivalents/litre
N	Number of transfer units
N_r	Number of reaction transfer units, Eqn. 3.13
P	Pressure
P_s	Pressure in the solution phase, Eqn. 5.5
P_r	Pressure in the resin phase, Eqn. 5.5
P_d	Peclet number
Q	Ion exchange resin capacity, equivalents/litre of packed bed
q_i	Resin phase concentration of species i, equivalents/litre of packed bed
R	Universal gas constant
R_i	Rate of mass transfer of species i ($1/L^3$)
Re	Reynolds number, $\frac{d_p F\rho}{6(1-\varepsilon)A\mu}$, Eqn. 3.16
Re'	Reynolds number, $\frac{d_p F\rho}{(1-\varepsilon)A\mu}$, Eqn. 3.32
r	Radial distance (L)
S	Surface area of particles per unit depth of bed, Eqn. 2.17, (L^2/L)
S	Constant in the Nernst equation
Sc	Schmidt number, $\frac{\mu}{\rho D}$
T	Absolute temperature, ^oK
T_L	Lag time (T)
t	Time (T)
$\underset{\sim}{U}$	Unit vector normal to the resin surface
V	Bed volume (L^3)
V_s	Solution volume (L^3)

V_D	Dead volume (L^3)
V_H^W	Bed volume of H-type resin in water (L^3)
V_i	Partial equivalent volume of species i, Eqn. 5.5
V_F	Weight equivalent average reference frame velocity (L/T)
W_i	Weight of species i, gm
X	Degree of cross-linking
X_i	Normalized solution phase concentration of species i
$\bar{X}_i$	Mean value of X_i at a particular cross-section of the column
$\bar{X}_i^*$	Equilibrium value of $\bar{X}_i$
$\bar{X}_i^o$	Feed value of $\bar{X}_i$
Y_i	Normalized particle phase concentration of species i
$\bar{Y}_i$	Mean value of Y_i at a particular cross-section of the column
$\bar{Y}_i^*$	Equilibrium value of $\bar{Y}_i$
$\bar{Y}_i^\infty$	Value of $\bar{Y}_i$ in equilibrium with $\bar{X}_i^o$
$\bar{Y}_i^o$	Value of $\bar{Y}_i$ at column presaturation
Z	The throughput ratio, $\frac{C_o(Ft - V\varepsilon - V_D)}{EQ}$
Z_i	Valence of species i
ΔV, ΔZV	Step-sizes in V, ZV respectively (L^3)
$\dot{A}$	Ion-size parameter, Eqn. 6B.9
α_j^i	Separation factor
γ_i, $\bar{\gamma}_i$	Individual activity coefficients in solution phase, particle phase respectively
γ_{XY}	Mean ionic activity coefficient of electrolyte XY, Eqn. 6B.7
ε	Packed bed voidage
μ	Solution viscosity (M/LT)
ρ	Solution density (M/L^3)
Σ	Summation operator
∇	Gradient operator

$\int$	Integration operator
θ	Bed volume per unit depth (L^3/L)
σ	Osmotic coefficient
ξ	Mechanism parameter, $\frac{\bar{k}_{ij}}{k_{ij}}$
β	Constant
δ & $\bar{\delta}$	Film thicknesses in solution phase and particle phase
ϕ, $\bar{\phi}$	Electrostatic potentials in solution phase, particle phase respectively
λ_i^o	Equivalent conductivity of species i at infinite dilution, sq.cm/ohm.gm.eq.
Γ_i, $\bar{\Gamma}_i$	Electrochemical potentials of species i in solution phase, particle phase respectively
μ_i, $\bar{\mu}_i$	Chemical potentials of species i in solution phase, particle phase respectively
$\mu_i^{\Delta}(T,P)$	Value of μ_i at standard state
$\|_i$	Evaluated at the solution-particle interface

REFERENCES

Acrivos, A.; I.E.C., 48(4), 703 (1956).

Allen, R.M.; "The Simulation of Fixed Bed Ion Exchange Columns" Ph.D. Thesis, University of Canterbury (1973).

Anderson, J. and R. Paterson; J.C.S. Faraday I, 1335 (1975).

Arnold, K.R. and H.L. Toor; A.I.Ch.E.J., 13 (1967).

Bagg, J. and G.A. Rechnitz; Anal. Chem., 1069 (1973).

Bajpai, R.K., A.K. Gupta and M.G. Rao; J.Phys.Chem., 77, 1288 (1973).

Bajpai, R.K., A.K. Gupta and M. Gopala Rao; A.I.Ch.E., 20(5), 989 (1974).

Bates, R.G. and M. Alfenaar; Nat.Bur.Stand.Spec.Publ. No. 314, edited by R.A. Durst, (1969).

Bates, R.G., B.R. Staples and R.A. Robinson; Anal.Chem., 42, 857 (1970).

Bates, R.G. and R.A. Robinson; Pure Appl.Chem., 575 (1973).

Bates, R.G.; "Determination of pH", Interscience London, (1973).

Bates, R.G.; Appl.Chem., 36, 407 (1973).

Bonner, O.D.; J.Phys.Chem., 58, (1954).

Bonner, O.D. and W.H. Payne; J.Phys.Chem., 58, (1954).

Boyd, G.E., A.W. Adamson and L.S. Myers Jr.; J.Am.Chem.Soc. 69, 2863 (1947).

Boyd, G.E., L.S. Myers Jr. and A.W. Adamson; J.Am.Chem.Soc. 69, 2849 (1947).

Bradley, W.G. and N.H. Sweed; A.I.Ch.E. Symposium Series 152, Vol 71, 59 (1975).

Clazie, Klein and Vermeulen; "Multicomponent Diffusion: Generalized Theory with Ion Exchange Application", U.S. Office of Saline Water R&D Progress Rept. 326 (1968).

Cooney, D.O. and E.N. Lightfoot; "Multicomponent Fixed-Bed Sorption of Intefering Solutes", Ind.Eng.Chem.Proc. Des.Dev. 5, 25 (1966).

Cooney, D.O. and F.P. Strusi; Ind.Eng.Chem.Fund., Vol 11, 123 (1972).

Cruickshank, E.H. and P. Meares; Trans.Faraday Soc., 53, 1289 (1957) and 54, 174 (1958).

Cussler, E.L. and M.M. Breuer; Nature, 235 (1972).

Dow Chemical Company; "Laboratory Manual", Midland, Michigan, (1971).

Dranoff, J.S. and L. Lapidus; Ind.Eng.Chem. 49, 1297 (1957).

Dranoff, J.S. and L. Lapidus; Ind.Eng.Chem., 50(1), 1648 (1958).

Dranoff, J.S. and L. Lapidus; "Ion Exchange in Ternary Systems" Ind.Eng.Chem., 53, 71 (1961).

Dranoff, J.S. and T.G. Smith; Ind.Eng.Chem.Fund, 3(3), 195 (1964)

Durst, R.A.; Nat.Bur.Stand.Spec.Publ. No. 314 (1969).

Eisenman, G.; "Glass electrodes for hydrogen and other cations", Marcel Dekker Inc., New York (1967).

Glaski, F.A.; M.S. Thesis, Northwestern University, (1960).

Glueckauf, E.; Trans.Faraday Soc., 51, 1540 (1955).

Graham, E.E.; Ph.D. Thesis, Northwestern University, (1970).

Harned, H.S. and B.B. Owen; "The physical chemistry of electrolyte solutions", Reinhold New York (1958).

Helfferich, F. and M.S. Plesset; J.Chem.Phys., 28, 418 (1958).

Helfferich, F.; "Ion Exchange", McGraw-Hill Book Co., New York, (1962).

Hering, B. and H. Bliss; A.I.Ch.E. Journal, Volume 9, No. 4, 495 (1963).

Hiester, N.K. and T. Vermeulen; Chem.Eng.Progr. 48, 505 (1952).

Hiester, N.K., E.F. Fields, R.C. Phillips and S.B. Radding; Chem.Eng.Progr. 50, 139 (1954).

Hiester, N.K., S.B. Radding, R.L. Nelson and T. Vermeulen; A.I.Ch.E. Journal 2, 404 (1956).

Hiester, N.K., T. Vermeulen and G. Klein; "Adsorption and Ion Exchange" in "Chemical Engineers Handbook", R.H. Perry, C.H. Chilton and S.D. Kirkpatrick; McGraw-Hill, New York (1963).

Jury, S.H.; A.I.Ch.E. Journal, Vol. 12, No. 6, 1124 (1967).

Kataoka, T., N. Sato and K. Ueyama; J.Chem.Eng.Japan, Vol. 1, No. 1, 38 (1968).

Kataoka, T., H. Yoshida and T. Yamada; J.Chem.Eng.Japan, Vol. 6 No. 2, 172 (1973).

Kataoka, T., H. Yoshida and H. Sanada; J.Chem.Eng.Japan, Vol. 7 No. 2, 105 (1974).

Kataoka T. and H. Yoshida; J.Chem.Eng.Japan, Vol. 10 No. 5, 74 (1976).

Kelly, E.G.; "Ion Exchange in Fixed Beds", Ph.D. Thesis, University of Otago (1966).

Kelly, E.G., R.M. Allen and A.M. Kennedy; "Australia National Committee", Inst.Chem.Engrs., Chemeca '70 Conference, Sydney (1970).

Klein, G., D. Tondeur and T. Vermeulen; "Multi-component Ion Exchange in Fixed Bed: General Properties of Equilibrium System", Ind.Eng.Chem. Fundamentals 6, 339 (1967).

Kraus, K.A. and R.J. Raridon; J.Phys.Chem., 63, 1901 (1959).

Lapidus, L.; "Digital Computation for Chemical Engineers", McGraw-Hill, New York (1962).

Leyendekkers, J.V.; Anal. Chem., 43, 1835 (1971).

Lupa, A.J.; "The Kinetics of Ion Exchange with Simultaneous Film and Particle Diffusion", Ph.D. Thesis, Northwestern University, (1967).

Miller, D.G.; J.Phys.Chem., 70, 2639 (1966).

Miller, D.G.; J.Phys.Chem., 71, 616 (1967).

Mills, R. and E.W. Godbole; J.Am.Chem.Soc., 82, 2395 (1960).

Marinsky, J.A., M.M. Reddy and S. Amdur; J. Phys.Chem., 77, 2128 (1973).

Mohan, M.S. and R.G. Bates; Nat.Bur.Stand.Spec.Publ. 450, 293 (1977).

Morig, C.R. and M.G. Rao; Chem.Eng.Sci., Volume 20, 889 (1965).

Myers, G.E. and G.E. Boyd; J.Phys.Chem., 60, 521 (1956).

Omatete, O.O.; "Column Dynamics for Ternary Ion Exchange", Ph.D dissertation in Chemical Engineering, University of California, Berkeley, (1971).

Orion Newsletter, Orion Research Incorporated; September (1969).

Orion Research; Instruction manual; potassium electrode, (1979).

Perry, R.H., C.H. Chilton and S.D. Kirkpatrick; "Chemical Engineers Handbook", 4th edition, McGraw-Hill (1963).

Pieroni, L.J. and J.S. Dranoff; A.I.Ch.E.J., 9, 42 (1963).

Porter, D.G. and R. Sawyer; "Automation of Analytical Methods: in Analytical Methods Volume 1", edited by F. Korte, Academic Press, New York (1974).

Rao, H.C., Suba and M.M. David; A.I.Ch.E., 3, 187 (1957).

Rao, Gopala, M. and M.M. David; A.I.Ch.E., 10, 297 (1964).

Robinson, R.A. and R.H. Stokes; "Electrolyte Solution", 2nd ed., Academic, New York (1959).

Salmon, J.E. and D.K. Hale; "Ion Exchange: A Laboratory Manual", Academic Press Inc., New York, (1959).

Samuelson, O.; "Ion Exchange Separations in Analytical Chemistry" Wiley, New York (1963).

Shatkay, A.; J.Phys.Chem., 71, 3853 (1967).

Sherwood, T.K., R.L. Pigford and C.R. Wilke; "Mass Transfer", McGraw-Hill, New York, (1975).

Stokes, R.H. and R.A. Robinson; J.Amer.Chem.Soc., 70, 1870 (1948).

Treybal, R.E.; "Mass Transfer Operations", McGraw-Hill Book Company, New York (1968).

Turner, J.C.R., M.R. Church, A.S.W. Johnson and C.B. Snowden; Chem.Eng.Sci., 21, 317 (1966).

Turner, J.C.R. and C.B. Snowden; Chem.Eng.Sci., 23, 221 and 1099 (1968).

Turner, J.C.R. and C.B. Snowden; Chem.Eng.Sci., 25, 1673 (1970).

Vanichseni, S.; "Mass Transfer Coefficient Correlation for Ion Exchange in Fixed Bed", B.E. Project Report, University of Canterbury (1970).

Viswanathan, S., D.P. Rao, S.Y. Kekre and M. Gopala Rao; "Ion Exchange in Process Industries", Soc.Chem.Ind., London (1969).

Vermeulen, T.; "Separation by Adsorption Methods", in Drew, T.B. and J.W. Hoopes (Eds), "Advances in Chemical Engineering", Vol 2, Academic Press, New York (1958).

Whitfield, M.; "Ion Selective Electrodes for the Analysis of Natural Waters", Australian Marine Sciences Association Sydney (1971).

Zerolit Testing Method; Zerolit Limited (1976).